UNIVERZITA KARLOVA
Přírodovědecká fakulta

Studijní program: Fyzikální chemie

Mgr. Zuzana Vosáhlová

Charakterizace a využití chromatografických módů s více interakčními mechanismy

Characterization and utilization of chromatographic modes with multiple interaction mechanisms

Disertační práce

Vedoucí disertační práce: doc. RNDr. Květa Kalíková, Ph.D.
Konzultant disertační práce: prof. RNDr. Eva Tesařová, CSc.

Praha 2024

Předkládaná disertační práce shrnuje výsledky získané během mého doktorského studia ve skupině Elektroforetických a chromatografických separačních metod (ECHMET) na Katedře fyzikální a makromolekulární chemie Přírodovědecké fakulty Univerzity Karlovy. Tato práce vznikla za podpory Grantové agentury České republiky (projekt č. 20-19655S) a za podpory programu CEEPUS (projekt č. CIII-RO-0010- 17-2223).

Prohlášení

Prohlašuji, že jsem tuto závěrečnou práci zpracovala samostatně a že jsem uvedla všechny použité informační zdroje a literaturu. Tato práce ani její podstatná část nebyla předložena k získání jiného nebo stejného akademického titulu.

Jsem si vědoma toho, že případné využití výsledků získaných v této práci mimo Univerzitu Karlovu je možné pouze po písemném souhlasu této univerzity.

V Praze dne 17.7. 2024

……..

Mgr. Zuzana Vosáhlová

Poděkování

A je to! Po deseti letech studia na PřF UK je čas poděkovat všem, kteří mě mou dlouhou cestou provázeli, podporovali mě a věřili, že jednou konečně přijde tahle chvíle.

V první řadě bych ráda poděkovala své školitelce Květě, díky níž mám za sebou spoustu let zajímavé práce, která mě každou chvíli posouvala dál, ale především mě hrozně bavila! Vždy jsi mě zvládla správně nasměrovat, poradit, ale zároveň jsi mě vedla k samostatnosti a kritickému myšlení. Děkuji Ti za důvěru a možnost pracovat na všech těch skvělých projektech.

Mé velké poděkování patří i Martinovi a Sylwii, kteří mě zasvětili do světa oligonukleotidů a svým přístupem ze mě udělali lepšího vědce.

Ráda bych poděkovala i Evě, především za její pozitivní přístup. Dále bych chtěla poděkovat všem, které jsem během svého doktorátu potkala, a kteří mi vždy dokázali zvednout náladu.

Poděkování patří i mým přátelům, především Zůze a Fijalce, a rodině. Nikdo z nich nemá vůbec tušení, co jsem tady celé ty roky dělala (něco s trubičkami naplněnými pískem?), ale vždy mě podporovali a byli trpěliví. Děkuji, že jste měli jen přiměřené množství všetečných otázek („K čemu to bude?“, „Kdy už skončíš?“, „Nechceš jít radši do práce?“) a nechali jste mě plnit si sny.

Mé největší poděkování patří mému manželovi. Děkuji Ti za všechny ty večery společně strávené na fakultě, když se jednomu nebo druhému protáhly experimenty. Děkuji Ti za to, že jsme si vždycky našli čas i na „normální“ život, díky čemuž nás věda nepřestala bavit. Jsi mým vysněným parťákem a vím, že spolu vždycky všechno zvládneme!

Obsah

Abstrakt

Předkládaná disertační práce se zabývá podrobnou charakterizací a využitím různých módů kapalinové chromatografie s více interakčními mechanismy pro analýzu biologicky aktivních látek, jako jsou například peptidy, proteiny nebo terapeutické oligonukleotidy. V první části práce byl detailně studován retenční/interakční mechanismus vybraných reverzních a mix-mód stacionárních fází, a to s velkým důrazem na popis elektrostatických interakcí. Pro jejich detailní charakterizaci byla vyvinuta nová metoda využívající čistě vodné mobilní fáze s různými hodnotami pH a modelové permanentně nabité analyty (včetně anorganických aniontů). Bylo ukázáno, že elektrostatické interakce mohou být důsledkem přítomnosti nejen ligandu s iontově výměnným charakterem (na mix-mód stacionárních fázích), ale i residuálních disociovaných silanolových skupin.

Pro popis retenčního chování peptidů a proteinů, tedy analytů zwitterionické povahy, byly vybrány stacionární fáze s mix-mód charakterem. Retence i tvar píků v těchto systémech jsou zásadně ovlivněny nejen pH vodné složky mobilní fáze, ale také koncentrací pufru. S cílem vyvinout jednoduché metody pro on-line štěpení proteinů byly charakterizovány chromatografické kolony s imobilizovaným trypsinem z hlediska vlivu chromatografických podmínek (teplota, pH mobilní fáze, průtok, obsah organické složky mobilní fáze) na aktivitu imobilizovaného trypsinu. V optimalizovaných podmínkách bylo provedeno on-line štěpení různých proteinů s následnou separací na mix-mód koloně. Získané výsledky byly porovnány s off-line štěpením pomocí „spin kolonek“, v případě cytochromu C i s analýzou jeho komerčně dostupného naštěpeného standardu.

Terapeutické thiofosfátové oligonukleotidy byly charakterizovány a analyzovány ve dvou různých módech, a to iontově-párovou chromatografií na reverzních fázích a hydrofilní interakční kapalinovou chromatografií. Oba systémy v optimalizovaných podmínkách neposkytují separaci diastereomerů, což je klíčové pro jejich spolehlivou analýzu. V prvním zmíněném módu byl podrobně studován vliv separační teploty, typu a koncentrace jak iontově-párového činidla, tak i jeho protiiontu na potlačení separace diastereomerů a rozlišení oligonukleotidů s různou délkou (*n* a *n-x*). Zjištěný vysoký potenciál hydrofilní interakční kapalinové chromatografie a její kompatibilita s hmotnostní detekcí byly využity při separaci a identifikaci nečistot a metabolitů terapeutického oligonukleotidu nusinersenu.

Abstract

The presented dissertation thesis focuses on the detailed characterization and utilization of various modes of liquid chromatography with multiple interaction mechanisms for analysis of biologically active compounds, such as peptides, proteins or therapeutic oligonucleotides. In the first part of the thesis, the retention/interaction mechanisms of selected reversed-phase and mixed-mode stationary phases were investigated thoroughly, with a strong emphasis on describing electrostatic interactions. For their detailed characterization, new method using pure aqueous mobile phases with different pH values and model permanently charged analytes (including inorganic anions) was developed. It's important to note that electrostatic interactions can be arise not only from the presence of ligands with ion-exchange properties (mixed-mode stationary phases) but also from residual dissociated silanols.

To describe the retention behavior of peptides and proteins, *i.e.* zwitterionic compounds, stationary phases with mixed-mode character were selected. The retention and peak shape in these systems are fundamentally affected not only by pH of aqueous part of the mobile phase, but also by the buffer concentration. With the aim of developing a simple method for on-line protein digestion, chromatographic columns with immobilized trypsin were characterized in terms of the effects of chromatographic conditions (temperature, pH of the mobile phase, flow rate, content of organic modifier in the mobile phase) on the activity of immobilized trypsin. Under optimized conditions, several proteins were on-line digested, followed by the separation of digests using mixed-mode column. The results were compared with off-line digestion using trypsin spin columns and, in the case of cytochrome C also with analysis of its commercially available digested standard.

Therapeutic phosphorothioate oligonucleotides were characterized and analyzed in two different modes, namely ion-pairing reversed-phase liquid chromatography and hydrophilic interaction liquid chromatography. Both systems do not provide separation of diastereomers under optimized conditions, which is crucial for their reliable analysis. In the first mentioned mode, the effect of the separation temperature, type and concentration of both the ion-pairing agent and its counterion on the suppression of diastereomeric separation and the resolution of oligonucleotides of different lengths (*n* and *n-x*) was comprehensively inspected. The discovered high potential of hydrophilic interaction liquid chromatography and its compatibility with mass detection were utilized for separation and identification of impurities and metabolites of the therapeutic oligonucleotide nusinersen.

Klíčová slova: interakční mechanismus, LFER, mix-mód chromatografie, štěpení proteinů, peptidy, oligonukleotidy

Key words: interaction mechanism, LFER, mixed-mode chromatography, protein digestion, peptides, oligonucleotides

Seznam zkratek a symbolů

Zkratky

ACN	acetonitril
AmAc	octan amonný
AEX	aniontově-výměnný charakter
BAPNA	*N*-α-benzoyl-L-arginin 4-nitroanilid hydrochlorid
BEH	„bridged ethylene hybrid“
C8	oktylová skupina
C18	oktadecylová skupina
CE	kapilární elektroforéza
CEX	kationtově-výměnný charakter
CSH	„charged surface hybrid“
DBAA	dibutylamonium acetát
DEA	diethylamin
DEAA	diethylamonium acetát
DHAA	dihexylamonium acetát
DIPAA	diisopropylamonium acetát
DPA	dipropylamin
DPAA	dipropylamonium acetát
FP	fluorfenyl
GC	plynová chromatografie
HA	hexylamin
HAA	hexylamonium acetát
HFIP	hexafluorisopropanol
HILIC	hydrofilní interakční kapalinová chromatografie
HPLC	vysokoúčinná kapalinová chromatografie
HSS	„high strength silica“
IEC	iontově-výměnná chromatografie
IMER	„immobilized enzyme reactor“ (imobilizovaný enzymatický reaktor)
IP	iontově-párový
IPRPLC	iontově-párová chromatografie na reverzních fázích
LFER	„linear free energy relationship“ (lineární vztah volných energií)
MeOH	methanol

MF	mobilní fáze
MM	mix-mód
MMC	mix-mód chromatografie
MS	hmotnostní spektrometrie
NPLC	normální mód kapalinové chromatografie
OAA	oktylamonium acetát
ON	oligonukleotid
PFP	pentafluorfenyl
PH	fenyl-hexyl
POM	polárně-organický mód
PS	thiofosfát
RPLC	reverzní mód kapalinové chromatografie
SEC	molekulová vylučovací chromatografie
SF	stacionární fáze
SFC	sub/superkritická fluidní chromatografie
TEA	triethylamin
TEAA	triethylamonium acetát
TIC	„total ion recording“
$TMFA^+$	trimethyfenylamonný kationt
UHPLC	ultra-vysokoúčinná kapalinová chromatografie
4-CBC	4-chlor-*N*-butylkathinon
4-CDC	4-chlor-*N,N*-dimethylkathinon
4-ClC	4-chlor-*N*-isopropylkathinon
4-CPRC	1-(4-chlorfenyl)-2-pyrrolidin-1-yl-pentan-1-on
4F-NPP	1-(4-fluorfenyl)-2-(isopropylamino)pentan-1-on

Symboly

A	kyselost vodíkové vazby (LFER)
a	regresní koeficient LFER rovnice
A_s	faktor asymetrie
B	basicita vodíkové vazby (LFER)
b	regresní koeficient LFER rovnice
c	úsek LFER rovnice

D^-	záporný náboj analytu (LFER)
d^-	regresní koeficient LFER rovnice
$D+$	kladný náboj analytu (LFER)
$d+$	regresní koeficient LFER rovnice
E	rozsah molární refrakce (LFER)
e	regresní koeficient LFER rovnice
f_p	šířka vzestupné části píku v 5 % jeho výšky
HI	hydrofobicita (Waltersův test)
k	retenční faktor
$k(u)$	retenční faktor uridinu (Tanakův test)
R^2	koeficient determinace
R_s	rozlišení dvou píků
S	dipolarita/ polarizibilita (LFER)
s	regresní koeficient LFER rovnice
SI	silanolová aktivita (Waltersův test)
t_M	mrtvý čas
t_R	retenční čas
V	McGowanův charakteristický objem (LFER)
v	regresní koeficient LFER rovnice
$w_{5\%}$	šířka píku v 5 % jeho výšky
$w_{50\%}$	šířka píku v 50 % jeho výšky
y	počet thiofosfátových substitucí
z	celkový efektivní náboj
α	selektivita
α(AX)	aniontově-výměnný charakter stacionární fáze (Tanakův test)
α(CH3)	selektivita k hydrofobním skupinám (Tanakův test)
α(CX)	kationtově-výměnný charakter stacionární fáze (Tanakův test)
α(OH)	selektivita k polárním skupinám (Tanakův test)
α(Tb/Tp)	kyselost povrchu stacionární fáze (Tanakův test)
α(V/A)	selektivita pro konfigurační isomery (Tanakův test)
α(2D/3D)	selektivita pro strukturní isomery (Tanakův test)

1 Úvod

1.1 Separační metody, chromatografie

S rostoucím počtem nejrůznějších nejen biologicky aktivních sloučenin využívaných ve farmacii, potravinářství a dalších odvětvích roste i poptávka po účinných, rychlých a robustních analytických metodách, a to zejména těch separačních [1,2]. Separační metody umožňují analyzovat komplexní vzorky a poskytovat informaci o několika přítomných analytech v rámci jedné analýzy, což je velmi efektivní z hlediska úspory času, a tedy i vynaložených finančních prostředků. Z moderních instrumentálních separačních metod můžeme zmínit například kapilární elektroforézu (CE), plynovou chromatografii (GC), sub/superkritickou fluidní chromatografii (SFC) a vysokoúčinnou kapalinovou chromatografii (HPLC) [3]. CE má ve svém základním uspořádání omezenou použitelnost pouze pro nabité analyty, vyznačuje se obecně nižší robustností než chromatografické metody [4]. GC je vhodnou technikou pro analýzu a separaci těkavých sloučenin. Optimalizace metody v GC je limitována mobilní fází (MF), inertní plynem, a proto nelze selektivitu systému ovlivňovat jejím složením [5], ale je nutné využití např. teplotních gradientů [6]. SFC je metodou s velkým potenciálem pro separaci nejen chirálních sloučenin, nicméně prozatím je v komerční sféře rutinně využívána daleko méně než kapalinová chromatografie [7].

HPLC, případně ultra-vysokoúčinná kapalinová chromatografie (UHPLC) je v současné době nejvíce využívanou analytickou separační metodou pro analýzu, separaci a purifikaci širokého spektra sloučenin a vzorků různého původu. Její největší předností je vysoká variabilita z důvodu možnosti použít různé kombinace stacionárních fází (SF) a MF, a tedy možnost pracovat v různých módech kapalinové chromatografie [8]. Na základě polarity analytů a typu SF rozeznáváme dva nejzákladnější módy kapalinové chromatografie, a to normální mód (NP) a reverzní mód (RP). NPLC, která je vhodná pro analýzu polárnějších látek, využívá polární SF v kombinaci s nepolárními organickými rozpouštědly, jako je například heptan, hexan nebo chloroform velmi často s přídavky polárních rozpouštědel jako je např. ethanol nebo propan-2-ol. Jako SF se nejčastěji využívá nemodifikovaný silikagel nebo silikagel modifikovaný polárními skupinami [9]. RPLC je naopak vhodná pro analýzu spíše nepolárních sloučenin a SF je v tomto módu méně polární než MF. SF bývá většinou silikagel modifikovaný oktadecylovými (C18), oktylovými (C8) nebo fenylovými ligandy, MF je pak nejčastěji směs vody nebo vodného

pufru s organickým rozpouštědlem, především acetonitrilem nebo methanolem [10]. Mezi další základní módy kapalinové chromatografie patří např. iontově-výměnná chromatografie (IEC, separující na základě náboje analytu) nebo molekulová vylučovací chromatografie (SEC, separující na základě velikosti analytu).

1.2 Chromatografie s více interakčními mechanismy

Všechny výše zmíněné módy kapalinové chromatografie mají jednu společnou charakteristiku, a to že retence analytů je řízena pouze jedním hlavním interakčním mechanismem. V případě RPLC se kromě „hydrofobní interakce“ může uplatňovat sekundární iontově-výměnná interakce s residuálními disociovanými silanolovými skupinami (**Obr. 1A**). Tato interakce je zpravidla považována za nežádoucí a nepředstavuje hlavní interakční mechanismus. Interakce především bazických analytů s residuálními disociovanými silanoly (nezreagovanými při pokrývání ligandem a dodatečně nechráněnými, tzv. „neendkapovanými“) způsobují zhoršení tvaru píků, a tedy i separační účinnosti [11]. S rostoucí komplexitou vzorků roste i poptávka po stacionárních fázích/módech, které budou dva a více interakčních mechanismů poskytovat účelně, a tím vykazovat jedinečnou selektivitu a zároveň variabilitu. V následujících třech podkapitolách jsou detailně popsány tři takové módy, které byly využívány v průběhu práce na publikacích zahrnutých v předkládané disertační práci.

1.2.1 Mix-mód chromatografie

V osmdesátých letech minulého století byl poprvé představen koncept chromatografie na tzv. smíšených fázích, neboli mix-mód chromatografie (MMC) [12]. Mix-mód (MM) SF jsou vyvíjeny tak, aby poskytovaly dva a více hlavních interakčních mechanismů významně se podílejících na retenci současně, a tím umožňovaly separovat široké spektrum sloučenin s rozdílnými vlastnostmi (například nabité a nepolární sloučeniny) v rámci jedné analýzy [13]. V principu je možné MM SF dosáhnout několika způsoby. Příkladem může být spojení dvou kolon v sérii s různými typy SF [14] nebo kombinace dvou různých materiálů v jedné koloně [15]. V současné době je nejrozšířenějším přístupem kovalentní modifikace nosiče (nejčastěji silikagelu) nebo ligandu různými typy funkčních skupin v rámci jedné SF [16]. Takové uspořádání zaručuje homogenní distribuci funkčních skupin a s tím související vysokou opakovatelnost měření. V případě bimodálního systému rozeznáváme tři základní typy kovalentní modifikace:

i) navázání dvou různých samostatných ligandů/funkčních skupin na povrch silikagelového nosiče (**Obr. 1B**); ii) vložení funkční skupiny do řetězce/skupiny s jiným charakterem (**Obr. 1C**); iii) vložení funkční skupiny na konec řetězce/skupiny s jiným charakterem (**Obr. 1D**) [17]. Všechny tři uvedené možnosti vykazují různé retenční chování, a to zejména z důvodu různé přístupnosti funkčních skupin.

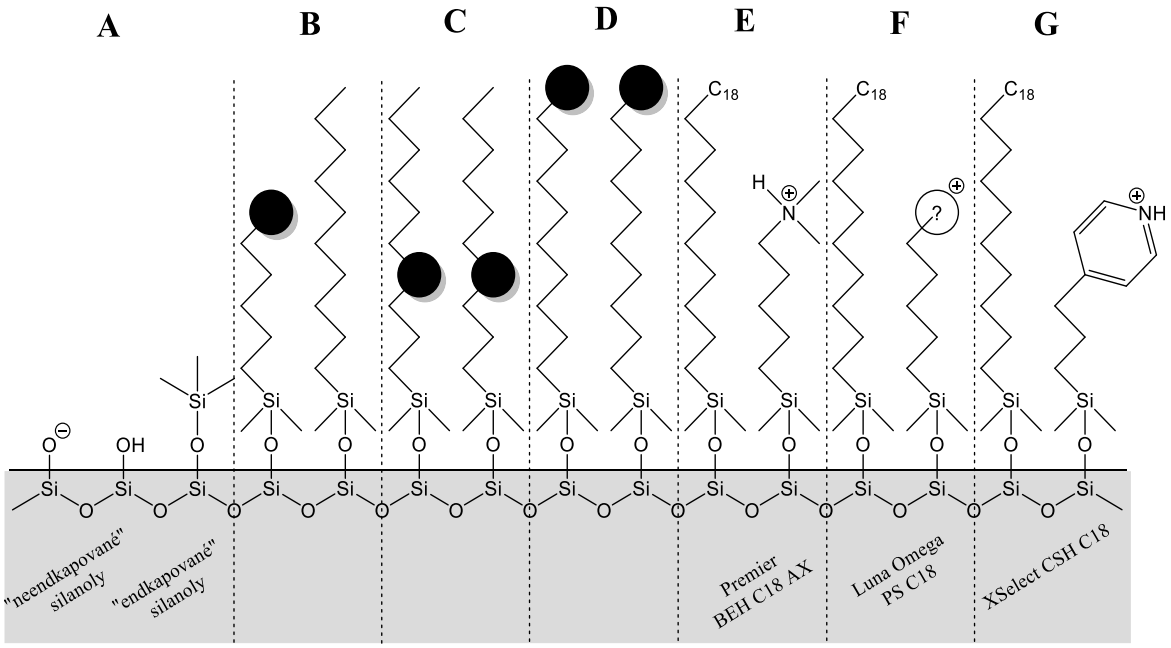

Obr. 1: Různé typy stacionárních fází. **A:** povrch silikagelového nosiče, **B, C, D:** možnosti umístění funkčních skupin na MM stacionárních fázích, **E:** MM stacionární fáze použitá v koloně Premier BEH C18 AX (kladně nabitá do pH 8-9), **F:** MM stacionární fáze použitá v koloně Luna Omega PS C18 (není známá přesná struktura), **G:** MM stacionární fáze použitá v koloně CSH C18 (kladně nabitá v omezeném rozsahu pH). Zobrazení SF je schematické a pro jednoduchost ukazuje monofunkční navázání ligandu na nosič ve všech případech (u kolon Premier BEH C18 AX a XSelect CSH C18 jsou ligandy navázány trifunkčně – podrobněji v Tabulce 3, str. 38-39).

MM SF můžeme rozdělit do čtyř základních skupin na základě kombinace tradičních chromatografických módů: RPLC-IEC, RPLC-hydrofilní interakční kapalinová chromatografie (HILIC), HILIC-IEC a RPLC-HILIC-IEC [18]. SF s RP charakterem jsou tvořeny hydrofobními ligandy, tedy především alkylovými řetězci (C8 nebo C18) [19,20] nebo fenylem [21]. HILIC SF obvykle obsahují polární amidy [21], aminokyseliny [22] nebo hydroxylové skupiny [20]. SF s IEC charakterem jsou tvořeny především kvarterním amoniem (aniontově-výměnný charakter, AEX) [23] nebo karboxylovými či sulfonovými skupinami (kationtově-výměnný charakter, CEX) [24]. Kombinací výše zmíněných

ligandů v rámci jedné SF lze dosáhnout unikátní selektivity a široké použitelnosti MM SF. Mezi další výhody MM SF patří i možnost větší nadávkované koncentrace vzorku [25].

V rámci předkládané disertační práce jsem se zabývala mimo jiné MM SF kombinujícími RP a AEX charakter, které obsahují hydrofobní C18 ligand a ionizovatelnou funkční skupinu poskytující kladný náboj (např. terciární alkylamin). Struktura takových SF je zobrazena na **Obr. 1E a F.** Zatímco pro kolonu Premier BEH C18 AX je struktura SF známá (**Obr. 1E**), o SF použité v koloně Luna Omega PS C18 je zveřejněno pouze to, že je přítomen kladný náboj (**Obr. 1F**). Kromě kolon s komerčním označením „mix-mód" lze na trhu najít i kolony prodávané jako „RPLC", které nicméně za určitých podmínek poskytují i mix-mód charakter [26]. Příkladem mohou být například kolony, jejichž stacionární fáze je tvořena ligandy navázanými na tzv. „charged surface hybrid" (CSH) částicích. CSH částice mají na povrchu kromě ligandu navázanou pyridylovou skupinu (**Obr. 1G**), která by měla být při pH < 7 kladně nabitá [27], a tím poskytovat MM charakter CSH SF. CSH částice s povrchovým nábojem byly navrženy především pro zlepšení tvaru píků bazických látek při analýze v kyselých MF s nízkou iontovou silou [28].

MM SF byly úspěšně využity pro analýzu různých biologicky aktivních sloučenin, jako jsou například aminokyseliny a peptidy [29,30], nukleové kyseliny [31], DNA a RNA deriváty [32] nebo protilátky [33,34].

1.2.2 Hydrofilní interakční kapalinová chromatografie

Pojem HILIC poprvé použil v roce 1990 Alpert [35], nicméně první experimenty byly v tomto uspořádání provedeny již o 15 let dříve [36]. HILIC je používán jako alternativa k NPLC pro analýzu polárních sloučenin, které by v klasické RPLC měly velmi nízkou nebo žádnou retenci nebo by byly špatně rozpustné v MF používané pro NPLC. Pro HILIC je charakteristické použití polární SF typické pro NPLC v kombinaci s méně polární MF, která je svým složením podobná MF používaným v RPLC. SF může být čistý silikagel, silikagel modifikovaný polárními skupinami (například amino, amido, kyano nebo diolovými skupinami) nebo tzv. zwitterionické SF, které nesou kladný i záporný náboj [37,38]. MF je tvořena směsí vodné složky (minimálně 2,5 obj. %) a méně polárního rozpouštědla, obvykle acetonitrilu (typicky více než 70 obj. %) [39]. Na rozdíl od RPLC má vodná složka MF v tomto uspořádání vyšší eluční sílu.

HILIC má oproti NPLC i RPLC řadu výhod, jako je například možnost analýzy polárních sloučenin za použití méně toxických rozpouštědel, než nabízí klasická NPLC. Zároveň jsou polární analyty lépe rozpustné v HILIC MF ve srovnání s NPLC MF. MF používané v HILIC jsou kompatibilní s hmotnostní detekcí [40]. K dosažení opakovatelných výsledků je ale nutná relativně dlouhá ekvilibrace systému. Nevýhodou může být i komplexnost retenčního mechanismu, která má za následek problematické porozumění a předvídání retenčního chování.

Základem retenčního mechanismu v HILIC je rozdělování analytu mezi dvě vrstvy MF, a to konkrétně mezi vodnou složkou obohacenou vrstvu MF imobilizovanou na povrchu SF a na acetonitril bohatou MF (**Obr. 2**). Na retenci má tedy vliv nejen polarita sloučenin (s rostoucí polaritou analytu roste jeho afinita k vodou obohacené vrstvě, a tím roste jeho retence), ale také stupeň solvatace SF [41]. Na povrchu SF dochází během solvatace k tvorbě gradientu, tzn. u povrchu SF je zastoupení vodné složky MF největší a s rostoucí vzdáleností od povrchu SF roste podíl acetonitrilu v MF [42]. Aby mohla vrstva obohacená vodnou složkou MF vzniknout, musí MF obsahovat minimálně již zmíněných 2,5 obj. % vodné složky [43]. S rostoucím obsahem vodné složky v MF pak klesá retence analytů, což je způsobeno rostoucí podobností vrstvy sorbované na povrchu SF s okolní MF [44].

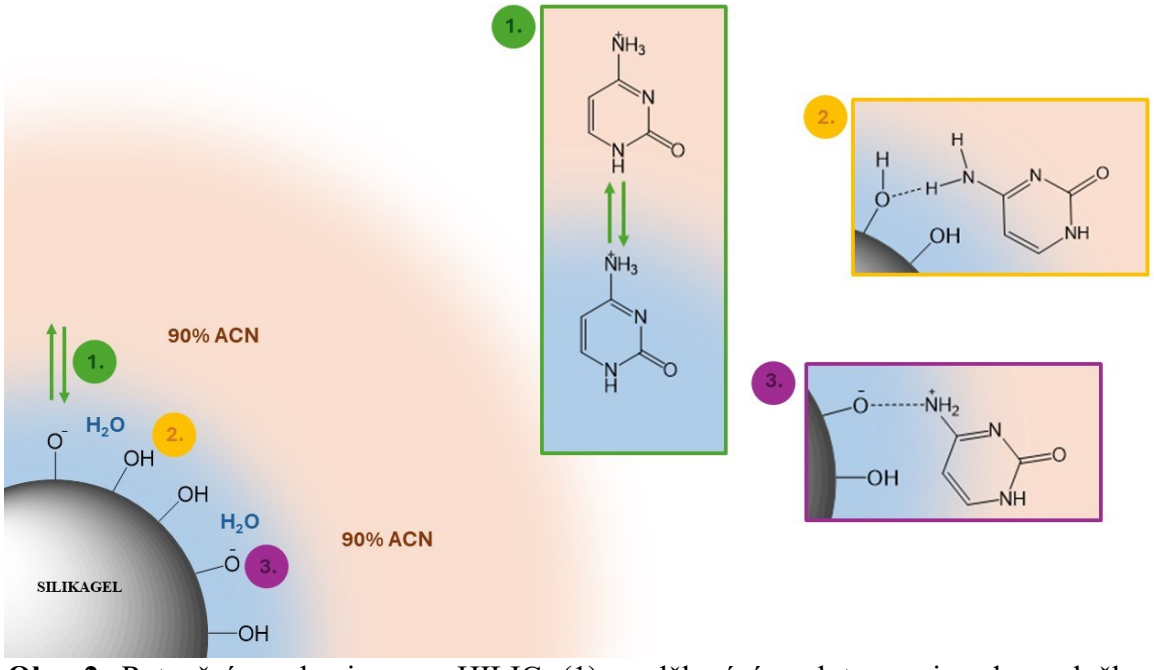

Obr. 2: Retenční mechanismus v HILIC. (1) rozdělování analytu mezi vodnou složkou obohacenou vrstvu MF imobilizovanou na povrchu SF a na acetonitril bohatou MF; (2) vodíkové interakce; (3) elektrostatické interakce.

Rozdělování analytů mezi vrstvy MF různě obohacené o vodnou nebo organickou složku ale není jediným mechanismem, který přispívá k retenci analytů v HILIC (**Obr. 2**). V závislosti na zvolených podmínkách (tj. výběr SF, výběr MF) může docházet i k interakci mezi analytem a přímo povrchem SF a mohou se tak uplatňovat například vodíkové interakce, elektrostatické interakce nebo interakce dipól-dipól [45,46].

HILIC se běžně využívá například pro farmaceutické analýzy [47,48], v metabolomice [49,50] a glykoproteomice [51], a to zejména z důvodu bezproblémové kompatibility s MS, která umožňuje analýzu i velmi komplexních vzorků.

1.2.3 Iontově-párová chromatografie na reverzní stacionární fázi

Iontově-párová chromatografie na reverzních fázích (IPRPLC) byla poprvé představena v 70. letech minulého století [52]. IPRPLC je zvláštním módem kapalinové chromatografie, který umožňuje separaci nabitých polárních analytů na klasických nepolárních RP SF, a to z důvodu přídavku iontově-párového (IP) činidla do MF [53]. Na mechanismus IPRPLC lze v zásadě nahlížet dvěma způsoby [54,55]: i) dynamické pokrytí SF IP činidlem a následná interakce nabitých analytů s nyní opačně nabitým povrchem SF (**Obr. 3A**); ii) tvorba iontových párů mezi IP činidlem a opačně nabitým analytem v MF a interakce těchto navenek elektroneutrálních iontových párů s nepolární stacionární fází (**Obr. 3B**). Tento systém tak vykazuje charakteristiky jak RPLC tak iontově-výměnné chromatografie (IEC), přičemž převládající mechanismus je určen mimo jiné koncentrací a hydrofobicitou IP činidla [56]. Rovněž je potřeba vhodně zvolit pH MF tak, aby analyty byly nabité a mohly interagovat s IP činidlem.

Jako IP činidla nesoucí záporný náboj, která se používají pro analýzu bazických analytů, se nejčastěji využívají alkylsulfonové kyseliny nebo perfluorované karboxylové kyseliny (např. trifluoroctová kyselina). Alkylsulfonáty nejsou kvůli své nízké těkavosti kompatibilní s MS detekcí. Jako IP činidla nesoucí kladný náboj, která jsou vhodná pro analýzu kyselých analytů, se využívají především alkylamoniové kationty.

Mezi největší výhody IPRPLC patří zejména možnost separovat nabité analyty za použití klasických RPLC kolon (a tedy bez nutnosti kupovat nové s jinou SF) a možnost separovat neutrální analyty od těch nabitých (na rozdíl od IEC). IPRPLC také nabízí velkou variabilitu ve výběru MF, z nichž některé jsou relativně dobře kompatibilní s MS detekcí (nebo alespoň lépe v porovnání s IEC). Nevýhodou IPRPLC je ve srovnání s RPLC menší robustnost, pomalé ustavování rovnováhy a perzistence některých IP činidel

v chromatografickém systému, což je velmi problematické především ve spojení s MS detekcí.

V současné době patří jednoznačně k největším aplikacím IPRPLC analýza terapeutických thiofosfátových oligonukleotidů, která je detailně popsána v kapitole 1.5.

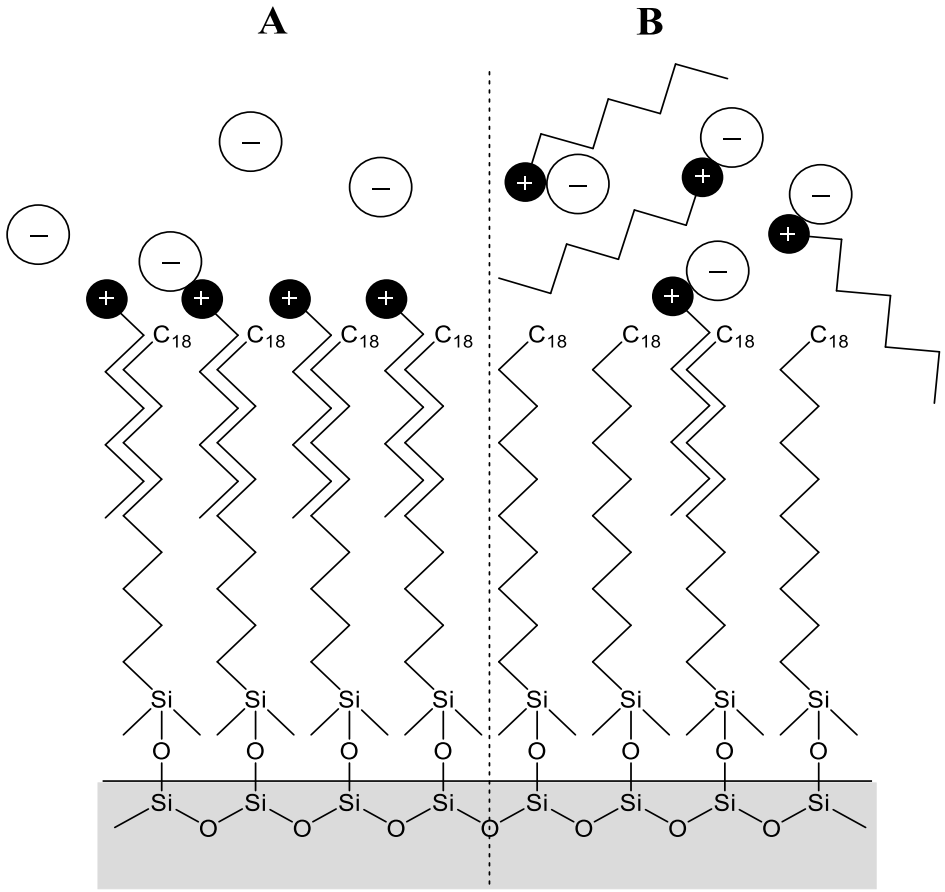

Obr. 3: Mechanismus IPRPLC (na příkladu záporně nabitého analytu v kombinaci s kladně nabitým hexylamoniem jako IP činidlem).

1.3 Charakterizace stacionárních fází

S rostoucí komplexitou retenčního mechanismu roste i důležitost charakterizace SF, resp. separačního systému. Detailní popis interakčních mechanismů (zejména pokud je jich více) je základem pro vhodnou volbu SF a MF k danému účelu. K popisu chromatografických systémů bylo navrženo několik jednoduchých chromatografických testů (například test podle Walterse [57] nebo Tanaky [58] používané především pro RPLC), které pro získání základních charakteristik/parametrů separačního systému využívají dvojici strukturně odlišných analytů. Výpočet jednotlivých parametrů a jejich význam jsou uvedeny v **Tabulce 1**.

Tabulka 1: Výpočet a význam jednotlivých parametrů pro testy podle Walterse a Tanaky, chromatografické podmínky pro daný test

WALTERSŮV TEST Mobilní fáze: acetonitril (ACN)/voda; 65/35 (*v/v*) Teplota kolony: 40 °C		
Hydrofobicita (*HI*)		*k* (antracen)/*k* (benzen)
Silanolová aktivita (*SI*)		*k* (antracen)/*k* (*N,N*-diethyltoluamid)
TANAKŮV TEST Mobilní fáze: ACN/20mM octan amonný, pH 4,7; 90/10 (*v/v*) Teplota kolony: 30 °C		
***k*(u)**	hydrofobicita/retentivita	*k* (uridin)
α(CH3)	hydrofobní charakter SF, selektivita k hydrofobním skupinám	*k* (uridin)/*k* (methyluridin)
α(OH)	hydrofilní charakter SF, selektivita k polárním skupinám, tloušťka vodné vrstvy (v HILIC)	*k* (uridin)/*k* (deoxyuridin)
α(V/A)	selektivita pro konfigurační isomery	*k* (vidarabin)/*k* (adenosin)
α(2D/3D)	selektivita pro strukturní isomery	*k* (2′-deoxyguanosin)/*k* (3′-deoxyguanosin)
α(AX)	aniontově-výměnný charakter SF	*k* (toluensulfonová kys.)/*k* (uridin)
α(CX)	kationtově-výměnný charakter SF	*k* (trimethylfenylamonium chlorid)/*k* (uridin)
α(Tb/Tp)	kyselost povrchu SF	*k* (theobromin)/*k* (theofylin)

Pro komplexnější charakterizaci interakčních vlastností separačního systému lze použít například model lineárních vztahů volných energií (linear free energy relationship, LFER) [59]. Tento semiempirický model umožňuje kvalitativně a kvantitativně popsat jednotlivé typy interakcí, které ovlivňují retenci a separaci analytů. Na základě LFER modelu je při použití dané MF možné charakterizovat, a především srovnávat různé SF z hlediska jejich interakčního potenciálu. Základní LFER model je běžně používaný především pro charakterizaci systémů s neutrálními SF, protože základní tvar LFER rovnice nezahrnuje příspěvky elektrostatických interakcí [60]. Z toho důvodu byla základní LFER rovnice rozšířena o další dva členy charakterizující kladný resp. záporný náboj

analytu při dané hodnotě pH mobilní fáze [61,62]. To umožňuje vhodnější aplikaci LFER modelu i pro SF s MM charakterem. Rozšířená LFER regresní funkce má následující tvar:

$$\log k = eE + sS + aA + bB + vV + d^{-}D^{-} + d^{+}D^{+} + c \qquad (1.1)$$

a vyjadřuje vztah mezi experimentálně zjištěnými retenčními faktory sady strukturně odlišných analytů (ve formě $\log k$) a deskriptory (velká písmena), které popisují fyzikálně-chemické vlastnosti a jsou tabelovány pro celou řadu analytů [63]. Regresní koeficienty/parametry systému (malá písmena) jsou získány multidimenzionální lineární regresí a charakterizují tendenci systému poskytovat daný typ interakce neboli rozdíl v síle dané interakce analyt-SF a analyt-MF. Pokud má regresní koeficient kladnou hodnotu, je daná interakce silnější mezi analytem a SF (v porovnání s interakcí analyt-MF) a daná interakce tak přispívá ke zvýšení retence analytu. Významy jednotlivých deskriptorů i regresních koeficientů jsou uvedeny v **Tabulce 2.**

Tabulka 2: Význam deskriptorů a regresních koeficientů v LFER rovnici

DESKRIPTORY	tabelované/vypočtené hodnoty	**REGRESNÍ KOEFICIENTY**	zjištěné hodnoty multidimenzionální lineární regresí
E	rozsah molární refrakce	e	schopnost interakce skrze n- a π- elektrony
S	dipolarita/ polarizibilita	s	schopnost interagovat interakcí dipól-dipól a dipól-indukovaný dipól
A	kyselost vodíkové vazby	a	proton-donorová schopnost tvořit vodíkové vazby
B	basicita vodíkové vazby	b	proton-akceptorová schopnost tvořit vodíkové vazby
V	McGowanův charakteristický objem	v	schopnost „hydrofobní“ interakce
D^-	záporný náboj analytu	d^-	schopnost elektrostatické interakce (pro kyseliny)
$D+$	kladný náboj analytu	d^+	schopnost elektrostatické interakce (pro báze)
		c	poměr objemů MF a SF + všechny ostatní nezahrnuté příspěvky k retenci

Deskriptory popisující elektrostatické vlastnosti analytu (D^- a D^+) jsou závislé na pH MF a nejsou tedy pro všechny hodnoty pH tabelované. Lze je ale snadno vypočítat následujícími rovnicemi:

$$D^- = \frac{10^{(\mathrm{pH}^* - \mathrm{pK}_a^*)}}{1 + 10^{(\mathrm{pH}^* - \mathrm{pK}_a^*)}} \tag{1.2}$$

$$D^+ = \frac{10^{(\mathrm{pK}_a^* - \mathrm{pH}^*)}}{1 + 10^{(\mathrm{pK}_a^* - \mathrm{pH}^*)}} \ , \tag{1.3}$$

kde pH^* značí pH vodně-organické MF a $\mathrm{p}K_a^*$ značí $\mathrm{p}K_a$ analytu v dané vodně-organické MF [64]. V praxi se k výpočtu těchto deskriptorů využívají standardní hodnoty $\mathrm{p}K_a$ a hodnoty pH změřené na pH metru kalibrovaném klasickými vodnými pufry.

Charakteristiky separačního systému vyjádřené regresními koeficienty se dají určit testováním rozsáhlé sady analytů. Vybraná testovací sada analytů musí obsahovat strukturně odlišné sloučeniny, aby jejich deskriptory rovnoměrně pokrývaly celou škálu možných interakcí. Výsledky multidimenzionální regrese pak umožní popsat, které typy interakcí mezi analytem a SF převládají (největší kladné hodnoty regresních koeficientů) a na základě toho lze určit aplikační potenciál testovaných kolon/separačních systémů.

1.4 Analýza peptidů/štěpných produktů proteinů

Pro proteomickou analýzu za využití kapalinové chromatografie je zásadním krokem štěpení velkých proteinů na menší fragmenty, které je možné identifikovat použitím MS detekce, tedy tzv. peptidové mapování [65]. Ke štěpení proteinů se velmi často využívá trypsin, vysoce specifický enzym štěpící proteiny hydrolýzou peptidové vazby na karboxylovém konci lysinu a argininu [66,67]. Pokud jsou tyto aminokyseliny následovány kyselým aminokyselinovým zbytkem, štěpení probíhá výrazně pomaleji, v případě následování prolinem štěpení neprobíhá vůbec [68]. Tato vysoká substrátová specifita souvisí s reaktivitou pozitivně nabitých postranních řetězců lysinu a argininu, což je zároveň velmi výhodné pro následnou interpretaci MS spekter [69,70]. Optimální podmínky pro aktivitu trypsinu jsou teplota 37 °C a pH ~ 7,0-8,0 [71]. Před samotným štěpením je nutné protein denaturovat (rozrušit jeho terciární strukturu) a zajistit tím rozložení proteinu a větší přístupnost lysinu a argininu pro následné štěpení. V případě proteinů obsahujících více než jeden cystein dochází k tvorbě disulfidických (S-S) můstků, které je potřeba podrobit redukci a alkylaci, aby mohlo dojít ke správnému procesu štěpení.

Jako denaturační činidlo lze využít například komerčně dostupnou směs močoviny, thiomočoviny a C_7BzO detergentu. K rozrušení S-S můstků se používá jako redukční činidlo například tributylfosfin. Následná alkylace SH skupin jodacetamidem vede k tvorbě karbamidomethyl-cysteinu, který znemožňuje opětovnou tvorbu S-S můstků.

Kromě samotného tryptického štěpení může docházet i k tvorbě semitryptických nebo nespecifických peptidových fragmentů [66]. Semitryptické fragmenty jsou charakteristické tím, že jedno z míst štěpení je tryptické, druhé ale může být za jakoukoliv aminokyselinou. Například minoritní chymotryptická nebo chymotrypsinu podobná aktivita vede k nespecifickému štěpení peptidové vazby na karboxylovém konci fenylalaninu, tyrosinu nebo leucinu [72]. Chymotryptická nebo tomu podobná aktivita může být důsledkem kontaminace trypsinu chymotrypsinem (v závislosti na dodavateli trypsinu) nebo důsledkem přítomnosti pseudotrypsinu (ψ-trypsin), který je produktem autolýzy trypsinu. V případě, že protein není zcela naštěpen, tzn. dojde k vynechání štěpného místa za lysinem nebo argininem, mluvíme o tzv. „missed cleavage“ fragmentech. Všechny tyto jevy zásadním způsobem komplikují vyhodnocování MS spekter [73].

Tryptické štěpení předcházející LC MS analýze může být provedeno několika způsoby. Nejpoužívanějším způsobem je tzv. štěpení v roztoku [74], pro které existuje velmi dobře popsaný standardizovaný protokol [75]. Tento přístup má nicméně několik nevýhod, jako je například dlouhá doba štěpení (až 24 hodin), autolýza trypsinu (lze zmírnit přídavkem Ca^{2+}), nutnost striktně dodržet teplotu během celého procesu štěpení a vysoká intolerance k organickým rozpouštědlům [76]. Některá z těchto omezení lze překonat imobilizací trypsinu na vhodný nosič, čímž vznikne tzv. imobilizovaný enzymatický reaktor („immobilized enzyme reactor”, IMER) [74]. Mezi hlavní výhody IMER patří především rychlost štěpení (v řádu minut) [77], zvýšená teplotní a pH stabilita a výrazné omezení autolýzy trypsinu [78]. IMER mohou být připravovány ve formě membrán, kapilár, čipů, spin kolonek nebo chromatografických kolon [79,80] a jsou dostupné jak ve vsádkovém tak průtokovém uspořádání. I přes jeho nesporné výhody není IMER uspořádání rutinně příliš využíváno, a to především z důvodu vyšší ceny a nedostatku informací pramenícího z časté absence standardizovaného protokolu. Ideálním řešením z hlediska úspory času a jednoduchosti celého procesu je tzv. on-line uspořádání, tedy přímé spojení trypsinového IMER a LC kolony v sérii, které je ale z důvodu nutnosti použít jednu MF pro štěpení i separaci štěpných produktů značně problematické (volba pH,

přítomnost organického rozpouštědla v MF) [81]. Častým kompromisem je tak například použití chromatografických trypsinových kolon v kombinaci s přepínacím ventilem, sběračem frakcí nebo v 2D uspořádání (tzv. pseudo on-line) [82–84].

Většina proteomických aplikací je prováděna za použití klasických RPLC C18 SF. Vzhledem k povaze peptidů/štěpných produktů proteinů se nabízí i možnost využít MM SF, které při vhodně zvoleném pH MF mohou poskytovat i elektrostatickou interakci, a tím výjimečnou selektivitu [85].

1.5 Analýza terapeutických thiofosfátových oligonukleotidů

Využití terapeutických oligonukleotidů (ON) v genové terapii v posledních letech významně roste [86,87]. V letech 2016-2023 tvořily více než 4 % z celkového počtu nově registrovaných léčiv [88]. Využívají se například k léčbě spinální svalové atrofie (nusinersen) [89] nebo cytomegalovirové infekce sítnice u pacientů s AIDS (fomivirsen) [90]. Terapeutické ON jsou na rozdíl od těch přirozeně se vyskytujících modifikované, aby se zvýšila jejich *in-vivo* odolnost proti endo- a exo-nukleasam a schopnost procházet do buňky [32,91].

Jedním z nejčastějších typů modifikace je tzv. thiofosfátová substituce, kdy dochází k nahrazení atomu kyslíku v jedné nebo více fosfátových skupinách sírou [92] (**Obr. 4**). Tím vzniká thiofosfátová vazba (PS), která do molekuly přináší chirální centrum (*). Důsledkem je vznik 2^y diastereomerů, kde *y* značí počet thiofosfátových substitucí [93]. Protože diastereomery mají různé fyzikálně-chemické vlastnosti, lze je separovat i na běžných C18 kolonách. Tvorba diastereomerů značně komplikuje chromatografickou analýzu PS ON, a to především těch s velkým počtem PS modifikací. Například v případě plně modifikovaného 21mer ON, což je typická délka terapeutických ON, se jedná o 1048576 diastereomerů (20 PS modifikací = 2^{20}). Pro chromatografickou analýzu je tak nutné potlačit separaci diastereomerů s cílem dosáhnout co nejužších píků, které budou umožňovat správné vyhodnocení nejen hlavního píku (například 21meru), ale také typických nečistot ze syntézy jako jsou 5´*n*-1, 5´*n*-2,…5´*n*-*x* mery (tedy ON zkrácené na 5´konci), případně 5´*n*+1 [94,95]. Na 3´nebo 5´konci může navíc docházet i k dalším procesům, jako je například cyklizace (thio)fosfátové skupiny, existence zbytkové (thio)fosfátové skupiny na 3´konci nebo deaminace nukleobáze, které ztěžují separaci a identifikaci nečistot [96,97]. Kromě samotné separace nečistot od hlavního píku současně s potlačením separace diastereomerů je pro analýzu thiofosfátových ON důležitá také

separace a identifikace metabolitů. Metabolity jsou krátké ON (*n-x)*, které vznikají v důsledku metabolismu podaného léčiva, tedy terapeutického ON, v těle pacienta. Jejich separace a identifikace je obvykle vzhledem k velkému počtu možných metabolitů, které jsou si strukturně velmi podobné, značně komplikovaná.

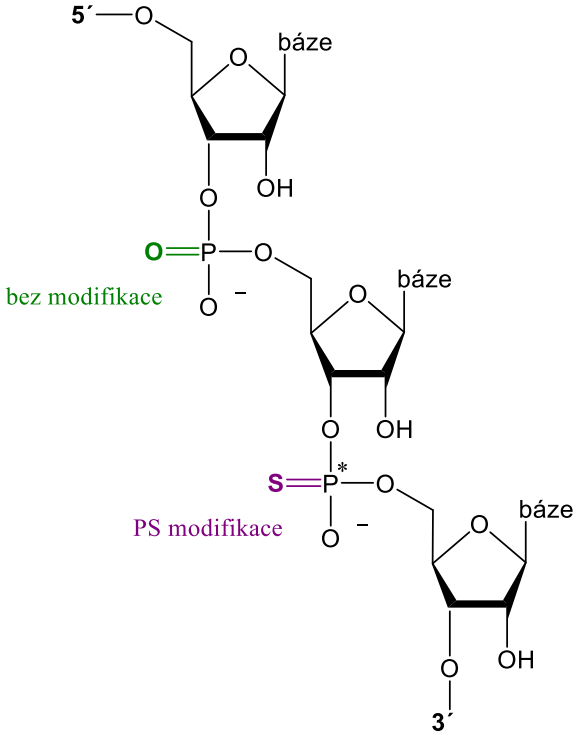

Obr. 4: Struktura RNA oligonukleotidu.

V současné době se pro potlačení separace diastereomerů využívá především dvou přístupů, a to IPRPLC nebo HILIC. V IPRPLC dochází k potlačení separace diastereomerů z důvodu přítomnosti IP činidla (např. alkylamonium acetátu) v MF, které má za následek potlačení hydrofobní interakce mezi ON a SF, která je zodpovědná za separaci diastereomerů. Uplatnění pouze elektrostatické interakce mezi nabitými skupinami ON a nabitou částí IP činidla nedokáže jednotlivé diastereomery zcela rozlišit [98,99]. Míra potlačení separace diastereomerů je samozřejmě závislá na několika faktorech, a to především na hydrofobicitě a koncentraci IP činidla, které ovlivňují míru pokrytí nepolární SF IP činidlem. Významnou roli hraje i teplota, která má vliv na tvorbu sekundárních struktur. Výhodou IPRPLC je jednoznačně vysoká selektivita, dobrá opakovatelnost a možnost výběru mnoha typů MF. Mezi nevýhody patří kontaminace instrumentace, a to především MS detektoru, hydrofobními IP činidly. Tomu se lze částečně vyvarovat použitím hexafluorisopropanolu (HFIP) v MF místo kyseliny octové. HFIP podporuje sorpci IP činidel na povrch stacionární fáze, a tím umožňuje použít méně hydrofobní

a méně koncentrovaná IP činidla za dosažení stejných výsledků [100–102]. HFIP navíc z důvodu své těkavosti nepotlačuje ionizaci ON a poskytuje tak dostatečný MS signál [103,104].

Druhou možností je využít HILIC SF, které ze své podstaty téměř neposkytují hydrofobní interakce a tedy ve většině případů za vhodných podmínek ani separaci diastereomerů [105,106]. Výhodou jsou MF bez IP činidel kontaminujících LC MS instrumentaci [107]. Nevýhodou je nutnost dlouhé ekvilibrace systému (především při gradientové eluci), často nedostatečný MS signál a omezené možnosti výběru podmínek při optimalizaci metod [108].

Analýza terapeutických ON je klíčová jak v průběhu jejich syntézy při kontrole čistoty, tak i následně při studiu jejich metabolismu v těle pacientů.

2 Cíle práce

Hlavním cílem práce byla podrobná charakterizace SF poskytujících více interakčních mechanismů a jejich následné využití pro analýzu biologicky aktivních sloučenin jako jsou proteiny nebo terapeutické ON. Dílčí cíle zahrnují:

I. Detailní charakterizaci SF z hlediska jejich interakčního potenciálu za využití jednoduchých chromatografických testů (např. Waltersův test) i komplexnějšího přístupu metodou LFER. Zvláštní důraz byl kladen na charakterizaci elektrostatických interakcí. Testovány byly kolony s různými ligandy, různými nosiči (různými typy částic), kolony prodávané pod označením RP i MM.

II. Zjištění aplikačního potenciálu MMC pro analýzu peptidů a proteinů (cytochromu C) a porovnání s klasickou RPLC. Vývoj rychlé a spolehlivé metody/uspořádání pro on-line štěpení proteinů – sériové zapojení trypsinové a MM chromatografické kolony umožňující štěpení a separaci štěpných produktů v rámci jedné analýzy za použití jedné MF kompatibilní s MS detekcí.

III. Podrobný popis vlivu různých chromatografických podmínek na retenci a analýzu terapeutických thiofosfátových ON v IPRPLC a HILIC. Testování vlivu hydrofobicity a koncentrace IP činidla, separační teploty a povahy protiiontu (kyselina octová *vs.* HFIP) na potlačení separace diastereomerů a rozlišení ON s různou délkou (především *n* a 5´*n*-1) v IPRPLC. Podrobný popis retenčního chování terapeutických ON a jejich možných metabolitů v HILIC. Aplikace zjištěných poznatků na analýzu metabolitů PS ON obsažených ve vzorcích plasmy pacientů léčených proti spinální svalové atrofii.

3 Parametry chromatografického systému

K popisu a vyhodnocení naměřených dat je používáno několik základních chromatografických parametrů. Parametry využité k charakterizaci separačního systému v rámci této disertační práce byly vypočteny softwarem Empower 3 podle následujících vztahů.

Retenční faktor (*k*) udává, kolikrát delší dobu stráví analyt interakcí se SF než v MF. Zavedení retenčního faktoru místo pouhého retenčního času je velmi výhodné především z hlediska možnosti porovnat různé separační systémy z různými mrtvými objemy/časy. Pro retenční faktor platí

$$k = \frac{t_R - t_M}{t_M} \tag{3.1}$$

kde t_R [min] je retenční čas daného analytu a t_M [min] mrtvý čas kolony, tj. eluční čas analytu, který neinteraguje se stacionární fází.

Rozlišení (R_s) charakterizuje míru separace dvou sousedních analytů/píků. Pokud je rozlišení R_s > 1,5, mluvíme o tzv. separaci na základní linii. Pro rozlišení platí

$$R_s = \frac{1{,}18\,(t_{R,2} - t_{R,1})}{w_{2;50\%} + w_{1;50\%}} \tag{3.2}$$

kde $t_{R,1}$ [min] a $t_{R,2}$ [min] jsou retenční časy dříve, respektive později eluujícího analytu, $w_{1;50\%}$a $w_{2;50\%}$ jsou šířky daného píku v 50 % jeho výšky.

Selektivita (α) udává poměr retencí dvou analytů. Pro selektivitu platí

$$\alpha = \frac{k_1}{k_2} \tag{3.3}$$

kde k_1 a k_2 jsou retenční faktory jednotlivých analytů.

Faktor symetrie (A_s) slouží k posouzení a porovnání tvaru píku (symetrie). Pokud je A_s > 1, píky mají tendenci chvostovat (tzv. tailing), naopak pokud je A_s <1, píky mají tendenci frontovat. Pro faktor symetrie platí

$$A_s = \frac{w_{5\%}}{2\,f_p} \tag{3.4}$$

kde $w_{5\%}$ je šířka píku v 5 % jeho výšky a f_p je šířka vzestupné části píku v 5 % jeho výšky.

4 Výsledky a diskuse

4.1 Podrobná charakterizace interakčního potenciálu vybraných stacionárních fází (Publikace I, Publikace II, Publikace III)

Vlastnosti SF, a tím i jejich interakční potenciál, jsou ovlivněny nejen samotným ligandem navázaným na povrchu nosiče (silikagelu) a endkapingem, ale také typem částic nosiče. V rámci námi testovaných SF od firmy Waters (jejich přehled je uveden v **Tabulce 3** na konci této podkapitoly, str. 38-39) se můžeme setkat se třemi základními typy částic, a to „bridged ethylene hybrid“ (BEH), „high strength silica“ (HSS) a „charged surface hybrid“ (CSH). BEH částice mají v silikagelovém nosiči vmezeřeny ethylenové můstky, které mají za následek zvýšenou chemickou i mechanickou odolnost a umožňují tak použití v širokém rozsahu teplot, tlaků i pH. Ethylenové můstky navíc snižují kyselost okolních silanolových skupin a potlačují tak rozmývání píků bazických analytů [109]. HSS částice poskytují vyšší retenci všech analytů z důvodu většího povrchu (velikost pórů 100 Å) v porovnání s BEH i CSH částicemi (velikost pórů 130 Å). Navíc mohou ve vyšší míře poskytovat iontově-výměnnou interakci skrz silanolové skupiny, což má za následek zvýšenou retenci bazických analytů. CSH částice naopak z důvodu přítomnosti kladného náboje v pH < 7 poskytují zvýšenou retenci kyselých analytů.

Pro základní porovnání vybraných kolon byl využit Waltersův test (**Obr. 5**). Silanolová aktivita (*SI*) závisí na počtu volných silanolových skupin na povrchu nosiče a s jejich rostoucím počtem stoupá i hodnota SI. Hodnota HI pak stoupá s rostoucí hydrofobicitou SF. Na **Obr. 5** je na první pohled patrné rozdělení na endkapované (nízká silanolová aktivita, světlé barvy) a neendkapované (vyšší silanolová aktivita, tmavé barvy) kolony. Modře označené kolony vykazující vyšší hydrofobicitu obsahují C18 ligandy, zeleně označené s nižší hydrofobicitou obsahují ligandy s aromatickým jádrem vázaným na kratších (propyl nebo hexyl) alkylových řetězcích. Nejvyšší hydrofobicitu vykazuje kolona s mix-mód charakterem Premier BEH C18 AX, naopak nejnižší neendkapovaná kolona XSelect HSS C18 SB, jejíž volné silanolové skupiny zvyšují polaritu SF. Porovnání dvou neendkapovaných kolon se stejným ligandem (pentafluorfenyl – označení PFP nebo FP), ale různým typem částic (XSelect HSS PFP a XSelect CSH FP) potvrzuje, že HSS částice mají větší množství volných silanolových skupin (a tedy i vyšší hodnotu SI) v porovnání s jinými typy částic.

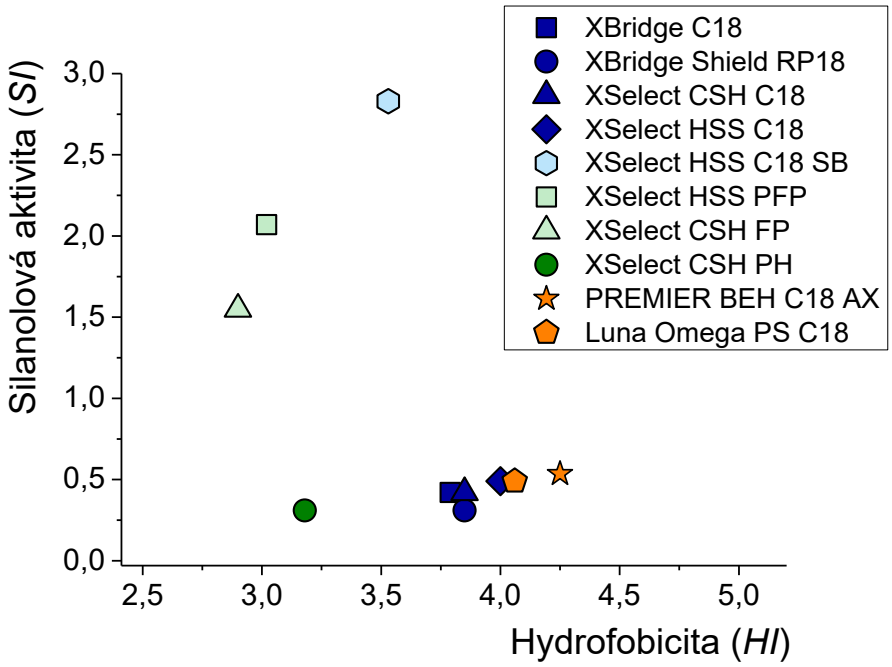

Obr. 5: Výsledky Waltersova testu pro vybrané kolony. Světlé barvy: neendkapované kolony; tmavé barvy: endkapované kolony; modrá barva: kolony s C18 ligandy; zelená barva: kolony s aromatickými ligandy, oranžová barva: mix-mód kolony. Podmínky Waltersova testu jsou uvedeny v **Tabulce 1** na str. 20. Převzato z Publikace I a Publikace IV.

Výsledky Waltersova testu velmi dobře korelují s výsledky získanými z LFER modelu (podle rovnice 1.1). LFER studie byla provedena ve třech typech MF, a to konkrétně ACN/365mM kyselina mravenčí, pH 2,1 40/60 (*v/v*), ACN/10mM octan amonný, pH 4,7 40/60 (*v/v*) a ACN/10mM octan amonný, pH 8,0 40/60 (*v/v*), aby bylo možné sledovat vliv pH vodné složky MF na jednotlivé typy interakcí. Pro všechny systémy odpovídaly dominantní interakce (nejvyšší absolutní hodnoty) koeficientům *v* (hydrofobicita, nejvyšší kladné hodnoty, tedy interakce preferovaná mezi analytem a SF) a *b* (proton-akceptorová schopnost tvořit vodíkové vazby, nejnižší záporné hodnoty, tedy interakce preferovaná mezi analytem a MF), což je typické pro RPLC [110]. Hodnoty všech regresních koeficientů pro všechny testované chromatografické systémy jsou přiloženy v Tabulce S1, S2 a S3 v Doplňkových datech, str. 72-74. Nejvyšší hydrofobicitu (nejvyšší hodnota koeficientu *v*) vykazovaly kolony XSelect HSS C18 a XSelect CSH C18, nejnižší pak kolona XSelect CSH FP, což přesně odpovídá výsledkům Waltersova testu (mix-mód kolona Premier BEH C18 AX nebyla v LFER testu zahrnuta). Při porovnání kolon s C18 ligandem z hlediska proton-akceptorové schopnosti tvořit vodíkové vazby byl

nejnižší rozdíl mezi SF a MF (tedy nejnižší absolutní hodnota koeficientu *b*) nalezen pro kolonu XSelect HSS C18 SB. To koreluje s její nejvyšší silanolovou aktivitou získanou z výsledků Waltersova testu. Při zvýšení pH vodné složky MF z 2,1 na 4,7 dochází ke zvýšení hodnot regresních koeficientů *v* pro všechny kolony. Navíc se začne uplatňovat elektrostatická interakce mezi kladně nabitými analyty a záporně nabitými disociovanými volnými silanoly na neendkapovaných SF (XSelect CSH FP, XSelect HSS C18 SB a XSelect HSS PFP), což se projevuje kladnými hodnotami regresního koeficientu d^+. Další zvýšení pH vodné složky MF na 8,0 způsobuje pokles v příspěvku hydrofobicity k retenci (nižší hodnoty koeficientu *v*). Vzhledem k tomu, že většina bazických analytů není již v pH 8,0 kladně nabitá, efekt volných silanolů popisovaný pomocí koeficientu d^+ není pro toto pH vypovídající.

Ačkoliv využití rozšířené regresní rovnice (rovnice 1.1) zahrnující i elektrostatické interakce poskytovalo vyšší hodnoty koeficientu determinace (R^2), vypovídající popis uplatnění elektrostatických interakcí pro různá pH vodné složky MF bylo možné získat jen částečně, a to především z důvodu obtížnosti najít větší množství strukturně odlišných permanentně nabitých analytů v celém rozsahu testovaných pH vhodných pro UV detekci. Z toho důvodu bylo nezbytné hledat další způsoby popisu elektrostatických interakcí.

Jednou z možností, jak získat základní přehled o uplatnění elektrostatických interakcí je analýza permanentně (nebo alespoň v celém měřeném rozsahu pH) kladně a záporně nabitých analytů v různých pH vodných složek MF. Čím více hodnot pH zvolíme, tím detailnější informaci získáme. Vzhledem k tomu, že jedním z cílů byl detailní popis chování CSH částic (tzn. zjistit, kdy jsou tyto částice kladně nabité a přispívají tím k retenci záporně nabitých analytů), byly zvoleny pH vodné složky MF s malými rozestupy v kyselé oblasti (pH 2,1; 2,5; 2,8; 3,5; 4,7). **Obr. 6** ukazuje trendy v retenci benzensulfonové kyseliny a trimethyfenylamonného kationtu ($TMFA^+$) v závislosti na pH vodné složky MF pro jednotlivé kolony. Výsledky potvrzují výskyt kladného náboje na povrchu CSH částic v pH 2,1, kde je retence záporně nabité benzensulfonové kyseliny značně vyšší v porovnání s kolonami s jinými typy částic (**Obr. 6A**). Retence benzensulfonové kyseliny s rostoucím pH postupně klesá, což indikuje ztrátu kladného náboje CSH částic s rostoucím pH MF. Na základě získaných dat lze usuzovat, že míra uplatnění kladného náboje na povrchu CSH částic klesá v následující řadě: XSelect CSH FP > XSelect CSH PH > XSelect CSH C18. Retence $TMFA^+$ v závislosti na pH ukazuje významné rozdíly mezi endkapovanými a neendkapovanými kolonami. Pro

neendkapované kolony pozorujeme významné zvýšení retence již při pH 4,7, ale především pak při pH 8,0, které je důsledkem elektrostatické interakce mezi $TMFA^+$ a volnými disociovanými silanoly. Tento efekt je ještě výraznější pro SF s HSS částicemi v porovnání s CSH částicemi (**Obr. 6B**). Stejných trendů bylo dosaženo i pro jiné nabité analyty, jako je například toluensulfonová kyselina nebo propranolol.

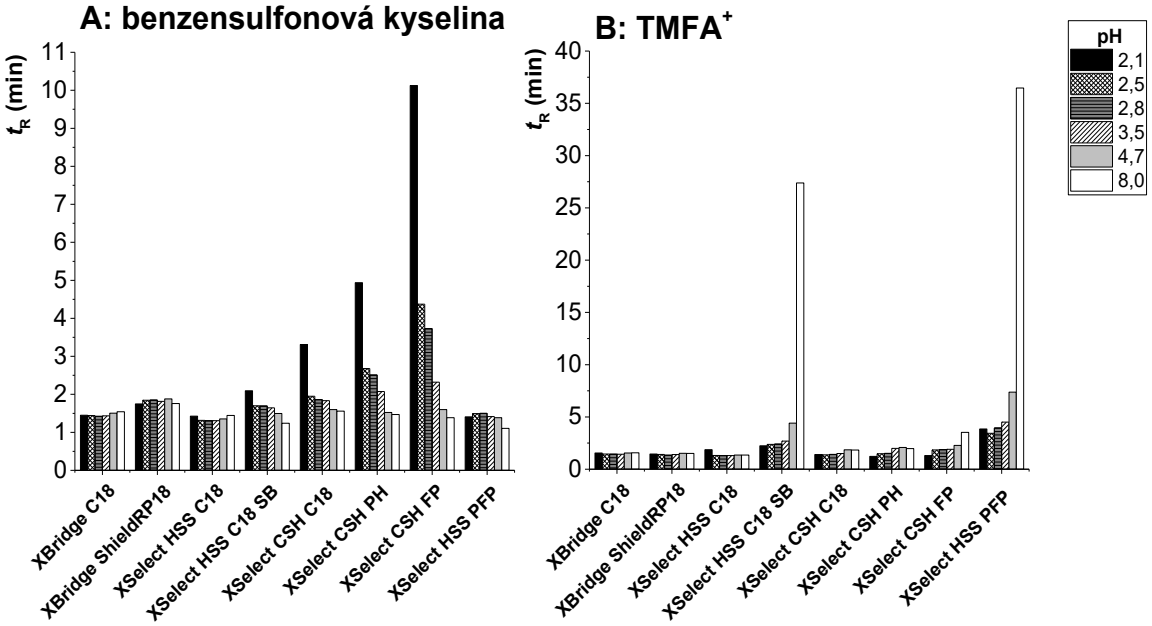

Obr. 6: Vliv pH na retenci permanentně nabitých analytů. A: benzensulfonová kyselina; B: $TMFA^+$. Složení MF: ACN/vodná složka, 40/60 (*v/v*). Vodné složky MF: 365mM kyselina mravenčí, pH 2,1; 10mM mravenčan amonný, pH 2,5; 10mM mravenčan amonný, pH 2,8; 10mM octan amonný, pH 3,5; 10mM octan amonný, pH 4,7 a 10mM octan amonný, pH 8,0. Převzato z Publikace I.

Pro detailnější popis elektrostatických interakcí byla vyvinuta a otestována nová metoda využívající pouze vodné MF (dichloroctová kyselina s vodným roztokem amoniaku) v rozmezí pH 2,5 - 9,0, které mají konstantní iontovou sílu, ale velmi nízkou pufrační kapacitu v rozmezí pH 4,5-6,5. Přítomnost organického rozpouštědla v MF ovlivňuje nejen pH MF, ale i pK_a analytů a funkčních skupin na povrchu SF, což může negativně ovlivnit interpretaci výsledků. Jako analyty, tedy sloučeniny s permanentním nábojem, byly vybrány dusičnany, jodidy, benzensulfonová kyselina a $TMFA^+$. Charakterizace elektrostatických interakcí analýzou anorganických aniontů je velmi výhodná především z důvodu absence hydrofobní interakce. Ze stejného důvody byly původně za účelem popisu kationtově-výměnného charakteru využity anorganické kationty Ag^+ a Cu^{2+}. Jejich analýza je při použití UV detektoru komplikovaná a výsledky nebylo

možné jednoznačně interpretovat. Celkem bylo charakterizováno jedenáct stacionárních fází, získané výsledky jsou shrnuty na **Obr. 7**. Pro neutrální SF (**Obr. 7A, B, C**) retence permanentně nabitých analytů nezávisí na pH mobilní fáze, pokud jsou tyto SF endkapované (plné znaky). Pro neendkapované SF (prázdné znaky) retence záporně nabitých analytů s rostoucím pH klesá, zatímco retence kladně nabitých analytů s pH roste. Interakce s disociovanými volnými silanoly způsobující tyto trendy se začíná výrazně uplatňovat již v pH ~ 4. Polární SF Torus DIOL (používaná v HILIC nebo SFC) vykazuje podobné trendy jako neendkapované SF, což naznačuje větší množství residuálních silanolů nebo jejich nedostatečné stínění diolovými ligandy.

Pro SF s CSH částicemi (**Obr. 7D, E, F**) můžeme vidět pokles retence záporně nabitých analytů a nárůst retence $TMFA^+$ s rostoucím pH, což indikuje výrazný aniontově-výměnný charakter v pH < 6, který poskytuje kladně nabitá pyridylová skupina na povrchu těchto částic. Pro endkapované SF zůstává retence v pH > 6 konstantní (typické RP chování), zatímco pro neendkapovanou kolonu (prázdné znaky) dochází k dalšímu poklesu retence pro záporně nabité analyty a prudkému zvýšení retence pro kladně nabité analyty. Výsledky také potvrzují již výše zmíněné, a to že aniontově výměnný charakter klesá v řadě XSelect CSH FP > XSelect CSH PH > XSelect CSH C18. Vzhledem k uniformitě CSH částic (a tedy i konstantnímu zastoupení nabitých skupin na jejich povrchu) se jedná pravděpodobně o důsledek různého stínění povrchu částic kvůli přítomnosti ligandů, a to v závislosti na délce jejich alkylového řetězce. Nejvíce stíněný je povrch SF obsahující C18 ligandy, nejméně pak povrch SF, která má aromatické jádro vázané pomocí propylového linkeru.

Mix-mód kolona Premier BEH C18 AX (**Obr. 7G, H, I**) vykazuje aniontově-výměnný charakter v širším rozsahu pH v porovnání s CSH kolonami (pK_a alkylaminu ~ 8-9; pK_a pyridylu ~ 5-6) [111]. V pH ~ 8 dochází k poklesu retence záporně nabitých analytů a zvýšení retence $TMFA^+$, což je důsledkem nejen ztráty aniontově-výměnného charakteru, ale i rostoucího uplatnění elektrostatické interakce s residuálními silanoly. Velmi podobné trendy byly pozorovány i pro SF Torus DEA s čistě aniontově-výměnným charakterem (pK_a diethylaminu ~10,6, bez přítomnosti C18 ligandu, **Obr. 7J, K, L**), kde pravděpodobně opět dochází k uplatnění interakce s residuálními silanoly.

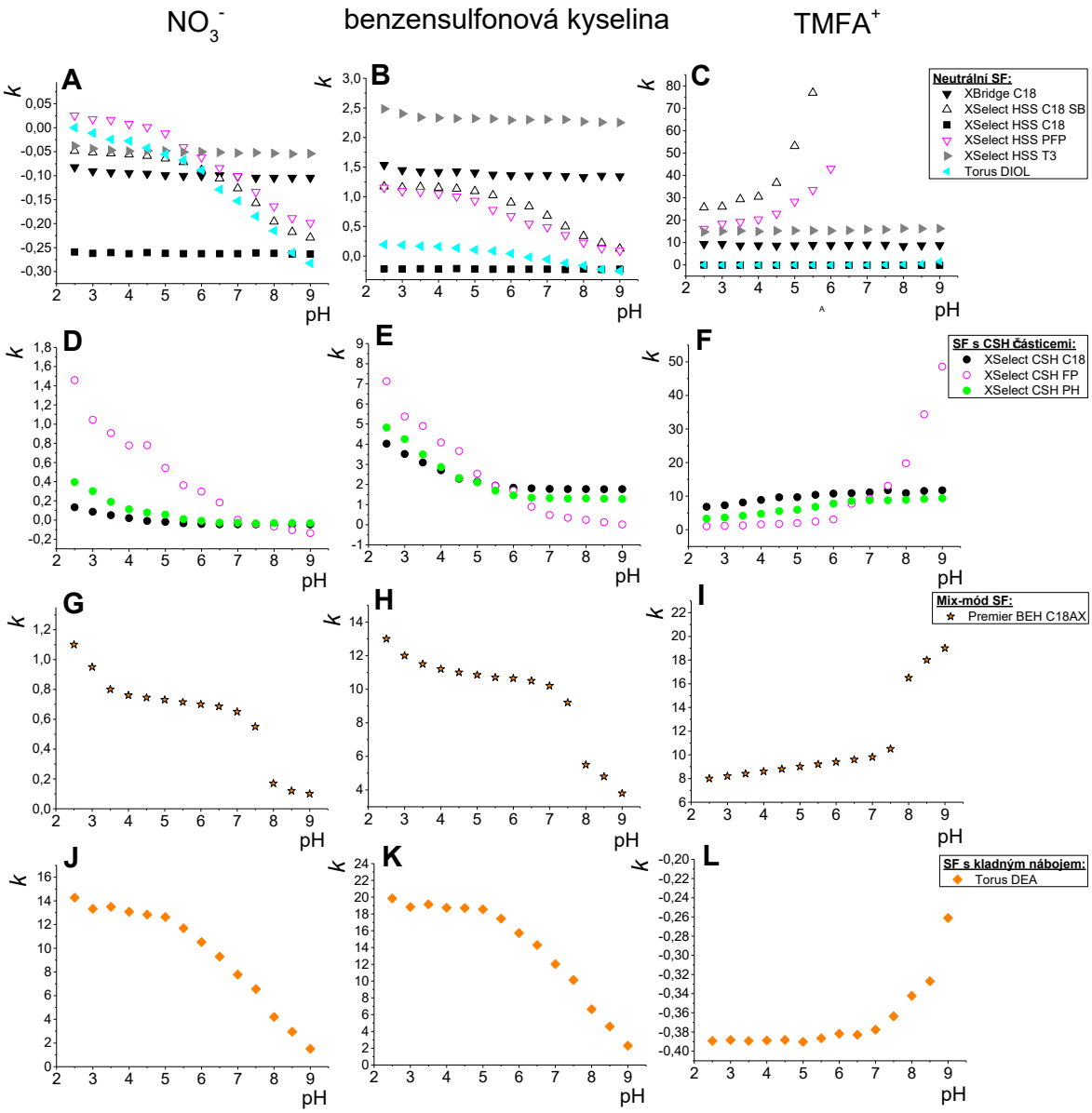

Obr. 7: Závislost retence nabitých analytů (dusičnany: A, D, G, J; benzensulfonová kyselina: B, E, H, K; $TMFA^+$: C, F, I, L) na pH MF pro různé typy SF (černé/šedé znaky: C18 ligandy; fialové znaky: fluorfenyl ligandy, zelené znaky: fenyl-hexyl ligandy; modré znaky: diolové ligandy; oranžové znaky: ligandy s aniontově-výměnným charakterem). Plné znaky značí endkapované SF, prázdné znaky neendkapované. Složení MF: 10mM dichloroctová kyselina s přídavkem vodného roztoku amoniaku k dosažení pH 2,5 – 9,0 (po 0,5 krocích). Převzato z Publikace II.

Klíčová role residuálních silanolů na endkapované mix-mód koloně Premier BEH C18 AX, která v důsledku vede k zwitterionickému charakteru této SF, byla dále podrobně zkoumána v publikaci [112], kde byl zároveň popsán i vliv přídavku acetonitrilu do MF na uplatnění těchto elektrostatických interakcí.

I přes detailní charakterizaci interakčního potenciálu jednotlivých SF je pro získání přehledu o jejich aplikačním potenciálu výhodné provést retenční analýzu různých skupin sloučenin (kyselých, bazických, neutrálních a zwitterionických) v různých pH vodných složek MF. Závislost retenčního času a symetrie píku na pH vodné složky MF pro jednotlivé zástupce z uvedených skupin (kyselé – ibuprofen, bazické – derivát kathinonu 1-(4-chlor-fenyl)-2-pyrrolidin-1-yl-pentan-1-on (4-CPRC), neutrální – β-naftoflavon, zwitterionické – dipeptid H-Tyr-Phe-OH) pro osm testovaných kolon je ukázána na **Obr. 8**. Pro neutrální sloučeniny (**Obr. 8A**) se dle očekávání retence ani symetrie píku příliš nemění se změnou pH vodné složky MF. Hodnota faktoru symetrie A_s je pro všechny testované podmínky blízká jedné, což indikuje velmi symetrické píky. Nejvyšší retence byla pozorována pro kolonu XSelect HSS C18, což koreluje s výsledky Waltersova testu i LFER modelu, kde tato SF vykazovala nejvyšší hydrofobicitu. Na příkladu kyselého analytu (ibuprofen, **Obr. 8B**) je vidět výrazný pokles retence s rostoucím pH, který je způsobem disociací karboxylové skupiny ibuprofenu (pK_a = 4,85), což vede ke zvýšení polarity. Při pH 8,0 dochází z důvodu negativního náboje analytu také ke zhoršení symetrie píků (hodnoty A_s ~ 0,6; „frontování“ píků) a celkově lze předpokládat, že bazické pH vodné složky MF není vhodné pro analýzu kyselých sloučenin. Retence ibuprofenu na jednotlivých kolonách opět velmi dobře koreluje s výsledky Waltersova testu. Bazické sloučeniny (derivát kathinonu, **Obr. 8C**) vykazují trend opačný, tedy zvýšení retence s rostoucím pH vodné složky MF. V kyselém pH jsou kathinony kladně nabité (a tedy polárnější a vykazující nižší retenci), v pH 8,0 jsou pak už jen částečně nabité (pK_a ~ 8,2), ale stále mohou interagovat s volnými silanoly, což jejich retenci výrazně zvyšuje (především na neendkapovaných kolonách, kde jejich retence na kolonách XSelect HSS C18 SB a XSelect HSS PFP přesáhla 60 minut). Vliv typu částic (CSH *vs.* HSS) na retenci bazických analytů je výrazný. Zatímco SF s CSH částicemi neposkytují v pH 2,1 téměř žádnou retenci kathinonů kvůli elektrostatické repulsi, HSS částice potvrdily svou vhodnost pro analýzu bazických sloučenin z důvodu jejich zvýšené retence. Tento efekt je nejvýraznější při porovnání kolon XSelect CSH FP a XSelect HSS PFP, kde druhá zmíněná kolona poskytuje výrazně vyšší retenci. Z hlediska symetrie píků lze shrnout, že v kyselém pH (2,1 a 4,7) mají píky tendenci chvostovat, zatímco v bazickém pH (8,0) „frontovat“. Dipeptidy jsou velmi polární analyty, jejichž retence je obecně v RPLC nízká. I při zvýšení obsahu vodné složky v MF z 60 na 80 obj.% nebylo možné dosáhnout dostatečných retencí v jiném pH než 2,1. Kolony s CSH částicemi opět poskytují nejnižší retence z důvodu

elektrostatické repulse s kladným nábojem analytu, který v tomto pH převažuje.

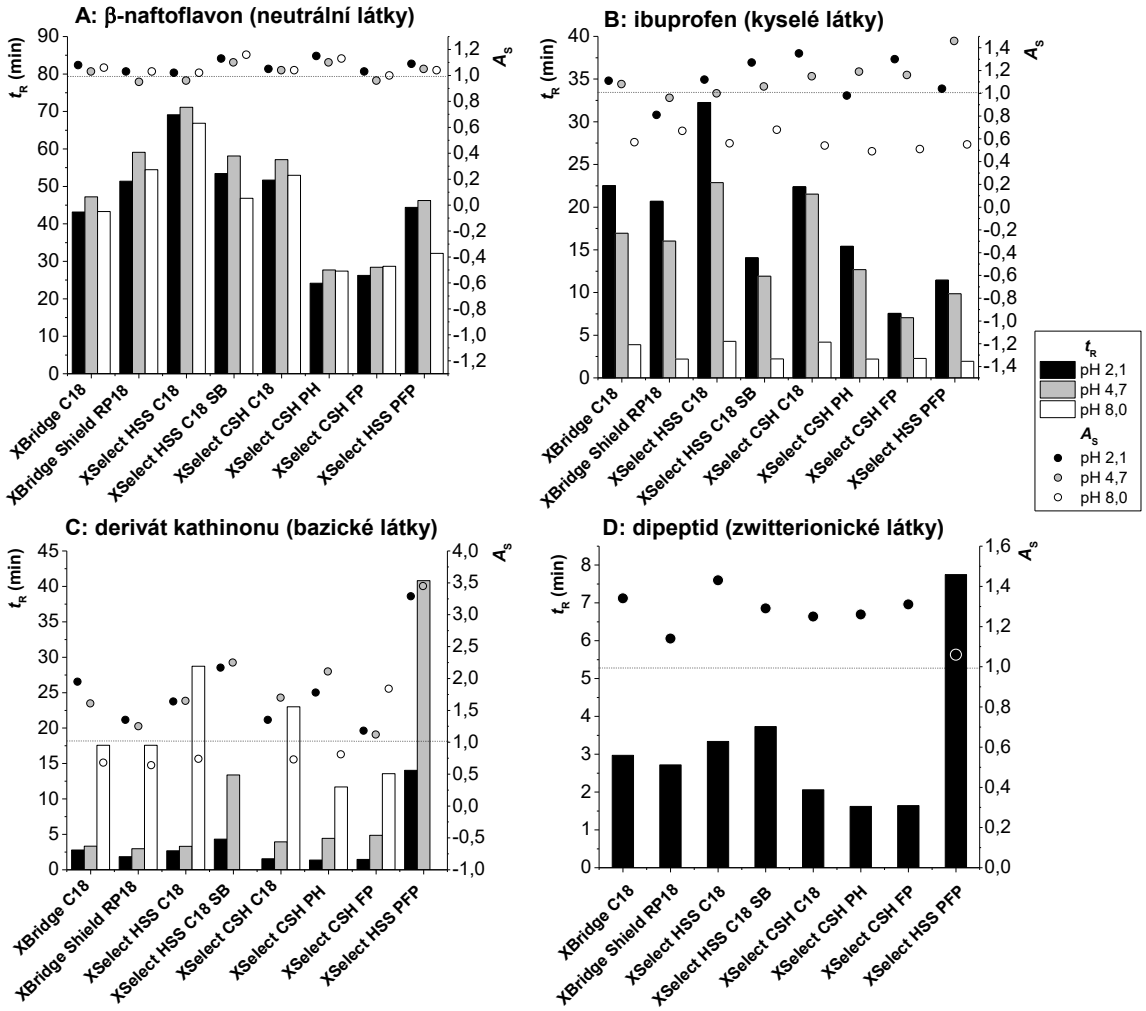

Obr. 8: Trendy v retenci a symetrii píků (A_S) pro jednotlivé zástupce z různých skupin analytů (A: β-naftoflavon, B: ibuprofen, C: derivát kathinonu 4-CPRC, D: H-Tyr-Phe-OH). Složení MF pro A,B,C: ACN/vodná složka, 40/60 (*v/v*); pro D: ACN/vodná složka, 20/80 (*v/v*). Vodné složky MF: 365mM kyselina mravenčí, pH 2,1; 10mM octan amonný, pH 4,7; 10mM octan amonný, pH 8,0. Přerušovaná linka značí ideální symetrii píku (A_S=1). Převzato z Publikace I.

Analýza modelových směsí v rámci výše uvedených skupin názorně ukazuje vynikající aplikační potenciál RPLC kolony XBridge C18 pro kyselé profeny v případě použití kyselé vodné složky MF, a naopak pro bazické deriváty kathinonu v případě použití mírně bazické vodné složky MF. V opačném případě dochází ke koeluci jednotlivých analytů a zhoršení tvaru píků (**Obr. 9**).

Pochopení retenčního/interakčního mechanismu pro jednotlivé stacionární fáze je klíčové pro správný výběr kolony s ohledem na charakter daných analytů. Důsledkem je

úspora času během optimalizace metody (není nutné zkoušet velké množství SF a MF), a tím i úspora rozpouštědel.

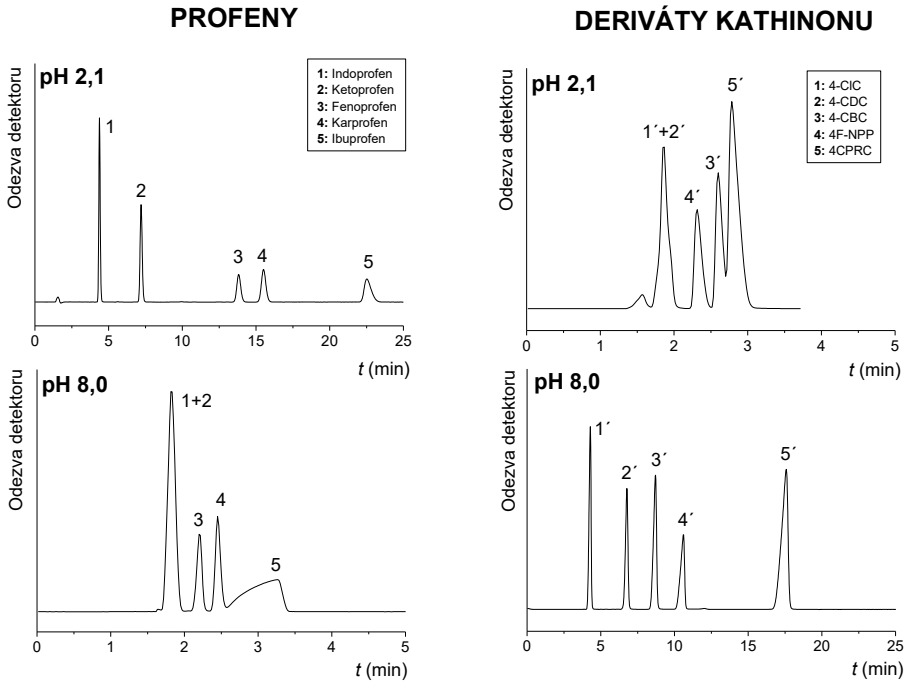

Obr. 9: Separace směsi kyselých profenů a bazických derivátů kathinonu (4-chlor-*N,N*-dimethylkathinon (4-CDC), 1-(4-chlorfenyl)-2-pyrrolidin-1-yl-pentan-1-on (4-CPRC), 4-chlor-*N*-butylkathinon (4-CBC), 1-(4-fluorfenyl)-2-(isopropylamino)pentan-1-on (4F-NPP), 4-chlor-*N*-isopropylkathinon (4-ClC) na koloně XBridge C18. Složení MF: ACN/vodná složka, 40/60 (*v/v*). Vodné složky MF: 365mM kyselina mravenčí, pH 2,1; 10mM octan amonný, pH 8,0. Data převzata z Publikace III.

Tabulka 3: Přehled testovaných stacionárních fází a jejich vlastností. Všechny kolony měly rozměry 150 × 4,6 mm a částice o velikosti 5 µm

Kolona	Struktura	Typ částic	Ligand	„Endkaping“	Skupina nesoucí náboj	Pokrytí ligandem (µmol·m^{-2})	Množství uhlíku v SF (%)	Velikost pórů (Å)	Objem pórů (cm^3·g^{-1})	Povrch (m^2·g^{-1})
XSelect® HSS C18	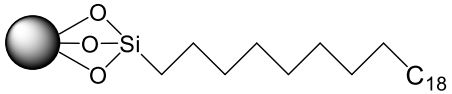	HSS	oktadecyl	ano	žádná	3,2	15	100	0,7	230
XSelect® HSS T3	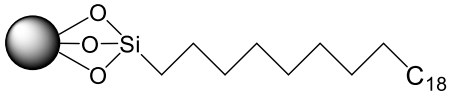	HSS	oktadecyl	ano	žádná	1,6	11	100	0,7	230
XSelect® HSS C18 SB	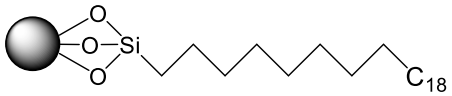	HSS	oktadecyl	ne	žádná	1,6	8	100	0,7	230
XSelect® HSS PFP	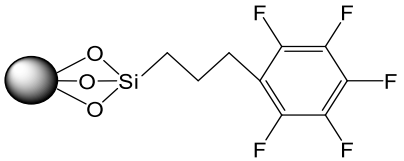	HSS	pentafluorfenyl	ne	žádná	3,2	7	100	0,7	230
XSelect® CSH™ C18	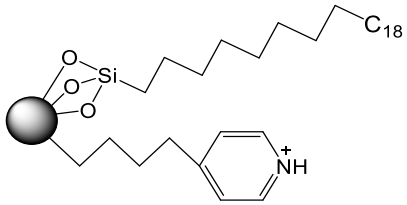	CSH	oktadecyl	ano	pyridyl	2,3	15	130	0,7	185
XSelect® CSH™ PH	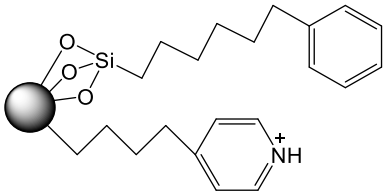	CSH	fenyl-hexyl	ano	pyridyl	2,3	14	130	0,7	185

XSelect® CSH™ FP	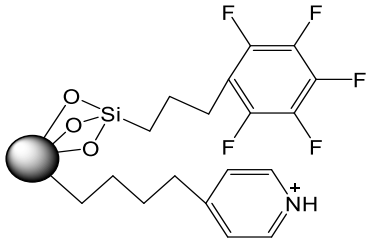	CSH	pentafluorfenyl	ne	pyridyl	2,3	10	130	0,7	185
XBridge® C18	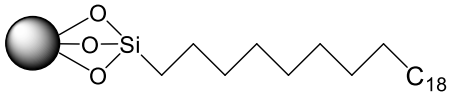	BEH	oktadecyl	ano	žádná	3,1	18	130	0,7	185
XBridge® Shield RP18	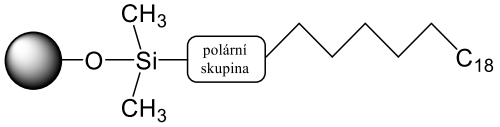	BEH	oktadecyl + karbamát	ano	žádná	3,3	17	130	0,7	185
Premier BEH C18 AX	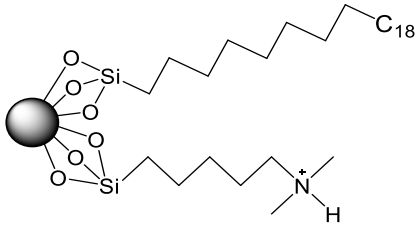	BEH	oktadecyl	ano	alkylamin	1,6	17	95	0,7	270
Torus™ DIOL	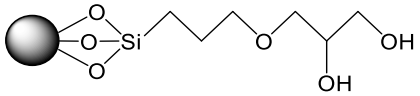	BEH	diol	ano	žádná	-	-	130	0,7	185
Torus™ DEA	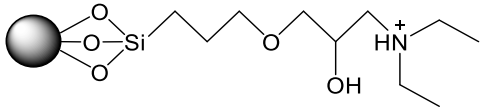	BEH	diethylamin	ano	diethylamin	-	-	130	0,7	185

Typy částic: HSS = high strength silica; CSH = charged surface hybrid; BEH = bridged ethylene hybrid; v případě SF s CSH částicemi není dostupný způsob navázání pyridylu na nosič; (-) nedostupná data

4.2 Mix-mód chromatografie pro analýzu peptidů a proteinů (Publikace IV, Publikace V, Publikace VI)

Peptidy a proteiny jsou relativně polární sloučeniny zwitterionické povahy, které mohou být i několikanásobně nabité. Z toho důvodu je vhodné pro jejich analýzu využít MMC, a to konkrétně SF kombinující RP a IEX charakter. Tyto SF mohou poskytovat odlišnou selektivitu v porovnání s klasickými C18 SF, které jsou pro proteomickou analýzu využívány nejčastěji. Při analýze zwitterionických analytů je důležité znát jejich celkový efektivní náboj (z) v jednotlivých pH a hodnotu isoelektrického bodu (pI). Hodnota z by měla být nulová v případě, že pH je rovno pI a analyt se tak nachází ve zwitterionické formě a chová se jako celek neutrálně. Hodnoty z a pI pro analyzované peptidy jsou uvedeny v **Tabulce 4**. Dipeptidy a enkefaliny neobsahují ve své struktuře žádnou aminokyselinu nesoucí další náboj a jejich celkový náboj tak závisí pouze na hodnotách pK_a karboxylových a amino- skupin na konci sekvence. Tyto peptidy jsou kladně nabité při pH 3,0 (z = 0,80), zwitterionické při pH 4,7 (z = 0,07) a částečně záporně nabité při pH 6,9 (z = -0,17). Leucin-enkefalinamid, který obsahuje amid karboxylové kyseliny a angiotensin II obsahující arginin a histidin (bazické aminokyseliny) ve své sekvenci, jsou kladně nabité v celém testovaném rozsahu pH.

Tabulka 4: Hodnoty isoelektrického bodu (pI) a celkového efektivního náboje (z) pro testované peptidy. Hodnoty byly vypočteny podle [113]. Převzato z publikace IV

	pI	***z* (pH 3,0)**	***z* (pH 4,7)**	***z* (pH 6,9)**
Angiotensin II	7,00	2,70	1,21	0,10
Met^{5}enkefalin	5,60	0,80	0,07	-0,17
Leucin enkefalinamid	8,70	1,00	1,00	0,83
Leucin enkefalin	5,60	0,80	0,07	-0,17
Dipeptidy	5,60	0,80	0,07	-0,17

Pro sloučeniny nacházející se ve zwitterionické formě ($z \sim 0$) je velmi obtížné odhadovat, jakým způsobem budou interagovat s MM SF, tedy zda převáží elektrostatická atrakce nebo repulse. Situace je o to komplikovanější, že z našich předchozích výsledků (Publikace II) vyplývá, že MM SF Premier BEH C18 AX má při vyšších hodnotách pH také zwitterionický charakter. Pro účely zjištění převládajícího typu elektrostatické interakce je vhodné provést analýzu při různých koncentracích pufrů v MF. Vyšší

koncentrace pufru způsobují inhibici elektrostatické interakce z důvodu soutěžení iontů analytu a iontů pufru o interakci se SF. Pokud s rostoucí koncentrací pufru roste i retence analytu, převládá elektrostatická repulse – rostoucí koncentrace pufru inhibuje repulsi mezi analytem a SF a retence analytu roste. Pokud naopak s rostoucí koncentrací pufru retence klesá, v systému převládá elektrostatická atrakce – rostoucí koncentrace pufru inhibuje elektrostatickou atrakci, což způsobuje pokles retence. Tyto efekty jsou znázorněny na příkladu dipeptidu H-Phe-Trp-OH pro tři různé kolony (dvě mix-mód a jednu s CSH částicemi) na **Obr. 10**. V pH 3,0 jednoznačně převládá elektrostatická repulse mezi kladně nabitým dipeptidem a kladně nabitým povrchem SF pro všechny kolony. Nejnižší retence na koloně Atlantis Premier BEH C18 AX (označení Atlantis je pro UHPLC kolony, SF je stejná jako v případě kolony Premier BEH C18 AX) naznačuje největší repulsi, tedy největší přístupnost kladného náboje na povrchu SF. Zvýšení retence na této koloně v pH 4,7 naznačuje vymizení elektrostatické repulse, a naopak uplatnění atrakce (retence s koncentrací klesá), ačkoliv dipeptid by měl mít v tomto pH celkový náboj kolem nuly (z = 0,07). V pH 6,9 je dipeptid částečně záporně nabitý a na jeho retenci na koloně Atlantis Premier BEH C18 AX se podílí elektrostatická atrakce s kladným nábojem na povrchu této SF. Na ostatních dvou kolonách (Luna Omega PS C18 a XSelect CSH C18) opačné trendy ukazují na uplatnění elektrostatické repulse, pravděpodobně s disociovanými residuálními silanoly.

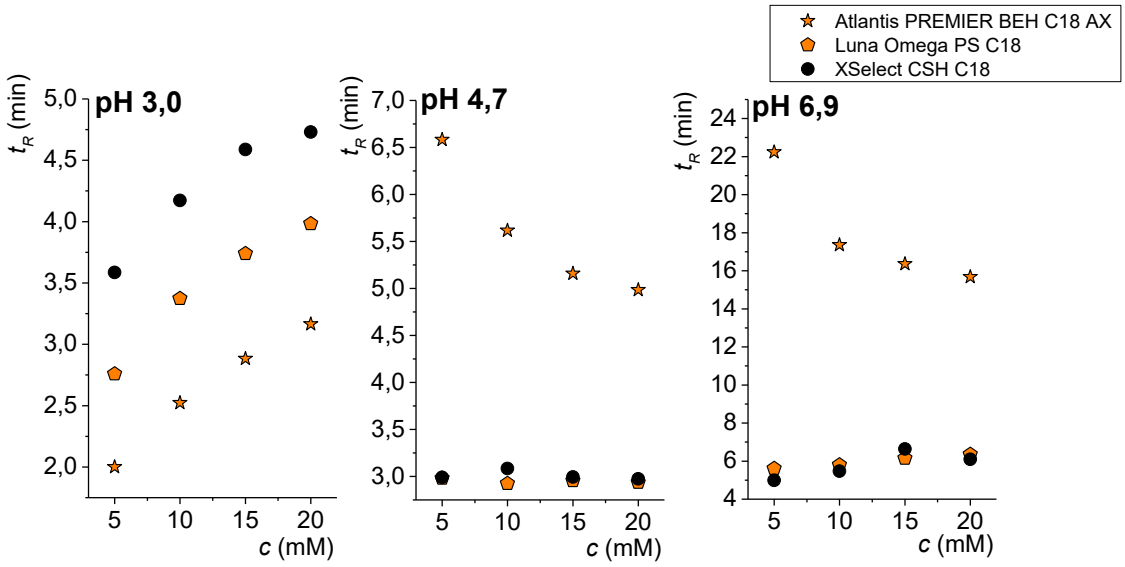

Obr. 10: Vliv koncentrace pufru na retenci dipeptidu H-Phe-Trp-OH pro různá pH vodné složky MF a tři kolony s MM charakterem. Složení MF: ACN/vodná složka, 15/85 (*v/v*). Vodné složky MF: mravenčan amonný, pH 3,0; octan amonný, pH 4,7; octan amonný, pH 6,9. Převzato z Publikace IV.

V MMC koncentrace pufru výrazně ovlivňuje nejen retenci, ale i symetrii píků (symetrie píků je do značné míry spojena s elektrostatickými interakcemi). V pH 3,0 bylo nejlepší symetrie dosaženo pro kolonu Atlantis Premier BEH C18 AX při 5mM koncentraci pufru. S rostoucí koncentrací se symetrie výrazně zhoršovala. Pro ostatní dvě kolony byly pozorovány značně chvostující píky (hodnoty A_s v rozmezí 4,5-9,5). V pH 4,7 byly trendy zcela opačné, tzn. mírně „frontující“ píky (hodnoty $A_s \sim 0{,}9$) pro kolony Luna Omega PS C18 a XSelect CSH C18 a zlepšující se symetrie s rostoucí koncentrací pro kolonu Atlantis Premier BEH C18 AX. MF s vodnou složkou o pH 6,9 poskytovala ve všech případech velmi široké píky, které nebylo možné správně vyhodnotit.

Na základě výše zmíněných poznatků lze vybrat podmínky vhodné pro analýzu peptidů. Po optimalizaci bylo dosaženo nejlepších výsledků (nejkratší čas analýzy, dobrá symetrie píků, rozlišení na základní linii) pro separaci 14 peptidů na koloně Atlantis Premier BEH C18 AX (**Obr. 11**).

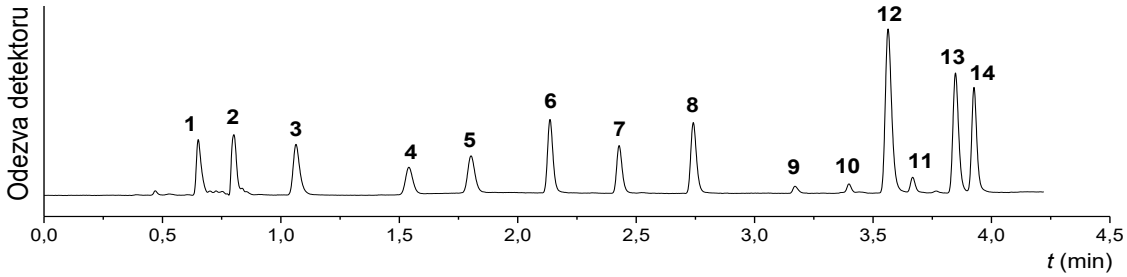

Obr. 11: Separace směsi 14 peptidů. Gradientová eluce: 0min=5% ACN; 1,5min=15% ACN; 3min=25% ACN; 6min=35% ACN. Vodná složka MF: 5mM mravenčan amonný, pH 3,0. Analyty: 1: H-Tyr-Ala-OH; 2: H-Ala-Tyr-OH; 3: H-Phe-Ala-OH; 4: H-Ala-Phe-OH; 5: H-Trp-Ala-OH; 6: H-Ala-Trp-OH; 7: H-Phe-Tyr-OH; 8: H-Tyr-Phe-OH; 9: Angiotensin II; 10: Leucin enkefalinamid; 11: H-Phe-Trp-OH; 12: Met^{5}enkefalin; 13: H-Trp-Phe-OH; 14: Leucin enkefalin. Převzato z publikace IV.

Obecně lze říct, že MM SF potvrdily svůj velký potenciál v proteomické analýze. Z toho důvodu jsme tento projekt rozšířili o další modelové peptidy (celkem 21 peptidů) s cílem určit a porovnat výsledky analýzy z hlediska separace a tvaru píků pro kyselé pH (pH 2,7; typické pH pro separaci peptidů) a bazické pH (pH 8,0; pH potřebné ke štěpení proteinů trypsinem). Pro tento projekt byly vybrány čtyři stacionární fáze – dvě MM (Atlantis Premier BEH C18 AX a Luna Omega PS C18), jedna RP s MM charakterem (XSelect CSH C18) a jedna RP (XBridge C18). Výsledky ukázaly, že pro většinu peptidů bylo dosaženo lepší symetrie a větší retence v MF o pH 8,0, což naznačuje slibné výsledky v oblasti on-line štěpení proteinů.

V další fázi projektu byl vybrán modelový protein cytochrom C, který je již velmi dobře prostudovaný z hlediska jeho štěpných fragmentů. Navíc je na trhu dostupný standard trypsinem naštěpeného cytochromu C, což nám umožnilo srovnat výsledky analýzy naštěpeného standardu, štěpení pomocí tzv. trypsinových „spin kolonek" a na závěr i námi vyvinuté metody/uspořádání pro on-line štěpení proteinů (viz dále, **Obr. 17**). Trypsinové „spin kolonky" byly vyvinuty jako alternativa ke štěpení v roztoku. Z důvodu imobilizace trypsinu na silikagelový nosič ve vysoké koncentraci je štěpení rychlé (15 minut samotné štěpení, cca 1 hodina včetně denaturace proteinu a promývání kolonek), není nutné kontrolovat teplotu a téměř nedochází k autolýze trypsinu. **Obr. 12** ukazuje porovnání analýzy standardu naštěpeného cytochromu C (**Obr. 12 A**) a cytochromu C naštěpeného za použití „spin kolonky" (**Obr. 12 B**). Největšími rozdíly jsou: a) chybějící chymotryptický fragment T19C při použití „spin kolonky", b) velké množství neznámých nečistot ve standardu naštěpeného cytochromu C. Obě zjištění potvrzují, že trypsinové „spin kolonky" jsou vysoce specifické a neposkytují téměř žádné chymotryptické, „miscleavage" nebo autolytické fragmenty. Naopak standard cytochromu C byl pravděpodobně získán štěpením v roztoku, pro které je přítomnost těchto fragmentů typická, a to především při delším čase štěpení. Pokud výsledky porovnáme s on-line štěpením (data v Publikaci VI), lze jednoznačně shrnout, že on-line štěpení poskytuje největší množství chymotryptických i „miscleavage" fragmentů, zároveň ale nepřicházíme o žádné tryptické fragmenty (v některých případech je dokonce při on-line štěpení možné identifikovat více tryptických fragmentů než při použití „spin kolonek").

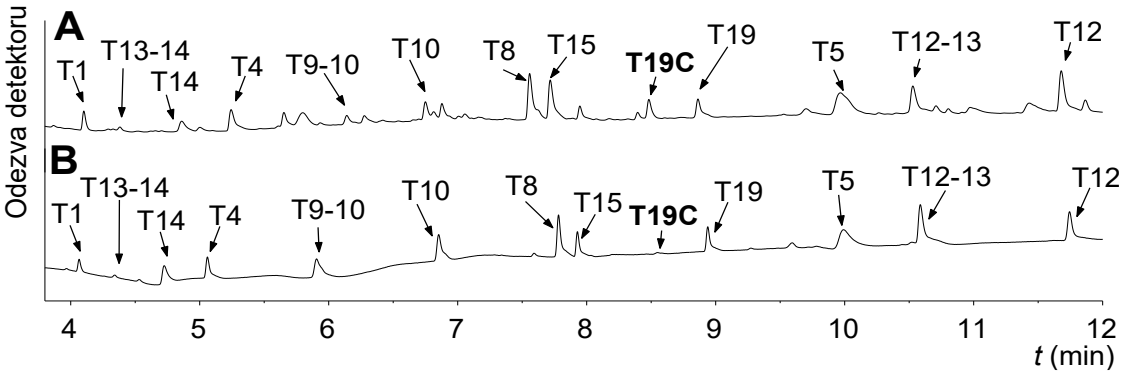

Obr. 12: Porovnání analýzy standardu naštěpeného cytochromu C (A) a cytochromu C naštěpeného za použití „spin kolonky" (B). Gradientová eluce: 0min=0% MF A; 8min=25% MF A; 10,5min=30% MF A; 12min=40% MF A. Složení MF: MF A: 0,1% kyselina mravenčí v ACN, MF B: 0,1% kyselina mravenčí ve vodě. Teplota kolony: 37 °C, UV detekce: 214 nm. Kolona: Luna Omega PS C18. Identifikaci jednotlivých fragmentů lze najít v Tabulce S4 v kapitole Doplňková data na str. 75. Převzato z Publikace V.

Koncept on-line štěpení (**Obr. 13**) nabízí výhodu velmi rychlé a jednoduché metody, která je použitelná na jakékoliv chromatografické instrumentaci bez nutnosti používat přepínací ventily nebo sbírat jednotlivé frakce a provádět 2D chromatografii. Velkou výzvou je kompatibilita MF, tedy MF vhodné pro štěpení a MF vhodné pro separaci štěpných produktů. MF, ve které bude docházet na IMER ke štěpení musí mít pH vhodné pro aktivitu trypsinu (pH~8) a nesmí obsahovat větší množství organického rozpouštědla.

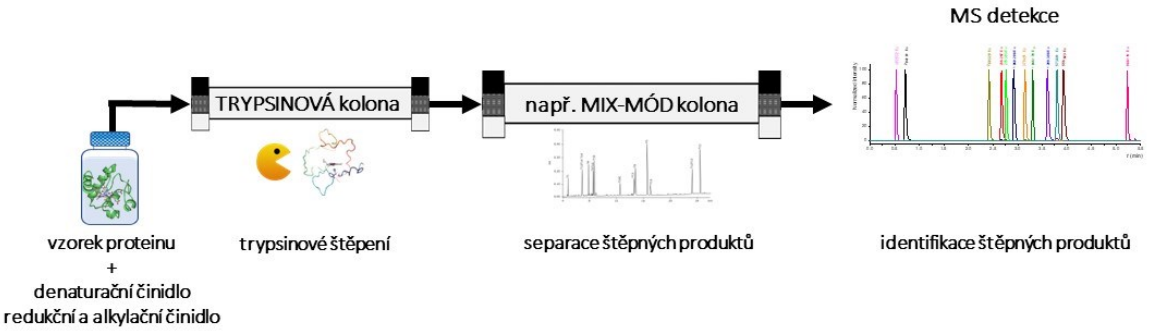

Obr. 13: Schéma uspořádání pro on-line štěpení proteinů a separaci štěpných fragmentů při použití sériově zapojených UHPLC kolon.

V první řadě bylo potřeba provést podrobnou charakterizaci testovaných IMER, tedy trypsinových kolon lišících se rozměry (30 × 2,1 mm a 50 × 1,0 mm) a pokrytím trypsinem (3,0 µmol m^{-2} a 5,0 µmol m^{-2}). Získané trendy byly velmi podobné pro všechny testované kolony, a proto budou dále ukázány výsledky pouze pro IMER s nižším pokrytím trypsinu (3,0 µmol m^{-2}), ale většími rozměry (a tedy i větším povrchem; 30 × 2,1 mm). IMER prototypy byly získány v rámci spolupráce se společností Waters. Aktivita IMER byla sledována analýzou *N*-α-benzoyl-L-arginin 4-nitroanilid hydrochloridu (BAPNA), který je trypsinem štěpen na benzoylarginin (vždy první eluující) a *p*-nitroanilin (vždy druhý eluující), tedy dva produkty detekovatelné UV detekcí. Nejprve byl zkoumán vliv množství substrátu (BAPNA) na aktivitu trypsinu, tedy štěpící kapacita IMER, a to v rozsahu od 1 do 200 µg nadávkovaného BAPNA (kombinace koncentrací 1 mg ml^{-1}; 5 mg ml^{-1}; 10 mg ml^{-1}; 15 mg ml^{-1}; 20 mg ml^{-1} a nadávkovaného objemu od 1 do 10 µl, z důvodu rozpustnosti). **Obr. 14** ilustruje, že v rozsahu do 120 µg nadávkovaného BAPNA nelze pozorovat téměř žádnou změnu v kapacitě trypsinového IMER a množství nenaštěpeného BAPNA je < 1 %. Nad 120 µg množství nenaštěpeného BAPNA stoupá až k hodnotě okolo 7 % pro 200 µg nadávkovaného substrátu. Pro lepší představu jsou na **Obr. 14** zobrazeny i chromatogramy pro dva krajní případy, tedy 1 µg a 200 µg

dávkovaného substrátu. Na základě získaných výsledků byla pro další experimenty vybrána koncentrace 10 mg ml^{-1} a dávkovaný objem 5 µl (50 µg BAPNA).

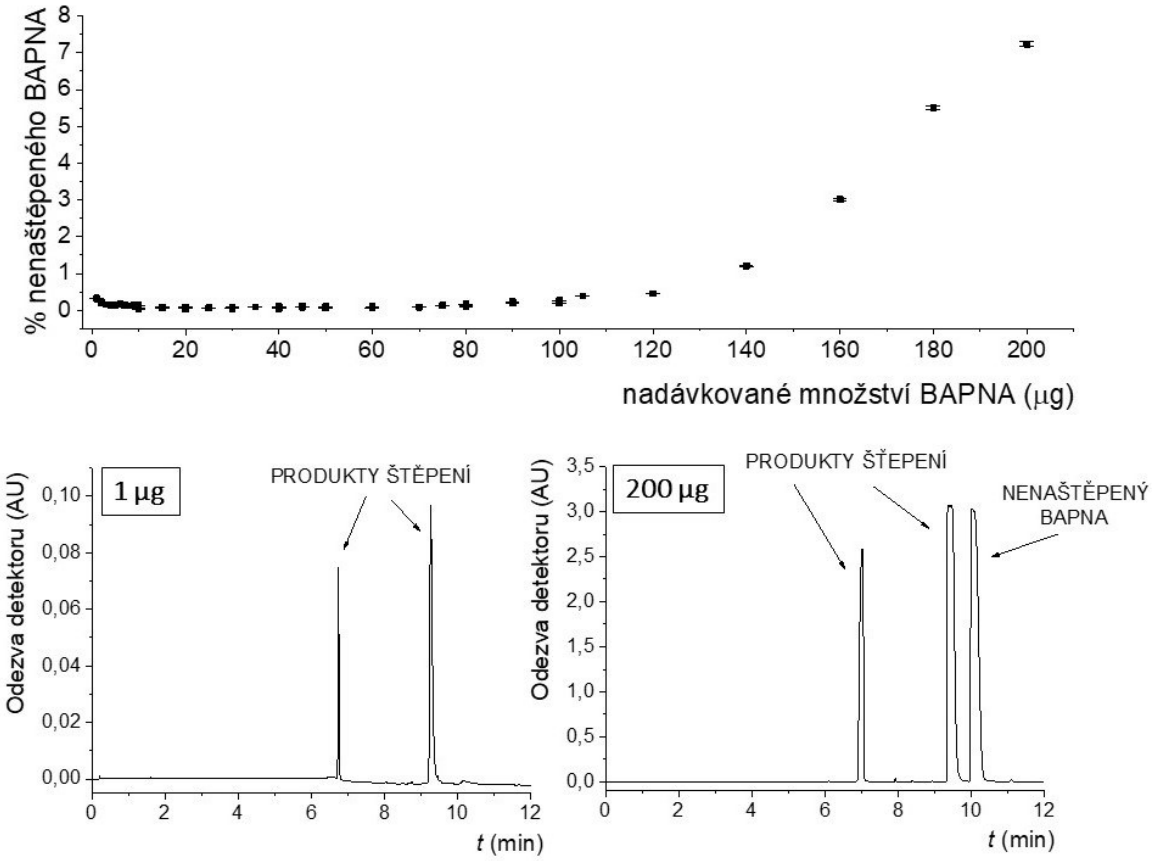

Obr. 14: Závislost množství nenaštěpeného substrátu (BAPNA) na jeho celkovém nadávkovaném množství. Každý bod je opatřen chybovou úsečkou, jejíž hodnota nepřekračuje ±0,4 %. Gradientová eluce: 0min=100% MF B; 2min=100% MF B; 8min=50% MF B. Složení MF: MF A: 26,5mM mravenčan amonný ve směsi ACN/voda, 80/20 (*v/v*); MF B: 26,5mM mravenčan amonný ve vodě. pH upraveno roztokem amoniaku na hodnotu 8,5. Teplota kolony: 37 °C, průtok 0,3 ml min^{-1}, UV detekce: 280 nm. Kolona: IMER 1 + Atlantis Premier BEH C18 AX. Pro názornost jsou chromatogramy ukázány při stejné vlnové délce, pro účely kvantifikace byla ale z důvodu velké odezvy pro 200 µg použita jiná vlnová délka a tomu odpovídající kalibrační závislost. Převzato z Publikace VI.

Pro aktivitu trypsinu je důležitá hodnota pH a teploty, a proto byl vliv těchto parametrů na aktivitu trypsinu sledován v chromatografickém systému. Navíc byl přidán i parametr průtoku MF, tedy doby, po kterou může být substrát v kontaktu s trypsinem. Jak je vidět na **Obr. 15**, v testovaném rozsahu má největší vliv na aktivitu trypsinu hodnota pH

MF. Již v pH 7,0 (tedy v okolí oblasti udávané jako pH optimální) je množství nenaštěpeného substrátu okolo 13 %, nad pH 8,0 jsou rozdíly zanedbatelné a téměř veškerý substrát je trypsinem naštěpen. Na pH optimum aktivity trypsinu má tak pravděpodobně vliv způsob imobilizace nebo zdroj trypsinu. V oblasti vlivu teploty na aktivitu trypsinu nebylo pozorováno nic neočekávaného a udávaná teplota minimálně 37 °C se potvrdila pro aktivitu trypsinu jako optimální. Vliv průtoku MF na aktivitu trypsinu byl sice malý, nicméně na uvedeném příkladu i tak dobře viditelný.

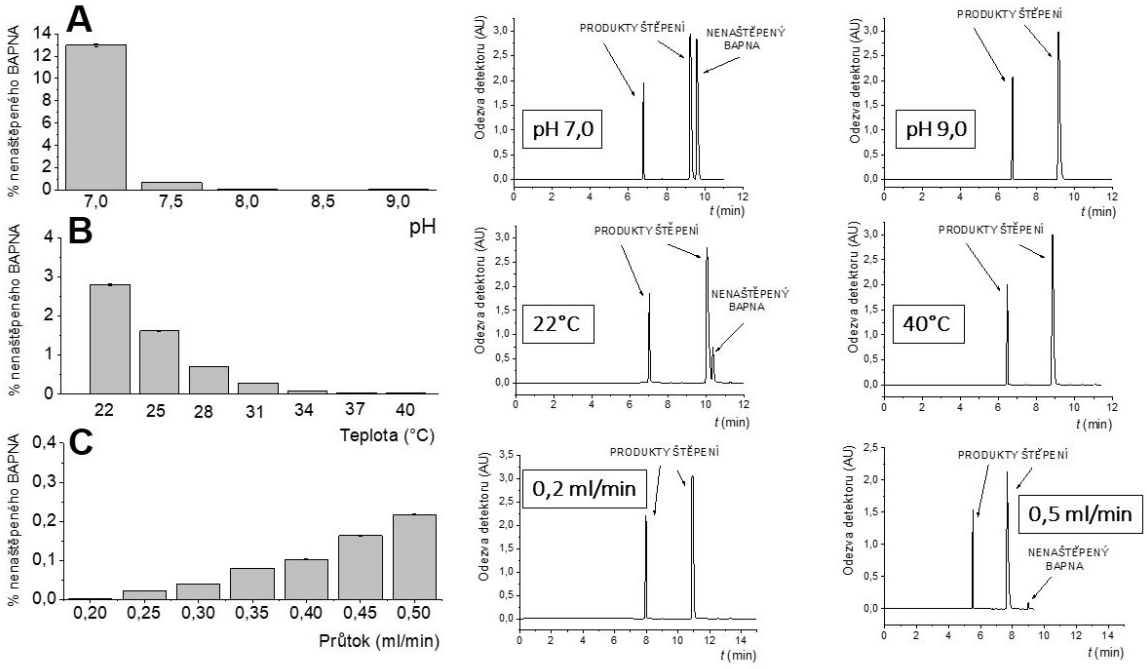

Obr. 15: Vliv pH MF, teploty a průtoku MF na aktivitu trypsinu (tj. množství nenaštěpeného substrátu, BAPNA). Každý sloupec je opatřen chybovými úsečkami, které nepřekračují ± 0,2 % pro A; ± 0,02 % pro B a ± 0,002 % pro C. Gradientová eluce: 0min=100% MF B; 2min=100% MF B; 8min=50% MF B. Složení MF: MF A: 26,5mM mravenčan amonný ve směsi ACN/voda, 80/20 (*v/v*); MF B: 26,5mM mravenčan amonný ve vodě. pH upraveno roztokem amoniaku na hodnotu 8,5 (kromě panelu A). Teplota kolony: 37 °C (kromě panelu B), průtok 0,3 ml min^{-1} (kromě panelu C), UV detekce: 280 nm. Kolona: IMER 1 + Atlantis Premier BEH C18 AX. Koncentrace vzorku: 10 mg ml^{-1}, nadávkovaný objem: 5µl. Převzato z Publikace VI.

Je známo, že trypsin je citlivý na přítomnost organických rozpouštědel. Z toho důvodu jsme se rozhodli otestovat vliv ACN a methanolu (MeOH) na aktivitu trypsinu, a to v případě, že bude organické rozpouštědlo přítomno v MF v počáteční fázi gradientu,

tedy ve fázi samotného štěpení (cca první 2 minuty). Na **Obr. 16** je vidět, že do 5-10 % organického rozpouštědla v MF se aktivita trypsinu výrazně nemění, přičemž pro MeOH klesá aktivita s rostoucím obsahem organického rozpouštědla výrazně méně. V případě ACN dochází okolo 37 obj. % ACN v MF ke ztrátě retence a koeluci BAPNA a jeho štěpných produktů. I přesto, že aktivita trypsinu je vyšší v přítomnosti MeOH v porovnání se stejným množstvím ACN, byla pro další experimenty vybrána MF s ACN. Důvodem je lepší tvar píků a kratší čas analýzy v případě MF s ACN a fakt, že i přes používání organického rozpouštědla ve vyšších koncentracích (cca 40 % na konci každého gradientu) byla aktivita trypsinu velmi dobře opakovatelná po více jak 300 nástřiků.

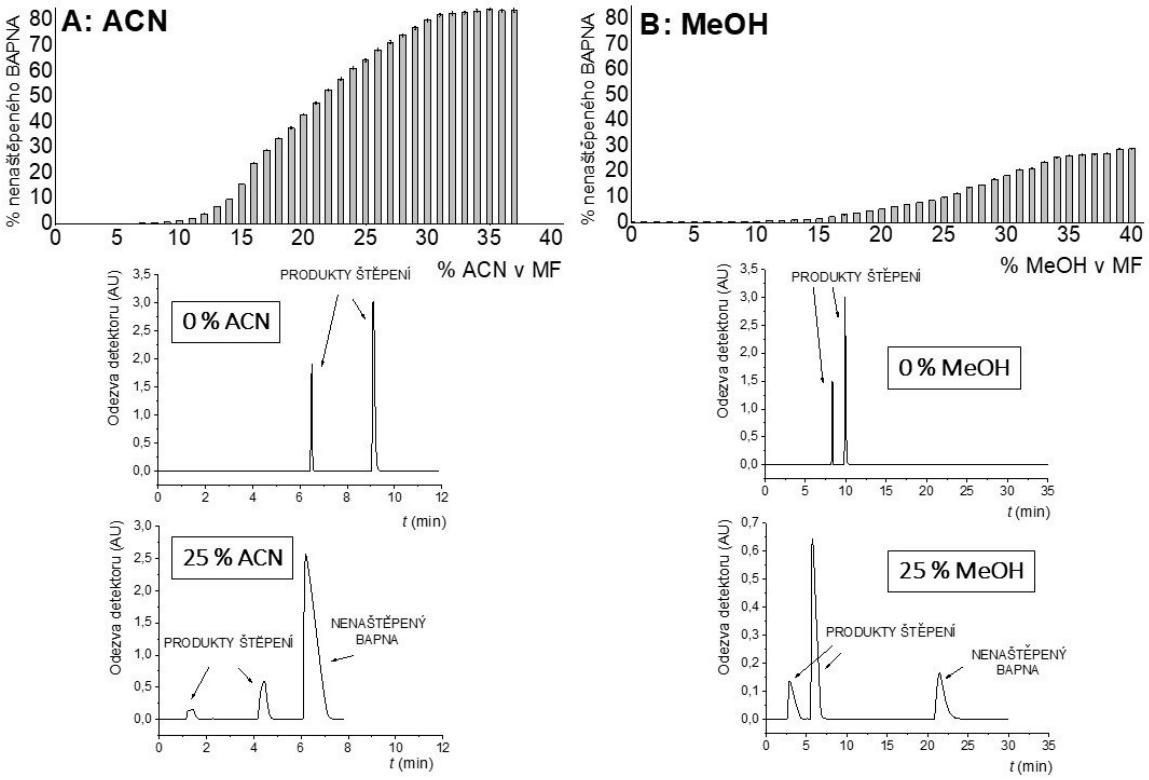

Obr. 16: Vliv množství a typu organického rozpouštědla na aktivitu trypsinu (tj. množství nenaštěpeného substrátu, BAPNA). Každý sloupec je opatřen chybovými úsečkami, které nepřekračují ± 0,7 %. Gradientová eluce: 0min=X% MF A; 2min= X% MF A; 8min=80% MF A; X = ⟨0; 80⟩. Složení MF: MF A: 26,5mM mravenčan amonný ve směsi ACN/voda, 50/50 (*v/v*); MF B: 26,5mM mravenčan amonný ve vodě. pH upraveno roztokem amoniaku na hodnotu 8,5. Množství organického rozpouštědla v MF je vypočítáno jako X/2. Teplota kolony: 37 °C; průtok 0,3 ml min^{-1}, UV detekce: 280 nm. Kolona: IMER 1 + Atlantis Premier BEH C18 AX; koncentrace vzorku: 10 mg ml^{-1}, nadávkovaný objem: 5µl. Převzato z Publikace VI.

Na základě získaných výsledků z on-line štěpení BAPNA byly pro on-line štěpení komplexnějších proteinů vybrány následující podmínky: MF pH 8,5; teplota kolony: 37 °C; gradient průtoku: 0,1 ml min^{-1} první dvě minuty gradientu, 0,2 ml min^{-1} ve třetí minutě a od čtvrté minuty průtok 0,3 ml min^{-1}. Tyto podmínky průtoku poskytují dostatečný čas pro efektivní štěpení a zároveň zajišťují přiměřeně dlouhý čas analýzy. V prvních třech minutách gradientu nebyl v MF přítomen žádný ACN a maximální obsah ACN v MF na konci gradientu byl 48 obj.% (60 obj.% MF A), což bylo nezbytné pro eluci všech štěpných produktů. Pro efektivní štěpení proteinů bylo do vzorku proteinu (přímo do vialky) přidáno denaturační činidlo (směs močoviny, thiomočoviny a C_7BzO). V případě proteinů tvořících disulfidické můstky bylo nutné přidat i redukční a alkylační krok (tributylfosfin a jodoacetamid, cca 2 hodiny dlouhý proces) zabraňující jejich tvorbě. Bez přídavku těchto činidel by nedocházelo ke štěpení za každým lysinem a argininem („miscleavage“), štěpné fragmenty by byly delší, nespecifické a těžko identifikovatelné. Při identifikaci jednotlivých fragmentů je nezbytné využití MS detekce spolu s kalkulátorem hmot jednotlivých fragmentů (Expasy, [114]).

Výsledky on-line štěpení cytochromu C v porovnání s analýzou jeho komerčně dostupného naštěpeného standardu a cytochromu C naštěpeného za použití „spin kolonek“ jsou na **Obr. 17**. Pro účely tohoto porovnání byly vybrány pouze fragmenty deklarované ve standardu naštěpeného cytochromu C (**Tabulka S4** v Doplňkových datech, str. 75). Jak již bylo zmíněno výše, použití „spin kolonek“ neposkytuje chymotryptický fragment T19C.

Kromě cytochromu C byla vyvinutá on-line metoda použita i pro štěpení myoglobinu a enolasy. Výsledky pro všechny tři proteiny potvrdily, že on-line štěpení poskytuje větší počet i vyšší množství „miscleavage“ a chymotryptických fragmentů v porovnání se štěpením za použití „spin kolonek“. Počet nalezených tryptických fragmentů byl srovnatelný pro všechny proteiny a celkově bylo identifikováno vždy přes 88 % sekvence (tzv. „sequence coverage“). Podobné trendy byly pozorovány i pro proteiny obsahující disulfidické můstky, tedy α-laktalbumin, β-laktoglobulin A, albumin a konalbumin, kde se vyšší počet nalezených fragmentů ukázal výhodný, a to z důvodu výrazně vyššího počtu nalezených tryptických fragmentů při on-line štěpení v porovnání se „spin kolonkami“.

Na základě získaných poznatků lze shrnout, že vyvinutá metoda pro on-line štěpení proteinů, tedy sériové zapojení trypsinové a analytické mix-mód kolony, se ukázala jako účinná technika, která výrazně šetří čas, a tím zvyšuje množství analyzovatelných vzorků.

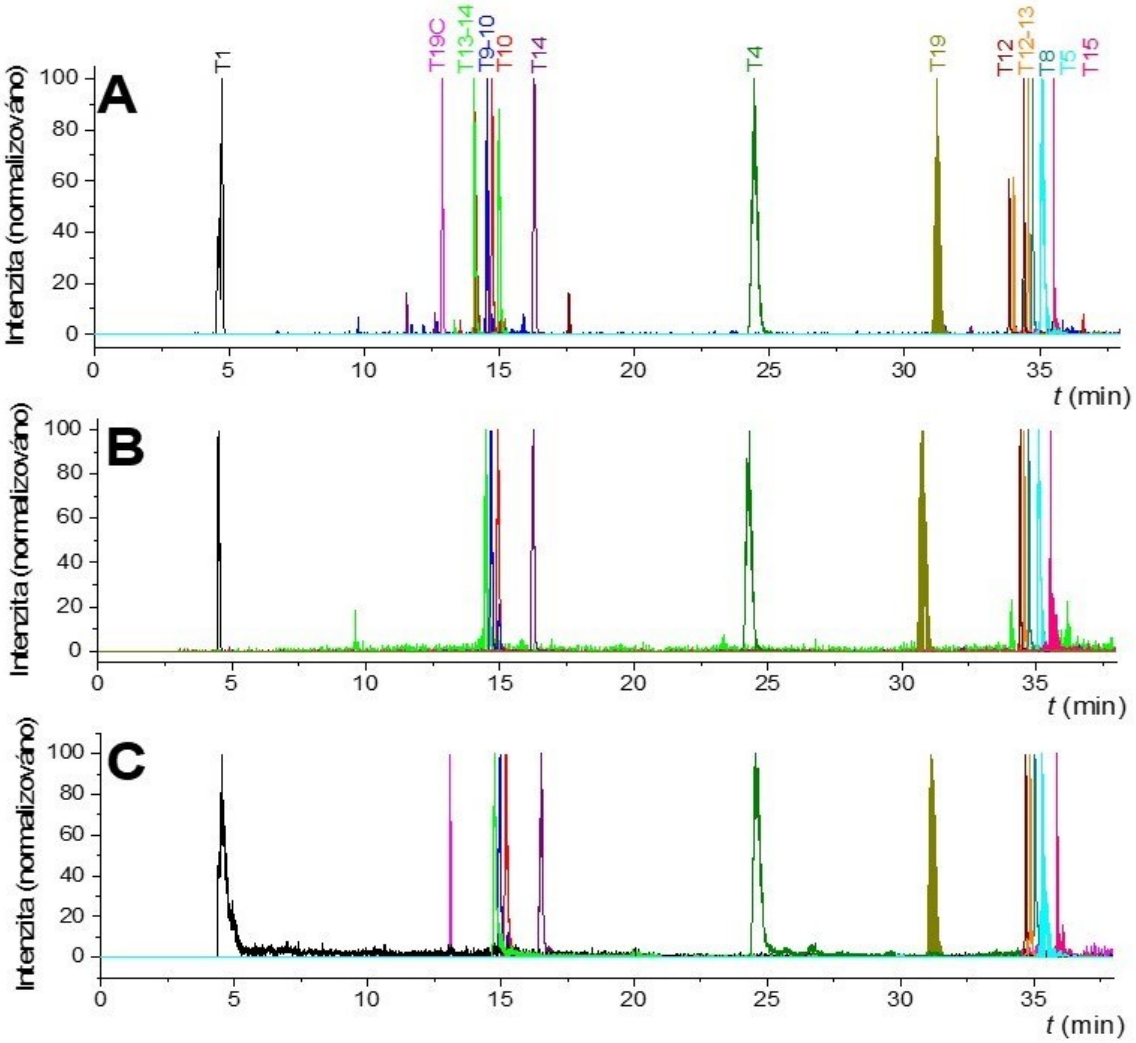

Obr. 17: Porovnání analýzy naštěpeného standardu cytochromu C (A), cytochromu C naštěpeného za použití „spin kolonek“ (B) a on-line štěpení cytochromu C (C). Ve všech případech byly použity stejné chromatografické podmínky a stejný gradient jako pro on-line štěpení. Převzato z Publikace VI.

4.3 Chromatografická charakterizace a analýza terapeutických thiofosfátových oligonukleotidů (Publikace VII, Publikace VIII, Publikace IX, Publikace X)

Nejpoužívanějším přístupem pro chromatografickou analýzu thiofosfátových ON je IPRPLC. Vliv typu/hydrofobicity a koncentrace jak samotného IP činidla, tak i protiiontu (octan *vs.* HFIP) na separaci diastereomerů ON byl popsán již dříve [115,116]. Komplexní práce vysvětlující a shrnující všechny tyto efekty vedoucí k lepšímu pochopení těchto jevů nebyla k dispozici. K seřazení IP činidel podle jejich hydrofobicity (a tedy teoreticky i podle jejich schopnosti potlačit separaci diastereomerů) je možné využít dvou přístupů. Prvním z nich je sledování množství ACN v MF, které je potřebné k eluci vybraného ON (viz Publikace VII). Čím vyšší je množství ACN, tím vyšší retenci ON IP činidlo poskytuje, a tím je IP činidlo hydrofobnější. Druhou možností je měření retence alkylaminů. Pokud jako MF zvolíme octan amonný nebo HFIP + vodný roztok amoniaku (v různých koncentracích, pH ~ 8), získáme zároveň informaci o tom, jak protiiont (octan *vs.* HFIP) a jeho koncentrace ovlivňuje sorpci alkylaminu na povrch stacionární fáze. Výsledky shrnuté na **Obr. 18** seřazují IP činidla podle jejich hydrofobicity (vyšší retence = víc hydrofobní). Na příkladu porovnání triethylaminu (TEA), dipropylaminu (DPA) a hexylaminu (HA) je vidět, že hydrofobicitu neovlivňuje pouze počet uhlíků v řetězci (všechny obsahují 6 uhlíků), ale také větvení uhlovodíkového řetězce (čím větší větvení, tím menší hydrofobicita). **Obr. 18** dále ukazuje, že přítomnost HFIP v MF podporuje sorpci alkylaminu na povrch SF více než octan a retence alkylaminů je tak vyšší. S rostoucí koncentrací protiiontu sorpce alkylaminu na povrch SF roste, tento efekt je však daleko výraznější pro MF s HFIP v porovnání s MF s octanem.

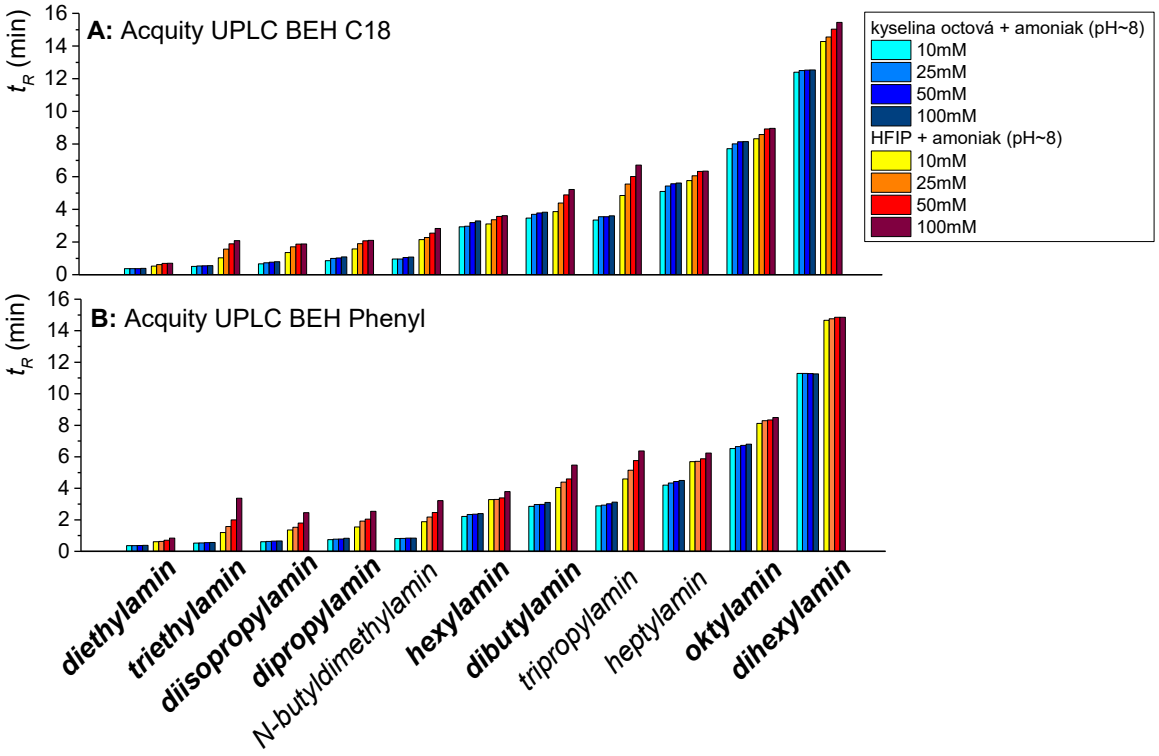

Obr 18: Retence alkylaminů na dvou typech SF (C18 a fenyl). Gradientová eluce: 0min=1% MF A; 22,5min=50% MF A. Složení MF: MF A: ACN, MF B: kyselina octová/HFIP + vodný roztok amoniaku, pH ~ 8; koncentrace soli 10mM, 25mM, 50mM a 100mM. Teplota kolony: 60 °C, průtok: 0,5 ml min^{-1}, MS detekce (QDa detektor). Tučně označené alkylaminy byly vybrány pro další měření. Převzato z Publikace VIII.

Důsledek zvýšené sorpce alkylaminu na povrch SF v přítomnosti HFIP v porovnání s octanem, a tedy efektivnější potlačení separace diastereomerů v případě HFIP MF je znázorněno na **Obr. 19 A**. Zatímco MF s octanem jako protiiontem poskytuje částečnou separaci diastereomerů (a to i přesto, že koncentrace samotného IP činidla i protiontu je vyšší), MF s HFIP plně potlačila separaci diastereomerů. Ohledně názvosloví, označení allPO značí nemodifikovaný ON, 1PS5´ označuje ON, který má 1PS modifikaci na 5´konci, označení 2PS3´5´center je pro ON obsahující 2PS modifikace na 3´konci, 2PS modifikace na 5´konci a 2PS modifikace uprostřed sekvence. Kompletní seznam všech testovaných ON je uveden v **Tabulce 5** na konci této podkapitoly, str. 60)

Vliv koncentrace protiiontu, konktrétně HFIP, na separaci diastereomerů je ilustrován na **Obr. 19 B**. S rostoucí koncentrací HFIP, tedy s rostoucím množstvím IP činidla sorbovaného na povrch SF (při stejné počáteční koncentraci IP činidla v MF) roste potlačení separace diastereomerů. **Obr. 19** potvrzuje hypotézy získané na základě měření

retence/sorpce alkylaminů na povrch SF v závislosti na typu a koncentraci použitého protiiontu v MF (**Obr. 18**).

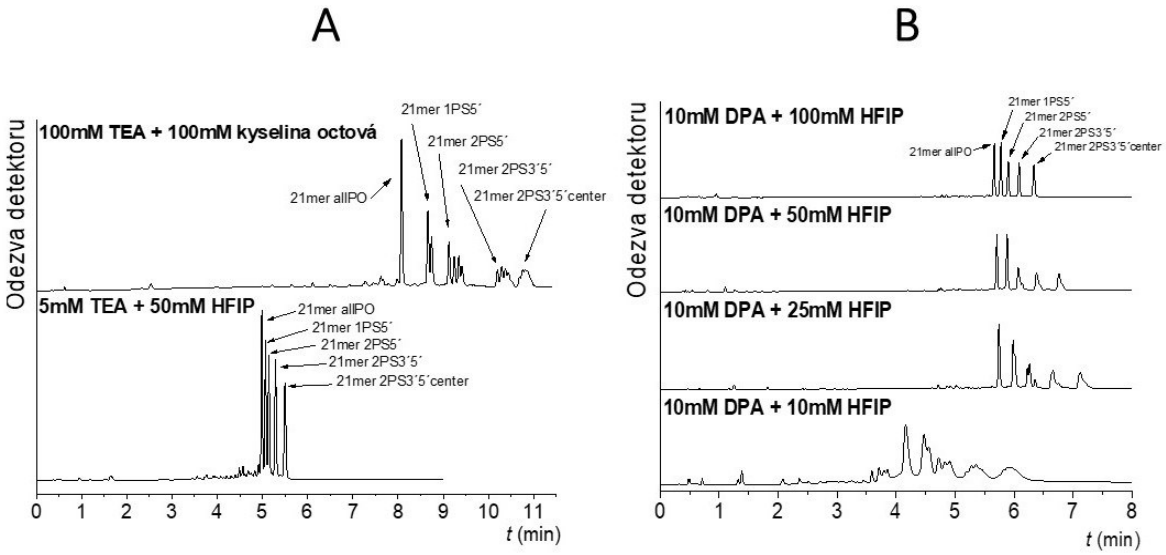

Obr. 19: Vliv protiiontu (octan *vs.* HFIP) na separaci diastereomerů, převzato z Publikace VII (A). Vliv koncentrace HFIP na separaci diastereomerů, převzato z Publikace VIII (B). Teplota kolony: 60 °C, UV detekce: 260 nm. Kolona: Acquity Premier UPLC BEH C18.

I přesto, že MF obsahující HFIP vykazují velmi slibné výsledky z hlediska sorpce IP činidla na povrch SF, a tím i potlačení separace diastereomerů, MF obsahující octan jako protiiont stále reprezentují většinu aplikací [117]. Důvodem je nižší selektivita HFIP systému vůči ON různé délky nebo ON lišících se počtem nebo pozicí PS modifikací v porovnání se systémem s octanem. Navíc HFIP je relativně drahá sloučenina, která je snadno oxidovatelná a není tak na vzduchu dlouhodobě stabilní. Vliv typu IP činidla (s octanem jako protiiontem) na separaci diastereomerů velmi dobře koreluje s předchozími výsledky, a tedy s rostoucí hydrofobicitou roste i potlačení separace diastereomerů (**Obr. 20**). V tomto trendu hraje významnou roli i fakt, že pro hydrofobnější IP činidla musí MF obsahovat více ACN, což vede k potlačení „hydrofobní interakce“, a tedy i potlačení separace diastereomerů.

Slabé IP systémy (červeně označené v **Obr. 20**) poskytují částečnou separaci diastereomerů a v některých případech je dokonce nemožné rozlišit mezi jednotlivými ON. Hydrofobnější (zeleně označené) IP systémy separaci diastereomerů plně potlačují, poskytují úzké píky a zároveň umožňují separaci jednotlivých ON lišících se počtem PS modifikací na základní linii. Trend rostoucího potlačení separace diastereomerů s rostoucí hydrofobicitou IP činidla však neplatí v celém rozsahu hydrofobicity IP činidel. Pro vysoce hydrofobní IP systémy (oranžová barva) v kombinaci s jejich vysokou koncentrací

(100mM) pozorujeme rozšířené píky, které naznačují částečnou separaci diastereomerů, což může komplikovat rozlišení jednotlivých ON. Obecně můžeme říct, že schopnost IP systému potlačit separaci diastereomerů může být popsána dvěma způsoby, a to: i) počtem separovaných píků/diastereomerů; ii) v případě pouze jednoho píku jeho šířkou (např. $w_{50\%}$, **Obr. 21A**). Na základě dat v **Obr. 20** lze shrnout, že nejlepší volbou z hlediska potlačení separace diastereomerů je využití např. 100mM HAA.

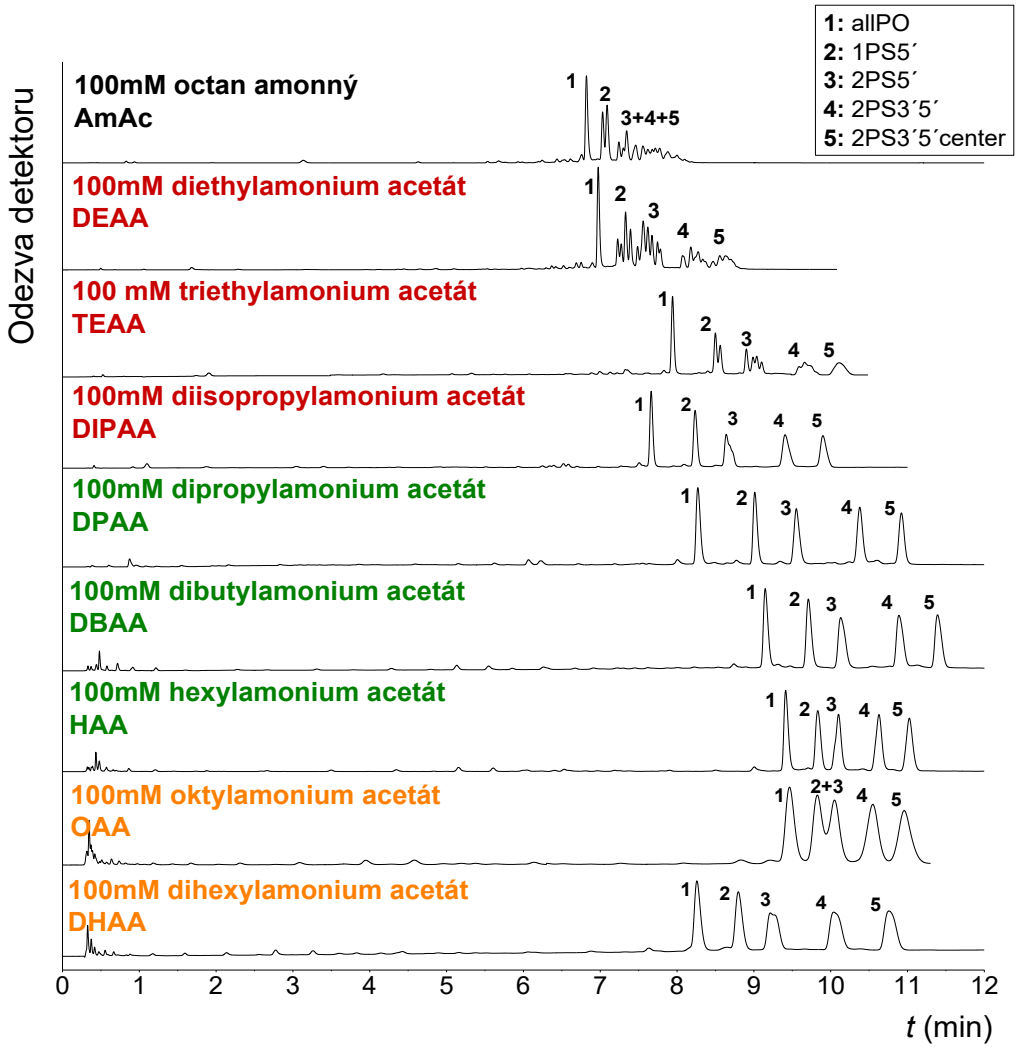

Obr. 20: Separace směsi 21mer ON lišících se v počtu PS modifikací. Gradientová eluce. Teplota kolony: 60 °C, UV detekce: 260 nm. Kolona: Acquity Premier UPLC BEH C18. Převzato z Publikace VII.

Kromě potlačení separace diastereomerů je dalším velmi důležitým parametrem v chromatografické analýze terapeutických PS ON rozlišení hlavního píku a jeho kratších nečistot, tedy rozlišení *n* a 5´*n-x* meru (např. 21meru a 20meru zkráceném na 5´ konci). Kratší mery (případně 5´*n*+1 mery) jsou pozůstatky ze syntézy a jsou typickými nečistotami každého vzorku ON. Jejich separace od hlavního píku je klíčová pro správné vyhodnocení a kvantifikaci hlavního píku. Hodnoty rozlišení *(R_s)* pro 21mer a 20mer (1PScenter ON) jsou uvedeny v **Obr. 21B**. S rostoucí hydrofobicitou a koncentrací IP činidla roste i rozlišení ON s různou délkou. Ve většině případů je žádoucí dosáhnout co největšího potlačení separace diastereomerů a zároveň co největšího rozlišení *n* a *n*-1 meru. Z toho důvodu je k volbě optimálního IP činidla nutné zkombinovat poznatky z **Obr. 21A** a **21B** a na základě kompromisu je pak možné vyzdvihnout IP systémy DBAA a HAA, které dostatečně splňují obě kritéria.

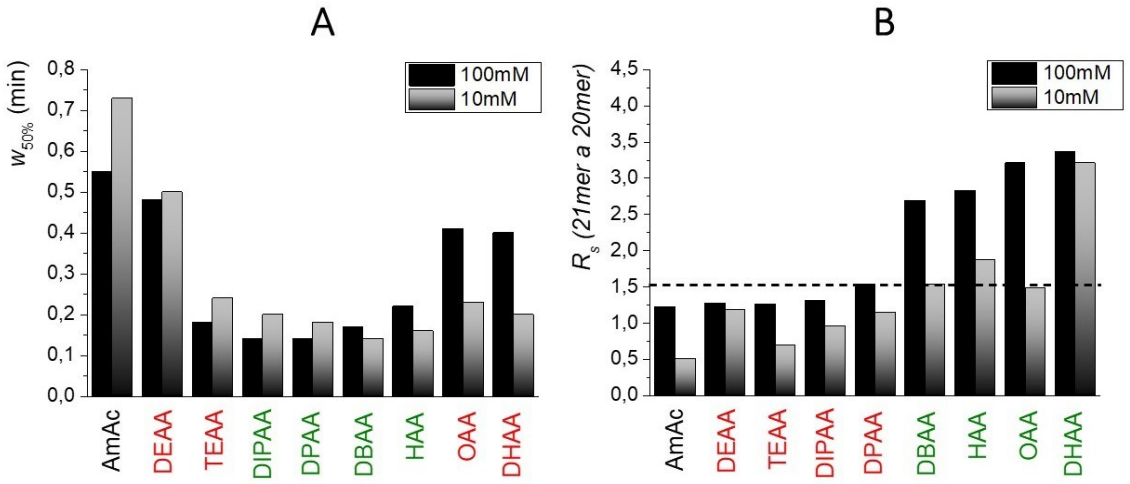

Obr. 21: Vliv typu a koncentrace IP činidla na: (A) šířku píku $w_{50\%}$, 21mer allPS; (B) rozlišení 21mer a 20mer, 21mer 1PScenter. Přerušovaná čára značí hranici rozlišení na základní linii. Červeně označené IP systémy jsou k danému účelu nevhodné, zeleně označené poskytují uspokojivé výsledky (úzké píky, rozlišení na základní linii). Teplota kolony: 60 °C. Převzato z Publikace VII.

Pro LC analýzu DNA i RNA oligonukleotidů je typická separační teplota 60 °C, a to z důvodu omezení tvorby sekundárních struktur, jako jsou např. homoduplexní smyčky a vlásenky nebo intermolekulární komplexy [118]. Jejich tvorba značně komplikuje analýzu ON a vede k rozšiřování píků. Separační teplota je významným chromatografickým parametrem a z toho důvodu jsme provedli první komplexní výzkum zabývající se vlivem teploty na separaci diastereomerů a rozlišení *n* a *n-x* meru, a to

v rozsahu teplot 20 °C až 90 °C. Teplotní rozmezí bylo vybráno s ohledem na teplotní stabilitu použitých kolon (kolony s BEH částicemi).

Vliv teploty na separaci diastereomerů je ukázán na **Obr. 22** na příkladu 21mer 2PS3´5´center ON (MF 100mM TEAA). S rostoucí teplotou nejprve klesá počet částečně separovaných diastereomerů (do 60 °C). S dalším nárůstem teploty, tedy nad běžně používaných 60 °C, dochází k dalšímu snižování šířky píku. I přesto, že TEAA patří ke slabým IP systémům, při vysokých teplotách (90 °C) lze dosáhnout úplného potlačení separace diastereomerů a získat užší píky než při běžně používaných 60 °C. Data pro ostatní ON a ostatní IP systémy vykazují velmi podobné trendy, tj. efektivnější potlačení separace diastereomerů s rostoucí teplotou.

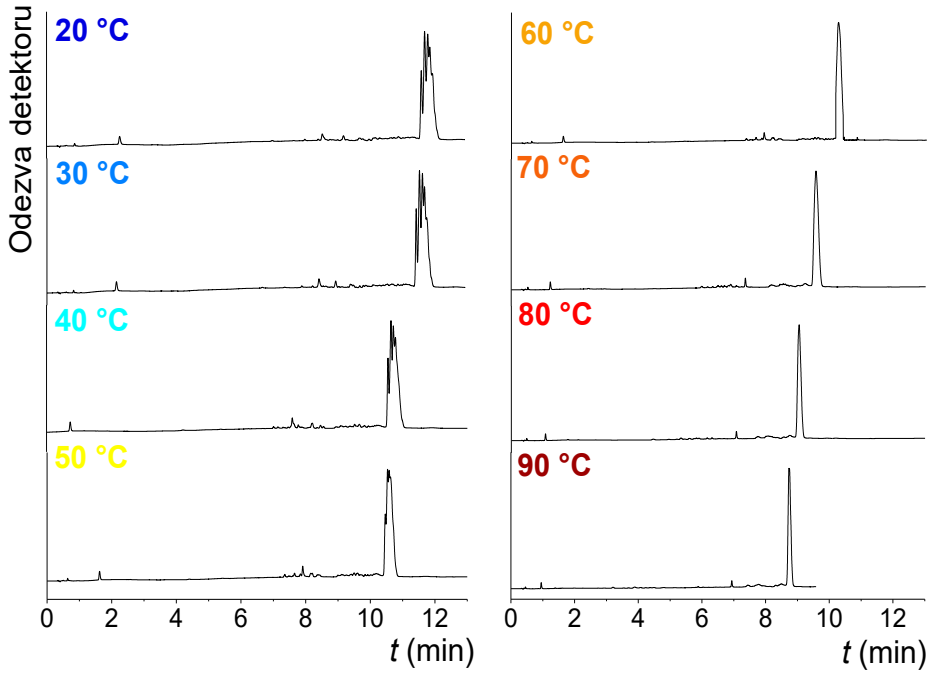

Obr. 22: Vliv teploty na separaci diastereomerů. Gradientová eluce: 0min=4% MF A, 20min=25% MF A. Složení MF: MF A: 100mM TEAA ve směsi ACN/voda, 80/20 (*v/v*); MF B: 100mM TEAA ve vodě, pH 8,0. ON: 21mer 2PS3´5´center. Převzato z Publikace IX.

Zúžení píku s rostoucí teplotou hraje velmi významnou roli v separaci *n* a *n-x* merů (**Obr. 23**). Čím užších píků jsme schopni dosáhnout, tím větší bude rozlišení ON s různou délkou. I pro slabé IP systémy (TEAA) jsme při teplotě 90 °C schopni dosáhnout alespoň částečné separace 21meru a jeho tří kratších nečistot (20mer, 19mer, 18mer). Stejně tak u vysoce hydrofobních IP systémů (OAA) vysoká teplota zásadním způsobem redukuje

šířku píku a umožňuje separaci 21meru a jeho nečistot na základní linii. Velmi podobné trendy byly pozorovány i pro IP systémy obsahující HFIP místo octanu (viz Publikace VII).

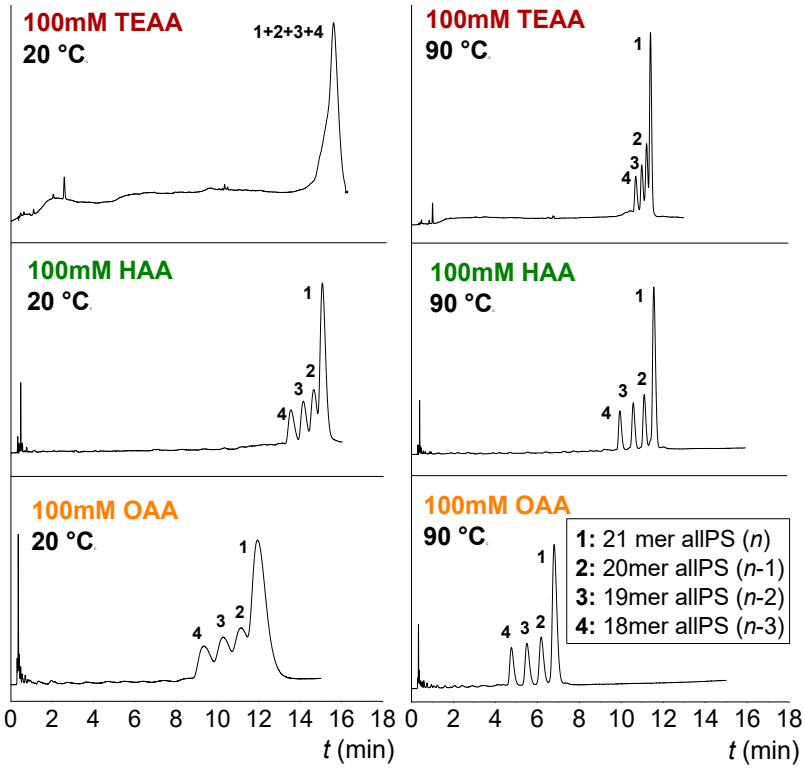

Obr. 23: Vliv teploty na separaci *n* a *n-x* merů (*x*=1,2,3). Gradientová eluce. Složení MF: MF A: 100mM alkylamonium acetát ve směsi ACN/voda, 80/20 (*v/v*); MF B: 100mM alkylamonium acetát ve vodě, pH 8,0. Převzato z Publikace IX.

Druhou možností, jak omezit separaci diastereomerů (kromě využití IPRPLC v kombinaci s vhodným IP systémem a teplotou), je využití vhodných HILIC systémů. Nespornou výhodou HILIC jsou MS kompatibilní MF, což je klíčové pro identifikaci nečistot i metabolitů. Z toho důvodu jsme do HILIC projektu přidali kratší oligonukleotidy (2-6mer), které svou délkou odpovídají možným metabolitům. Hlavním cílem bylo podrobně charakterizovat chromatografické chování ON v HILIC a vyvinout metodu aplikovatelnou na analýzu vzorků plasmy dětí léčených Spinrazou (terapeutický ON nusinersen) proti spinální svalové atrofii. Jako kolona byla vybrána Acquity Premier BEH Amide, která se ukázala jako nejvhodnější pro analýzu ON v HILIC.

V první řadě bylo potřeba optimalizovat složení MF z hlediska separace různých ON (délka, počet PS modifikací) a tvaru píků. MF (mravenčan amonný) o pH 3,0 se ukázala jako nevhodná, protože nedošlo k eluci ON do 60 minut, což je pravděpodobně

způsobeno silnou nespecifickou interakcí mezi ON a kovovým povrchem LC instrumentace. pH 4,7 poskytovalo v porovnání s pH 6,8 a 8,0 širší píky vedoucí k menšímu rozlišení *n* a *n-x* merů. Měření při různých koncentracích mravenčanu amonného (5-25mM, pH 8,0) ukázalo, že s rostoucí koncentrací klesá šířka píků a zlepšuje se tak separace různě dlouhých ON. Amidová SF prokázala svůj velký potenciál pro analýzu krátkých ON (2-6mer), což je dáno vysokou selektivitou jak pro různě dlouhé ON, tak i ON s různým počtem PS modifikací (**Obr. 24**). Čas analýzy by samozřejmě bylo možné na úkor selektivity zkrátit změnou gradientu a stále by bylo zachováno rozlišení na základní linii.

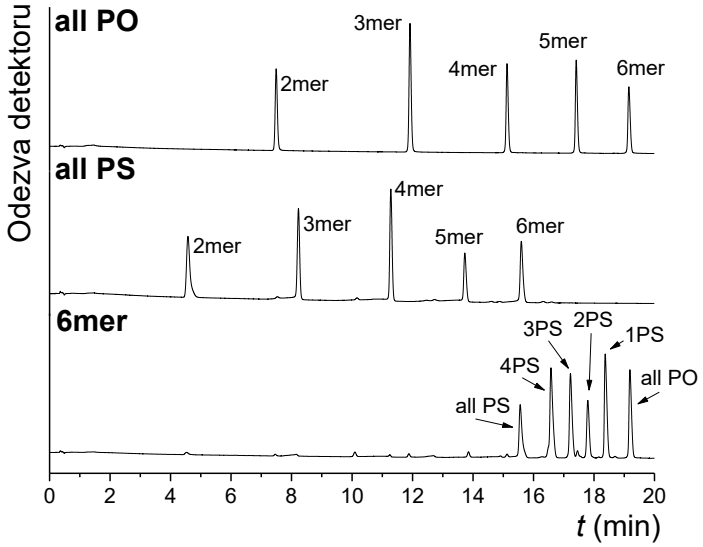

Obr. 24: Separace ON v závislosti na jejich délce a počtu PS modifikací. Gradientová eluce: 0min=97% MF A, 25min=55% MF A. Složení MF: MF A: ACN; MF B: 25mM mravenčan amonný, pH 8,0. Teplota kolony: 40 °C, UV detekce: 260 nm. Kolona: Acquity Premier BEH Amide (1,7 μm, 50×2,1 mm). allPO značí nemodifikovaný ON, allPS značí plně modifikovaný ON. Převzato z Publikace X.

Vzhledem k tomu, že pro komplexnější analýzu nečistot a metabolitů je nezbytné využití MS detekce, bylo složení MF upraveno tak, aby poskytovalo co největší MS signál. Mravenčan amonný byl nahrazen octanem amonným a jeho koncentrace byla snížena z 25mM na 10mM. K udržení konstantní iontové síly byl octan amonný přidán do obou složek MF. Poslední změnou bylo pH, které bylo z důvodu snazší přípravy, a tedy i vyšší opakovatelnosti změněno z pH 8,0 na pH 6,8. Takto upravené podmínky nezpůsobily žádné zásadní změny v analýze nečistot OL1 ani OL2, dvou sekvenčních analogů nusinersenu (sekvence zobrazeny v **Tabulce 5** na konci této podkapitoly, str. 60).

LC MS analýza nečistot analytu OL2 (zcela PS modifikovaného sekvenčního analogu nusinersenu), je zobrazena na **Obr. 25**. V optimalizovaných podmínkách bylo možné identifikovat 28 nečistot, převážně ON zkrácených na 5´nebo 3´konci nebo kratších ON se zbytkovou fosfátovou skupinou (1 nečistota) nebo cyklickou fosfátovou skupinou (8 nečistot). V případě OL1 (nemodifikovaného analogu nusinersenu) jsme identifikovali 26 nečistot s vyšším zastoupením nečistot se zbytkovou fosfátovou skupinou.

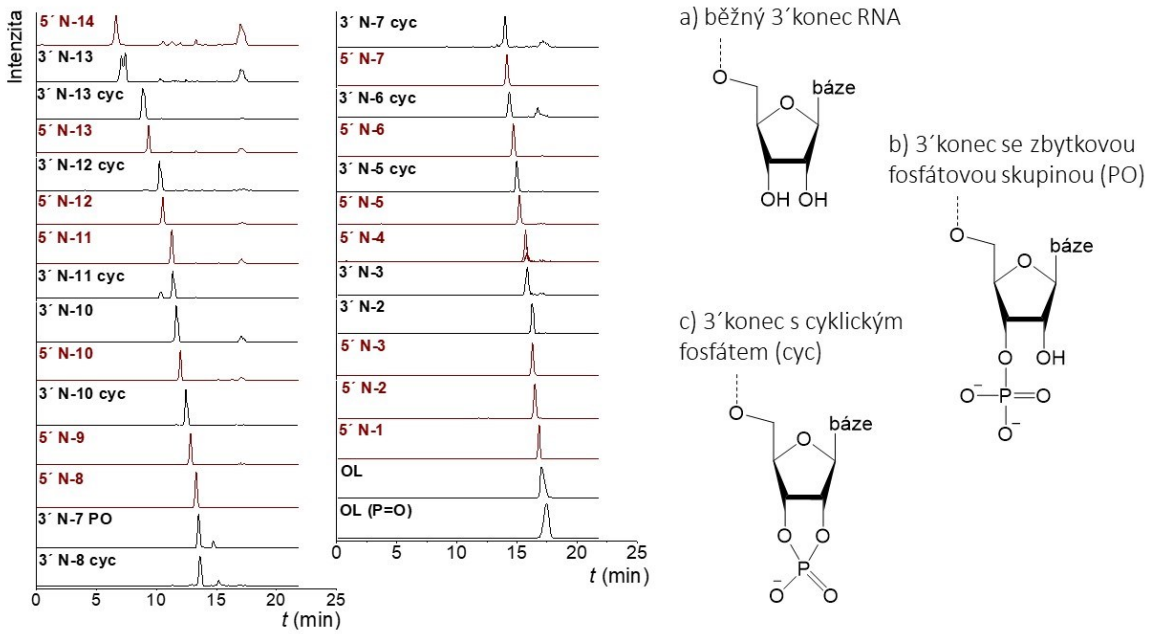

Obr. 25: Analýza nečistot zcela modifikovaného sekvenčního analogu nusinersenu (OL2). Gradientová eluce: 0min=100% MF A, 1min=100% MF A, 21min=50% MF A. Složení MF: MF A: 10mM octan amonný v ACN/voda, 75/25 (*v/v*); MF B: 10mM octan amonný ve vodě, pH 6,8. Teplota kolony: 40 °C, MS detekce (QDa detektor). Kolona: Acquity Premier BEH Amide (1,7 µm, 50×2,1 mm) Označení: 5´n-14 označuje ON zkrácený na 5´konci o 14 nukleobází oproti hlavnímu ON onačenému OL; cyc označuje přítomnost cyklického fosfátu, PO přítomnost zbytkové fosfátové skupiny na 3´konci; (P=O) označuje, že v sekvenci se na jednom místě vyskytuje místo thiofosfátu fosfát. Převzato z Publikace X.

V rámci spolupráce s Dr. Sylwii Studzińskou z polské univerzity Mikuláše Koperníka v Toruni jsme měli možnost analyzovat vzorky plasmy pacientů léčených Spinrazou (obsahující terapeutický ON nusinersen) proti spinální svalové atrofii. Vzorky plasmy byly odebírány léčeným pacientům po třetí dávce Spinrazy, která se aplikuje přímo do mozkomíšního moku lumbální punkcí. Vzorky pro LC analýzu byly dále podrobeny

extrakci kapalina-kapalina (fenol/chloroform/isoamyl alkohol (25:24:1 *v/v/v*)) k odstranění proteinů a lipidů ze vzorku. Analýza metabolitů nusinersenu ve vzorku plasmy je ukázána na **Obr. 26**. Celkem bylo nalezeno 11 metabolitů, ale pouze některé z nich bylo možné s jistotou identifikovat (Tabulka S5 v Doplňkových datech, str. 76). Ačkoliv měření probíhalo na MS detektoru typu Q-ToF a bylo využito fragmentačních spekter, identifikace takto krátkých ON je velmi náročná. Navíc tyto metabolity obsahují kromě thiofosfátové modifikace ještě dva další typy modifikací, a to 2'-O-methoxyethylovou skupinu na ribose a methylované cytosiny a uridiny. Na **Obr. 26** je také vidět, že nebylo možné dosáhnout separace všech metabolitů, a to ani přesto, že pro jejich analýzu byla použita třikrát delší kolona (15 cm) než pro všechny ostatní experimenty.

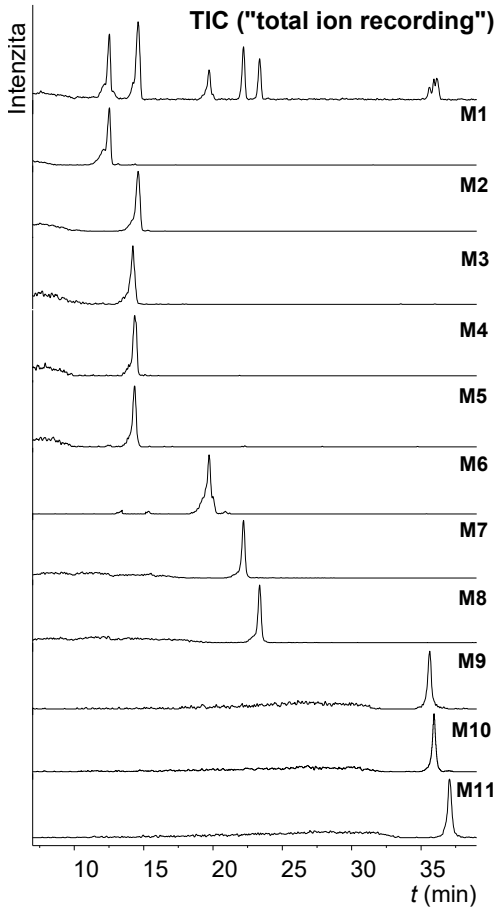

Obr. 26: Analýza vzorku plasmy dětí léčených Spinrazou (účinná látka nusinersen) proti spinální svalové atrofii. Gradientová eluce: 0min=100% MF A, 1min=100% MF A, 60min=80% MF A. Složení MF: MF A: 10mM octan amonný v ACN/voda, 75/25 (*v/v*); MF B: 10mM octan amonný ve vodě, pH 6,8. Teplota kolony: 40 °C, MS detekce (Q-ToF). Kolona: Acquity Premier BEH Amide (1,7 µm, 150×2,1 mm). Převzato z Publikace X.

Tabulka 5: Seznam testovaných ON, jejich sekvence a pozice PS modifikace (*)

OZNAČENÍ	SEKVENCE
delší ON (studium nečistot)	
21mer allPO	5′-TTT TAG CAT TTT TAC GAT TTT-3′
21mer 1PS3′	5′-TTT TAG CAT TTT TAC GAT TT*T-3′
21mer 1PS5′	5′-T*TT TAG CAT TTT TAC GAT TTT-3′
21mer 1PScenter	5′-TTT TAG CAT T*TT TAC GAT TTT-3′
21mer 2PS3′	5′-TTT TAG CAT TTT TAC GAT T*T*T-3′
21mer 2PS5′	5′-T*T*T TAG CAT TTT TAC GAT TTT-3′
21mer 2PScenter	5′-TTT TAG CAT T*T*T TAC GAT TTT-3′
21mer 1PS3′5′	5′-T*TT TAG CAT TTT TAC GAT TT*T-3′
21mer 2PS3′5′	5′-T*T*T TAG CAT TTT TAC GAT T*T*T-3′
21mer 2PScenter3′5′	5′-T*T*T TAG CAT T*T*T TAC GAT T*T*T-3′
21 mer allPS	5′-T*T*T * T*A*G * C*A*T * T*T*T * T*A*C * G*A*T * T*T*T-3′
allPS 20mer (5′N-1)	5′ T*T * T*A*G * C*A*T * T*T*T * T*A*C * G*A*T * T*T*T 3′
allPS 19mer (5′N-2)	5′ T*T*A*G * C*A*T * T*T*T * T*A*C * G*A*T * T*T*T 3′
allPS 18mer (5′N-3)	5′ T*A*G * C*A*T * T*T*T * T*A*C * G*A*T * T*T*T 3′
kratší ON (studium metabolitů)	
2mer allPO	5′ TT 3′
2mer allPS	5′ T*T 3′
3mer allPO	5′ TTT 3′
3mer allPS	5′ T*T*T 3′
4mer allPO	5′ TTTT 3′
4mer allPS	5′ T*T*T*T 3′
5mer allPO	5′ TTTTT 3′
5mer allPS	5′ T*T*T*T*T 3′
6mer allPO	5′ TTTTTT 3′
6mer 1PS3′	5′ TTTTT*T 3′
6mer 2PS3′	5′ TTTT*T*T 3′
6mer 3PS3′	5′ TTT*T*T*T 3′
6mer 4PS3′	5′ TT*T*T*T*T 3′
6mer allPS	5′ T*T*T*T*T*T 3′
Analogy nusinersenu	
OL1 allPO 18 mer (RNA)	5' UCACUUUCAUAAUGCUGG 3'
OL2 allPS 18 mer (RNA)	5' U*C*A*C*U*U*U*C*A*U*A*A*U*G*C*U*G*G 3'
Nusinersen	
[2'-O-(2-methoxyethyl)] 5′mU*mC*A*mC*mU*mU*mU*mC*A*mU*A*A*mU*G*mC-mU*G*G 3′	

allPO značí nemodifikovaný ON, allPS značí plně modifikovaný ON, 5′N-1 značí ON zkrácený o 1 nukleobázi na 5′konci (typická nečistota)

5 Závěr

Předkládaná disertační práce je souborem 10 publikací, které lze rozdělit do tří na sebe navazujících tematických celků.

První část práce je věnována detailní charakterizaci interakčního potenciálu vybraných stacionárních fází. K tomuto účelu byly použity jak jednoduché chromatografické testy (např. Waltersův test), tak i komplexnější přístupy (LFER model), jejichž výsledky jednoznačně korelují. Kromě vlivu typu samotného ligandu a endkapingu byl ukázán i velmi významný vliv typu částic na retenci, selektivitu a tvar píků. Zatímco SF s BEH částicemi vykazují konstantní chromatografické chování v celém rozsahu pH, CSH částice poskytují aniontově-výměnný charakter v pH < 6 z důvodu přítomnosti pyridylové skupiny na jejich povrchu. HSS částice významně umocňují efekt residuálních silanolů, který se začíná projevovat již v pH ~ 5 zvýšením retence kladně nabitých analytů, a naopak snížením retence analytů záporně nabitých. Mix-mód kolona Premier BEH C18AX vykazovala nejvyšší hydrofobicitu z testovaných kolon a zároveň poskytovala aniontově-výměnný charakter až do pH ~ 7,5, a to z důvodu přítomnosti terciárního amonia. Pro detailní charakterizaci elektrostatických interakcí byla vyvinuta nová metoda, která využívá čistě vodné MF se stabilní iontovou silou, které je možné připravit v malých rozestupech pH (dichloroctová kyselina + vodný roztok amoniaku). Aplikační potenciál testovaných kolon byl následně ověřen pro čtyři skupiny modelových sloučenin s různým charakterem, a to i) profeny (kyselé analyty); ii) deriváty kathinonů (bazické analyty); iii) flavony (neutrální analyty) a iv) dipeptidy (zwitterionické analyty).

Na základě dat získaných podrobnou charakterizací interakčních možností různých SF, byly pro druhou část práce zaměřenou na chromatografii peptidů a proteinů vybrány kolony s mix-mód charakterem. Výběr vhodného pH a koncentrace vodné složky MF se ukázal jako klíčový pro různě dlouhé peptidy, a to nejen z hlediska retence, ale také symetrie píků. Na základě komplexního popisu vlivu různých chromatografických podmínek na retenci a symetrii píků peptidů byla vyvinuta nová metoda pro on-line štěpení proteinů s následnou separací na mix-mód koloně v UHPLC. Před samotným on-line štěpením proteinů byl testován vliv chromatografických podmínek (teplota, pH, průtok, přítomnost organického modifikátoru) na aktivitu imobilizovaného trypsinu v IMER. Na základě získaných poznatků byly vybrány následující podmínky: teplota 37 °C; pH 8,5; gradient průtoku bez přítomnosti ACN na počátku gradientu, kdy dochází k samotnému

štěpení. V těchto podmínkách bylo následně on-line naštěpeno několik proteinů. Pro všechny proteiny byl získán srovnatelný nebo vyšší počet tryptických fragmentů v porovnání s off-line štěpením za využití „spin kolonek“, naopak množství i počet chymotryptických fragmentů a tzv. „miscleavage“ fragmentů byl v případě on-line štěpení větší. Vzhledem k využití MS detekce není vyšší množství těchto fragmentů významnou komplikací.

Třetí část práce je zaměřena na velmi aktuální téma, tj. terapeutické oligonukleotidy ve dvou módech kapalinové chromatografie, a to IPRPLC a HILIC. Oba módy jsou charakteristické komplexním retenčním mechanismem, ve kterém se uplatňuje více druhů interakčních mechanismů. Pro IPRPLC byl proveden detailní výzkum vlivu typu/hydrofobicity a koncentrace IP činidla (alkylamonium) a protiiontu (octan *vs.* HFIP) na potlačení separace diastereomerů thiofosfátových oligonukleotidů a rozlišení hlavního oligonukleotidu (*n*) a jeho kratšího analogu (*n-x* meru). Středně hydrofobní IP systémy (např. DBAA nebo HAA) vykazovaly nejvyšší selektivitu pro různě dlouhé ON a zároveň významně potlačovaly separaci diastereomerů thiofosfátových ON. Nahrazení octanu za HFIP vede k účinnějšímu potlačení separace diastereomerů (při použití stejného IP alkylaminu), ale snižuje selektivitu vůči ON s různou délkou. Detailní testování chromatografických podmínek ukázalo, že separační teplota hraje v analýze terapeutických PS ON významnou roli. S rostoucí teplotou roste potlačení separace diastereomerů, čímž dochází ke zúžení píků, což má za následek zlepšení separace ON s různou délkou. HILIC představuje alternativu k IPRPLC a při správném pochopení retenčních/interakčních mechanismů vykazuje vysoký potenciál pro separaci a následnou identifikaci nečistot a metabolitů PS ON, a to především z důvodu její bezproblémové kompatibility s MS detekcí. V optimalizovaných podmínkách byla identifikována řada nečistot analogu terapeutického ON nusinersenu. Výběr vhodných podmínek vedl k separaci a identifikaci několika metabolitů nusinersenu ve vzorku plasmy pacienta léčeného Spinrazou (účinná látka nusinersen), což potvrzuje vhodnost HILIC/MS metod pro reálné aplikace.

6 Zdroje

[1] A.D. LaFleur, K.A. Schug, A review of separation methods for the determination of estrogens and plastics-derived estrogen mimics from aqueous systems, Anal. Chim. Acta 696 (2011) 6–26. https://doi.org/10.1016/j.aca.2011.03.054.

[2] W. Fu, J. Min, W. Jiang, Y. Li, W. Zhang, Separation, characterization and identification of microplastics and nanoplastics in the environment, Sci. Total Environ. 721 (2020) 137561. https://doi.org/10.1016/j.scitotenv.2020.137561.

[3] E. de Rijke, P. Out, W.M.A. Niessen, F. Ariese, C. Gooijer, U.A.Th. Brinkman, Analytical separation and detection methods for flavonoids, J. Chromatogr. A 1112 (2006) 31–63. https://doi.org/10.1016/j.chroma.2006.01.019.

[4] K.D. Altria, Overview of capillary electrophoresis and capillary electrochromatography, J. Chromatogr. A 856 (1999) 443–463. https://doi.org/10.1016/S0021-9673(99)00830-4.

[5] D.J. Beale, F.R. Pinu, K.A. Kouremenos, M.M. Poojary, V.K. Narayana, B.A. Boughton, K. Kanojia, S. Dayalan, O.A.H. Jones, D.A. Dias, Review of recent developments in GC–MS approaches to metabolomics-based research, Metabolomics 14 (2018) 152. https://doi.org/10.1007/s11306-018-1449-2.

[6] P. Boeker, J. Leppert, Flow Field Thermal Gradient Gas Chromatography, Anal. Chem. 87 (2015) 9033–9041. https://doi.org/10.1021/acs.analchem.5b02227.

[7] I. Gavrilović, B. Wüst, J. Danaceau, E. Braidman, X. de la Torre, F. Botrè, M.K. Parr, D. Cowan, Routine application of SFC-MS in doping control: Analysis of 3 × 1000 urine samples using three different SFC-MS instruments, Drug Test. Anal. (2024) 1-11. https://doi.org/10.1002/dta.3652.

[8] C. Gita, K. Krishna, A review of HPLC technique covering its pharmaceutical, environmental, forensic, clinical and other applications, Int. J. Pharm. Chem. Anal. 6 (2019) 27–39. https://doi.org/10.18231/j.ijpca.2019.006.

[9] T. Yoshida, Peptide Separation in Normal Phase Liquid Chromatography, Anal. Chem. 69 (1997) 3038–3043. https://doi.org/10.1021/ac9702204.

[10] P. Žuvela, M. Skoczylas, J. Jay Liu, T. Bączek, R. Kaliszan, M.W. Wong, B. Buszewski, Column Characterization and Selection Systems in Reversed-Phase High-Performance Liquid Chromatography, Chem. Rev. 119 (2019) 3674–3729. https://doi.org/10.1021/acs.chemrev.8b00246.

[11] J.M. Herrero-Martínez, A. Méndez, E. Bosch, M. Rosés, Characterization of the acidity of residual silanol groups in microparticulate and monolithic reversed-phase columns, J. Chromatogr. A 1060 (2004) 135–145. https://doi.org/10.1016/j.chroma.2004.04.015

[12] L.A. Kennedy, W. Kopaciewicz, F.E. Regnier, Multimodal liquid chromatography columns for the separation of proteins in either the anion-exchange or hydrophobic-interaction mode, J. Chromatogr. A 359 (1986) 73–84. https://doi.org/10.1016/0021-9673(86)80063-2

[13] H. Qiu, A.K. Mallik, M. Takafuji, S. Jiang, H. Ihara, New poly(ionic liquid)-grafted silica multi-mode stationary phase for anion-exchange/reversed-phase/hydrophilic interaction liquid chromatography, The Analyst 137 (2012) 2553–2555. https://doi.org/10.1039/c2an35348b.

[14] T. Marunouchi, M. Ono, T. Nakajima, Y. Ito, T. Aketo, Simultaneous determination of active ingredients in an ophthalmic solution by isocratic tandem-mode HPLC connected reverse phase column and strong cation exchange column, J. Pharm. Biomed. Anal. 40 (2006) 331–337. https://doi.org/10.1016/j.jpba.2005.08.018.

[15] J.T. Eleveld, H.A. Claessens, J.L. Ammerdorffer, A.M. van Herk, C.A. Cramers,

Evaluation of mixed-mode stationary phases in liquid chromatography for the separation of charged and uncharged oligomer-like model compounds, J. Chromatogr. A 677 (1994) 211–227. https://doi.org/10.1016/0021-9673(94)80150-9.

[16] R. Nogueira, M. Lämmerhofer, W. Lindner, Alternative high-performance liquid chromatographic peptide separation and purification concept using a new mixed-mode reversed-phase/weak anion-exchange type stationary phase, J. Chromatogr. A 1089 (2005) 158–169. https://doi.org/10.1016/j.chroma.2005.06.093

[17] K. Zhang, X. Liu, Reprint of "Mixed-mode chromatography in pharmaceutical and biopharmaceutical applications," J. Pharm. Biomed. Anal. 130 (2016) 19–34. https://doi.org/10.1016/j.jpba.2016.09.013.

[18] L. Wang, W. Wei, Z. Xia, X. Jie, Z.Z. Xia, Recent advances in materials for stationary phases of mixed-mode high-performance liquid chromatography, TrAC Trends Anal. Chem. 80 (2016) 495–506. https://doi.org/10.1016/j.trac.2016.04.001.

[19] X. Qiao, L. Zhang, N. Zhang, X. Wang, X. Qin, H. Yan, H. Liu, Imidazolium embedded C8 based stationary phase for simultaneous reversed-phase/hydrophilic interaction mixed-mode chromatography, J. Chromatogr. A 1400 (2015) 107–116. https://doi.org/10.1016/j.chroma.2015.04.060.

[20] Q. Wang, M. Ye, L. Xu, Z. Shi, A reversed-phase/hydrophilic interaction mixed-mode C18-Diol stationary phase for multiple applications, Anal. Chim. Acta 888 (2015) 182–190. https://doi.org/10.1016/j.aca.2015.06.058.

[21] H. Aral, K.S. Çelik, R. Altındağ, T. Aral, Synthesis, characterization, and application of a novel multifunctional stationary phase for hydrophilic interaction/reversed phase mixed-mode chromatography, Talanta 174 (2017) 703–714. https://doi.org/10.1016/j.talanta.2017.07.014

[22] Y. Li, Z. Xu, Y. Feng, X. Liu, T. Chen, H. Zhang, Preparation and Evaluation of Poly-l-Lysine Stationary Phase for Hydrophilic Interaction/Reversed-Phase Mixed-Mode Chromatography, Chromatographia 74 (2011) 523–530. https://doi.org/10.1007/s10337-011-2120-5.

[23] M. Mattarozzi, N. Riboni, M. Maffini, S. Scarpella, F. Bianchi, M. Careri, Reversed-phase and weak anion-exchange mixed-mode stationary phase for fast separation of medium-, long- and very long chain free fatty acids by ultra-high-performance liquid chromatography-high resolution mass spectrometry, J. Chromatogr. A 1648 (2021) 462209. https://doi.org/10.1016/j.chroma.2021.462209.

[24] F. Yang, Q. Bai, K. Zhao, D. Gao, L. Tian, Preparation of a novel weak cation exchange/hydrophobic interaction chromatography dual-function polymer-based stationary phase for protein separation using "thiol–ene click chemistry," Anal. Bioanal. Chem. 407 (2015) 1721–1734. https://doi.org/10.1007/s00216-014-8400-9.

[25] N.H. Davies, M.R. Euerby, D.V. McCalley, A study of retention and overloading of basic compounds with mixed-mode reversed-phase/cation-exchange columns in high performance liquid chromatography, J. Chromatogr. A 1138 (2007) 65–72. https://doi.org/10.1016/j.chroma.2006.10.002.

[26] Z. Kadlecová, K. Kalíková, M. Ansorge, M. Gilar, E. Tesařová, The effect of particle and ligand types on retention and peak shape in liquid chromatography, Microchem. J. 159 (2020) 105466. https://doi.org/10.1016/j.microc.2020.105466.

[27] F. Gritti, G. Guiochon, Adsorption behaviors of neutral and ionizable compounds on hybrid stationary phases in the absence (BEH-C18) and the presence (CSH-C18) of immobile surface charges, J. Chromatogr. A 1282 (2013) 58–71. https://doi.org/10.1016/j.chroma.2013.01.024.

[28] S. Khater, C. West, E. Lesellier, Characterization of five chemistries and three particle sizes of stationary phases used in supercritical fluid chromatography, J. Chromatogr. A 1319 (2013) 148–159. https://doi.org/10.1016/j.chroma.2013.10.037.
[29] P. Kozlik, J. Vaclova, K. Kalikova, Mixed-mode hydrophilic interaction/ion-exchange liquid chromatography – Separation potential in peptide analysis, Microchem. J. 165 (2021) 106158. https://doi.org/10.1016/j.microc.2021.106158.
[30] S. Alharthi, A. Ali, M. Iqbal, A. Ibrar, B. Ahmad, S. Nisa, F. Mabood, Preparation of mixed-mode stationary phase for separation of peptides and proteins in high performance liquid chromatography, Sci. Rep. 12 (2022) 4061. https://doi.org/10.1038/s41598-022-08074-7.
[31] M. Hosokawa, K. Goto, S. Tanaka, K. Ueda, S. Iwakawa, K. Ogawara, Optimization of Analytical Conditions for Hydrophilic Nucleic Acids Using Mixed-Mode and Reversed-Phase Pentabromobenzyl Columns, Chem. Pharm. Bull. 68 (2020) 1233–1237. https://doi.org/10.1248/cpb.c20-00448.
[32] A. Goyon, P. Yehl, K. Zhang, Characterization of therapeutic oligonucleotides by liquid chromatography, J. Pharm. Biomed. Anal. 182 (2020) 113105. https://doi.org/10.1016/j.jpba.2020.113105.
[33] M. Song, H. Yang, W. Cao, Q. Liu, Separation of bispecific antibody related impurities with mixed-mode chromatography, Process Biochem. 132 (2023) 110–120. https://doi.org/10.1016/j.procbio.2023.07.004.
[34] Milne, J.J., Mixed-Mode Chromatography and Its Role in Monoclonal Antibody Purification. In: Loughran, S.T., Milne, J.J. (eds) Protein Chromatography. Methods in Molecular Biology, 2699 (2023) 15-29. https://doi.org/10.1007/978-1-0716-3362-5_2
[35] A.J. Alpert, Hydrophilic-interaction chromatography for the separation of peptides, nucleic acids and other polar compounds, J. Chromatogr. A 499 (1990) 177–196. https://doi.org/10.1016/S0021-9673(00)96972-3.
[36] J.C. Linden, C.L. Lawhead, Liquid chromatography of saccharides, J. Chromatogr. A 105 (1975) 125–133. https://doi.org/10.1016/S0021-9673(01)81096-7
[37] M.R. Gama, R.G. da Costa Silva, C.H. Collins, C.B. Bottoli, Hydrophilic interaction chromatography, TrAC Trends Anal. Chem. 37 (2012) 48–60. https://doi.org/10.1039/9781839163524-00069
[38] X. Liu, Y. Jiang, F. Zhang, Z. Li, B. Yang, Preparation and evaluation of a polymer-based sulfobetaine zwitterionic stationary phase, J. Chromatogr. A 1649 (2021) 462229. https://doi.org/10.1016/j.chroma.2021.462229.
[39] D.V. McCalley, Is hydrophilic interaction chromatography with silica columns a viable alternative to reversed-phase liquid chromatography for the analysis of ionisable compounds?, J. Chromatogr. A 1171 (2007) 46–55. https://doi.org/10.1016/j.chroma.2007.09.047
[40] E. Cífková, R. Hájek, M. Lísa, M. HolĽapek, Hydrophilic interaction liquid chromatography mass spectrometry of (lyso)phosphatidic acids, (lyso)phosphatidylserines and other lipid classes, J. Chromatogr. A 1439 (2016) 65–73. https://doi.org/10.1016/j.chroma.2016.01.064.
[41] Y. Guo, N. Bhalodia, B. Fattal, I. Serris, Evaluating the Adsorbed Water Layer on Polar Stationary Phases for Hydrophilic Interaction Chromatography (HILIC), Separations 6 (2019) 19. https://doi.org/10.3390/separations6020019
[42] B. Buszewski, S. Noga, Hydrophilic interaction liquid chromatography (HILIC)-a powerful separation technique, Anal. Bioanal. Chem. 402 (2012) 231–247. https://doi.org/10.1007/s00216-011-5308-5.

[43] D.V. McCalley, U.D. Neue, Estimation of the extent of the water-rich layer associated with the silica surface in hydrophilic interaction chromatography, J. Chromatogr. A 1192 (2008) 225–229. https://doi.org/10.1016/j.chroma.2008.03.049.
[44] P. Hemstrom, K. Irgum, Hydrophilic interaction chromatography, J. Sep. Sci. 29 (2006) 1784–1821. https://doi.org/10.1002/jssc.200600199.
[45] D.V. McCalley, Study of the selectivity, retention mechanisms and performance of alternative silica-based stationary phases for separation of ionised solutes in hydrophilic interaction chromatography, J. Chromatogr. A 1217 (2010) 3408–3417. https://doi.org/10.1016/j.chroma.2010.03.011.
[46] Y. Guo, Recent progress in the fundamental understanding of hydrophilic interaction chromatography (HILIC), Analyst 140 (2015) 6452–6466. https://doi.org/10.1039/c5an00670h.
[47] C. Erkmen, W.H. Gebrehiwot, B. Uslu, Hydrophilic Interaction Liquid Chromatography (HILIC): Latest Applications in the Pharmaceutical Researches, Curr. Pharm. Anal. 17 (2021) 316–345. https://doi.org/10.2174/1573412916666200402101501
[48] G. Szabovik, Z. Béni, HILIC-UV determination of lysine and chloride counterions in active pharmaceutical ingredients, J. Pharm. Biomed. Anal. 226 (2023) 115245. https://doi.org/10.1016/j.jpba.2023.115245.
[49] F. Hosseinkhani, L. Huang, A.-C. Dubbelman, F. Guled, A.C. Harms, T. Hankemeier, Systematic Evaluation of HILIC Stationary Phases for Global Metabolomics of Human Plasma, Metabolites 12 (2022) 165. https://doi.org/10.3390/metabo12020165.
[50] N.V. Basov, A.D. Rogachev, M.A. Aleshkova, E.V. Gaisler, Y.S. Sotnikova, Y.V. Patrushev, T.G. Tolstikova, O.I. Yarovaya, A.G. Pokrovsky, N.F. Salakhutdinov, Global LC-MS/MS targeted metabolomics using a combination of HILIC and RP LC separation modes on an organic monolithic column based on 1-vinyl-1,2,4-triazole, Talanta 267 (2024) 125168. https://doi.org/10.1016/j.talanta.2023.125168.
[51] K. Molnarova, P. Kozlík, Comparison of Different HILIC Stationary Phases in the Separation of Hemopexin and Immunoglobulin G Glycopeptides and Their Isomers, Molecules 25 (2020) 4655. https://doi.org/10.3390/molecules25204655.
[52] S. Eksborg, P.-O. Lagerström, R. Modin, G. Schill, Ion-pair chromatography of organic compounds, J. Chromatogr. A 83 (1973) 99–110. https://doi.org/10.1016/S0021-9673(00)97031-6
[53] G. Schill, High performance ion-pair chromatography, J. Biochem. Biophys. Methods 18 (1989) 249–270. https://doi.org/10.1016/0165-022x(89)90035-3.
[54] C. Horvath, W. Melander, I. Molnar, P. Molnar, Enhancement of retention by ion-pair formation in liquid chromatography with nonpolar stationary phases, Anal. Chem. 49 (1977) 2295–2305.
[55] J.C. Kraak, K.M. Jonker, J.F.K. Huber, Solvent-generated ion-exchange systems with anionic surfactants for rapid separations of amino acids, J. Chromatogr. A 142 (1977) 671–688. https://doi.org/10.1016/S0021-9673(01)92076-X.
[56] S.L. Gelhaus, W.R. LaCourse, Separation of modified 2′-deoxyoligonucleotides using ion-pairing reversed-phase HPLC, J. Chromatogr. B 820 (2005) 157–163. https://doi.org/10.1016/j.jchromb.2005.02.024.
[57] M.J. Walters, Classification of octadecyl-bonded liquid chromatography columns., J.-Assoc. Off. Anal. Chem. 70 (1987) 465–469.
[58] K. Kimata, K. Iwaguchi, S. Onishi, K. Jinno, R. Eksteen, K. Hosoya, M. Araki, N. Tanaka, Chromatographic Characterization of Silica C18 Packing Materials.

Correlation between a Preparation Method and Retention Behavior of Stationary Phase, J. Chromatogr. Sci. 27 (1989) 721–728. https://doi.org/10.1093/chromsci/27.12.721.
[59] M.H. Abraham, Scales of solute hydrogen-bonding: their construction and application to physicochemical and biochemical processes, Chem. Soc. Rev. 22 (1993) 73–83. https://doi.org/10.1039/CS9932200073
[60] S. Soriano-Meseguer, E. Fuguet, M.H. Abraham, A. Port, M. Rosés, Linear free energy relationship models for the retention of partially ionized acid-base compounds in reversed-phase liquid chromatography, J. Chromatogr. A 1635 (2021) 461720. https://doi.org/10.1016/j.chroma.2020.461720.
[61] M.H. Abraham, W.E. Acree, Descriptors for ions and ion-pairs for use in linear free energy relationships, J. Chromatogr. A 1430 (2016) 2–14. https://doi.org/10.1016/j.chroma.2015.07.023.
[62] M.H. Abraham, Y.H. Zhao, Determination of Solvation Descriptors for Ionic Species: Hydrogen Bond Acidity and Basicity, J. Org. Chem. 69 (2004) 4677–4685. https://doi.org/10.1021/jo049766y.
[63] C.F. Poole, S.N. Atapattu, S.K. Poole, A.K. Bell, Determination of solute descriptors by chromatographic methods, Anal. Chim. Acta 652 (2009) 32–53. https://doi.org/10.1016/j.aca.2009.04.038
[64] D. Sykora, E. Tesarová, D.W. Armstrong, Practical considerations of the influence of organic modifiers on the ionization of analytes and buffers in reversed-phase LC, LC GC N. Am. 20 (2002) 974–981.
[65] X. Wang, S.G. Codreanu, B. Wen, K. Li, M.C. Chambers, D.C. Liebler, B. Zhang, Detection of Proteome Diversity Resulted from Alternative Splicing is Limited by Trypsin Cleavage Specificity, Mol. Cell. Proteomics 17 (2018) 422–430. https://doi.org/10.1074/mcp.RA117.000155.
[66] J.M. Burkhart, C. Schumbrutzki, S. Wortelkamp, A. Sickmann, R.P. Zahedi, Systematic and quantitative comparison of digest efficiency and specificity reveals the impact of trypsin quality on MS-based proteomics, J. Proteomics 75 (2012) 1454–1462. https://doi.org/10.1016/j.jprot.2011.11.016.
[67] E. Vandermarliere, M. Mueller, L. Martens, Getting intimate with trypsin, the leading protease in proteomics, Mass Spectrom. Rev. 32 (2013) 453–465. https://doi.org/10.1002/mas.21376.
[68] J.V. Olsen, S.-E. Ong, M. Mann, Trypsin Cleaves Exclusively C-terminal to Arginine and Lysine Residues, Mol. Cell. Proteomics 3 (2004) 608–614. https://doi.org/10.1074/mcp.T400003-MCP200.
[69] A.F.M. Altelaar, J. Munoz, A.J.R. Heck, Next-generation proteomics: towards an integrative view of proteome dynamics, Nat. Rev. Genet. 14 (2013) 35–48. https://doi.org/10.1038/nrg3356.
[70] M. Naldi, U. Černigoj, A. Štrancar, M. Bartolini, Towards automation in protein digestion: Development of a monolithic trypsin immobilized reactor for highly efficient on-line digestion and analysis, Talanta 167 (2017) 143–157. https://doi.org/10.1016/j.talanta.2017.02.016.
[71] W. Rick, Trypsin, in: H.U. Bergmeyer (Ed.), Methods Enzym. Anal. 2 (1974) 1013–1024. https://doi.org/10.1016/B978-0-12-091302-2.50099-2.
[72] H. Schaefer, D.C. Chamrad, K. Marcus, K.A. Reidegeld, M. Blüggel, H.E. Meyer, Tryptic transpeptidation products observed in proteome analysis by liquid chromatography-tandem mass spectrometry, PROTEOMICS 5 (2005) 846–852. https://doi.org/10.1002/pmic.200401203.
[73] F. Dycka, V. Franc, P. Frycák, M. Raus, P. Rehulka, R. Lenobel, G. Allmaier, M.

Marchetti-Deschmann, M. Sebela, Evaluation of Pseudotrypsin Cleavage Specificity Towards Proteins by MALDI-TOF Mass Spectrometry, Protein Pept. Lett. 22 (2015) 1123–1132. https://doi.org/10.2174/0929866522666151008151617
[74] T. Šlechtová, M. Gilar, K. Kalíková, S.M. Moore, J.W. Jorgenson, E. Tesařová, Performance comparison of three trypsin columns used in liquid chromatography, J. Chromatogr. A 1490 (2017) 126–132. https://doi.org/10.1016/j.chroma.2017.02.024.
[75] L.R. Riviere, P. Tempst, Enzymatic digestion of proteins in solution, Curr. Protoc. Protein Sci. (1995) 11–1. https://doi.org/10.1002/0471140864.ps1101s00
[76] B. Stefansson, L. Helgadóttir, S. Olafsdottir, Á. Gudmundsdottir, J.B. Bjarnason, Characterization of cold-adapted Atlantic cod (Gadus morhua) trypsin I - Kinetic parameters, autolysis and thermal stability, Comp. Biochem. Physiol. B Biochem. Mol. Biol. 155 (2010) 186–194. https://doi.org/10.1016/j.cbpb.2009.11.004.
[77] S. Moore, S. Hess, J. Jorgenson, Characterization of an immobilized enzyme reactor for on-line protein digestion, J. Chromatogr. A 1476 (2016) 1–8. https://doi.org/10.1016/j.chroma.2016.11.021.
[78] F.E. Regnier, J. Kim, Accelerating trypsin digestion: the immobilized enzyme reactor, Bioanalysis 6 (2014) 2685–2698. https://doi.org/10.4155/bio.14.216.
[79] S. A. Currivan, W. Q. Chen, R. Wilson, E.S. Rodriguez, N. Upadhyay, D. Connolly, P. N. Nesterenko, B. Paull, Multi-lumen capillary based trypsin micro-reactor for the rapid digestion of proteins, Analyst 143 (2018) 4944–4953. https://doi.org/10.1039/C8AN01330F.
[80] S. Liu, H. Bao, L. Zhang, G. Chen, Efficient proteolysis strategies based on microchip bioreactors, J. Proteomics 82 (2013) 1–13. https://doi.org/10.1016/j.jprot.2013.02.012
[81] G. Massolini, E. Calleri, Immobilized trypsin systems coupled on-line to separation methods: Recent developments and analytical applications, J. Sep. Sci. 28 (2005) 7–21. https://doi.org/10.1002/jssc.200401941.
[82] G.W. Slysz, D.C. Schriemer, On-column digestion of proteins in aqueous-organic solvents, Rapid Commun. Mass Spectrom. 17 (2003) 1044–1050. https://doi.org/10.1002/rcm.1022.
[83] D. López-Ferrer, K. Petritis, N.M. Lourette, B. Clowers, K.K. Hixson, T. Heibeck, D.C. Prior, L. Paša-Tolić, D.G.I. Camp, M.E. Belov, R.D. Smith, On-line Digestion System for Protein Characterization and Proteome Analysis, Anal. Chem. 80 (2008) 8930–8936. https://doi.org/10.1021/ac800927v.
[84] A. Goyon, B. Scott, K. Kurita, C. Maschinot, K. Meyer, P. Yehl, K. Zhang, On-line Sequencing of CRISPR Guide RNAs and Their Impurities via the Use of Immobilized Ribonuclease Cartridges Attached to a 2D/3D-LC–MS System, Anal. Chem. 94 (2022) 1169–1177. https://doi.org/10.1021/acs.analchem.1c04350.
[85] Z. Kadlecová, P. Kozlík, E. Tesařová, M. Gilar, K. Kalíková, Characterization and comparison of mixed-mode and reversed-phase columns; interaction abilities and applicability for peptide separation, J. Chromatogr. A 1648 (2021) 462182. https://doi.org/10.1016/j.chroma.2021.462182.
[86] E.C. Kuijper, A.J. Bergsma, W.W.M.P. Pijnappel, A. Aartsma-Rus, Opportunities and challenges for antisense oligonucleotide therapies, J. Inherit. Metab. Dis. 44 (2021) 72–87. https://doi.org/10.1002/jimd.12251.
[87] S. Bajan, G. Hutvagner, RNA-Based Therapeutics: From Antisense Oligonucleotides to miRNAs, Cells 9 (2020) 137. https://doi.org/10.3390/cells9010137.
[88] D. Al Shaer, O. Al Musaimi, F. Albericio, B.G. de la Torre, 2023 FDA TIDES

(Peptides and Oligonucleotides) Harvest, Pharmaceuticals 17 (2024) 243. https://doi.org/10.3390/ph17020243.
[89] E.E. Neil, E.K. Bisaccia, Nusinersen: A Novel Antisense Oligonucleotide for the Treatment of Spinal Muscular Atrophy, J. Pediatr. Pharmacol. Ther. 24 (2019) 194–203. https://doi.org/10.5863/1551-6776-24.3.194.
[90] M. Bege, A. Borbás, Rise and fall of fomivirsen, the first approved gene silencing medicine – A historical review, Acta Pharm. Hung. 92 (2022) 38–44. https://doi.org/10.33892/aph.2022.92.38-44.
[91] B.P. Monia, J.F. Johnston, H. Sasmor, L.L. Cummins, Nuclease Resistance and Antisense Activity of Modified Oligonucleotides Targeted to Ha-ras, J. Biol. Chem. 271 (1996) 14533–14540. https://doi.org/10.1074/jbc.271.24.14533.
[92] T.C. Roberts, R. Langer, M.J.A. Wood, Advances in oligonucleotide drug delivery, Nat. Rev. Drug Discov. 19 (2020) 673–694. https://doi.org/10.1038/s41573-020-0075-7.
[93] D. Yu, E.R. Kandimalla, A. Roskey, Q. Zhao, L. Chen, J. Chen, S. Agrawal, Stereo-enriched phosphorothioate oligodeoxynucleotides: synthesis, biophysical and biological properties, Bioorg. Med. Chem. 8 (2000) 275–284. https://doi.org/10.1016/S0968-0896(99)00275-8.
[94] W.J. Stec, G. Zon, B. Uznański, Reversed-phase high-performance liquid chromatographic separation of diastereomeric phosphorothioate analogues of oligodeoxyribonucleotides and other backbone-modified congeners of dna, J. Chromatogr. A 326 (1985) 263–280. https://doi.org/10.1016/S0021-9673(01)87452-5.
[95] Z. Kadlecová, K. Kalíková, E. Tesařová, M. Gilar, Phosphorothioate oligonucleotides separation in ion-pairing reversed-phase liquid chromatography: Effect of ion-pairing system, J. Chromatogr. A 1676 (2022) 463201. https://doi.org/10.1016/j.chroma.2022.463201.
[96] D. Capaldi, A. Teasdale, S. Henry, N. Akhtar, C. den Besten, S. Gao-Sheridan, M. Kretschmer, N. Sharpe, B. Andrews, B. Burm, J. Foy, Impurities in Oligonucleotide Drug Substances and Drug Products, Nucleic Acid Ther. 27 (2017) 309–322. https://doi.org/10.1089/nat.2017.0691.
[97] J. Kim, B. Basiri, C. Hassan, C. Punt, E. van der Hage, C. den Besten, M.G. Bartlett, Metabolite Profiling of the Antisense Oligonucleotide Eluforsen Using Liquid Chromatography-Mass Spectrometry, Mol. Ther. - Nucleic Acids 17 (2019) 714–725. https://doi.org/10.1016/j.omtn.2019.07.006.
[98] M. Donegan, J.M. Nguyen, M. Gilar, Effect of ion-pairing reagent hydrophobicity on liquid chromatography and mass spectrometry analysis of oligonucleotides, J. Chromatogr. A 1666 (2022) 462860. https://doi.org/10.1016/j.chroma.2022.462860.
[99] S. Studzińska, R. Rola, B. Buszewski, The impact of ion-pairing reagents on the selectivity and sensitivity in the analysis of modified oligonucleotides in serum samples by liquid chromatography coupled with tandem mass spectrometry, J. Pharm. Biomed. Anal. 138 (2017) 146–152. https://doi.org/10.1016/j.jpba.2017.02.014.
[100] K.J. Fountain, M. Gilar, J.C. Gebler, Analysis of native and chemically modified oligonucleotides by tandem ion-pair reversed-phase high-performance liquid chromatography/electrospray ionization mass spectrometry, Rapid Commun. Mass Spectrom. 17 (2003) 646–653. https://doi.org/10.1002/rcm.959.
[101] N. Li, N.M. El Zahar, J.G. Saad, E.R.E. van der Hage, M.G. Bartlett, Alkylamine ion-pairing reagents and the chromatographic separation of oligonucleotides, J. Chromatogr. A 1580 (2018) 110–119.

https://doi.org/10.1016/j.chroma.2018.10.040.
[102] M. Gilar, K.J. Fountain, Y. Budman, J.L. Holyoke, H. Davoudi, J.C. Gebler, Characterization of Therapeutic Oligonucleotides Using Liquid Chromatography with On-line Mass Spectrometry Detection, Oligonucleotides 13 (2003) 229–243. https://doi.org/10.1089/154545703322460612.
[103] A. Apffel, J.A. Chakel, S. Fischer, K. Lichtenwalter, W.S. Hancock, Analysis of Oligonucleotides by HPLC−Electrospray Ionization Mass Spectrometry, Anal. Chem. 69 (1997) 1320–1325. https://doi.org/10.1021/ac960916h.
[104] L. Guo, A.J. Worth, C. Mesaros, N.W. Snyder, J.D. Glickson, I.A. Blair, Diisopropylethylamine/hexafluoroisopropanol-mediated ion-pairing ultra-high-performance liquid chromatography/mass spectrometry for phosphate and carboxylate metabolite analysis: utility for studying cellular metabolism, Rapid Commun. Mass Spectrom. 30 (2016) 1835–1845. https://doi.org/10.1002/rcm.7667.
[105] T. Chen, S. Tang, Y. Fu, J.G. Napolitano, K. Zhang, Analytical techniques for characterizing diastereomers of phosphorothioated oligonucleotides, J. Chromatogr. A 1678 (2022) 463349. https://doi.org/10.1016/j.chroma.2022.463349.
[106] A. Goyon, M.S. Blevins, J.G. Napolitano, D. Nguyen, M. Goel, B. Scott, J. Wang, S.G. Koenig, T. Chen, K. Zhang, Characterization of antisense oligonucleotide and guide ribonucleic acid diastereomers by hydrophilic interaction liquid chromatography coupled to mass spectrometry, J. Chromatogr. A 1708 (2023) 464327. https://doi.org/10.1016/j.chroma.2023.464327.
[107] J.M. Sutton, G.J. Guimaraes, V. Annavarapu, W.D. van Dongen, M.G. Bartlett, Current State of Oligonucleotide Characterization Using Liquid Chromatography–Mass Spectrometry: Insight into Critical Issues, J. Am. Soc. Mass Spectrom. 31 (2020) 1775–1782. https://doi.org/10.1021/jasms.0c00179.
[108] M. Huang, X. Xu, H. Qiu, N. Li, Analytical characterization of DNA and RNA oligonucleotides by hydrophilic interaction liquid chromatography-tandem mass spectrometry, J. Chromatogr. A 1648 (2021) 462184. https://doi.org/10.1016/j.chroma.2021.462184.
[109] J. Olšovská, M. Jurková, Nové trendy v kapalinové chromatografii a jejich využití v analýze piva a pivovarských surovin. Část 1. Teoretický úvod., Kvas. Prům. 58 (2012) 30–35. https://doi.org/10.18832/kp2012005.
[110] R.-I. Chirita, C. West, S. Zubrzycki, A.-L. Finaru, C. Elfakir, Investigations on the chromatographic behaviour of zwitterionic stationary phases used in hydrophilic interaction chromatography, J. Chromatogr. A 1218 (2011) 5939–5963. https://doi.org/10.1016/j.chroma.2011.04.002
[111] T.H. Walter, M. Blaze M. T., C. Boissel, Electrospray ionization mass spectrometry ion suppression/enhancement caused by column bleed for three mixed-mode reversed-phase/anion-exchange high-performance liquid chromatography columns, Rapid Commun. Mass Spectrom. 35 (2021) e9098. https://doi.org/10.1002/rcm.9098.
[112] M. Malý, Z. Kadlecová, P. Dubský, K. Kalíková, Semi-empirical description of a retention of small organic probes on AtlantisTM Premier BEH C18 AX mixed-mode column under varying pH and organic modifier conditions, Microchem. J. 191 (2023) 108910. https://doi.org/10.1016/j.microc.2023.108910
[113] K. Shimura, K. Kamiya, H. Matsumoto, K. Kasai, Fluorescence-Labeled Peptide pI Markers for Capillary Isoelectric Focusing, Anal. Chem. 74 (2002) 1046–1053. https://doi.org/10.1021/ac0108010.
[114] PeptideMass, https://web.expasy.org/peptide_mass/ (accessed May 30, 2024).
[115] M. Donegan, J.M. Nguyen, M. Gilar, Effect of ion-pairing reagent hydrophobicity

on liquid chromatography and mass spectrometry analysis of oligonucleotides, J. Chromatogr. A 1666 (2022) 462860. https://doi.org/10.1016/j.chroma.2022.462860.
[116] M. Enmark, J. Bagge, J. Samuelsson, L. Thunberg, E. Örnskov, H. Leek, F. Limé, T. Fornstedt, Analytical and preparative separation of phosphorothioated oligonucleotides: columns and ion-pair reagents, Anal. Bioanal. Chem. 412 (2020) 299–309. https://doi.org/10.1007/s00216-019-02236-9.
[117] T. Fornstedt, M. Enmark, Separation of therapeutic oligonucleotides using ion-pair reversed-phase chromatography based on fundamental separation science, J. Chromatogr. Open 3 (2023) 100079. https://doi.org/10.1016/j.jcoa.2023.100079.
[118] S.M. McCarthy, M. Gilar, J. Gebler, Reversed-phase ion-pair liquid chromatography analysis and purification of small interfering RNA, Anal. Biochem. 390 (2009) 181–188. https://doi.org/10.1016/j.ab.2009.03.042.
[119] S. Shin, H.-J. Yang, J. Kim, J. Kim, J. Lee, K.H. Park, H.S. Kim, J. Kim, Clarification of a peak at m/z 1634 from tryptically digested cytochrome c, J. Mass Spectrom. 47 (2012) 1576–1581. https://doi.org/10.1002/jms.3119.

7 Doplňková data

Tabulka S1: Hodnoty regresních koeficientů LFER modelu podle rovnice 1.1. (statisticky významné koeficienty jsou uvedeny tučně). Složení MF: ACN/kyselina mravenčí, pH 2,1; 40/60 (*v/v*). Deskriptory D^- and D^+ byly vypočteny za použití pH vodně-organické MF (pH* 2,4)

Kolona		*a*	*b*	*d*⁻	*d*⁺	*e*	*s*	*v*	*c*	R^2	*N*
XSelect CSH C18	hodnota	**-0,46**	**-1,65**	0,13	**-0,37**	0,24	-0,23	**1,77**	**-0,64**		
	p-hodnota	0,00	0,00	0,64	0,00	0,06	0,11	0,00	0,00	0,936	68
	±CI	0,21	0,23	0,53	0,22	0,25	0,29	0,33	0,31		
XSelect CSH FP	hodnota	**-0,32**	**-1,12**	0,15	**-0,36**	**0,22**	-0,13	**1,09**	**-0,60**		
	p-hodnota	0,00	0,00	0,41	0,00	0,01	0,18	0,00	0,00	0,937	68
	±CI	0,14	0,15	0,37	0,15	0,17	0,20	0,23	0,22		
XSelect CSH PH	hodnota	**-0,31**	**-1,33**	0,00	**-0,42**	0,18	-0,18	**1,41**	**-0,55**		
	p-hodnota	0,00	0,00	0,99	0,00	0,07	0,12	0,00	0,00	0,941	68
	±CI	0,16	0,18	0,42	0,18	0,20	0,23	0,26	0,24		
XSelect HSS C18	hodnota	**-0,54**	**-1,64**	0,10	**-0,37**	0,25	-0,29	**1,75**	**-0,39**		
	p-hodnota	0,00	0,00	0,73	0,00	0,06	0,06	0,00	0,02	0,933	68
	±CI	0,22	0,24	0,56	0,24	0,26	0,21	0,35	0,33		
XSelect HSS C18 SB	hodnota	**-0,51**	**-1,22**	-0,34	**-0,36**	0,18	-0,14	**1,45**	**-0,62**		
	p-hodnota	0,00	0,00	0,11	0,00	0,06	0,20	0,00	0,00	0,946	68
	±CI	0,16	0,17	0,41	0,17	0,19	0,22	0,26	0,24		
XSelect HSS PFP	hodnota	**-0,32**	**-1,43**	**-0,51**	**0,37**	**0,25**	-0,20	**1,40**	**-0,56**		
	p-hodnota	0,00	0,00	0,02	0,00	0,02	0,09	0,00	0,00	0,924	68
	±CI	0,17	0,18	0,43	0,18	0,20	0,23	0,27	0,25		
XBridge C18	hodnota	**-0,57**	**-1,47**	0,03	**-0,29**	**0,27**	**-0,31**	**1,57**	**-0,44**		
	p-hodnota	0,00	0,00	0,91	0,02	0,05	0,05	0,00	0,01	0,921	68
	±CI	0,22	0,24	0,57	0,24	0,27	0,31	0,35	0,34		
XBridge Shield RP18	hodnota	**-0,33**	**-1,61**	-0,03	**-0,38**	**0,27**	-0,21	**1,54**	**-0,50**		
	p-hodnota	0,00	0,00	0,89	0,00	0,02	0,13	0,00	0,00	0,936	68
	±CI	0,19	0,21	0,50	0,21	0,23	0,27	0,31	0,29		

±CI interval spolehlivosti, R^2 koeficient determinace, *N* počet analytů v LFER modelu

Tabulka S2: Hodnoty regresních koeficientů LFER modelu podle rovnice 1.1. (statisticky významné koeficienty jsou uvedeny tučně). Složení MF: ACN/10mM octan amonný, pH 4,7; 40/60 (*v/v*). Deskriptory D^- and D^+ byly vypočteny za použití pH vodně-organické MF (pH* 5,4)

Kolona		*a*	*b*	d^-	d^+	*e*	*s*	*v*	*c*	R^2	*N*
XSelect CSH C18	hodnota	**-0,40**	**-1,57**	**-0,50**	**-0,33**	-0,03	**-0,17**	**2,02**	**-0,58**		
	p-hodnota	0,00	0,00	0,00	0,00	0,71	0,04	0,00	0,00	0,978	66
	±CI	0,13	0,12	0,15	0,15	0,14	0,16	0,21	0,18		
XSelect CSH FP	hodnota	**-0,37**	**-1,59**	-0,03	**0,22**	-0,08	0,05	**1,47**	**-0,57**		
	p-hodnota	0,00	0,00	0,77	0,06	0,48	0,70	0,00	0,00	0,924	66
	±CI	0,20	0,19	0,23	0,23	0,22	0,25	0,32	0,28		
XSelect CSH PH	hodnota	**-0,32**	**-1,43**	**-0,24**	**-0,18**	-0,05	-0,10	**1,74**	**-0,55**		
	p-hodnota	0,00	0,00	0,00	0,01	0,40	0,17	0,00	0,00	0,975	66
	±CI	0,12	0,11	0,13	0,14	0,13	0,14	0,19	0,16		
XSelect HSS C18	hodnota	**-0,56**	**-1,77**	**-0,32**	**-0,46**	-0,01	-0,12	**2,10**	**-0,46**		
	p-hodnota	0,00	0,00	0,01	0,00	0,96	0,29	0,00	0,00	0,965	66
	±CI	0,18	0,17	0,21	0,21	0,20	0,22	0,29	0,25		
XSelect HSS C18 SB	hodnota	**-0,48**	**-1,33**	**-0,46**	**0,24**	-0,05	-0,10	**1,76**	**-0,64**		
	p-hodnota	0,00	0,00	0,00	0,00	0,54	0,23	0,00	0,00	0,966	66
	±CI	0,14	0,13	0,15	0,16	0,15	0,17	0,22	0,19		
XSelect HSS PFP	hodnota	**-0,40**	**-1,40**	**-0,49**	**0,33**	-0,04	0,00	**1,54**	**-0,44**		
	p-hodnota	0,00	0,00	0,00	0,00	0,51	0,98	0,00	0,00	0,970	66
	±CI	0,12	0,12	0,14	0,15	0,14	0,15	0,20	0,17		
XBridge C18	hodnota	**-0,51**	**-1,64**	**-0,34**	**-0,39**	0,02	-0,15	**1,99**	**-0,61**		
	p-hodnota	0,00	0,00	0,00	0,00	0,82	0,17	0,00	0,00	0,967	66
	±CI	0,17	0,16	0,19	0,20	0,19	0,21	0,28	0,24		
XBridge Shield RP18	hodnota	**-0,43**	**-1,86**	-0,06	**-0,56**	-0,12	0,09	**1,96**	**-0,62**		
	p-hodnota	0,00	0,00	0,67	0,00	0,35	0,53	0,00	0,00	0,936	66
	±CI	0,24	0,22	0,27	0,28	0,26	0,29	0,38	0,33		

±CI interval spolehlivosti, R^2 koeficient determinace, *N* počet analytů v LFER modelu

Tabulka S3: Hodnoty regresních koeficientů LFER modelu podle rovnice 1.1. (statisticky významné koeficienty jsou uvedeny tučně). Složení MF: ACN/10mM octan amonný, pH 8,0; 40/60 (*v/v*). Deskriptory D^- and D^+ byly vypočteny za použití pH vodně-organické MF (pH* 7,8)

Kolona		*a*	*b*	d^-	d^+	*e*	*s*	*v*	*c*	R^2	*N*
XSelect CSH C18	hodnota	**-0,63**	**-1,60**	**-0,28**	-0,04	0,18	-0,09	**1,32**	-0,17		
	p-hodnota	0,00	0,00	0,00	0,77	0,13	0,48	0,00	0,25	0,942	64
	±CI	0,21	0,20	0,19	0,28	0,24	0,27	0,34	0,30		
XSelect CSH FP	hodnota	**-0,49**	**-1,03**	**-0,40**	0,17	**0,30**	-0,02	**0,68**	-0,10		
	p-hodnota	0,00	0,00	0,00	0,11	0,00	0,84	0,00	0,36	0,935	64
	±CI	0,16	0,15	0,14	0,21	0,18	0,20	0,25	0,22		
XSelect CSH PH	hodnota	**-0,48**	**-1,60**	**-0,43**	0,21	0,05	0,06	**1,23**	-0,23		
	p-hodnota	0,00	0,00	0,00	0,08	0,66	0,61	0,00	0,07	0,950	64
	±CI	0,18	0,17	0,16	0,24	0,21	0,23	0,29	0,26		
XSelect HSS C18	hodnota	**-0,59**	**-1,69**	**-0,39**	-0,09	0,23	-0,15	**1,43**	-0,02		
	p-hodnota	0,00	0,00	0,00	0,55	0,06	0,28	0,00	0,89	0,945	64
	±CI	0,22	0,21	0,20	0,29	0,25	0,28	0,34	0,31		
XSelect HSS C18 SB	hodnota	**-0,55**	**-1,05**	**-0,49**	0,14	**0,30**	**-0,27**	**1,19**	-0,23		
	p-hodnota	0,00	0,00	0,00	0,21	0,00	0,02	0,00	0,06	0,944	64
	±CI	0,18	0,16	0,16	0,23	0,20	0,23	0,27	0,24		
XSelect HSS PFP	hodnota	**-0,58**	**-1,20**	**-0,39**	0,08	0,13	-0,07	**1,00**	0,04		
	p-hodnota	0,00	0,00	0,00	0,49	0,20	0,56	0,00	0,76	0,939	63
	±CI	0,18	0,17	0,17	0,25	0,20	0,23	0,30	0,26		
XBridge C18	hodnota	**-0,69**	**-1,71**	-0,03	0,10	**0,53**	-0,33	**1,29**	**-0,43**		
	p-hodnota	0,00	0,00	0,81	0,59	0,00	0,07	0,00	0,03	0,906	64
	±CI	0,30	0,27	0,26	0,38	0,33	0,37	0,45	0,41		
XBridge Shield RP18	hodnota	**-0,63**	**-1,69**	-0,18	-0,07	0,26	0,03	**1,34**	**-0,52**		
	p-hodnota	0,00	0,00	0,14	0,66	0,08	0,87	0,00	0,01	0,912	64
	±CI	0,27	0,24	0,24	0,35	0,30	0,33	0,41	0,37		

±CI interval spolehlivosti, R^2 koeficient determinace, *N* počet analytů v LFER modelu

Tabulka S4: Fragmenty a jejich hodnoty *m/z* deklarované ve standardu naštěpeného cytochromu C.

Fragment	Pozice	Sekvence	Hmotnost (Da)	$[M+H]^+$	$[M+2H]^{2+}$
T1	2-6	GDVEK (+acetyl)	546,5780	**589**	
T4	10-14	IFVQK	633,7887	**634**	
T5	15-23	CAQCHTVEK (+hem)	2250,43		**817** [119]
T8	29-39	TGPNLHGLFGR	1168,3206		**585**
„miscleavage“ T9-10	40-54	KTGQAPGFSYTDANK	1584,7057		**793**
T10	41-54	TGQAPGFSYTDANK	1456,5316		**729**
T12	57-73	GITWGEETLMEYLENPK	2010,2459		**1006**
„miscleavage“ T12-13	57-74	GITWGEETLMEYLENPKK	2138,4200		**1070**
„miscleavage“ T13-14	74-80	KYIPGTK	805,9726		**404**
T14	75-80	YIPGTK	677,7985	**678**	
T15	81-87	MIFAGIK	779,0081	**780**	
T19	93-100	EDLIAYLK	964,1265	**965**	
chymotryptický T19C	93-98	EDLIAY	722,7930	**723**	

Tabulka S5: Sekvence pravděpodobných metabolitů nusinersenu, jejich hmoty a hodnoty *m/z*

Označení	Hodnota *m/z*	Náboj	Metabolit			
			Dekonvolutní hmota [Da]	Předpovězená hmota [Da]	Pravděpodobná sekvence	Pravděpodobný metabolit
M1	617,73718 1236,47773	-2 -1	1237,4760	1236	A*mU*G*	5'N-11+3'N-4
M2	696,77176 1394,54477	-2 -1	1395,5441	1395	G*mU*mC*MoeR mU*G*mC*MoeR	5'N-15+3'N-1 or 5'N-12+3'N-3
M3	601,77687	-2	1205,5537	1205	mC*A*mU* mU*mC*A* A*mC*mU*	5'N-7+3'N-8 or 3'N-15 or 5'N-2+3'N-13
M4	661,2532	-2	1324,5046	1325	*A*mU*G*	5'N-11+3'N-4
M5	595,75245	-2	1193,5049	1194	mC*mU*mU* mU*mU*mC*	5'N-3+3'N-12 or 5'N-5+3'N-10
M6	697,26371	-2	1396,5274	-	neidentifikováno	-
M7	653,26689 1307,53331	-2 -1	1308,5333	1308	*A*A*mU* *mU*A*A*	5'N-10+3'N-5 or 5'N-9+3'N-6
M8	731,317095	-2	1464,6340	1464	*mU*mU*mU*MoeR	5'N-4+3'N-11
M9	728,76776	-2	1459,5355	1458	A*mC*mU*MoeR* mU*mC*A*MoeR* mC*A*mU*MoeR*	5'N-2+3'N-13 or 5'N-6+3'N-9 or 5'N-7+3'N-8
M10	771,29979	-2	1544,5995	1543	G*G*mU*mC	3'N-14
M11	806,8181	-2	1615,6362	1614	A*mU*A*A*	5'N-8+3'N-6

Prohlášení o autorském podílu na vědeckých publikacích

Zuzana Vosáhlová je první autorkou všech deseti publikací zahrnutých v této disertační práci. U publikací III, VII, VIII a IX prováděla autorka veškeré chromatografické experimenty a vyhodnocení dat. U ostatních publikací autorka prováděla většinu chromatografických experimentů a vyhodnocení dat, vyjma např. experimentů s MS instrumentací typu QToF, která není v naší laboratoři k dispozici. Autorka se významně podílela na psaní všech rukopisů.

V Praze 17. července 2024

…….

doc. RNDr. Květa Kalíková, Ph.D.
vedoucí práce

Seznam publikací

Publikace I:
Kadlecová, Z., Kalíková, K., Ansorge, M., Gilar, M., Tesařová, E. The Effect of Particle and Ligand Types on Retention and Peak Shape in Liquid Chromatography. *Microchem. J.* **2020**, *159*, 105466.

Publikace II:
Kadlecová, Z., Kalíková, K., Folprechtová, D., Tesařová, E., Gilar, M. Method for Evaluation of Ionic Interactions in Liquid Chromatography. *J. Chromatogr. A* **2020**, *1625*, 461301.

Publikace III:
Kadlecová, Z., Kalíková, K., How ligand and particle types affect retention and separation of structurally diverse biologically active compounds in HPLC. *Monatshefte Für Chem. - Chem. Mon*. **2021**, *152*, 1081–1088.

Publikace IV:
Kadlecová, Z., Kozlík, P., Tesařová, E., Gilar, M., Kalíková, K., Characterization and comparison of mixed-mode and reversed-phase columns; interaction abilities and applicability for peptide separation. *J. Chromatogr. A* **2021**, *1648*, 462182.

Publikace V:
Kadlecová Z., Boudová H., Kalíková K., The benefits of mixed-mode chromatography columns for separation of peptides and protein digests. *Monatshefte Für Chem. - Chem. Mon*. **2023,** *154*, 993-1002.

Publikace VI:
Vosáhlová-Kadlecová Z., Gilar M., Molnárová K., Kozlík P., Kalíková K., Mixed-mode column allows simple direct coupling with immobilized enzymatic reactor for on-line protein digestion, *J. Chrom. B* **2023**, *1228*, 123866.

Publikace VII:
Kadlecová, Z., Kalíková, K., Tesařová, E., Gilar, M., Phosphorothioate oligonucleotides separation in ion-pairing reversed-phase liquid chromatography: Effect of ion-pairing system. *J. Chromatogr. A* **2022**, *1676*, 463201.

Publikace VIII:
Vosáhlová Z., Gilar M., Kalíková K., Impact of ion-pairing systems choice on diastereomeric selectivity of phosphorothioated oligonucleotides in reversed-phase liquid chromatography, *J. Chromatogr. A* **2024,** *1730,* 465074.

Publikace IX:
Kadlecová, Z., Kalíková, K., Tesařová, E., Gilar, M., Phosphorothioate oligonucleotides separation in ion-pairing reversed-phase liquid chromatography: Effect of temperature. *J. Chromatogr. A* **2022**, *1681*, 463473.

Publikace X:
Vosáhlová Z., Kalíková K., Gilar M., Szymarek J., Mazurkiewicz-Bełdzińska M., Studzińska S., Hydrophilic interaction liquid chromatography with mass spectrometry for the separation and identification of antisense oligonucleotides impurities and nusinersen metabolites, *J. Chromatogr. A* **2024**, *1713*, 464535.

Publikace I

The Effect of Particle and Ligand Types on Retention and Peak Shape in Liquid Chromatography

Kadlecová, Z., Kalíková, K., Ansorge, M., Gilar, M., Tesařová, E.
Microchemical Journal, **2020**, *159*, 105466.

Microchemical Journal 159 (2020) 105466

Contents lists available at ScienceDirect

Microchemical Journal

journal homepage: www.elsevier.com/locate/microc

The effect of particle and ligand types on retention and peak shape in liquid chromatography

Zuzana Kadlecová[a], Květa Kalíková[a,*], Martin Ansorge[a], Martin Gilar[b], Eva Tesařová[a]

[a] Department of Physical and Macromolecular Chemistry, Faculty of Science, Charles University, Hlavova 8, 12843 Prague, Czech Republic
[b] Waters Corporation, 34 Maple Street, Milford, MA 01757, USA

ARTICLE INFO

Keywords:
Linear free energy relationship
Particle type
Ligand type
Liquid chromatography
Interactions
Retentivity

ABSTRACT

A well performed, detailed characterization of stationary phase properties can serve as a useful tool for choice of suitable separation environment for a given purpose. This work shows effects of particle type/technology and ligand chemistry on retention and peak shape of neutral, acidic, basic and zwitterionic compounds. Eight columns differing in endcapping technology, particle type and ligand bonded were evaluated, namely XSelect CSH C18, XSelect CSH Phenyl-Hexyl, XSelect CSH Fluoro-Phenyl, XSelect HSS C18, XSelect HSS C18 SB, XSelect HSS PFP, XBridge C18 and XBridge Shield RP18. A simple Walters test for evaluation of hydrophobicity and silanol activity was performed. Mobile phases composed of acetonitrile and aqueous part (pH 2.1; pH 4.7 and pH 8.0) were used. More detailed description of interactions participating in the retention mechanism was provided by the linear free energy relationship model. For a more detailed characterization of possible electrostatic interactions, compounds with permanent charge across selected pH range were used. A good agreement between the Walters test results, the expanded linear free energy relationship model, and the test of ionic-interactions was observed, suggesting that each testing method provides value for characterization of the solute-stationary phase interactions.

1. Introduction

With growing sample complexity, demand on chromatographic sorbents performance is increasing. New sorbents with unique properties can contribute to better separation of a wide range of analytes. Retention of analytes is affected by a number of sorbent parameters, such as carrier (typically silica gel), particle ligand type, pore size, or additional sorbent modifications (embedded polar groups, endcapping, charged groups); differences in all of these parameters lead to different LC performance [1–3]. Companies supplying chromatographic columns investigate new particle technologies to achieve the required efficiency and selectivity of the separation systems. In this study, all chromatographic columns were obtained from a single manufacturer to ensure that the results are affected only by differences in particle and ligand types of the stationary phase (SP) [4].

One of the commonly used group of SPs is based on bridged ethylene hybrid (BEH) particles [5–8]. XBridge™ columns utilize BEH particles to achieve greater sorbent stability in wide pH range (pH 1–12), longer lifetime and usage at higher temperature than conventional silica sorbents. Among the most commonly used is the XBridge C18 column; the complementary XBridge Shield RP18 column is also available, where embedded carbamate group in the bonded ligand structure provides alternative selectivity (notably for phenolic compounds) compared to SPs with straight alkyl chain [9,10]. BEH sorbents are utilized for reversed-phase (RP) and hydrophilic interaction liquid chromatography (HILIC) in both high performance liquid chromatography (HPLC) and ultra-high performance liquid chromatography (UPLC) variations [11,12]. The XSelect™ family of chromatographic columns uses two different particle technologies - charged surface hybrid (CSH) and high strength silica (HSS) particles. CSH particles incorporate a low-level surface positive charge moiety-pyridyl. The sorbents have been shown to improve peak shape of basic molecules in acidic low-ionic-strength mobile phases (MPs) [13]. BEH particles are neutral in the whole range of pH, while CSH particles are protonated at

Abbreviations: ACN, acetonitrile; BEH, bridged ethylene hybrid; CSH, charged surface hybrid; FP, fluoro-phenyl; HI, hydrophobicity index; HILIC, hydrophilic interaction liquid chromatography; HPLC, high performance liquid chromatography; HSS, high strength silica; LFER, linear free-energy relationship; MP, mobile phase; PFP, pentafluoro-phenyl; PH, phenyl-hexyl; RP, reversed phase; RPLC, reversed phase liquid chromatography; SFC, supercritical-fluid chromatography; SI, silanol index; SP, stationary phase; UPLC, ultra-high performance liquid chromatography

* Corresponding author.
E-mail address: kalikova@natur.cuni.cz (K. Kalíková).

https://doi.org/10.1016/j.microc.2020.105466
Received 15 June 2020; Received in revised form 22 July 2020; Accepted 25 August 2020
Available online 30 August 2020
0026-265X/

pH < 7 [14]. At pH < 6, a low anion-exchange retention for inorganic ions was observed [15]. The presence of positive charge on the CSH columns makes them potentially applicable for mixed-mode chromatography [16,17]. Three different ligands are available on the CSH sorbent – octadecyl (C18), phenyl-hexyl (PH) and pentafluorophenyl (PFP).

The HSS particle technology has been reportedly developed as an alternative to BEH and CSH particles. The HSS columns provide higher retention of all compounds because of their larger surface (pore diameter 100 Å) in comparison with BEH and CSH columns (pore diameter 130 Å). Moreover, due to the higher possibility of ion-exchange interactions, basic compounds retention may be enhanced on HSS columns. Five SPs with different ligands bonded to HSS particles are commercially available – HSS T3 (trifunctional C18), HSS C18, HSS C18 SB, HSS PFP (pentafluoro-phenyl) and HSS CN (cyano-propyl) [18]. The type of the ligand, the particle type and the presence/absence of endcapping significantly affect SP properties.

In order to simplify the choice of the proper SP for a given purpose, several tests have been proposed [eg. 19–21]. One of the commonly used tests designed for characterization of reversed SPs is the Walters test, which describes hydrophobicity and silanol activity of the SPs [22]. It is based on two predominant retention mechanisms occurring in RPLC – hydrophobic and silanophilic interactions. Proportions of these interactions depend on the hydrocarbon coverage and the amount of unreacted silanol sites [23]. The residual free silanol groups can contribute to retention and peak tailing of basic compounds [24]. Walters proposed the relative retention of anthracene and benzene in acetonitrile/water 65/35 (*v*/*v*) MP for the hydrophobicity test, and the relative retention of anthracene and *N*,*N*-diethyltoluamide in pure acetonitrile for the characterization of the silanol activity. Other tests based on similar principles are available in the literature, for example the Galushko test [25] or the Engelhardt test [26].

In order to gain a deeper insight on the interactions taking part in the separation mechanism and thus, for a more complex characterization of chromatographic columns, several approaches were proposed [27]. Among them, the linear free-energy relationship method (LFER), often named as the solvation parameter model, is widely used [28–30]. The regression function mostly used in RPLC, is shown in the Eq. (1) [31]:

$$\log k = eE + sS + aA + bB + vV + c \quad (1)$$

where k is the retention factor of solute, descriptors E, S, A, B and V are the properties of solute, namely excess molar refraction (E), dipolarity/polarizability (S), hydrogen bond acidity and basicity (A *or* B) and McGowan characteristic volume (V), respectively. All these parameters are well described and tabulated for a large variety of compounds [32]. Corresponding lower-case letters are representatives of the separation system and characterize the magnitude of differences in the given interaction type between the SP and MP. They describe the tendency of interactions through *n*- and π- electrons, *e*; the dipolarity/polarizability and willingness to participate in dipole-dipole and dipole-induced dipole interactions, *s*; hydrogen bond interactions, *a* and *b*; and dispersion interactions/hydrophobicity, *v*. Constant *c* obtained as an intercept from LFER is related to phase ratio and any other possible interactions not covered by the model in the Eq. (1).

This regression function (Eq. (1)) was modified [33] and extended [34,35], by taking into account dissociation of solutes and their electrostatic interactions, resulting in an improved LFER model presented in Eq. (2):

$$\log k = eE + sS + aA + bB + vV + d^{-}D^{-} + d^{+}D^{+} + c \quad (2)$$

The electrostatic interactions of analytes are represented by the terms D^- and D^+. The system constants d^- and d^+ characterize the attractive and repulsive interactions in the separation system. The descriptors correspond to negative charge carried by anionic and zwitterionic species (D^-) and a positive charge carried by cationic and zwitterionic species (D^+). They are defined as degree of ionization according to the Eqs. (3) and (4):

$$D^{-} = \frac{10^{(\mathrm{pH}^{*} - \mathrm{pK}_a^{*})}}{1 + 10^{(\mathrm{pH}^{*} - \mathrm{pK}_a^{*})}} \quad (3)$$

$$D^{+} = \frac{10^{(\mathrm{pK}_a^{*} - \mathrm{pH}^{*})}}{1 + 10^{(\mathrm{pK}_a^{*} - \mathrm{pH}^{*})}} \quad (4)$$

where pH* stands for the pH of hydro-organic MP and pK_a* is the negative decadic logarithm of dissociation constant of a given species in that MP. In order to obtain the exact values of ${}^{s}_{s}$pH in hydro-organic MP, organic buffers would need to be used for the calibration of pH electrode. However, in common practice, aqueous buffers are used for calibration and ${}^{w}_{s}$pH (pH*) of hydro-organic phase is determined instead. Moreover, the aqueous dissociation constants, K_a, are also commonly used [34,36].

The LFER was implemented as a useful tool for both solute-solvent/phase interaction study and column characterization in HPLC e.g. [37–42], as well as in gas chromatography e.g. [43,44], electrokinetic chromatography e.g. [45,46] and supercritical-fluid chromatography (SFC) e.g. [47,48].

The aim of this work was to investigate differences in interaction/retention possibilities among chromatographic columns with different types of sorbents and surface chemistry ligands in LC. The influence of the particle type (specifically HSS, CSH and BEH) has been previously studied in detail in SFC system [49]. Four sets of structurally different analytes, i.e. neutral, acidic, basic, zwitterionic, were used for evaluation and comparison of peak shapes and columns retentivity. The Walters test served for a basic characterization of hydrophobicity and silanol activity. In order to obtain more general information about the contribution of individual interactions in the tested separation systems, the extended LFER model (Eq. (2)) was used in this study. For additional characterization of possible electrostatic interactions, compounds with a permanent charge across the selected pH range were used.

2. Materials and methods

2.1. Instrumentation

All chromatographic measurements were performed using the Waters Alliance system (Waters Corporation, Milford, CT, USA) consisting of Waters 2695 Separation Module, Waters 2996 Photodiode Array Detector, autosampler 717 Plus, and Waters Alliance Series column heater. Empower software was used for system control and data acquisition. The following eight columns were tested: XSelect® CSH™ C18, XSelect® CSH™ Phenyl-Hexyl, XSelect® CSH™ Fluoro-Phenyl, XSelect® HSS C18, XSelect® HSS C18 SB, XSelect® HSS PFP, XBridge® C18, XBridge® Shield RP18. All tested columns, particle size 5 µm, 150 × 4.6 mm I.D., were obtained from Waters Corporation (Milford, CT, USA).

2.2. Chemicals and reagents

Acetonitrile (Chromasolv® gradient grade, for HPLC, ≥99.9%), methanol (Chromasolv® gradient grade, for HPLC, ≥99.9%), ammonium acetate (purity ≥ 98%), ammonium formate (purity ≥ 97%), formic acid (purity ≥ 95%), acetic acid (purity ≥ 99%) and ammonium hydroxide solution (28.0–30.0% NH_3) were supplied by Sigma-Aldrich (St. Louis, MO, USA). Sodium hydroxide solution for HPCE (0.1 N Sodium hydroxide) was supplied by Agilent Technologies (Santa Clara, CA, USA). All of the naphtoflavones (α-naphthoflavone, β-naphthoflavone, 3-hydroxy-α-naphthoflavone and 3-hydroxy-β-naphthoflavone), profens (ibuprofen, indoprofen, carprofen, ketoprofen and fenoprofen), *N*,*N*-diethyltoluamide, benzenesulfonic acid, toluenesulfonic acid and trimethylphenylammonium chloride were purchased in analytical grade purity from Sigma-Aldrich (St. Louis, MO, USA).

Dipeptides (H-Tyr-Phe-OH, H-Phe-Tyr-OH, H-Ala-Trp-OH, H-Trp-Ala-OH) were supplied by Bachem (Bubendorf, Switzerland). Cathinone derivatives (4-chloro-*N*-butylcathinone (4-CBC), 4-chloro-*N,N*-dimethylcathinone (4-CDC), 4-chloro-*N*-isopropylcathinone (4-ClC), 1-(4-fluorophenyl)-2-(isopropylamino)pentan-1-on (4F-NPP), 1-(4-chlorophenyl)-2-pyrrolidin-1-yl-pentan-1-one (4-CPRC)) were purchased from internet vendors. For structures of the compounds see Table S1 in Supporting material. The list of 74 test solutes for LFER measurements (all of analytical grade purity), which were supplied by Sigma-Aldrich (St. Louis, MO, USA), and their corresponding descriptors is shown in the Supporting material Table S2.

2.3. Procedures

The stock solutions of analytes were prepared by dissolving the analytes in methanol at concentration 1 mg mL^{-1} (for solid samples) and 10 µL mL^{-1} (for liquid samples). Several compounds (dipeptides, xanthine and guanine) were dissolved in a mixture of methanol and water/sodium hydroxide because of their poor solubility in methanol. The first system peak was used as a dead time marker. All measurements were performed in triplicate.

The MPs composed of acetonitrile and aqueous part in volumetric ratio 40/60 (*v/v*) were used for analysis of sets of analytes and the LFER measurement. Volumetric ratio 20/80 (*v/v*) was used for separation of dipeptides. The following aqueous parts of MPs were used for experiments: formic acid, pH 2.1; 10 mM ammonium formate buffer, pH 2.5; 10 mM ammonium formate buffer, pH 2.8; 10 mM ammonium acetate buffer, pH 3.5; 10 mM ammonium acetate buffer, pH 4.7 and 10 mM ammonium acetate buffer, pH 8.0. For calculation of buffer constituent concentrations, and corresponding pH values, PeakMaster 6 software (freeware, downloadable at echmet.natur.cuni.cz) was used [50]. 10 mM ammonium formate buffer was prepared by dissolving appropriate amount of ammonium formate in deionized water and adjusted with formic acid to reach pH 2.5 or 2.8. 10 mM ammonium acetate buffer was prepared by dissolving appropriate amount of ammonium acetate in deionized water and adjusted with acetic acid to reach pH 3.5 or 4.7 or with ammonia to reach pH 8.0. The buffers were filtered with 0.45 µm syringe filters (Whatman, GE Healthcare, Chicago, IL, USA) before use. Aqueous solution of formic acid pH 2.1 (365 mM) was prepared by diluting appropriate volume of formic acid with water.

MP flow rate was 1 mL min^{-1}. Injection volume was 5 µL and detection wavelengths were 220 nm, 254 nm and 280 nm. All chromatographic measurements were performed at column temperature 25 °C, except the Walters test which was performed at column temperature 40 °C. The sample temperature was 20 °C for all measurements. Marvin software (product of ChemAxon company), was used for calculation of log *D* values in the corresponding pH of aqueous part of the MP and for calculation of pK_a values of analytes. Multiple linear regression analysis of log k versus the solute descriptors was performed using NCSS software (Kaysville, UT, USA) [51].

3. Results and discussion

3.1. Walters test

In order to determine hydrophobicity and silanol activity of selected columns, the Walters test was performed. Its results are presented in Fig. 1. The silanol index (SI) depends on the number of unreacted and non-endcapped silanol groups on the SP surface. With increasing number of free silanol groups, SI reaches higher values. The hydrophobicity index (HI) value increases with the hydrophobicity of the SP. A group of four columns with octadecyl ligand which exhibit similar hydrophobicity and silanol activity (XBridge C18, XBridge Shield RP18, XSelect CSH C18 and XSelect HSS C18) is obvious in Fig. 1. All these columns have high HI because of the long hydrophobic alkyl chain in their structure and the highest HI value was found for the XSelect HSS

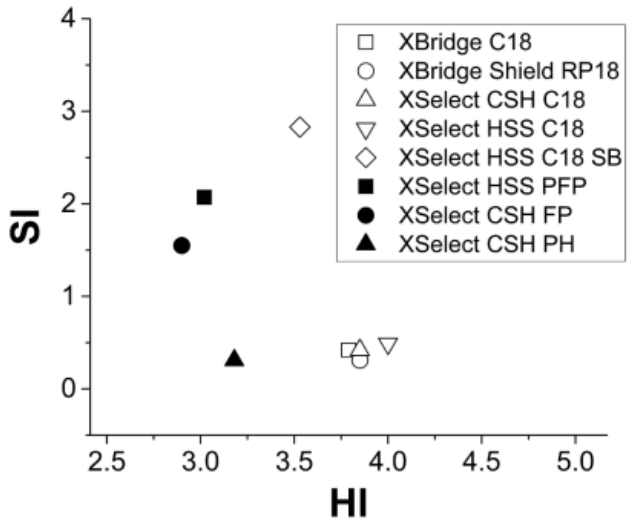

Fig. 1. Results of Walters test; silanol index, SI, and hydrophobicity index, HI. Open markers denote C18 columns, filler markers are used for phenyl or (penta) fluoro-phenyl columns.

C18 column. In addition, all these SPs are endcapped, which corresponds to their low SI value. In contrast, the column XSelect HSS C18 SB is not endcapped – it has much higher silanol index, and lower hydrophobic index compared to the other tested SPs with octadecyl ligand. The remaining three columns (XSelect CSH FP, XSelect HSS PFP and XSelect CSH PH) are less hydrophobic, because they have a shorter alkyl chain (propyl or hexyl) terminated with aromatic ring. The XSelect CSH PH column is endcapped, which corresponds to low SI value, similarly to other endcapped columns. The XSelect CSH FP and XSelect HSS PFP columns show mutual similarity, i.e. lower HI and high SI values, because both are not endcapped. Furthermore, these two columns contain the same ligand but are bonded to a different type of particles. The simple test summarized in Fig. 1, tells about basic properties and differences of the SPs. The obtained facts correspond to the more complex LFER method results, which will be discussed later.

3.2. Retention of structurally different groups of compounds

Differences in retentivity of the columns and peak symmetry were investigated by analysis of four structurally diverse sets of analytes: neutral compounds (naphtoflavones), acidic compounds (profens), basic compounds (cathinone derivatives), and zwitterionic compounds (dipeptides). MPs were composed of ACN and aqueous part, i.e. formic acid, pH 2.1; 10 mM ammonium acetate buffer, pH 4.7 or pH 8.0 40/60 (*v/v*), except for the dipeptides where volumetric ratio 20/80 (*v/v*) was used instead.

Retention and peak shapes of neutral naphtoflavones were almost unaffected by the pH of the MP. This is in an agreement with their inability to become charged within the tested pH range. Fig. 2A shows trends in retentivity and peak symmetry for the most retained β-naphtoflavone. Peaks exhibit good symmetry (symmetry factor about 1) in the tested pH range for all columns. Results also show that the fastest elution can be achieved on the XSelect CSH FP and XSelect CSH PH columns. On the other hand, the highest retention was observed on the XSelect HSS C18 column, which correlates with the highest HI value obtained by the Walters test. As retention in RPLC depends much on the polarity of analytes, the calculated log *D* values (Table S1 in Supporting material) correlate with the observed retention behavior. The experimental data for more detailed description are summarized in Tables S3, S5 and S7 in Supporting material.

Aqueous part of MP pH 8.0 is inappropriate for acidic profens. Profens are negatively charged (i.e. they are more polar, see the log *D*

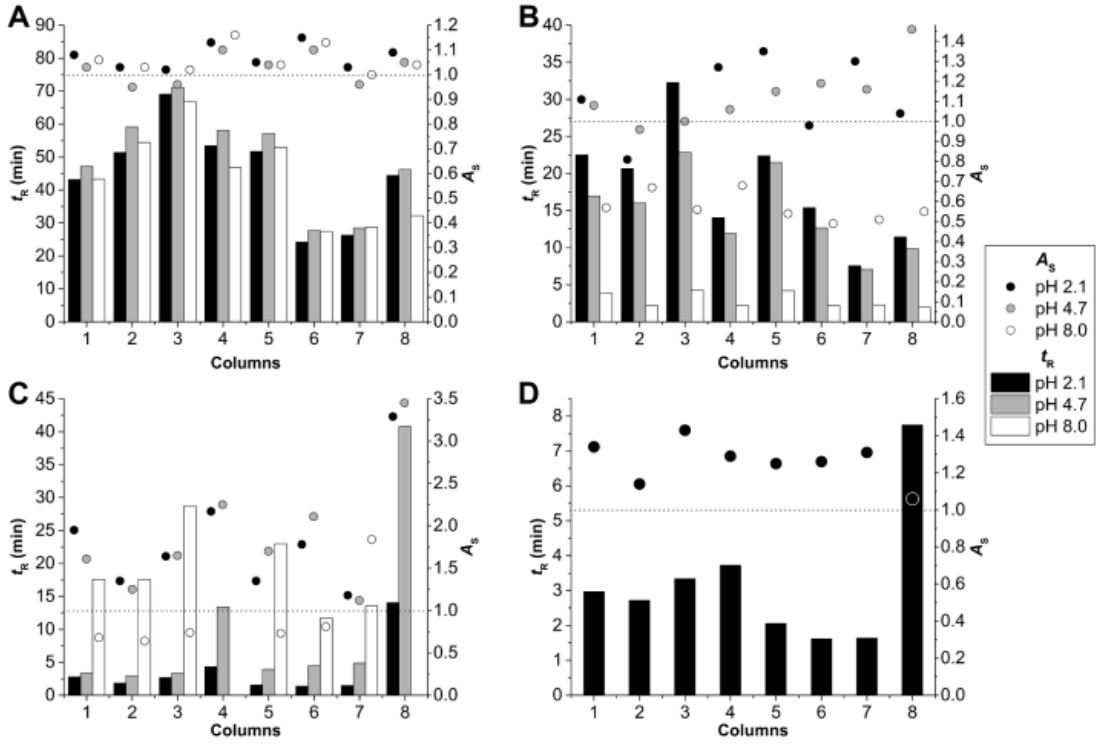

Fig. 2. Trends in retentivity and peak symmetry (A_s) for individual compounds from 4 different groups of analytes (A: β- naphtoflavone, B: ibuprofen, C: 4-CPRC, D: H-Tyr-Phe-OH). MP composition for A,B,C: ACN/aqueous part, 40/60 (*v*/*v*); for D: ACN/aqueous part, 20/80 (*v*/*v*). Retention times were used instead of retention factors because of elution with or before dead time marker in some cases. Columns: 1-XBridge C18; 2-XBridge Shield RP18; 3-XSelect HSS C18; 4-XSelect HSS C18 SB; 5-XSelect CSH C18; 6-XSelect CSH PH; 7-XSelect CSH FP; 8-XSelect HSS PFP. The dotted line symbolized the ideal peak symmetry.

values in Table S1 in Supporting material) so, their retention is much lower and peaks much broader at basic pH than at acidic pH of the MP. Trends in retention and peak symmetry for ibuprofen are shown in Fig. 2B. The results clearly indicate decrease in retention with increasing pH of the MP. The longest retention was observed on the XSelect HSS C18 column (the same as for naphtoflavones). The shortest retention of profens provide fluoro-phenyl class of columns. This corresponds with HI values obtained from the Walters test. Worse peak symmetry (fronting peaks) in basic MP is also evident.

Retention and peak symmetry of basic cathinone derivatives are also strongly influenced by the MP pH. Trends for the most retained 4-CPRC are shown in Fig. 2C. MPs composed of aqueous part of pH 4.7 or pH 8.0 caused prolonged retention compared to pH 2.1. In acidic MPs cathinone derivatives are positively charged (more polar and thus less retained), while at basic pH the majority of tested cathinones is charged only partially (see pKa values in Table S1 in Supporting material). The dependence of retention of cathinone derivatives on the sorbent chemistry is also evident. They have almost no retention on all the CSH columns (Tables S3-A and S3-B in Supporting material). This can be attributed to repulsive interactions between the positively charged analytes and the positively charged CSH particle surface. The most significant difference was observed between the XSelect HSS PFP and the XSelect CSH FP columns. The column XSelect HSS PFP showed the highest retention for cathinone derivatives, while these analytes were practically unretained on the latter column (Tables S3-A and S3-B in Supporting material). Both columns have the same ligand but bonded to different particle types. Similar effect was observed for the XSelect CSH C18 (low retention) and the XSelect HSS C18. In general, HSS particles provide higher retention of basic compounds and are more suitable for separation of polar analytes in comparison with other particle types. Symmetry of peaks strongly depends on pH of the MP. Fig. 2C shows that on all tested columns (except for the XSelect CSH FP) 4-CPRC tends to tail at acidic MP while fronting was observed in basic pH. Similar effects were observed for all cathinones (see Tables S3, S5 and S7 in Supporting material). Fig. 2C also confirms that CSH particles provide better peak shape of basic compounds in acidic low-ionic-strength MPs. The significance of particle technology is evident from the comparison of fluoro-phenyl class of columns, XSelect CSH FP and XSelect HSS PFP, and also from the comparison of C18 type columns, CSH C18 with XBridge C18 and HSS C18 columns. Peak symmetry is much better on the columns with CSH particles at pH 2.1.

Polar zwitterionic compounds, dipeptides, need a higher amount of aqueous part in the MP to be retained. Generally, the MP ACN/formic acid, pH 2.1; 20/80 (*v*/*v*) is the most suitable for dipeptides (see Tables S4-A and S4-B in Supporting material). MPs composed of aqueous part of pH 4.7 or pH 8.0 cause very low retention (see Table S6 in Supporting material). Fig. 3 documents the differences among columns with the same ligand, but bonded to different particle type (see also Tables S4-A and S4-B in Supporting material). The comparison of XSelect HSS C18 × XSelect CSH C18 and XSelect HSS PFP × XSelect CSH FP clearly shows that the HSS columns exhibit higher retention of dipeptides compared to the CSH columns with the same ligand. Repulsion of positively charged dipeptides and positively charged CSH particles in acidic pH of the MP is responsible for these results. Fig. 2D shows retention and peak symmetry of H-Tyr-Phe-OH. Very low retention of the dipeptide on the CSH columns was observed, whereas the highest retention accompanied with the best peak symmetry was acquired on the XSelect HSS PFP column.

3.3. LFER

The retention of 74 structurally different analytes with known descriptors were included to the LFER model (see Table S2 in Supporting material). The LFER study was performed in three MPs, namely ACN/formic acid, pH 2.1, ACN/10 mM ammonium acetate, pH 4.7 and ACN/10 mM ammonium acetate, pH 8.0 40/60 (*v*/*v*). Both LFER Eqs. (1) and

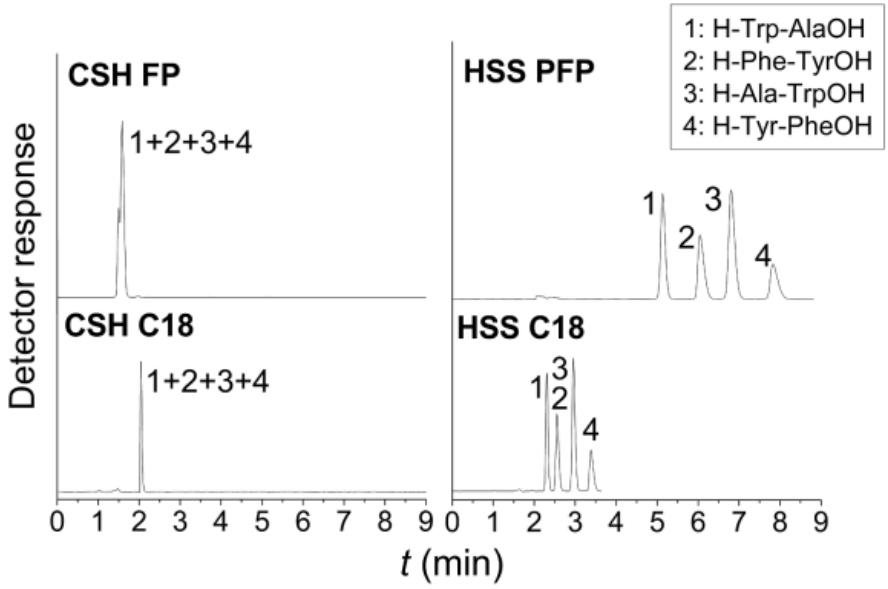

Fig. 3. Chromatograms of separation of dipeptides, effect of column particles type. MP: ACN/formic acid, pH 2.1; 20/80 (*v/v*).

Table 1
Regression coefficients (statistically significant in bold) of the LFER Eq. (2), MP: ACN/formic acid, pH 2.1; 40/60 (*v/v*). Calculated from LFER Eq. (2) where descriptors D^- and D^+ were calculated using pH of hydro-organic MP (pH* 2.4).

Column		*a*	*b*	d^-	d^+	*e*	*s*	*v*	*c*	R^2	*N*
XSelect CSH C18	value	**−0.46**	**−1.65**	0.13	**−0.37**	0.24	−0.23	**1.77**	**−0.64**		
	p-value	0.00	0.00	0.64	0.00	0.06	0.11	0.00	0.00	0.936	68
	± CI	0.21	0.23	0.53	0.22	0.25	0.29	0.33	0.31		
XSelect CSH FP	value	**−0.32**	**−1.12**	0.15	**−0.36**	**0.22**	−0.13	**1.09**	**−0.60**		
	p-value	0.00	0.00	0.41	0.00	0.01	0.18	0.00	0.00	0.937	68
	± CI	0.14	0.15	0.37	0.15	0.17	0.20	0.23	0.22		
XSelect CSH PH	value	**−0.31**	**−1.33**	0.00	**−0.42**	0.18	−0.18	**1.41**	**−0.55**		
	p-value	0.00	0.00	0.99	0.00	0.07	0.12	0.00	0.00	0.941	68
	± CI	0.16	0.18	0.42	0.18	0.20	0.23	0.26	0.24		
XSelect HSS C18	value	**−0.54**	**−1.64**	0.10	**−0.37**	0.25	−0.29	**1.75**	**−0.39**		
	p-value	0.00	0.00	0.73	0.00	0.06	0.06	0.00	0.02	0.933	68
	± CI	0.22	0.24	0.56	0.24	0.26	0.21	0.35	0.33		
XSelect HSS C18 SB	value	**−0.51**	**−1.22**	−0.34	**−0.36**	0.18	−0.14	**1.45**	**−0.62**		
	p-value	0.00	0.00	0.11	0.00	0.06	0.20	0.00	0.00	0.946	68
	± CI	0.16	0.17	0.41	0.17	0.19	0.22	0.26	0.24		
XSelect HSS PFP	value	**−0.32**	**−1.43**	**−0.51**	**0.37**	**0.25**	−0.20	**1.40**	**−0.56**		
	p-value	0.00	0.00	0.02	0.00	0.02	0.09	0.00	0.00	0.924	68
	± CI	0.17	0.18	0.43	0.18	0.20	0.23	0.27	0.25		
XBridge C18	value	**−0.57**	**−1.47**	0.03	**−0.29**	**0.27**	**−0.31**	**1.57**	**−0.44**		
	p-value	0.00	0.00	0.91	0.02	0.05	0.05	0.00	0.01	0.921	68
	± CI	0.22	0.24	0.57	0.24	0.27	0.31	0.35	0.34		
XBridge Shield RP18	value	**−0.33**	**−1.61**	−0.03	**−0.38**	**0.27**	−0.21	**1.54**	**−0.50**		
	p-value	0.00	0.00	0.89	0.00	0.02	0.13	0.00	0.00	0.936	68
	± CI	0.19	0.21	0.50	0.21	0.23	0.27	0.31	0.29		

± CI confidence interval, R^2 coeficient of determination, *N* number of analytes used for LFER model

(2) were evaluated. Application of the Eq. (2) led to a slight increase of the coefficients of determination, R^2, in comparison with the Eq. (1) – see Tables 1-3 and Tables S8-S10 in Supporting material. Table 1 summarizes calculated regression coefficients of the LFER Eq. (2) in the MP with formic acid. The distribution of positive and negative values of the regression coefficients corresponds with general description of RP mode. The dominant and opposite interactions participating in all of the tested systems are described by the coefficients *v* and *b*, respectively, which is typical for RPLC systems [34]. The XSelect HSS C18 and XSelect CSH C18 columns showed the highest hydrophobicity (highest value of the coefficient *v*). This is consistent with results of the Walters test. Both columns have the same carbon load but they differ in particle technology and ligand density (higher for XSelect HSS C18). The most polar of tested C18 columns was the XSelect HSS C18 SB with the lowest coefficient *v* and HI values. This column has the lowest carbon load and is not endcapped. The XBridge C18 and XBridge Shield RP18 columns with 18% and 17% carbon load, respectively, exhibit similar hydrophobicity, meaning that incorporated carbamate group embedded to the latter column does not significantly change column hydrophobicity. In general, lower hydrophobicity was observed for phenyl-based columns in comparison with all the C18 columns.

The second dominant interaction type expressed by the coefficient *b* (Table 1) is preferred in the MP (negative values of the regression coefficient). Among the C18 columns, the lowest difference between the SP and MP in hydrogen bond acidity (the lowest absolute value of the regression coefficient *b*) was observed for the XSelect HSS C18 SB, which correlates with the highest silanol activity calculated from the Walters test. The highest difference in hydrogen bond acidity was

Table 2
Regression coefficients (statistically significant in bold) of the LFER Eq. (2), MP: ACN/10 mM ammonium acetate buffer, pH 4.7; 40/60 (*v/v*). Calculated from LFER Eq. (2) where descriptors D^- and D^+ were calculated using pH of hydro-organic MP (pH* 5.4).

Column		*a*	*b*	d^-	d^+	*e*	*s*	*v*	*c*	R^2	*N*
XSelect CSH C18	value	**−0.40**	**−1.57**	**−0.50**	**−0.33**	−0.03	**−0.17**	**2.02**	**−0.58**		
	p-value	0.00	0.00	0.00	0.00	0.71	0.04	0.00	0.00	0.978	66
	± CI	0.13	0.12	0.15	0.15	0.14	0.16	0.21	0.18		
XSelect CSH FP	value	**−0.37**	**−1.59**	−0.03	**0.22**	−0.08	0.05	**1.47**	**−0.57**		
	p-value	0.00	0.00	0.77	0.06	0.48	0.70	0.00	0.00	0.924	66
	± CI	0.20	0.19	0.23	0.23	0.22	0.25	0.32	0.28		
XSelect CSH PH	value	**−0.32**	**−1.43**	**−0.24**	**−0.18**	−0.05	−0.10	**1.74**	**−0.55**		
	p-value	0.00	0.00	0.00	0.01	0.40	0.17	0.00	0.00	0.975	66
	± CI	0.12	0.11	0.13	0.14	0.13	0.14	0.19	0.16		
XSelect HSS C18	value	**−0.56**	**−1.77**	**−0.32**	**−0.46**	−0.01	−0.12	**2.10**	**−0.46**		
	p-value	0.00	0.00	0.01	0.00	0.96	0.29	0.00	0.00	0.965	66
	± CI	0.18	0.17	0.21	0.21	0.20	0.22	0.29	0.25		
XSelect HSS C18 SB	value	**−0.48**	**−1.33**	**−0.46**	**0.24**	−0.05	−0.10	**1.76**	**−0.64**		
	p-value	0.00	0.00	0.00	0.00	0.54	0.23	0.00	0.00	0.966	66
	± CI	0.14	0.13	0.15	0.16	0.15	0.17	0.22	0.19		
XSelect HSS PFP	value	**−0.40**	**−1.40**	**−0.49**	**0.33**	−0.04	0.00	**1.54**	**−0.44**		
	p-value	0.00	0.00	0.00	0.00	0.51	0.98	0.00	0.00	0.970	66
	± CI	0.12	0.12	0.14	0.15	0.14	0.15	0.20	0.17		
XBridge C18	value	**−0.51**	**−1.64**	**−0.34**	**−0.39**	0.02	−0.15	**1.99**	**−0.61**		
	p-value	0.00	0.00	0.00	0.00	0.82	0.17	0.00	0.00	0.967	66
	± CI	0.17	0.16	0.19	0.20	0.19	0.21	0.28	0.24		
XBridge Shield RP18	value	**−0.43**	**−1.86**	−0.06	**−0.56**	−0.12	0.09	**1.96**	**−0.62**		
	p-value	0.00	0.00	0.67	0.00	0.35	0.53	0.00	0.00	0.936	66
	± CI	0.24	0.22	0.27	0.28	0.26	0.29	0.38	0.33		

± CI confidence interval, R^2 coeficient of determination, *N* number of analytes used for LFER model

observed for the XSelect CSH C18 and XSelect HSS C18 columns, which show the highest hydrophobicity. Among the phenyl/PFP class of columns, the XSelect CSH FP column shows the lowest hydrophobicity ($v = 1.09$), and the lowest absolute value of the coefficient *b*.

The regression coefficient *a*, expressing hydrogen bond basicity, is statistically significant and negative in all the separation systems tested. The absolute values of the coefficient *a* are much smaller than those of the coefficient *b*. It means that the effect of hydrogen bond basicity on the retention is smaller than that of hydrogen bond acidity (*b*).

The regression coefficient *s*, describing the phase's ability to interact with dipolar and/or polarizable solutes, is statistically insignificant for almost all of the separation systems/columns. We conclude that dipolar interactions do not significantly participate on the retention of analytes on the SPs investigated in this study.

The *e* coefficient expressing interactions with n- and π- electrons is statistically significant for both fluorophenyl-based columns and for both XBridge octadecyl columns. The obtained values of the coefficient *e* are small (ranged between 0.22 and 0.27) as compared to the values of other coefficients (see Table 1).

The coefficients d^- and d^+ in Eq. (2) describe ionic interactions. Generally, the coefficient d^- describes the difference between the SP and MP acting as a cation. The coefficient d^- is statistically insignificant for all the separation systems tested except for the system with the XSelect HSS PFP column where this interaction type is preferred between the analytes and the MP. The coefficient d^+ is negative for all separation systems tested (except for that with the XSelect HSS PFP column), hence this interaction type is preferred between the analyte and the MP. In the buffer of pH 2.1 the free silanol groups are uncharged and do not contribute to electrostatic interactions and thus, to the value of coefficient d^+. Therefore, positively charged analytes will preferably interact with the MP. The intercept *c* relating to the phase ratio and interactions, which are not covered by the regression coefficients of the LFER equation is statistically significant and negative in all the separation systems tested.

Comparing regression coefficient values obtained using Eq. (1) (see Tables S8) and Eq. (2) (see Table 1) it can be seen that the trend is the same for all the regression coefficients.

The buffer/MP pH has a great impact on the coefficients of the LFER equation. The LFER results obtained for all columns using the Eq. (2) in the MP composed of ACN/10 mM ammonium acetate buffer, pH 4.7 are summarized in Table 2. The coefficient *v* increased in all the tested separation system compared to the systems with acidic MP discussed above (see Table 1). The absolute value of coefficient *b* increased or did not change within confidence interval (CI). The values of coefficient *a* did not change within CI with the MP pH change. Interactions described by the coefficients *e* and *s* do not significantly contribute to the retention. The effect of free silanol groups at non-endcapped columns becomes apparent at the MP aqueous part pH 4.7. All the separation systems with these columns, i.e. XSelect CSH FP, XSelect HSS C18 SB and XSelect HSS PFP, show positive values of the coefficient d^+ (Table 2). At this pH both the free silanol groups and bases are charged, which is why the retention of positively charged analytes increases. This effect is also obvious in Fig. 4. The CSH-based sorbents show minor anionic interactions with analytes [13,15,52]. As shown previously, the degree of ionic attraction/repulsion increases in the order XSelect CSH C18 < XSelect CSH PH < XSelect CSH FP [15]. This is consistent with the distribution of the coefficient d^- values for the CSH-based columns (Table 2). The highest difference in this interaction type (the highest negative value of the d^- coefficient) between the SP and MP was observed for the CSH C18 column. On the other hand, the lowest difference (comparable in both SP and MP) was observed for the CSH FP sorbent. As the anionic interactions of CSH-based sorbents are expected to be minor their contribution to the overall retention is low (low values of d^- coefficients) compared to e.g. "hydrophobicity". The same trend of the d^- coefficient values for CSH-based sorbents was observed with the more acidic MP composed of ACN/10 mM ammonium acetate buffer, pH 3.5 where the pyridyl groups of CSH sorbent are positively charged – see Tables S11 and S12 in Supporting info. For a more detailed description of the electrostatic interactions in various pH of the MPs see 3.4 "Evaluation of electrostatic interactions". The intercept *c* is negative again.

Comparing the regression coefficient values obtained using the Eq. (1) (see Table S9) and the Eq. (2) (Table 2) it can be seen that the trend is the same for all the coefficients within CI.

An increase of pH of the aqueous part of MP to pH 8.0 leads to changes of strength of the individual interactions (Table 3). The

Table 3
Regression coefficients (statistically significant in bold) of the LFER Eq. (2), MP: ACN/10 mM ammonium acetate buffer. pH 8.0; 40/60 (*v/v*). Calculated from LFER Eq. (2) where descriptors D^- and D^+ were calculated using pH of hydro-organic MP (pH* 7.8).

Column		*a*	*b*	d^-	d^+	*e*	*s*	*v*	*c*	R^2	*N*
XSelect CSH C18	value	**−0.63**	**−1.60**	**−0.28**	−0.04	0.18	−0.09	**1.32**	−0.17		
	p-value	0.00	0.00	0.00	0.77	0.13	0.48	0.00	0.25	0.942	64
	± CI	0.21	0.20	0.19	0.28	0.24	0.27	0.34	0.30		
XSelect CSH FP	value	**−0.49**	**−1.03**	**−0.40**	0.17	**0.30**	−0.02	**0.68**	−0.10		
	p-value	0.00	0.00	0.00	0.11	0.00	0.84	0.00	0.36	0.935	64
	± CI	0.16	0.15	0.14	0.21	0.18	0.20	0.25	0.22		
XSelect CSH PH	value	**−0.48**	**−1.60**	**−0.43**	0.21	0.05	0.06	**1.23**	−0.23		
	p-value	0.00	0.00	0.00	0.08	0.66	0.61	0.00	0.07	0.950	64
	± CI	0.18	0.17	0.16	0.24	0.21	0.23	0.29	0.26		
XSelect HSS C18	value	**−0.59**	**−1.69**	**−0.39**	−0.09	0.23	−0.15	**1.43**	−0.02		
	p-value	0.00	0.00	0.00	0.55	0.06	0.28	0.00	0.89	0.945	64
	± CI	0.22	0.21	0.20	0.29	0.25	0.28	0.34	0.31		
XSelect HSS C18 SB	value	**−0.55**	**−1.05**	**−0.49**	0.14	**0.30**	**−0.27**	**1.19**	−0.23		
	p-value	0.00	0.00	0.00	0.21	0.00	0.02	0.00	0.06	0.944	64
	± CI	0.18	0.16	0.16	0.23	0.20	0.23	0.27	0.24		
XSelect HSS PFP	value	**−0.58**	**−1.20**	**−0.39**	0.08	0.13	−0.07	**1.00**	0.04		
	p-value	0.00	0.00	0.00	0.49	0.20	0.56	0.00	0.76	0.939	63
	± CI	0.18	0.17	0.17	0.25	0.20	0.23	0.30	0.26		
XBridge C18	value	**−0.69**	**−1.71**	−0.03	0.10	**0.53**	−0.33	**1.29**	**−0.43**		
	p-value	0.00	0.00	0.81	0.59	0.00	0.07	0.00	0.03	0.906	64
	± CI	0.30	0.27	0.26	0.38	0.33	0.37	0.45	0.41		
XBridge Shield RP18	value	**−0.63**	**−1.69**	−0.18	−0.07	0.26	0.03	**1.34**	**−0.52**		
	p-value	0.00	0.00	0.14	0.66	0.08	0.87	0.00	0.01	0.912	64
	± CI	0.27	0.24	0.24	0.35	0.30	0.33	0.41	0.37		

± CI confidence interval, R^2 coeficient of determination, *N* number of analytes used for LFER model.

contribution of hydrophobicity (coefficient *v*) to the retention is lower at this pH. The coefficients *a* and *b*, describing hydrogen bonding interactions, are negative and statistically significant in all the separation systems tested. A higher difference of hydrogen bond basicity (coefficient *a*) between the SP and MP was observed with basic MP. In the acidic MPs it was observed that the absolute values of the coefficient *a* are much smaller than those of the coefficient *b*. The interactions described by the regression coefficient *s* influence the retention of analytes only in the separation system with the XSelect HSS C18 SB column. The negative coefficient *s* decreases retention of analytes that can interact by these interactions. Compared to the MP with buffer pH of 4.7, the interactions described by the coefficient *e* increase the retention of analytes on three columns, namely XSelect CSH FP, XSelect HSS C18 SB and XBridge C18. In separation systems with other columns this interaction type is comparable in the SP and MP. Regarding the electrostatic interactions, the effect of the CSH dopant was not noticed at basic pH as CSH becomes uncharged above the pH of 6–7. The coefficient d^- if statistically significant is negative, meaning that this interaction type is preferred between the analyte and the MP. The effect of free silanol groups which can be described by the coefficient d^+ is not reflected correspondingly in basic pH as the majority of basic analytes became uncharged at this pH. For a more detailed description of electrostatic interactions in various pH of the MPs see section "Evaluation of electrostatic interactions".

Comparing the regression coefficient values obtained using Eq. (1) (see Table S10) and Eq. (2) (Table 3), it can be seen that the Eq. (2) offers better fit with the chromatographic data.

Discussion can be found in the literature as to whether it is more appropriate to use the aqueous buffer pH to calculate the D^- and D^+ descriptors instead of the apparent hydro-organic pH of the MP [53]. We decided to primarily use the apparent hydro-organic pH for the D^- and D^+ descriptors calculations and the obtained LFER results are discussed above. The descriptors D^+ and D^- were also calculated for the aqueous buffer pH and the LFER model was performed (data not shown). Comparing the obtained regression coefficients the trend is the same for both types of D^+ and D^- calculations. So, we can conclude that no substantial change in the regression coefficients was observed.

To summarize, two dominant interaction types were observed in all the tested chromatographic systems. Hydrophobicity, expressed by the coefficient *v*, is preferred between the analyte and the SP and reaches

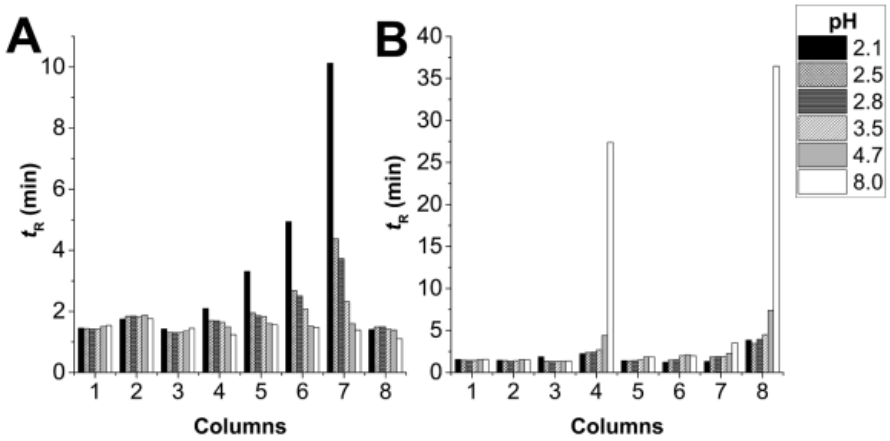

Fig. 4. Effect of pH on retention of benzenesulfonic acid (A) and trimethylphenylammonium cation (B) for all tested columns. MP composition: ACN/aqueous part; 40/60 (*v/v*). Retention time was used instead of retention factor because of the elution before dead time marker in some cases. Columns: 1-XBridge C18; 2-XBridge Shield RP18; 3-XSelect HSS C18; 4-XSelect HSS C18 SB; 5-XSelect CSH C18; 6-XSelect CSH PH; 7-XSelect CSH FP; 8-XSelect HSS PFP.

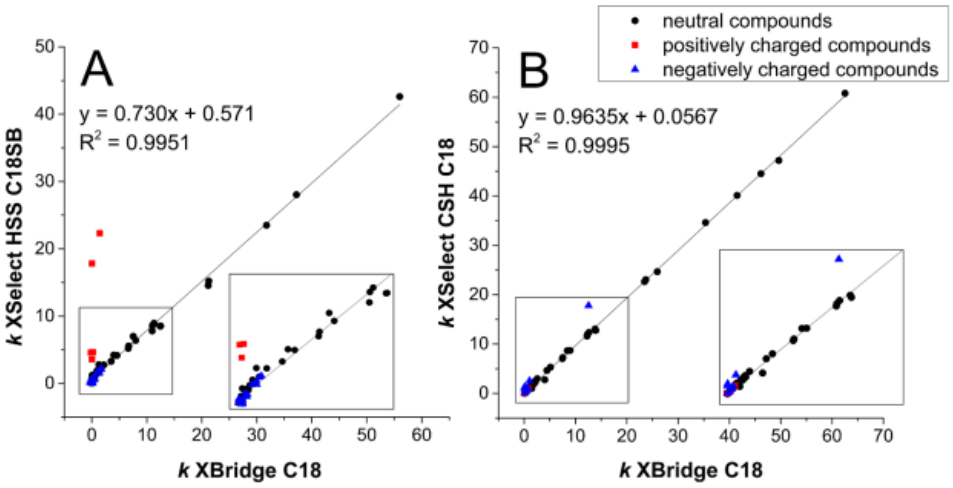

Fig. 5. Correlation of retention factors *k of* compound from LFER set and permanently charged compounds on the XBridge C18 column versus column XSelect HSS C18SB (A) and column XSelect CSH C18 (B). MP composition: ACN/aqueous part; 40/60 (*v/v*). Aqueous parts: 10 mM ammonium acetate; pH = 8.0 (A) and formic acid; pH = 2.1 (B). Only the black dots data series were used for the calculation of regression trend.

the highest values for C18 columns. The second dominant interaction, hydrogen bond basicity, expressed by the coefficient *b*, is stronger between the analyte and the MP. Ionic interactions between the analyte and SP particles are strongly influenced by the mobile phase pH, since protonation and dissociation of the analyte and SP particles depend on the MP pH. At buffer pH 4.7 the prolonged retention of positively charged basic compounds was observed on non-endcapped columns as is reflected by the positive value of the coefficient d^+. Positive charge on the surface of CSH particles in acidic buffers pH was confirmed (the coefficient d^-). The contribution of ionic interactions is much lower than of hydrophobicity and hydrogen bond basicity as these columns are marketed as RP columns.

3.4. Evaluation of electrostatic interactions

The ability of the SPs to interact by electrostatic interactions was further investigated by analysis of permanently negatively charged acids (benzenesulfonic acid, pKa = -2.36; toluenesulfonic acid, pKa = -2.14) and permanently positively charged trimethylphenyl ammonium cation. Another base (propranolol, pKa = 9.67) from the LFER set can be also used for evaluation of electrostatic interactions – see Figure S1 in Supporting material. All measurements were performed in MPs composed of ACN/aqueous part, 40/60 (*v/v*) with the aqueous parts of pH values 2.1; 2.5; 2.8; 3.5; 4.7 and 8.0.

Fig. 4A shows the dependence of the benzenesulfonic acid retention on the pH of the aqueous part of the MP for all tested columns. The results confirm the presence of positive charge on the surface of CSH particles at pH 2.1, i.e. significantly higher retention of negatively charged acid on columns with CSH particles in comparison with columns containing other particle types. Retention of benzenesulfonic acid on the three CSH columns gradually decreases with increasing pH. The same trends were observed for toluenesulfonic acid (see Supporting material, Figure S2). The degree of "electrostatic interactions" on individual columns with CSH particles decreases as follows: XSelect CSH FP > XSelect CSH PH > XSelect CSH C18, which is in agreement with the LFER results and previously published results [15].

Fig. 4B shows the dependence of the retention of positively charged trimethylphenylammonium cation on the pH of aqueous part of the MP. The results clearly show differences in endcapping. Non-endcapped columns (XSelect HSS C18 SB, XSelect CSH FP and XSelect HSS PFP) provide increase in retention of trimethylphenylammonium cation at pH 4.7 and pH 8.0 in comparison with other columns and pH of MPs. At pH 8.0, non-endcapped silanol groups are fully dissociated and they can interact with positively charged analytes. Retention is even higher for non-endcapped HSS particles. HSS particles provide higher retention because of the smaller pore diameter and thus larger surface in comparison with other particle types. The same effect was observed for propranolol (see Supporting material, Figure S1).

For further comparison of retentivity of C18 columns, the experimentally measured retention factors *k* of 74 analytes (the LFER analytes plus permanently charged analytes) obtained on neutral column (XBridge C18) and columns with ion-exchange properties (HSS C18SB, CSH C18) were plotted. Fig. 5 clearly shows a high degree of similarity in retention of neutral compounds between each pair of sorbents since all columns are based on the same chemistry. Fig. 5A shows positively charged outliers, which are relatively more retained on the XSelect HSS C18SB column in basic conditions. On the other hand, Fig. 5B shows negatively charged outliers, which are more retained on the XSelect CSH C18 column in acidic conditions in comparison with the neutral XBridge C18 column. These dependencies support the LFER results that retention is mainly influenced by hydrophobicity, but electrostatic interactions also play an important role in the retention of charged analytes.

4. Conclusions

In conclusion, column retentivity depends not only on the type of ligand bonded to the carrier but also on the type of particles and endcapping technology. In this work, eight columns differing in particle type, i.e. charged surface hybrid (CSH), high strength silica (HSS) or bridged ethylene hybrid (BEH); the ligand bonded, i.e. octadecyl, phenyl, fluorophenyl, and the endcapping technology were evaluated and compared. Significant differences among the SPs were observed.

The Walters test is useful in sorting the columns into groups according to their polarity. First group, comprising of more hydrophobic C18 columns, showed lower silanol activity. The only exception was the XSelect HSS C18 SB column, which is not endcapped and thus exhibits lower hydrophobicity and higher silanol index. Second group of columns exhibited lower hydrophobicity because of shorter alkyl chain terminated with aromatic ring. The values of LFER hydrophobicity coefficient *v* and hydrogen bond basicity coefficient *b* were consistent with the Walters test trends. Hydrogen bond basicity had lower impact on retention compared to hydrogen bond acidity. The effect of other interaction types depended on the MP pH, since the pH of MP affects protonation and dissociation of both analytes and of the SPs. In other words, buffer pH can strongly alter the strength of interactions responsible for retention. Based on the LFER findings, silanol and ionic interactions are important contributors to the retention in RPLC. On the other hand, the retention of neutral naphtoflavones is nearly unaffected by the MP pH.

Evaluation of electrostatic interactions was performed by analysis of permanently positively and negatively charged compounds. The

presence of a positive charge on the surface of CSH particles in acidic buffer pH was confirmed. The results also showed increasing retention of positively charged compounds on non-endcapped columns in basic pH of the MP. It confirms that endcapping technology has a great impact on retention behavior and selectivity.

The results from LFER well correlated with those obtained from the Walters test and the electrostatic interactions evaluation and can provide an explanation of differences among columns in terms of retentivity. Modification of the classic LFER with charge related terms was useful to detect ionic interaction of analytes with selected types of SPs.

CRediT authorship contribution statement

Zuzana Kadlecová: Investigation, Formal analysis, Writing - original draft, Writing - review & editing. **Květa Kalíková:** Investigation, Formal analysis, Writing - original draft, Funding acquisition, Conceptualization, Writing - review & editing. **Martin Ansorge:** Investigation, Formal analysis, Writing - original draft. **Martin Gilar:** Methodology, Resources, Writing - review & editing. **Eva Tesařová:** Writing - review & editing.

Declaration of Competing Interest

The authors declare that they have no known competing financial interests or personal relationships that could have appeared to influence the work reported in this paper.

Acknowledgements

The authors gratefully acknowledge financial support from Czech Science Foundation [Project No. CSF 20-19655S]. Authors thank to Dominik Gilar for proofreading the manuscript. Authors also want to express their gratitude to Prof. Martin Schmid for his generous gift of cathinone derivatives.

Appendix A. Supplementary data

Supplementary data to this article can be found online at https://doi.org/10.1016/j.microc.2020.105466.

References

[1] F. Gritti, T. McDonald, M. Gilar, Impact of the column hardware volume on resolution in very high pressure liquid chromatography non-invasive investigations, J. Chromatogr. A. 1420 (2015) 54–65, https://doi.org/10.1016/j.chroma.2015.09.079.
[2] C.F. Poole, Reversed-phase liquid chromatography system constant database over an extended mobile phase composition range for 25 siloxane-bonded silica-based columns, J. Chromatogr. A. 1600 (2019) 112–126, https://doi.org/10.1016/j.chroma.2019.04.027.
[3] M.R. Euerby, P. Petersson, Chromatographic classification and comparison of commercially available reversed-phase liquid chromatographic columns containing polar embedded groups/amino endcappings using principal component analysis, J. Chromatogr. A. 1088 (2005) 1–15, https://doi.org/10.1016/j.chroma.2004.10.027.
[4] K. Plachká, F. Švec, L. Nováková, Ultra-high performance supercritical fluid chromatography in impurity control: Searching for generic screening approach, Anal. Chim. Acta. 1039 (2018) 149–161, https://doi.org/10.1016/j.aca.2018.07.008.
[5] E.S. Grumbach, D.M. Diehl, U.D. Neue, The application of novel 1.7 µm ethylene bridged hybrid particles for hydrophilic interaction chromatography, J. Sep. Sci. 31 (2008) 1511–1518, https://doi.org/10.1002/jssc.200700673.
[6] L. Nováková, I. Kaufmannová, R. Jánská, Evaluation of hybrid hydrophilic interaction chromatography stationary phases for ultra-HPLC in analysis of polar pteridines, J. Sep. Sci. 33 (2010) 765–772, https://doi.org/10.1002/jssc.200900734.
[7] K.D. Wyndham, J.E. O'Gara, T.H. Walter, K.H. Glose, N.L. Lawrence, B.A. Alden, G.S. Izzo, C.J. Hudalla, P.C. Iraneta, Characterization and Evaluation of C18 HPLC Stationary Phases Based on Ethyl-Bridged Hybrid Organic/Inorganic Particles, Anal. Chem. 75 (2003) 6781–6788, https://doi.org/10.1021/ac034767w.
[8] O. Kozlov, Z. Kadlecová, M. Gilar, T. Gondová, K. Kalíková, E. Tesařová, Systematic evaluation of selected supercritical fluid chromatography diol- and diethylamine-based columns for application in hydrophilic interaction liquid chromatography, Sep. Sci. PLUS. 2 (2019) 81–88, https://doi.org/10.1002/sscp.201900023.
[9] C. Moretton, G. Crétier, H. Nigay, J.-L. Rocca, Quantification of 4-Methylimidazole in Class III and IV Caramel Colors: Validation of a New Method Based on Heart-Cutting Two-Dimensional Liquid Chromatography (LC-LC), J. Agric. Food Chem. 59 (2011) 3544–3550, https://doi.org/10.1021/jf104464f.
[10] A. Ribas-Agustí, R. Cáceres, M. Gratacós-Cubarsí, C. Sárraga, M. Castellari, A Validated HPLC-DAD Method for Routine Determination of Ten Phenolic Compounds in Tomato Fruits, Food Anal. Methods. 5 (2012) 1137–1144, https://doi.org/10.1007/s12161-011-9355-5.
[11] K.J. Fountain, J. Xu, D.M. Diehl, D. Morrison, Influence of stationary phase chemistry and mobile-phase composition on retention, selectivity, and MS response in hydrophilic interaction chromatography, J. Sep. Sci. 33 (2010) 740–751, https://doi.org/10.1002/jssc.200900660.
[12] BEH (Ethylene Bridged Hybrid) Technology : Waters, (n.d.). https://www.waters.com/waters/en_US/BEH-(Ethylene-Bridged-Hybrid)-Technology/nav.htm?cid=134618172&locale=en_US (accessed January 20, 2020).
[13] F. Gritti, G. Guiochon, Effect of the pH and the ionic strength on overloaded band profiles of weak bases onto neutral and charged surface hybrid stationary phases in reversed-phase liquid chromatography, J. Chromatogr. A. 1282 (2013) 113–126, https://doi.org/10.1016/j.chroma.2013.01.063.
[14] F. Gritti, G. Guiochon, Adsorption behaviors of neutral and ionizable compounds on hybrid stationary phases in the absence (BEH-C18) and the presence (CSH-C18) of immobile surface charges, J. Chromatogr. A. 1282 (2013) 58–71, https://doi.org/10.1016/j.chroma.2013.01.024.
[15] Z. Kadlecová, K. Kalíková, D. Folprechtová, E. Tesařová, M. Gilar, Method for evaluation of ionic interactions in liquid chromatography, J. Chromatogr. A. 1625 (2020) 461301, , https://doi.org/10.1016/j.chroma.2020.461301.
[16] P.C. Iraneta, K.D. Wyndham, D.R. McCabe, T.H. Walter, A Review of Waters Hybrid Particle Technology, Part 3. Charged Surface Hybrid (CSH) Technology and its Use in Liquid Chromatography, Waters Milford Mass. (2010).
[17] B.A. Alden, K.M. Smith, P.D. Rainville, T.H. Walter, M. Gilar, Retention of anions on charged surface hybrid columns, in: Washington DC, United States, 2018.
[18] XSelect HPLC Columns Selectivity of Basic Compounds : Waters, (n.d.). https://www.waters.com/waters/en_US/XSelect-HPLC-Columns-Selectivity-of-Basic-Compounds-/nav.htm?cid=10165804&alias=Alias_xselect_CHEMISTRY&locale=j (accessed January 21, 2020).
[19] K. Vyňuchalová, P. Jandera, Selectivity Tests of Stationary Phases for Reversed-Phase HPLC, Anal. Lett. 44 (2011) 1640–1662, https://doi.org/10.1080/00032719.2010.520393.
[20] L. Janečková, K. Kalíková, Z. Bosáková, E. Tesařová, Study of interaction mechanisms on zirconia-based polystyrene HPLC column, J. Sep. Sci. 33 (2010) 3043–3051, https://doi.org/10.1002/jssc.201000391.
[21] M.J. Ruiz-Angel, S. Pous-Torres, S. Carda-Broch, M.C. García-Alvarez-Coque, Performance of different C18 columns in reversed-phase liquid chromatography with hydro-organic and micellar-organic mobile phases, J. Chromatogr. A. 1344 (2014) 76–82, https://doi.org/10.1016/j.chroma.2014.04.011.
[22] M.J. Walters, Classification of octadecyl-bonded liquid chromatography columns, J.-Assoc. Off. Anal. Chem. 70 (1987) 465–469.
[23] H.A. Claessens, M.A. van Straten, C.A. Cramers, M. Jezierska, B. Buszewski, Comparative study of test methods for reversed-phase columns for high-performance liquid chromatography, J. Chromatogr. A. 826 (1998) 135–156, https://doi.org/10.1016/S0021-9673(98)00749-3.
[24] S.D. Rogers, J.G. Dorsey, Chromatographic silanol activity test procedures: the quest for a universal test, J. Chromatogr. A. 892 (2000) 57–65, https://doi.org/10.1016/S0021-9673(00)00722-6.
[25] S.V. Galushko, The calculation of retention and selectivity in reversed-phase liquid chromatography II, Methanol-water eluents, Chromatographia. 36 (1993) 39–42, https://doi.org/10.1007/BF02263833.
[26] H. Engelhardt, M. Jungheim, Comparison and characterization of reversed phases, Chromatographia. 29 (1990) 59–68.
[27] D. Sykora, J. Vozka, E. Tesarova, Chromatographic methods enabling the characterization of stationary phases and retention prediction in high-performance liquid chromatography and supercritical fluid chromatography, J. Sep. Sci. 39 (2016) 115–131, https://doi.org/10.1002/jssc.201501023.
[28] R.I. Amos, P.R. Haddad, R. Szucs, J.W. Dolan, C.A. Pohl, Molecular modeling and prediction accuracy in Quantitative Structure-Retention Relationship calculations for chromatography, TrAC Trends Anal. Chem. 105 (2018) 352–359.
[29] H. Xian, H. Peng, X. Wang, D. Long, R. Ni, J. Chen, S. Li, Z. Zhang, J. Peng, Preparation and evaluation a mixed-mode stationary phase with imidazolium and carboxyl group for high performance liquid chromatography, Microchem. J. 150 (2019) 104131, , https://doi.org/10.1016/j.microc.2019.104131.
[30] X. Wang, H. Peng, J. Peng, C. Gong, Y. He, F. Chen, Y. Chen, S. Li, Preparation and evaluation of a polar embedded diphenylethene bonded stationary phase for High Performance Liquid Chromatography, Microchem. J. 142 (2018) 195–201, https://doi.org/10.1016/j.microc.2018.06.034.
[31] M.H. Abraham, Scales of solute hydrogen-bonding: their construction and application to physicochemical and biochemical processes, Chem. Soc. Rev. 22 (1993) 73–83.
[32] C.F. Poole, S.N. Atapattu, S.K. Poole, A.K. Bell, Determination of solute descriptors by chromatographic methods, Anal. Chim. Acta. 652 (2009) 32–53.
[33] M. Rosés, D. Bolliet, C.F. Poole, Comparison of solute descriptors for predicting retention of ionic compounds (phenols) in reversed-phase liquid chromatography using the solvation parameter model, J. Chromatogr. A. 829 (1998) 29–40.
[34] R.-I. Chirita, C. West, S. Zubrzycki, A.-L. Finaru, C. Elfakir, Investigations on the chromatographic behaviour of zwitterionic stationary phases used in hydrophilic interaction chromatography, J. Chromatogr. A. 1218 (2011) 5939–5963.
[35] M.H. Abraham, Y.H. Zhao, Determination of Solvation Descriptors for Ionic Species:

Hydrogen Bond Acidity and Basicity, J. Org. Chem. 69 (2004) 4677–4685, https://doi.org/10.1021/jo049766y.
[36] D. Sykora, E. Tesarová, D.W. Armstrong, Practical considerations of the influence of organic modifiers on the ionization of analytes and buffers in reversed-phase LC, LC GC N. Am. 20 (2002) 974–981.
[37] X. Subirats, M.H. Abraham, M. Rosés, Characterization of hydrophilic interaction liquid chromatography retention by a linear free energy relationship. Comparison to reversed-and normal-phase retentions, Anal. Chim. Acta. 1092 (2019) 132–143.
[38] C.S. Bagwill, S. Wireduaah, B. Cusworth, J. Korba, C.C. Kirkpatrick, M. Lewis, A.M. Stalcup, Use of HPLC retention to investigate new P descriptors designed to represent ion-π interactions, J. Liq. Chromatogr. Relat. Technol. 43 (2020) 83–93, https://doi.org/10.1080/10826076.2019.1667822.
[39] E. Lemasson, Y. Richer, S. Bertin, P. Hennig, C. West, Characterization of Retention Mechanisms in Mixed-Mode HPLC with a Bimodal Reversed-Phase/Cation-Exchange Stationary Phase, Chromatographia. 81 (2018) 387–399, https://doi.org/10.1007/s10337-018-3477-5.
[40] B. Danylec, C. Kulsing, J.C. Topete, M.T. Matyska, J.J. Pesek, R.I. Boysen, M.T. Hearn, Application of linear solvation energy relationships and principal component analysis methods for the prediction of the retention behaviour of E-resveratrol analogues with substituted silica hydride stationary phases, Anal. Chim. Acta. 1090 (2019) 159–171.
[41] H. Larbi, L. Didaoui, M. Righezza, Characterization of stationary phases based on monosubstituted benzene retention indices using correspondence factor analysis and linear solvation energy relationships in RPLC, J. Iran. Chem. Soc. 15 (2018) 2295–2305, https://doi.org/10.1007/s13738-018-1418-8.
[42] G. Kučerová, K. Kalíková, H. Procházková, M. Popr, J. Jindřich, P. Coufal, E. Tesařová, Chromatographic Characterization of a New Cationic β-CD Based Stationary Phase Prepared by Dynamic Coating, Chromatographia. 79 (2016) 529–536, https://doi.org/10.1007/s10337-016-3050-z.
[43] P. Siriviboon, C. Tungkaburee, N. Weerawongphrom, C. Kulsing, Direct equations to retention time calculation and fast simulation approach for simultaneous material selection and experimental design in comprehensive two dimensional gas chromatography, J. Chromatogr. A. 1602 (2019) 425–431.
[44] Y. Nolvachai, C. Kulsing, P.J. Marriott, In silico modeling of hundred thousand experiments for effective selection of ionic liquid phase combinations in comprehensive two-dimensional gas chromatography, Anal. Chem. 88 (2016) 2125–2131.
[45] J.R. McGettrick, N.H. Williamson, A.T. Sutton, C.P. Palmer, Performance and selectivity of cationic nanoparticle pseudo-stationary phases in electrokinetic chromatography, Electrophoresis. 38 (2017) 730–737.
[46] J. Lu, X. Ni, Y. Cao, X. Ma, G. Cao, Electrokinetic chromatographic characterization of novel catanionic surfactants vesicle as pseudostationary phase, Electrophoresis. 36 (2015) 312–318.
[47] C. West, E. Lemasson, K. Nagai, T. Shibata, P. Franco, S. Bertin, P. Hennig, E. Lesellier, Characterization of novel polymer-based pyridine stationary phases for supercritical fluid chromatography, Chromatographia. 82 (2019) 143–152.
[48] O. Kozlov, Z. Kadlecová, E. Tesařová, K. Kalíková, Evaluation of separation properties of stationary phases in supercritical fluid chromatography; deazapurine nucleosides case study, Microchem. J. 150 (2019) 104137, , https://doi.org/10.1016/j.microc.2019.104137.
[49] S. Al Hamimi, M. Sandahl, M. Armeni, C. Turner, P. Spégel, Screening of stationary phase selectivities for global lipid profiling by ultrahigh performance supercritical fluid chromatography, J. Chromatogr. A. (1548 (2018)) 76–82, https://doi.org/10.1016/j.chroma.2018.03.024.
[50] M. Malý, M. Dovhunová, M. Dvořák, G.S. Gerlero, P.A. Kler, V. Hruška, P. Dubský, Generalized model of the linear theory of electromigration and its application to electrokinetic chromatography: Theory and software PeakMaster 6—Next Generation, Electrophoresis 40 (2019) 683–692, https://doi.org/10.1002/elps.201800400.
[51] J.L. Hintze, NCSS user's guide II, NCSS Kaysville UT USA. (2007).
[52] M.A. Lauber, S.M. Koza, S.A. McCall, B.A. Alden, P.C. Iraneta, K.J. Fountain, High-Resolution Peptide Mapping Separations with MS-Friendly Mobile Phases and Charge-Surface-Modified C18, Anal. Chem. 85 (2013) 6936–6944, https://doi.org/10.1021/ac401481z.
[53] L. Taraba, T. Křížek, O. Hodek, K. Kalíková, P. Coufal, Characterization of polyaniline-coated stationary phases by using the linear solvation energy relationship in the hydrophilic interaction liquid chromatography mode using capillary liquid chromatography, J. Sep. Sci. 40 (2017) 677–687, https://doi.org/10.1002/jssc.201600785.

Publikace II

Method for Evaluation of Ionic Interactions in Liquid Chromatography

Kadlecová, Z., Kalíková, K., Folprechtová, D., Tesařová, E., Gilar, M.
Journal of Chromatography A, **2020**, *1625*, 461301.

Journal of Chromatography A 1625 (2020) 461301

Contents lists available at ScienceDirect

Journal of Chromatography A

journal homepage: www.elsevier.com/locate/chroma

Method for evaluation of ionic interactions in liquid chromatography

Zuzana Kadlecová [a], Květa Kalíková [a], Denisa Folprechtová [a], Eva Tesařová [a], Martin Gilar [b,*]

[a] Department of Physical and Macromolecular Chemistry, Faculty of Science, Charles University, Hlavova 8, 128 43 Prague 2, Czech Republic
[b] Waters Corporation, 34 Maple Street, Milford, MA 01757, USA

ARTICLE INFO

Article history:
Received 29 April 2020
Revised 29 May 2020
Accepted 31 May 2020
Available online 3 June 2020

Keywords:
Ionic interactions
Silanols
Reversed-phase
Mixed-mode
Inorganic ions

ABSTRACT

In this work we utilized basic and acidic analytes to investigate the ionic interaction participation in retention behavior of selected reversed-phase and polar columns. The test analytes included nitrate, benzenesulfonate and trimethylphenylammonium ions. The fully aqueous mobile phase comprising 10 mM dichloroacetic acid buffered with ammonia solution to desirable pH was used for retention experiments. Developed method was utilized to study the ionic interactions of stationary phases in pH range between 2.5 and 9.0. We demonstrate that selected sorbents used for reversed-phase and hydrophilic interaction chromatography separations exhibit cation- or anion-exchange interactions. We compare the results to novel Atlantis PREMIER BEH C18 AX mixed-mode column that combines reversed-phase and anion-exchange interaction modes. We evaluated the relative retention strength of selected columns for anionic and cationic analytes.

1. Introduction

In reversed-phase liquid chromatography (RP LC) the retention is dominated by hydrophobic interactions, while in hydrophilic interaction liquid chromatography (HILIC) the dominant retention mode is ascribed to analyte partitioning between stagnant water rich layer at the sorbent surface and acetonitrile rich mobile phase [1]. It is known that additional interactions (dipoles, H-bond acidity/basicity, ionic silanol interactions) may participate in both types of chromatography [2–4], but those are regarded as secondary, or even undesirable interactions [5,6].

Some of the modern RP stationary phases, such as charged surface hybrid sorbents (CSH) [7,8], have population of ionizable functional groups bonded to surface with the goal to improve peak shapes for basic molecules [7–10]. Other commercial stationary phases with charged ligands bonded to surface in addition to RP or HILIC chemistry are marketed as mixed-mode columns [10–12], for example Primesep columns [13], Scherzo columns [14,15] Acclaim columns [16,17] or Atlantis PREMIER BEH C18 AX column [18]. The goal of additional ionic interactions is to provide an alternative selectivity to common RP and HILIC columns. While mixed-mode columns may provide desirable retention of ionic species that would otherwise be unretained by RP (HILIC) mode, the contribution of secondary retention mechanism can make the method development more complex [19].

Various versions of mixed-mode stationary phases recently prepared were reviewed by Sýkora et al. [20]. Commercially available stationary phases were reviewed by Zhang and Liu [11] and Mansour and Danielson [21]. Novel mixed-mode stationary phases were applied to separation of small organic molecules and inorganic anions/cations [22–27]. While multiple columns capable of mixed-mode interactions are available to users, the relative contribution of selected separation modes to analyte retention is not well known. For example, the anionic interaction of Charged Surface Hybrid RP sorbents with analytes is expected to be minor [7,8], while Primesep or Acclaim mixed-mode family columns exhibit relatively strong retention for ionic analytes [12–14,16,17,19]. Selected HILIC stationary phases based on silica or immobilized charged ligands provide for ionic interactions that participate in the overall analytes retention [28–31]. Contribution of silanols to retention of basic compound in RP LC is well known [2,32–34]; it has been also recognized as one of the retention modes in HILIC not only with silica columns, but also with derivatized silica surfaces [28,30,35–40].

Many stationary phases provide secondary mode of interactions alongside the main retention mechanism, e.g. ionic interactions in RP and HILIC columns [5,32,39,41,42], yet they are not marketed as mixed-mode columns. A clarification of the terminology used in the literature would be useful. We suggest that term mixed-mode chromatography is reserved to columns where two or more retention modes contribute substantially to analytes retention. However, the contribution of multiple retention modes to analyte retention is often unknown. The methods for column characterization are

* Corresponding author.
E-mail address: Martin_Gilar@waters.com (M. Gilar).

https://doi.org/10.1016/j.chroma.2020.461301
0021-9673/

needed. In this work we focus on ionic interactions in addition to hydrophobic interactions.

Method for characterization of ionic interactions in liquid chromatography has not been standardized yet. Useful tests were proposed by various groups [3,4,33,39,43–46]. Mixed-mode properties of columns combining RP with ionic interactions were tested with hydrophobic analytes (polycyclic aromatic hydrocarbons, alkylbenzenes, phthalates and phenols) and highly polar charged analytes (such as nucleobases or small organic anions) [22,25,27].

Inorganic anions were also used to test anion-exchange properties of the sorbents. Nitrates, nitrites, iodides, iodates, bromides, bromates and thiocyanates are most often used for this purpose [22–24,26,32]. Cation-exchange nature of stationary phases can be investigated using organic (choline) or inorganic (potassium, magnesium, sodium, zinc, lithium) cations [27,32]. The advantage of polar inorganic ions (cations and anions) is that they are not retained in RP mode, hence they probe only ionic interactions with the sorbent.

Mixed-mode columns combining ionic interactions with either RP or HILIC retention mode are now available to users [11,13,14,19,20,47]. However, the information about the stationary phase structure, nature of charged ligand, and its pKa is not always reported by manufacturers. An information about a degree of ionic interactions of available columns is of primary interest for the analysts. The method development will differ for sorbents with low and high ion-exchange activity. For example, the columns with high degree of ionic interactions will require greater buffer concentrations to ensure the elution of charged analytes. When the mobile phase compatibility with mass spectrometry detection is desired, the low concentration of volatile salts used as eluent is preferred [7,14,18].

The goal of this study is to develop a method suitable for evaluation of ionic interactions in liquid chromatography. The study included representative examples of reversed-phase sorbents (C18, Phenyl-hexyl and Fluoro-Phenyl chemistry) with endcapped, non-endcapped, charged-surface hybrid stationary phases [7–9], and mixed-mode Atlantis Premier BEH C18 AX column. In addition to reversed-phase stationary phases we studied selected sorbents with hydrophilic surface chemistry such as diol and diol modified with diethylamine.

2. Experimental

2.1. Materials and reagents

Acetonitrile (Chromasolv® gradient grade, for HPLC), dichloroacetic acid (ReagentPlus®, purity ≥ 99%), ammonia solution (28.0-30.0% NH_3), benzenesulfonic acid (purity ≥ 98%), and trimethylphenylammonium chloride (purity ≥ 98%) were purchased from Sigma-Aldrich (St. Louis, USA). Thiourea (purity ≥ 99%), potassium iodide, and potassium nitrate (purity ≥ 99.8%) were purchased from Lachema (Brno, Czech Republic). Deionized water was purified with Rowapur and Ultrapur system from Watrex (Prague, Czech Republic).

2.2. LC instrumentation and columns

All chromatographic measurements were performed on the Waters Alliance system (Waters Chromatography, Milford, USA) consisting of 2690 D Separation Module, 2487 Dual λ Absorbance Detector, 717 Plus autosampler, and Waters Alliance Series column heater. Empower 2 software was used for data acquisition and analysis. The columns tested in the study were obtained from Waters (Milford, USA). The column description and properties are summarized in Table 1. All columns sized 150 × 4.6 mm, particle size 5 μm.

2.3. Experimental procedures

Stock solutions of analytes were prepared by dissolving the analytes in deionized water at concentration 1 mg mL^{-1}. Aqueous mobile phases (MPs) without presence of organic solvent modifiers were used. They were prepared by adjusting 10 mM aqueous solution of dichloroacetic acid with ammonia solution to reach the pH values from 2.5 to 9.0 with 0.5 steps. The rationale for using fully aqueous MPs is two-fold. (i) pH of MP, pKa of analytes, and pKa of stationary phases are not affected by organic solvent. (ii) polar compounds are often separated in RP and mixed mode RP under aqueous mobile phases to achieve desirable retention [10,18]. The effect of buffer concentration in MP on retention was tested on Torus DEA column (pH=3.0, buffer concentration of MP ranged from 10 mM to 50 mM with 10 mM increments). Flow rate was 1 mL min^{-1}, injection volume was 5 μL. Detection wavelengths were 240 nm for nitrates and iodides and 254 nm for benzenesulfonic acid, and trimethylphenylammonium ions. All measurements were performed at column temperature 25 °C. The column was equilibrated with the MP for 40 min before the first injection. Individual measurements were repeated three times and averaged. Thiourea was used as a dead time (t_M) marker; t_M was determined with MP composed of acetonitrile/deionized water 70/30 (v/v) to eliminate the residual hydrophobic retention of thiourea in aqueous MPs.

ChemAxon software (product of ChemAxon company) was used for calculation of pKa values of analytes and MP components.

3. Results and discussion

3.1. Development of method for estimation of ionic interactions with sorbent

Ionic and hydrophobic interactions with stationary phases were evaluated with charged test analytes in the wide range of mobile phase pH. Nitrate, iodide and benzenesulfonate anions represented negatively charged markers while trimethylphenylammonium cation was selected as positively charged marker. The inorganic nitrate and iodide ions were chosen as analytes that are retained by ionic interactions only (no hydrophobic retention mechanism). Inorganic anions were previously used in chromatographic research as void volume markers since they are not retained in RP LC [48,49]. Nitrate and other selected ions can be conveniently monitored by ultra-violet (UV) or alternatively by MS detectors [32,50].

Organic ions selected for the study have modest retention in RP mode, therefore they can be eluted from the selected columns with fully aqueous MPs. Protonation/deprotonation of analytes strongly affects their retention in RP LC [51–53]. The rationale of using permanently charged test compounds was to evaluate the protonation/deprotonation of sorbent in wide range of mobile phase pH. The change of sorbent surface ionization is expected to be reflected in the test samples retention [32].

The MP was prepared from 10 mM dichloroacetic acid solution buffered with concentrated ammonia solution in range of pH 2.5 – 9.0 in 0.5 pH increments. The dichloroacetic acid was selected for its low pKa value ~ 2.3 (estimated by ChemAxon software). Our first approach utilized ammonium formate and acetate buffers, but the protonation of acids at pH below their respective pKa values decreases an effective concentration of formate and acetate ions in the buffer. Due to this effect the retention of anionic test analytes on positively charged sorbents increased dramatically even if the protonation of stationary phase did not change. Therefore, we prepared buffers from dichloroacetic acid buffered with ammonia solution (pKa 8.9). This MP should provide nearly constant concentration of dichloroacetate and ammonium ions in pH range ~ 3.5 –

Table 1
Properties of columns used in the study.[a]

Column[a]	Ligand Structure	Sorbent type	Charge modifier	Endcapping	Ligand density ($\mu mol \cdot m^{-2}$)	Carbon load (%)	Pore diameter (Å)	Pore volume ($cm^3 \cdot g^{-1}$)	Surface area ($m^2 \cdot g^{-1}$)
XSelect CSH C18	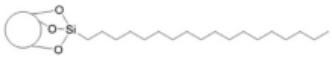	CSH	pyridyl	proprietary	2.3	15	130	0.7	185
XSelect CSH Phenyl-Hexyl	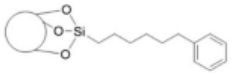	CSH	pyridyl	proprietary	2.3	14	130	0.7	185
XSelect CSH Fluoro-Phenyl	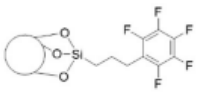	CSH	pyridyl	none	2.3	10	130	0.7	185
XSelect HSS T3	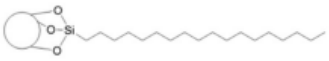	HSS	none	proprietary	1.6	11	100	0.7	230
XSelect HSS C18 SB	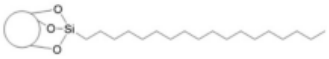	HSS	none	none	1.6	8	100	0.7	230
XSelect HSS PFP	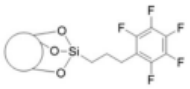	HSS	none	none	3.2	7	100	0.7	230
XBridge C18	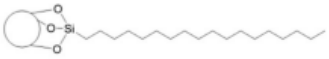	BEH	none	proprietary	3.1	18	130	0.7	185
Atlantis BEH C18 AX	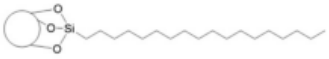	BEH	alkylamine	proprietary	1.6	17	95	0.7	270
Torus DIOL	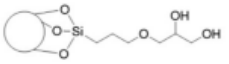	BEH	none	proprietary	n.a.	n.a.	130	0.7	185
Torus DEA	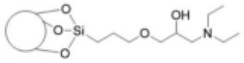	BEH	none	proprietary	n.a.	n.a	130	0.7	185

[a] 150 × 4.6 mm column packed with 5 µm sorbent.

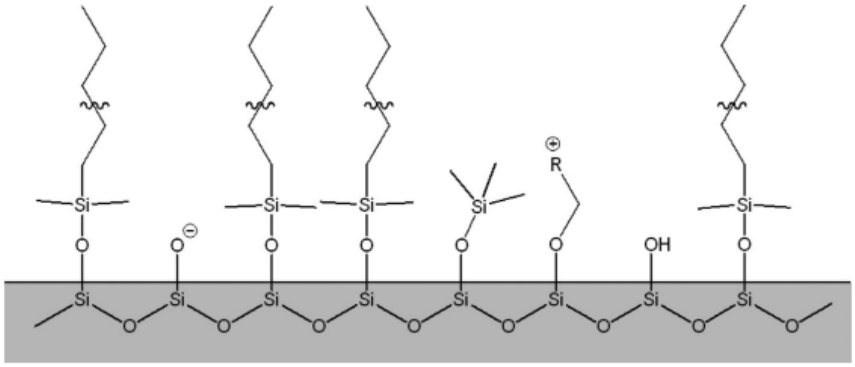

Fig. 1. Schematic representation of silica stationary phase surface chemistry with bonded alkyl groups, negatively charged silanol group, bonded positively charged moiety R, and silanol endcapping.

8.0. The downside of our choice is the low buffering capacity in the pH range 4.5 - 6.5.

Fig. 1 shows a schematic representation of silica-based sorbent derivatized with alkyl ligand, endcapped with trimethylsilyl moiety, and derivatized with positively charged group. Negatively charged residual (not endcapped) silanols can act as cation-exchange moieties [6,32,54], while positively charged surface groups may facilitate anion-exchange interaction mechanism in addition to reversed-phase retention [8]. Recent trend in column research is to combine anion or cation interactions with HILIC or RP mode to modify the retention and selectivity of stationary phase to address specific analytical applications [11,14,15].

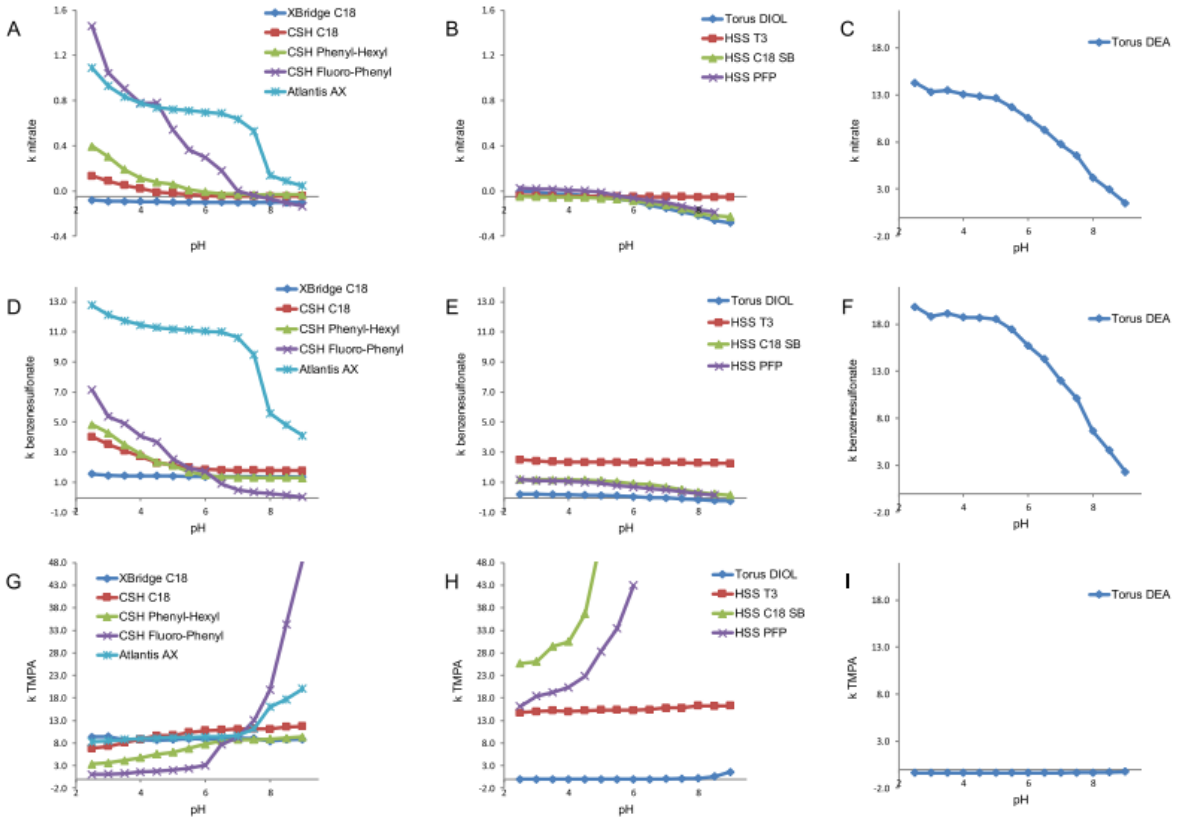

Fig. 2. Experimentally measured retention factor *k* versus the mobile phase pH for nitrate anion (A, B, C), benzenesulfonate anion (D, E, F) and trimethylphenylammonium cation (G, H, I). Panels A, D, and G compare reversed phase columns based on hybrid-silica sorbents. Panels B, E, and H compare silica based C18 column and polar Torus DIOL column. Panels C, F, and I show results for Torus DEA column with dominant anion-exchange retention mode. MP for all experiments was 10 mM dichloroacetic acid adjusted to desirable pH with ammonium hydroxide.

3.2. Ionic interactions investigation of selected columns

Fig. 2 compares retention trends of negatively charged nitrate (panels A, B, C) and benzenesulfonate anions (panels D, E, F) with trends of positively charged trimethylphenylammonium cation (panels G, H, I). Negatively charged iodide ions showed similar trends as nitrate ions (see Supplementary Fig. S1). For better clarity we divided evaluated columns into three groups. First group (Fig. 2, panels A, D, G) represents hybrid-silica RP sorbents. Hybrid-silica sorbents are similar to conventional silica particles, but their formulation includes organofunctional silanes [9,55–57]. Although they have similar morphology as silica, hybrid-silica sorbents exhibit higher pH stability, and less pronounced tailing for basic analytes [56], presumably due to lower acidity of residual surface silanols. A separate class of sorbents known as Charged Surface Hybrid (CSH) is hybrid-silica modified with ionizable pyridyl ligand. Published reports recommend CSH sorbents for separation of peptides, basic analytes [7–10] and as a column with alternative selectivity to conventional C18 sorbents [58].

First group of columns include XBridge C18 sorbent (hybrid-silica with C18 chemistry) which shows no significant change of retention for test analytes within pH range 2.5 – 9.0 (Fig. 2A,D,G). We conclude that XBridge C18 does not exhibit significant ionic-interactions. In comparison, CSH reversed-phase sorbents show distinct increase of retention of anionic analytes at acidic mobile phase pH when the pyridyl surface modifier (pKa~5–6) is positively charged. Fig. 2A and D show that all CSH columns retain nitrate and benzenesulfonate more strongly than XBridge C18 column. Furthermore, trimethylphenylammonium cation retention is suppressed at acidic pH compared to neutral XBridge C18 column (Fig. 2G). These observations suggest that CSH sorbents have anion-exchange properties at pH<6 in addition to RP retention. The degree of ionic attraction/repulsion increases in the order CSH C18 < CSH Phenyl-Hexyl < CSH Fluoro-Phenyl. This is intriguing observation, since all CSH sorbents have the same concentration of pyridyl ligand at the surface [59]. The different ionic-interaction strength is presumably due to steric shielding of a surface charge with RP ligand. Relatively long C18 ligand shields the ionic interactions more effectively than shorter Phenyl-Hexyl and shortest Fluoro-Phenyl ligands (see Table 1 for structures).

Fig. 2A,D,G indicate that above pH 6 the pyridyl surface groups of CSH sorbents are discharged [18] and ionic interactions no-longer contribute to retention. Retention factors of analytes on CSH C18 and CSH Phenyl-Hexyl columns remain constant and the retention strength is comparable to neutral XBridge C18 sorbent (Figs. 2A, B). On the other hand, CSH Fluoro-Phenyl column behaves differently. The retention of trimethylphenylammonium cation sharply increases at basic pH (Fig. 2G), while the retention of anions decreases (Fig. 2A, D). The observed cation-exchange activity of CSH Fluoro-Phenyl sorbent is due to non-endcapped silanols on the surface that act as cation-exchange sites above pH ~6–7.

The first group includes mixed-mode Atlantis Premier BEH C18 AX column. The column combines RP (C18) and anion-exchange retention modes. Because alkylamine is stronger base than pyridyl group (amine pKa ~ 10.6), Atlantis Premier BEH C18 AX column retains anions in wider pH range than CSH columns (Fig. 2A, D). Retention trends on Atlantis Premier BEH C18 AX reveal a decrease in

anionic retention and increase in cation retention at pH 7–8, which suggests diminished contribution of ionic retention mode. This is far from expected pKa of alkylamine surface modifier, when we would expect loss of sorbent surface charge. A possible explanation is that residual silanols remaining on the surface after endcapping become deprotonated in vicinity of pH 7 and alter the overall surface charge via formation of zwitter ions with surface bound amines.

Comparison of second group of columns is shown in Fig. 2, panels B, E, H. The group includes silica C18 sorbents with exception of polar hybrid-silica Torus DIOL column. Torus DIOL was designed for Supercritical Fluid Chromatography (SFC), but it is applicable also for HILIC separations [60]. RP columns in the second group include HSS T3 (C18 sorbent) with endcapped silanols, HSS C18 SB (SB refers to selectivity for bases), and HSS PFP bonded with pentafluorophenyl ligand. The latter two RP sorbents are not endcapped (Table 1).

Fig. 2B, E, H show that HSS T3 column has minimal ionic interactions with test analytes; the retention factors do not change significantly with mobile phase pH. In contrast, the non-endcapped HSS C18 SB and HSS PFP columns exhibit strong cation-exchange interactions as the silanols become more charged at increased pH (repulsion of anions and attraction of cations). Because of this behavior the HSS C18 SB stationary phase is recommended as column with "orthogonal" selectivity to endcapped C18 columns (e.g. HSS T3). It is important to understand that the apparent selectivity differences are ionic in nature; relative retention of neutral analytes is not strongly affected [2,43,51].

Fig. 2B shows slightly negative retention factor for nitrate anion below pH 6. Although it is difficult to measure retention factor near zero (due to peak shape and difficulties to precisely measure column void volume), this observation suggests an exclusion of nitrate from the sorbent pores due to ionic repulsion. Decrease in retention was observed also for benzenesulfonate on non-endcapped HSS C18 SB and HSS PFP columns in Fig. 2E, but the retention factor remains above zero because of hydrophobic interactions.

Polar Torus DIOL column shows minimal retention for test analytes (Fig. 2B, E, H). The observed repulsion of anions on Torus DIOL column at basic pH resembles the cation-exchange interactions of non-endcapped columns. This behavior is intriguing, because polymeric diol layer is expected to effectively shield all surface silanols. It is unclear whether portion of hybrid-silica silanols remains accessible for chromatographic interactions, or whether hydrolyzed epoxy siloxanes moieties become an alternative source of silanols on the bonded surface.

The third group includes Torus DEA, the only column in the set with primary anion-exchange retention mode (Fig. 2C,F,I). Torus DEA sorbent, originally designed for SFC, is prepared by polymerization of epoxy siloxanes on hybrid silica as described above for Torus DIOL phase, followed by derivatization with diethylamine moiety and ring opening of remaining epoxides. Diethylamine ligand with pKa of ~ 10.6 is fully charged below pH ~ 9. The column was included in the study for comparison with CSH and Atlantis Premier BEH C18 AX columns.

As expected, the retention of inorganic nitrate and benzenesulfonate ions on Torus DEA is significantly higher compared to all tested columns (Fig. 2C, F). Surprisingly, the anion-exchange retention gradually diminishes for MP above pH~5. The retention loss occurs well above the pKa value of DEA ligand. This observation is reminiscent to trends obtained with Atlantis Premier BEH C18 AX column. It is unclear whether this retention behavior is due to the same mechanism that is deprotonation of residual silanols of Torus DEA sorbent, which results in formation of zwitter-ions and decreases DEA surface charge.

Fig. 2I illustrates that overall positively charged Torus DEA sorbent repels the trimethylphenylammonium cation from the surface. The analyte elutes before the column void volume (retention factor lower than zero).

To further elucidate the retention mechanism of Torus DEA column we performed experiments with different concentrations of ammonium dichloroacetate (10 to 50 mM) in the MP. A decrease in retention of anionic compounds at elevated ammonium dichloroacetate concentration was observed, a behavior consistent with anion-exchange chromatography retention mode (see Supplementary Fig. S2).

Further inspection of results in Fig. 2 suggests additional conclusions about retention mechanism of selected columns. For example, anion-exchange retention factors of nitrate and benzenesulfonate on Torus DEA are comparable (Fig. C, F), while substantial retention differences were observed for nitrate and benzenesulfonate on CSH and on Atlantis Premier BEH C18 AX columns, respectively (Fig. 2A, D). It appears that retention contribution of ion-exchange and RP modes is not simply additive, but multiplicative, as proposed by Neue and colleagues [6]. Retention models for retention prediction of ion-exchange-RP mixed-mode chromatography are subject of current research [61].

To our knowledge only Hydrophobic Subtraction Model database [3,4,62] included comprehensive database of RP columns. The database enables user to compare limited information about cation or anion exchange activity of columns. The method proposed in this work could be useful for comparison of relative ionic interaction strength of sorbents across wide range of MP pH.

4. Conclusions

The method for investigation of ionic interactions of chromatographic sorbents was proposed. Nitrate marker was selected for testing anionic interactions without a measurable hydrophobic (RP) retention. Benzenesulfonic acid and trimethylphenylammonium markers were chosen as anionic and cationic analytes suitable for characterization of ionic and hydrophobic interactions of columns with aqueous mobile phases.

The obtained data illustrate that ionic interactions participate in retention of both reversed-phase and polar (HILIC) columns to various degrees. We made the following conclusions:

(i) CSH columns exhibit mild anion-exchange interactions at pH below 6.0. This is due to pyridyl modifier present on CSH sorbents surface that becomes charged in acidic pH. At pH above 6.0 the pyridyl moiety is discharged; retention of CSH C18 becomes similar to XBridge C18 column.

(ii) Sorbents with non-endcapped silanols (HSS C18 SB, HSS PFP, CSH Fluoro-Phenyl) have strong ionic activity above pH ~7. Free silanols provide cation-exchange interactions with basic analytes. No significant silanol interactions was evident for endcapped RP sorbents tested (XBridge C18, HSS T3, CSH Phenyl-Hexyl, CSH C18).

(iii) Torus DIOL column shows minor cation-exchange activity in the pH range 6.0 - 9.0. This activity was apparent from behavior of both cationic and anionic test analytes.

(iv) Torus DEA polar column has no observable RP retention; the retention is dominated by anion-exchange activity due to the presence of immobilized positively charged amino groups.

(v) Atlantis Premier BEH C18 AX column has anion-exchange activity in full range of investigated pH 2.5–9.0. The anionic retention diminishes above pH 7, well before expected pKa value of primary alkylamine surface modifier. We speculate that this behavior is related to deprotonation of residual silanols on the sorbent surface leading to diminished surface charge.

It should be pointed out that the developed test can provide only a relative comparison of ionic and hydrophobic interactions for the tested sorbents. Overall retention depends not only on the

immobilized ligands but also on the sorbents phase ratio that is closely related to sorbent pore size or morphology.

The focus of the presented study was to evaluate ionic interactions of selected columns. Many questions remain unanswered, for example whether the surface modification of RP columns with charged moiety alters their hydrophobic retentivity [24] or to what extent the ionic and hydrophobic retentions are synergistic. In other words, whether ionic and hydrophobic interactions mutually enhance their retention strength.

In the subsequent study we plan to investigate mixed-mode columns available on the market with wider set of analytes including both charged and neutral analytes.

Declaration of Competing Interest

The authors declare that they have no known competing financial interests or personal relationships that could have appeared to influence the work reported in this paper.

CRediT authorship contribution statement

Zuzana Kadlecová: Methodology, Investigation, Writing - review & editing, Visualization. **Květa Kalíková:** Conceptualization, Supervision, Writing - review & editing, Visualization. **Denisa Folprechtová:** Investigation, Methodology, Writing - review & editing, Visualization. **Eva Tesařová:** Conceptualization, Funding acquisition, Supervision. **Martin Gilar:** Conceptualization, Writing - original draft.

Acknowledgement

The authors gratefully acknowledge the financial support of the Czech Science Foundation, Grant No 20-19655S.

Supplementary materials

Supplementary material associated with this article can be found, in the online version, at doi:10.1016/j.chroma.2020.461301.

References

[1] A.J. Alpert, Hydrophilic-interaction chromatography for the separation of peptides, nucleic acids and other polar compounds, J. Chromatogr. 499 (1990) 177–196.
[2] D.H. Marchand, P.W. Carr, D.V. McCalley, U.D. Neue, J.W. Dolan, L.R. Snyder, Contributions to reversed-phase column selectivity. II. Cation exchange, J. Chromatogr. A 1218 (2011) 7110–7129.
[3] L.R. Snyder, J.W. Dolan, P.W. Carr, The hydrophobic-subtraction model of reversed-phase column selectivity, J. Chromatogr. A 1060 (2004) 77–116.
[4] A.R. Johnson, C.M. Johnson, D.R. Stoll, M.F. Vitha, Identifying orthogonal and similar reversed phase liquid chromatography stationary phases using the system selectivity cube and the hydrophobic subtraction model, J. Chromatogr. A 1249 (2012) 62–82.
[5] U.D. Neue, Stationary phase characterization and method development, J. Sep. Sci. 30 (2007) 1611–1627.
[6] U.D. Neue, K. Tran, A. Mendez, P.W. Carr, The combined effect of silanols and the reversed-phase ligand on the retention of positively charged analytes, J. Chromatogr. A 1063 (2005) 35–45.
[7] M.A. Lauber, S.M. Koza, S.A. McCall, B.A. Alden, P.C. Iraneta, K.J. Fountain, High-resolution peptide mapping separations with MS-friendly mobile phases and charge-surface-modified C18, Anal. Chem. 85 (2013) 6936–6944.
[8] F. Gritti, G. Guiochon, Effect of the pH and the ionic strength on overloaded band profiles of weak bases onto neutral and charged surface hybrid stationary phases in reversed-phase liquid chromatography, J. Chromatogr. A 1282 (2013) 113–126.
[9] F. Gritti, G. Guiochon, Adsorption behaviors of neutral and ionizable compounds on hybrid stationary phases in the absence (BEH-C18) and the presence (CSH-C18) of immobile surface charges, J. Chromatogr. A 1282 (2013) 58–71.
[10] T.H. Walter, B.A. Alden, C. Boissel, J. Field, N. Lawrence, D. Osterman, A. Patel, A new mixed-mode reversed-phase/anion-exchange stationary phase based on hybrid particles, Application note 720006742en (2020) 8.
[11] K. Zhang, X. Liu, Mixed-mode chromatography in pharmaceutical and biopharmaceutical applications, J. Pharm. Biomed .Anal. 128 (2016) 73–88.
[12] M. Lammerhofer, M. Richter, J. Wu, R. Nogueira, W. Bicker, W. Lindner, Mixed–mode ion-exchangers and their comparative chromatographic characterization in reversed-phase and hydrophilic interaction chromatography elution modes, J. Sep. Sci. 31 (2008) 2572–2588.
[13] J. Li, S. Shao, M.S. Jaworsky, P.T. Kurtulik, Simultaneous determination of cations, zwitterions and neutral compounds using mixed-mode reversed-phase and cation-exchange high-performance liquid chromatography, J. Chromatogr. A 1185 (2008) 185–193.
[14] M. Biba, E. Jiang, B. Mao, D. Zewge, J.P. Foley, C.J. Welch, Factors influencing the separation of oligonucleotides using reversed-phase/ion-exchange mixed–mode high performance liquid chromatography columns, J. Chromatogr. A 1304 (2013) 69–77.
[15] A.A. Kazarian, P.N. Nesterenko, P. Soisungnoen, R. Burakham, S. Srijaranai, B. Paull, Comprehensive analysis of pharmaceutical products using simultaneous mixed-mode (ion-exchange/reversed-phase) and hydrophilic interaction liquid chromatography, J. Sep. Sci. 37 (2014) 2138–2144.
[16] S.H. Park, M. De Pra, P.R. Haddad, S. Grosse, C.A. Pohl, F. Steiner, Localised quantitative structure-retention relationship modelling for rapid method development in reversed-phase high performance liquid chromatography, J. Chromatogr. A (2019) 460508.
[17] C. Hao, D. Morse, F. Morra, X. Zhao, P. Yang, B. Nunn, Direct aqueous determination of glyphosate and related compounds by liquid chromatography/tandem mass spectrometry using reversed-phase and weak anion-exchange mixed-mode column, J. Chromatogr. A 1218 (2011) 5638–5643.
[18] T.H. Walter, B.A. Alden, M. Blaze, C. Boissel, M. DeLano, J. Field, N. Lawrence, D. Osterman, A. Patel, Characterization of new MS-compatible mixed-mode reversed-phase/anion-exchange HPLC columns, J. Chromatogr. A (2020) Submitted for publication.
[19] E.C. Pinto, M.D.S. Goncalves, L.M. Cabral, D.W. Armstrong, V.P. de Sousa, Development and validation of a stability-indicating HPLC method for topiramate using a mixed-mode column and charged aerosol detector, J. Sep. Sci. 41 (2018) 1716–1725.
[20] D. Sykora, P. Rezanka, K. Zaruba, V. Kral, Recent advances in mixed-mode chromatographic stationary phases, J. Sep. Sci. 42 (2019) 89–129.
[21] F.R. Mansour, N.D. Deanielson, Multimodal liquid chromatography of small molecules, Anal. Methods 5 (2013) 4955–4972.
[22] H. Qiu, A.K. Mallik, M. Takafuji, S. Jiang, H. Ihara, New poly(ionic liquid)-grafted silica multi-mode stationary phase for anion-exchange/reversed-phase/hydrophilic interaction liquid chromatography, Analyst 137 (2012) 2553–2555.
[23] M. Sun, J. Feng, C. Luo, X. Liu, S. Jiang, Benzimidazole modified silica as a novel reversed-phase and anion-exchange mixed-mode stationary phase for HPLC, Talanta 105 (2013) 135–141.
[24] Q. Song, K. Zhao, H. Xia, J. Liu, Q. Bai, A novel reversed-phase and weak anion-exchange mixed-mode stationary phase based on horizontal polar-copolymerized approach for separation of small organic molecules and inorganic anions, Talanta 197 (2019) 592–598.
[25] P. Zhang, J. Chen, L. Jia, N-methylimidazolium-functionalized monolithic silica column for mixed-mode chromatography, J. Chromatogr. A 1218 (2011) 3459–3465.
[26] M. Sun, J. Feng, S. Liu, C. Xiong, X. Liu, S. Jiang, Dipyridine modified silica–a novel multi-interaction stationary phase for high performance liquid chromatography, J. Chromatogr. A 1218 (2011) 3743–3749.
[27] K. Zhang, L. Dai, N.P. Chetwyn, Simultaneous determination of positive and negative pharmaceutical counterions using mixed-mode chromatography coupled with charged aerosol detector, J. Chromatogr. A 1217 (2010) 5776–5784.
[28] D.V. McCalley, A study of column equilibration time in hydrophilic interaction chromatography, J. Chromatogr. A 1554 (2018) 61–70.
[29] D.V. McCalley, Managing the column equilibration time in hydrophilic interaction chromatography, J. Chromatogr. A 1612 (2020) 460655.
[30] D.S. Bell, Retention and selectivity of stationary phases used in HILIC, LC GC N. Am. 33 (2015) 90–101.
[31] K.D. Berthelette, T.H. Walter, M. Gilar, F. Gritti, T.S. MacDonald, M. Soares, Evaluating MISER chromatography as a tool for characterizing HILIC column equilibration, J. Chromatogr. A (2020) 460931.
[32] A. Mendez, E. Bosch, M. Roses, U.D. Neue, Comparison of the acidity of residual silanol groups in several liquid chromatography columns, J. Chromatogr. A 986 (2003) 33–44.
[33] U.D. Neue, B.A. Alden, T.H. Walter, Universal procedure for the assessment of the reproducibility and the classification of silica-based reversed-phase packings II. Classification of reversed-phase packings, J. Chromatogr. A 849 (1999) 101–116.
[34] N.S. Wilson, M.D. Nelson, J.W. Dolan, L.R. Snyder, P.W. Carr, Column selectivity in reversed-phase liquid chromatography II. Effect of a change in conditions, J. Chromatogr. A 961 (2002) 195–215.
[35] W. Bicker, J. Wu, H. Yeman, K. Albert, W. Lindner, Retention and selectivity effects caused by bonding of a polar urea-type ligand to silica: a study on mixed-mode retention mechanisms and the pivotal role of solute-silanol interactions in the hydrophilic interaction chromatography elution mode, J. Chromatogr. A 1218 (2011) 882–895.
[36] M. Gilar, A. Jaworski, Retention behavior of peptides in hydrophilic-interaction chromatography, J. Chromatogr. A 1218 (2011) 8890–8896.
[37] K. Kalíková, P. Kozlík, M. Gilar, E. Tesařová, Properties of two amide-based hydrophilic interaction liquid chromatography columns, J. Sep. Sci. 36 (2013) 2421–2429.

[38] D.V. McCalley, Study of retention and peak shape in hydrophilic interaction chromatography over a wide pH range, J. Chromatogr. A 1411 (2015) 41–49.
[39] M.E. Ibrahim, Y. Liu, C.A. Lucy, A simple graphical representation of selectivity in hydrophilic interaction liquid chromatography, J. Chromatogr. A 1260 (2012) 126–131.
[40] S. Van Dorpe, V. Vergote, A. Pezeshki, C. Burvenich, K. Peremans, B. De Spiegeleer, Hydrophilic interaction LC of peptides: columns comparison and clustering, J. Sep. Sci. 33 (2010) 728–739.
[41] Y. Wang, M.F. Wahab, Z.S. Breitbach, D.W. Armstrong, Carboxylated cyclofructan 6 as a hydrolytically stable high efficiency stationary phase for hydrophilic interaction liquid chromatography and mixed mode separations, Anal. Methods 8 (2016) 6038–6045.
[42] Y. Hou, F. Zhang, X. Liang, B. Yang, X. Liu, P.K. Dasgupta, Poly(vinyl alcohol) modified porous graphitic carbon stationary phase for hydrophilic interaction liquid chromatography, Anal. Chem. 88 (2016) 4676–4681.
[43] U.D. Neue, J.E. O'Gara, A. Mendez, Selectivity in reversed-phase separations Influence of the stationary phase, J. Chromatogr. A 1127 (2006) 161–174.
[44] K. Kimata, K. Iwaguchi, K. Onishi, K. Jinno, R. Eksteen, K. Hosoya, M. Araki, N. Tanaka, Chromatographic characterization of silica C18 Packing Materials. Correlation between a Preparation Method and Retention Behavior of Stationary Phase, J. Sep. Sci. 27 (1989) 721–728.
[45] M.J. Walters, Classification of octadecyl-bonded liquid chromatography columns, J. Assoc. Off. Anal. Chem. 70 (1987) 465–469.
[46] R.K. Lindsey, B.L. Eggimann, D.R. Stoll, P.W. Carr, M.R. Schure, J.I. Siepmann, Column selection for comprehensive two-dimensional liquid chromatography using the hydrophobic subtraction model, J. Chromatogr. A 1589 (2019) 47–55.
[47] R. Nogueira, D. Lubda, A. Leitner, W. Bicker, N.M. Maier, M. Lammerhofer, W. Lindner, Silica-based monolithic columns with mixed-mode reversed-phase/weak anion-exchange selectivity principle for high-performance liquid chromatography, J. Sep. Sci. 29 (2006) 966–978.
[48] P. Jiang, D. Wu, C.A. Lucy, Determination of void volume in normal phase liquid chromatography, J. Chromatogr. A 1324 (2014) 63–70.
[49] S. Jung, S. Ehlert, M. Pattky, U. Tallarek, Determination of the interparticle void volume in packed beds via intraparticle Donnan exclusion, J. Chromatogr. A 1217 (2010) 696–704.
[50] R. Linda, L.W. Lim, T. Takeuchi, Poly(ethylene oxide)-bonded stationary phase for separation of inorganic anions in capillary ion chromatography, J. Chromatogr. A 1294 (2013) 117–121.
[51] U.D. Neue, A. Mendez, Selectivity in reversed-phase separations: general influence of solvent type and mobile phase pH, J. Sep. Sci. 30 (2007) 949–963.
[52] M. Gilar, P. Olivova, A.E. Daly, J.C. Gebler, Two-dimensional separation of peptides using RP-RP-HPLC system with different pH in first and second separation dimensions, J. Sep. Sci. 28 (2005) 1694–1703.
[53] M. Gilar, P. Olivova, A.E. Daly, J.C. Gebler, Orthogonality of separation in two-dimensional liquid chromatography, Anal. Chem. 77 (2005) 6426–6434.
[54] U.D. Neue, C.H. Phoebe, K. Tran, Y.F. Cheng, Z. Lu, Dependence of reversed-phase retention of ionizable analytes on pH, concentration of organic solvent and silanol activity, J. Chromatogr. A 925 (2001) 49–67.
[55] Y.F. Cheng, T.H. Walter, Z.L. Lu, P. Iraneta, B.A. Alden, C. Gendreau, U.D. Neue, J.M. Grassi, J.L. Carmody, J.E. OGara, R.P. Fisk, Hybrid organic-inorganic particle technology: breaking through traditional barriers of HPLC separations, LC-GC 18 (2000) 1162–1172.
[56] K.D. Wyndham, J.E. O'Gara, T.H. Walter, K.H. Glose, N.L. Lawrence, B.A. Alden, G.S. Izzo, C.J. Hudalla, P.C. Iraneta, Characterization and evaluation of C18 HPLC stationary phases based on ethyl-bridged hybrid organic/inorganic particles, Anal. Chem. 75 (2003) 6781–6788.
[57] E.S. Grumbach, D.M. Diehl, U.D. Neue, The application of novel 1.7 microm ethylene bridged hybrid particles for hydrophilic interaction chromatography, J. Sep. Sci. 31 (2008) 1511–1518.
[58] G. Glauser, F. Schweizer, T.C. Turlings, P. Reymond, Rapid profiling of intact glucosinolates in Arabidopsis leaves by UHPLC-QTOFMS using a charged surface hybrid column, Phytochem. Anal. 23 (2012) 520–528.
[59] B.A. Alden, K.M. Smith, P. Rainville, T.H. Walter, M. Gilar, Retention of Anions on Charged Surface Hybrid Columns, EAS poster Library number: PSTR134990442, 2019.
[60] O. Kozlov, Z. Kadlecova, M. Gilar, T. Gondova, K. Kalikova, E. Tesafova, Systematic evaluation of selected supercritical fluid chromatography diol- and diethylamine-based columns for application in hydrophilic interaction liquid chromatography, Sep. Sci. Plus 2 (2019) 81–88.
[61] J.L. Dores-Sousa, J. De Vos, W.T. Kok, S. Eeltink, Probing selectivity of mixed–mode reversed-phase/weak-anion-exchange liquid chromatography to advance method development, J. Chromatogr. A 1570 (2018) 75–81.
[62] http://www.hplccolumns.org/about/index.php, Hydrophobic subtraction model Column database, 2020.

Publikace III

How ligand and particle types affect retention and separation of structurally diverse biologically active compounds in HPLC

Kadlecová, Z., Kalíková, K.
Monatshefte Für Chemie - Chemical Monthly, **2021**, *152*, 1081–1088.

Monatshefte für Chemie - Chemical Monthly (2021) 152:1081–1088
https://doi.org/10.1007/s00706-021-02807-6

ORIGINAL PAPER

How ligand and particle types affect retention and separation of structurally diverse biologically active compounds in HPLC

Zuzana Kadlecová[1] · Květa Kalíková[1]

Received: 19 March 2021 / Accepted: 21 June 2021 / Published online: 17 August 2021

Abstract

In this work, effects of particle and ligand types on retention and separation of sets of neutral (naphthoflavones), acidic (profens), basic (cathinones), and zwitterionic (dipeptides) biologically active compounds are shown in detail and discussed. Nine columns differing in ligand and particle types were tested, namely XSelect HSS C18, XSelect HSS C18 SB, XSelect HSS PFP, XSelect CSH C18, XSelect CSH Phenyl-Hexyl, XSelect CSH Fluoro-Phenyl, XBridge C18, XBridge Shield RP18, and Atlantis PREMIER BEH C18 AX. Various mobile phases differing in acetonitrile/aqueous part volume ratio and aqueous part pH, i.e. pH = 2.1, pH = 4.7, and pH = 8.0 were tested and compared in terms of analytes´ retention and separation. Results showed significant effect of ionic interactions resulting from particle types used or additional ionisable functional groups bonded to the surface on retention and separation of charged compounds. All tested sets of compounds were baseline separated but different conditions, that is column type and mobile phase composition, were needed.

Graphic abstract

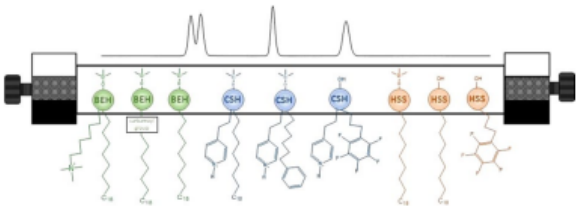

Keywords High-pressure liquid chromatography · Ligand · Particle type · Separation performance · Resolution

Introduction

Recently, the supply and the demand for new chromatographic sorbents have been increasing. Chromatographic columns are supplied by several manufacturers, and each has different "know-how" concerning the production process and innovation. Retention and separation potential of the columns are affected by the number of factors, which includes: carrier type, ligand type, particle type, pore size, and various sorbent modifications (e.g. endcapping, charged moiety) [1–5]. Companies involved in the development of new stationary phases are continuously improving columns´ efficiency, including research in the field of particle technology. The choice of particle type can fundamentally affect not only retention but also the peak shape [6]. In this work, all chromatographic columns were obtained from a single manufacturer to ensure that the results are affected only by differences in particle and ligand types of the stationary phase and not by differences in packing procedure [7, 8].

In this work, we compare columns with different ligands and three different particle types: bridged ethylene hybrid (BEH) particles, charged surface hybrid (CSH) particles, and high-strength silica (HSS) particles. Columns with BEH particles are commonly available on the market under the designation XBridge™. Special BEH particles´ structure is

✉ Květa Kalíková
kalikova@natur.cuni.cz

[1] Department of Physical and Macromolecular Chemistry, Faculty of Science, Charles University, Hlavova 8, 12843 Prague, Czech Republic

designed to achieve longer lifetime and greater sorbent stability in wide pH range (pH 1–12). Simultaneously, XBridge columns allow using at higher temperatures and pressures in comparison with conventional silica sorbents [9, 10]. One of the most common columns from this family is XBridge C18 column [11]. A complementary column to conventional octadecyl-based columns, especially in terms of the selectivity for phenolic compounds, is the XBridge Shield RP18 column [12]. This column contains embedded carbamate group in the bonded octadecyl structure, which is responsible for different selectivity. A special case is a mixed-mode column Atlantis PREMIER BEH C18 AX, which utilizes BEH particles to bond both octadecyl ligands and anion-exchange groups [13, 14].

The XSelect™ family of chromatographic columns includes two different particle types, CSH and HSS. The CSH particles contain pyridyl groups (pK_A ~ 5–6) as charge modifiers bonded to the surface of the particles. This low-level surface charge can improve peak shape of basic compounds in acidic low-ionic strength mobile phases [15]. The presence of a positive charge on stationaryphase surface is limited by pH of mobile phase. Pyridyl group is positively charged at pH < 7, but anion-exchange mechanism for inorganic ions was confirmed at pH < 6 [13]. Three different ligands bonded to CSH particles were tested—octadecyl, phenyl-hexyl (PH), and pentafluorophenyl (PFP).

The HSS particle technology was developed specifically to complement the chromatographic performance of BEH and CSH particles [16]. Compared to them, HSS particles´ higher silanophilicity offers increased retention of polar compounds [15]. Moreover, smaller pore diameters (100×10^{-10} m) and thus larger surface of HSS particles provide increased retention of all compounds in comparison with BEH and CSH columns of same dimension, which are available in 130×10^{-10} m variants [16, 17]. Three HSS columns were used in this work: XSelect HSS C18, XSelect HSS C18 SB, and XSelect HSS PFP.

The endcapping also significantly affects columns retentivity, selectivity and thus separation behavior. Non-endcapped columns containing free silanol groups can provide electrostatic interactions in mobile phases, where free silanol groups are dissociated. This causes enhanced retention of positively charged compounds and reduced retention of negatively charged compounds [6].

The aim of this work was to describe the differences among nine chromatographic columns under isocratic reversed-phase mobilephase conditions. The effect of the particle type, ligand type, and endcapping technology was investigated in terms of columns applicability for the separation of structurally diverse compounds. Four sets of structurally different analytes, i.e. neutral naphthoflavones, acidic profens, basic cathinones, and zwitterionic dipeptides, in various pH of aqueous part of mobile phase and organic modifier/aqueous part volume ratios can provide comprehensive information about retentivity, selectivity, and separation behavior of the columns.

Results and discussion

The differences in retentivity and selectivity of nine tested columns (for their basic properties see Table 1) were examined by analysis of four structurally diverse sets of analytes in different mobile phases. Mobile phases were composed of acetonitrile and aqueous part, i.e. formic acid, pH = 2.1, 10 mM ammonium acetate buffer, pH = 4.7, or 10 mM ammonium acetate buffer, pH = 8.0. Two ratios of acetonitrile/aqueous part, 60/40 and 40/60 (*v*/*v*), were tested for all the columns and for all sets of analytes. In some cases, additional volume ratios were used to improve separation: acetonitrile/aqueous part 70/30, 50/50, 30/70, and 20/80 (*v*/*v*). List of all analytes, their corresponding structures, pK_A and log *D* values is shown in Table S1 in Supporting Material.

Table 1 Basic properties of nine tested columns, the information can be found at www.waters.com

Column	Particle type	Ligand	Endcapping	Charge modifier
XSelect® HSS C18	HSS	Octadecyl	Yes	None
XSelect® HSS C18 SB	HSS	Octadecyl	No	None
XSelect® HSS PFP	HSS	Pentafluorophenyl	No	None
XSelect® CSH™ C18	CSH	Octadecyl	Yes	Pyridyl
XSelect® CSH™ Phenyl-Hexyl	CSH	Phenyl-hexyl	Yes	Pyridyl
XSelect® CSH™ Fluoro-Phenyl	CSH	Pentafluorophenyl	No	Pyridyl
XBridge® C18	BEH	Octadecyl	Yes	None
XBridge® Shield RP18	BEH	Octadecyl + carbamate group	Yes	None
Atlantis™ PREMIER BEH C18 AX	BEH	Octadecyl	Yes	Alkylamine

Particle types: *HSS* high-strength silica, *CSH* charged surface hybrid, *BEH* bridged ethylene hybrid

Naphthoflavones

As can be expected, retention and peak shape of neutral naphthoflavones are almost unaffected by pH of aqueous part of mobile phase. Peak symmetry factors for all tested naphthoflavones in all tested conditions are close to 1. The retention order of naphthoflavones was the same for all tested columns in all the tested mobile phases. The only exception was XSelect HSS PFP column, which will be discussed later. As retention in reversed-phase chromatography depends much on polarity of analytes, the calculated log *D* values (see Table S1 in Supporting Material) correlate with observed retention order. More polar hydroxylated α- and β-naphthoflavones eluted before nonhydroxylated α- and β-naphthoflavones. In each pair α-derivative eluted before β-derivative. Using XSelect HSS PFP column, change in the elution order with changing in acetonitrile/aqueous part ratio was observed for all tested mobile phases pHs. Figure 1 shows that hydroxylated α- and β- naphthoflavones eluted before nonhydroxylated α- and β- naphthoflavones in all conditions, but the change in elution order of α- and β-derivatives in both pairs was observed. In mobile phase composed of acetonitrile /10 mM ammonium acetate buffer, pH = 8.0; 60/40 (*v*/*v*) β-derivatives were eluted before α-derivatives. Increasing amount of the aqueous part in mobile phase, i.e. acetonitrile / 10 mM ammonium acetate buffer, pH = 8.0; 50/50 (*v*/*v*) resulted in co-elution of appropriate α- and β-derivatives. Further increase in aqueous part in mobile phase (acetonitrile / 10 mM ammonium acetate buffer, pH = 8.0; 40/60 (*v*/*v*)) led to partial separation, but in opposite elution order of α- and β-derivatives.

Generally, octadecyl columns and column XSelect HSS PFP exhibit higher retention of naphthoflavones than other columns. The highest retention provides mixed-mode column Atlantis PREMIER BEH C18 AX. Baseline separation of naphthoflavones could be achieved within 8 min in mobile phase composed of acetonitrile/aqueous part; 70/30 (*v*/*v*) on the following columns: XBridge C18, XBridge Shield RP18, XSelect HSS C18, Xselect CSH C18, XSelect CSH PH, and Atlantis PREMIER BEH C18 AX. Mobilephase composition acetonitrile/aqueous part 40/60 (*v*/*v*) enabled baseline separation of naphthoflavones on XSelect HSS C18 SB column (analysis time 60 min) and XSelect CSH FP column (analysis time 30 min)—see Tables S3 and S5 in Supporting Material. All chromatographic data obtained for naphthoflavones are summarized in Tables S2, S3, S5, S6, S9, and S10 in Supporting Material.

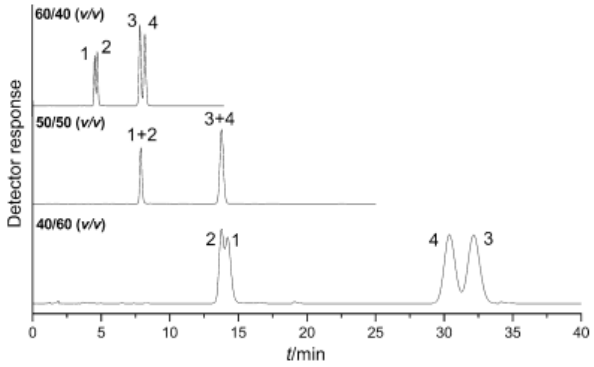

Fig. 1 Chromatograms of separation of naphthoflavones, change in retention order with changing of mobilephase composition. Mobilephase composition: acetonitrile / 10 m M ammonium acetate buffer, pH = 8.0 in three different acetonitrile/aqueous part ratios, column: XSelect HSS PFP. Peak identification—1: 3-hydroxy-β-naphthoflavone; 2: 3-hydroxy-α-naphthoflavone; 3: β-naphthoflavone; 4: α-naphthoflavone

Profens

Retention of acidic profens decreases with increasing pH of aqueous part of mobile phase on all the columns. Since profens are negatively charged at basic pH (i.e. they are more polar, see the log *D* values in Table S1 in Supporting Material), aqueous part of mobile phase of pH = 8.0 is not suitable for their retention and separation in RP chromatography (see Fig. 2 for example). Retention of profens is low and peaks are broadened with great tendency to front at pH = 8.0. Mobile phases composed of aqueous parts of pH = 2.1 and pH = 4.7 appear more suitable for profens separation in terms of their retention and symmetry factors (close to 1). While on all reversed-phase octadecyl-based columns change of the pH of mobile phase aqueous part from 2.1 to 4.7 caused a decrease in retention, the retention increased on mixed-mode column Atlantis PREMIER BEH C18 AX and small increase in retention on XSelect CSH C18 column is also evident (see Tables S3, S6, and Fig. 3). It is caused by the

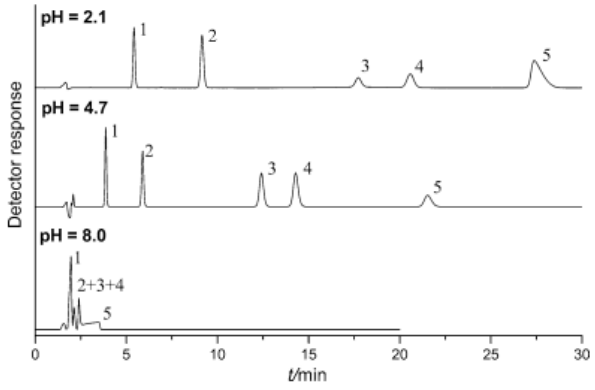

Fig. 2 Chromatograms of separation of profens. Mobilephase composition: acetonitrile/aqueous part, 40/60 (*v*/*v*). Column: XSelect CSH C18. Peak identification—1: indoprofen; 2: ketoprofen; 3: fenoprofen; 4: carprofen; 5: ibuprofen

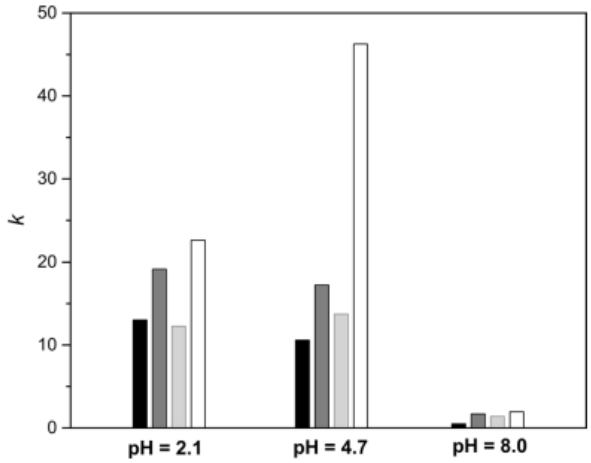

Fig. 3 Dependence of retention factor of ibuprofen on mobile phase pH for XBridge C18 column (black), XSelect HSS C18 (dark gray), XSelect CSH C18 column (light gray), and Atlantis PREMIER BEH C18 AX column (white). Mobilephase composition: acetonitrile/aqueous part, 40/60 (*v/v*)

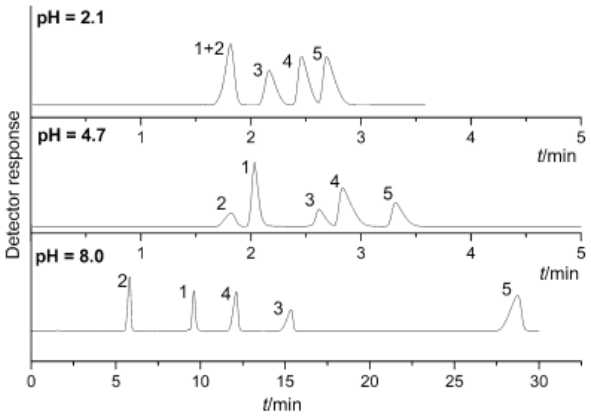

Fig. 4 Chromatograms of separation of cathinone derivatives, effect of aqueous part pH on retention and separation. Mobile-phase composition: acetonitrile/aqueous part; 40/60 (*v/v*); aqueous part: formic acid, pH = 2.1; 10 mM ammonium acetate buffer, pH = 4.7 and pH = 8.0. Column: XSelect HSS C18. Peak identification—1: 4-CDC; 2: 4-ClC; 3: 4F-NPP; 4: 4-CBC; 5: 4-CPRC

occurrence of electrostatic interactions between positively charged stationary phase and partially negatively charged ibuprofen ($pK_A = 4.85$) in mobile phase composed of aqueous part of pH = 4.7. The increase in retention on column XSelect CSH C18 is small in comparison with mixed-mode column, because the charge on column XSelect CSH C18 at pH = 4.7 does not play so important role. Figure 3 also shows that positively charged mixed-mode column Atlantis PREMIER BEH C18 AX at mobile phase with aqueous part of pH = 8.0 does not provide longer retention of profens in comparison with other columns. This behavior was previously explained in [13] as follows: "residual silanols remaining on the surface after endcapping become deprotonated in vicinity of pH = 7 and alter the overall surface charge via formation of zwitterions with surface bound amines."

Column Atlantis PREMIER BEH C18 AX provides the highest retention of profens at aqueous parts of pH = 2.1 and pH = 4.7. In mobile phases composed of acetonitrile/aqueous part of pH = 2.1 or 4.7; 50/50 (*v/v*), baseline separation can be achieved within 16 min and 37 min, respectively. In mobile phases composed of acetonitrile/aqueous part, pH = 2.1 or pH = 4.7; 40/60 (*v/v*), columns XSelect HSS C18 SB, XSelect CSH PH, and XSelect HSS PFP provided baseline separation within 15 min; columns XBridge C18, XSelect HSS C18, and XSelect CSH C18 within 30 min. In some cases, the change in volume ratio of acetonitrile/aqueous part or using gradient elution could improve the separation and shorten the analysis time. Under the same mobile-phase composition, lower selectivity, i.e. separation of only four profens, on XBridge Shield RP18 (within 20 min) and XSelect CSH FP (within 10 min) was obtained. Retention order of profens was the same on all the columns in acidic mobile phases and corresponds to calculated log *D* values (Table S1 in Supporting Material): indoprofen, ketoprofen, fenoprofen, carprofen, and ibuprofen. Only pentafluorophenyl ligand bonded to different particles caused a switch in elution order of the last two eluting profens, i.e. ibuprofen eluted before carprofen, on columns XSelect CSH FP and XSelect HSS PFP. This behavior confirms different selectivity of the columns.

Cathinone derivatives

Retention of basic cathinone derivatives is also strongly influenced by the aqueous part pH [18]. Increasing pH of aqueous part of mobile phase caused prolongation of retention compared to lower pH values (Fig. 4). Cathinone derivatives are very polar in acidic pH, which causes their low retention in reversed-phase conditions, and less polar in basic pH, which results from the change in their charge. Figure 4 also shows change in elution order with pH change. In mobile phase composed of aqueous part of pH = 2.1 and pH = 4.7, cathinone derivatives are positively charged, while at basic pH, the majority of tested cathinones is charged only partially. pK_A values of the cathinone derivatives are around 8.2 (see Table S1 in Supporting Material) and 4-chloro-*N,N*-dimethylcathinone (4-CDC) is nearly neutral ($pK_A = 6.8$). Retention behavior also correlates with calculated log *D* values (see Table S1 in Supporting Material). The highest log *D* value for 1-(4-chlorophenyl)-2-(pyrrolidin-1-yl) pentan-1-one (4-CPRC) correlates with the highest retention

on all columns in all three tested pH values of aqueous parts of mobile phase. Compounds 4-chloro-*N*-butylcathinone (4-CBC) and 1-(4-fluorophenyl)-2-(isopropylamino)pentan-1-one (4F-NPP) have similar log *D* values (0.29 and 0.25 in acidic conditions; 3.09 and 3.00 in basic conditions) and they are eluted always next to each other. Similar rule works for 4-chloro-*N*-isopropylcathinone (4-ClC) and 4-CDC in basic mobile phase (log *D* values 2.60 and 2.57, respectively). The elution order was the same for all the columns, where cathinones were retained. In aqueous part of mobile phase of pH = 2.1 and pH = 4.7, the retention order was as follows: 4-ClC, 4-CDC, 4F-NPP, 4-CBC, and 4-CPRC (see Tables S3, S6, and S7 in Supporting Material). Retention order in basic mobile phase was rather different: 4-ClC, 4-CDC, 4-CBC, 4F-NPP, and 4-CPRC (see Tables S10 and S11 in Supporting Material). Only phenyl-based columns showed the same retention order in acidic and basic mobile phases. Based on these results and calculated log *D* values, it can be assumed that the retention and the change in the retention order of cathinone derivatives is affected by more types of interactions participating in the interaction/separation mechanism. This confirms different selectivity of the columns. Figure 4 also shows the effect of aqueous part pH on peak shape. Generally, in aqueous part of pH = 8.0, peaks of cathinone derivatives show tendency to front (except for column XSelect CSH FP), while in aqueous parts of pH = 2.1 and pH = 4.7, they exhibit tendency to tail.

The dependence of retention and separation of cathinone derivatives on the type of the column particles is also evident. Figure 5 shows differences in retention of 4-CBC among column without charge modifier XBridge C18, column XSelect CSH C18 with pyridyl group as a charge modifier, mixed-mode column Atlantis PREMIER BEH C18 AX with alkylamine as charge modifier and non-endcapped column without charge modifier XSelect HSS C18 SB. Cathinones had almost no retention on all CSH columns in acidic mobile phase. Their very low retention can be attributed to repulsive interactions between positively charged analytes and positively charged CSH particle surface. This effect diminished at pH = 4.7, where electrostatic repulsion of cathinones from CSH particles decreased. For the same reason, i.e. electrostatic repulsion, mixed-mode column at pH = 2.1 and pH = 4.7 is not suitable for cathinones. At pH = 8.0, cathinones are only partially positively charged and retention on all columns is higher. As can be seen from Fig. 5, the retention in all tested mobile phases is the highest for non-endcapped column XSelect HSS C18 SB, because of its higher surface. Moreover, at pH of aqueous parts 4.7 and 8.0, electrostatic attraction with free silanol groups increases retention of cathinones. This effect is the most significant in mobile phase with aqueous part of pH = 8.0, where free silanol groups are fully dissociated.

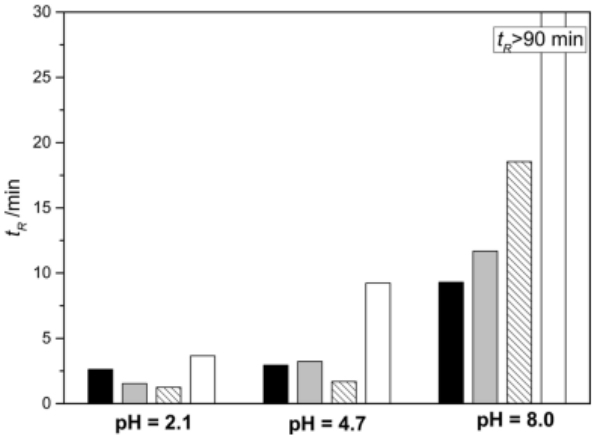

Fig. 5 Differences in retention of 4-CBC on four different columns. Mobilephase composition: acetonitrile/aqueous part; 40/60 (*v*/*v*); aqueous part: formic acid, pH = 2.1; 10 mM ammonium acetate buffer, pH = 4.7; 10 mM ammonium acetate buffer, pH = 8.0. Columns: XBridge C18 (black), XSelect CSH C18 (gray), Atlantis PREMIER BEH C18 AX (dashed), and XSelect HSS C18 SB (white). Retention times were used instead of retention factors because of elution before dead time marker in some cases

The most significant difference in retention of cathinones attributed to the particle type was observed between XSelect HSS PFP and XSelect CSH FP columns (columns with the same ligand bonded to the different particles) in mobile phase composed of aqueous part of pH = 2.1. Column XSelect HSS PFP showed the highest retention for cathinone derivatives, while these analytes were almost not retained on the column with CSH particles, because of the significant electrostatic repulsion (Table S3 in Supporting Material). Similar effect was observed for XSelect CSH C18 (almost no retention) and XSelect HSS C18 (baseline separation in acetonitrile/formic acid, pH = 2.1; 30/70 (*v*/*v*) within 6 min). Comparing the columns, XSelect HSS C18 SB column seems to be the best choice for separation of cathinone derivatives in terms of fast analysis and baseline separation (mobile phase acetonitrile/formic acid, pH = 2.1; 40/60 (*v*/*v*), analysis time 5 min). The baseline separation of these compounds was observed also on XBridge C18 and XBridge Shield RP18 columns within 16 min in mobile phase acetonitrile/formic acid, pH = 2.1; 20/80 (*v*/*v*). Regarding the basic aqueous part of mobile phase, 50 volume % of aqueous part was the best solution for the majority of columns for providing baseline separation of cathinone derivatives (Table S11 in Supporting Material).

Dipeptides

Dipeptides are polar compounds which need a higher amount of aqueous part in the mobile phase to be retained

and separated. Generally, the mobile phase acetonitrile/formic acid, pH = 2.1; 20/80 (*v*/*v*) is suitable for baseline separation of dipeptides on all columns with HSS particles and XBridge C18 column. Retention order in this mobile phase was as follows: H-Trp-Ala-OH, H-Phe-Tyr-OH, H-Ala-Trp-OH, and H-Tyr-Phe-OH on XBridge C18, XSelect HSS C18, XSelect HSS C18 SB, and XSelect HSS PFP. Separation of only three dipeptides (within 3 min) can be achieved on column XBridge Shield RP18 in mobile phase acetonitrile/formic acid, pH = 2.1; 20/80 (*v*/*v*). On the other hand, the mobile phase composed of acetonitrile/formic acid, pH = 2.1 was not suitable for dipeptide separation on mixed-mode column Atlantis PREMIER BEH C18 AX and all columns with CSH particles, probably due to the electrostatic repulsion resulting in very weak retention (see Tables S4 in Supporting Material). Enhanced retention of dipeptides can be achieved on mixed-mode column Atlantis PREMIER BEH C18 AX using aqueous part of pH = 4.7 and pH = 8.0 (see Fig. 6). The change in retention order with the change of mobile phase pH was observed for this column. In mobile phase composed of acetonitrile/aqueous part of pH = 4.7 20/80 or 10/90 (*v*/*v*), retention order was as follows: H-Trp-Ala-OH, H-Ala-Trp-OH, H-Phe-Tyr, and H-Tyr-Phe-OH, while mobile phase composed of acetonitrile/aqueous part of pH = 8.0; 20/80 or 10/90 (*v*/*v*) provides following retention order: H-Ala-Trp-OH, H-Trp-Ala-OH, H-Tyr-Phe-OH, and H-Phe-Tyr-OH.

The results show that the type of the column particles plays again an important role (see Table S4 in Supporting Material). It was confirmed that columns with HSS particles provide higher retention and thus better separation compared to columns with CSH particles, due to the repulsion of CSH particles with positively charged dipeptides.

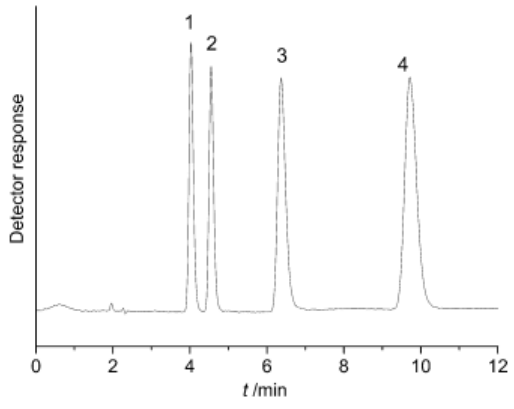

Fig. 6 Chromatograms of separation of dipeptides. Mobilephase composition: acetonitrile / 10 mM ammonium acetate buffer, pH = 4.7; 10/90 (*v*/*v*). Column: Atlantis PREMIER BEH C18 AX. Peak identification—1: H-Tyr-Ala-OH; 2: H-Ala-Trp-OH; 3: H-Phe-Tyr-OH; 4: H-Tyr-Phe-OH

The aqueous parts of pH = 4.7 and pH = 8.0 are not suitable for separation of dipeptides on all tested columns except for mixed-mode column (see Tables S8 and S12 in Supporting Material). On the other hand, aqueous part of pH = 2.1 is not suitable for separation of dipeptides on mixed-mode column. This behavior can be related to the zwitterionic character of dipeptides which causes bad peak shapes and very low retention under certain conditions.

Conclusion

To conclude, columns retentivity and selectivity differ with the ligand type, as well as with the particle type and endcapping technology. In this work, nine columns differing in particle and ligand types and endcapping technology were compared in terms of applicability to the separation of four sets of structurally diverse compounds. Table 2 shows the appropriate separation conditions, i.e. column type and mobilephase composition, for specific groups of analytes.

Generally, retention and separation of neutral naphthoflavones were almost unaffected by pH of mobile phase. The only exception was XSelect HSS PFP column, where decrease in retention in basic pH of mobile phase was observed. Separation of acidic profens can be performed only in acidic pH of mobile phase, basic pH of mobile phase provided weak retention and bad peak shapes. Basic cathinone derivatives cannot be separated on mixed-mode column Atlantis PREMIER BEH C18 AX and columns with CSH particles in acidic pH of mobile phase since they are positively charged. On the other hand, basic pH of mobile phase provided prolonged retention of cathinone derivatives and allowed baseline separation on all the columns. Mobile phase composed of aqueous part of pH = 2.1 was suitable for dipeptides baseline separation on all columns with HSS particles and XBridge C18 column while the mobile phases with aqueous parts of pH = 4.7 and pH = 8.0 were suitable for separation on mixed-mode column Atlantis PREMIER BEH C18 AX.

Endcapping of the columns also significantly affects their chromatographic behavior. For example, non-endcapped column XSelect HSS C18 SB provides significantly higher retention of positively charged cathinones in basic pH of mobile phase in comparison with endcappped column XSelect HSS C18, due to the electrostatic attraction with dissociated free silanol groups.

We were able to baseline separate all sets of selected compounds in various conditions, such as column type and mobilephase composition. Application potential for analysis of structurally diverse biologically active compounds of all tested columns was proved.

Table 2 Summary of the suitability of the columns for separation of the sets of analytes

	Aqueous part of pH = 2.1				Aqueous part of pH = 4.7				Aqueous part of pH = 8.0			
	Neutral	Acidic	Basic	Zwitterionic	Neutral	Acidic	Basic	Zwitterionic	Neutral	Acidic	Basic	Zwitterionic
XSelect® HSS C18	✓	✓	✓	✓	✓	✓	✓	*X*	✓	*X*	✓	*X*
XSelect® HSS C18 SB	✓	✓	✓	✓	✓	✓	✓	*X*	✓	*X*	> 90 min	*X*
XSelect® HSS PFP	✓	✓	✓	✓	✓	✓	✓	*X*	✓	*X*	> 90 min	*X*
XSelect® CSH™ C18	✓	✓	*X*	*X*	✓	✓	✓	*X*	✓	*X*	✓	*X*
XSelect® CSH™ Phenyl-Hexyl	✓	✓	*X*	*X*	✓	✓	✓	*X*	✓	*X*	✓	*X*
XSelect® CSH™ Fluoro-Phenyl	✓	✓	*X*	*X*	✓	✓	✓	*X*	✓	*X*	✓	*X*
XBridge® C18	✓	✓	✓	✓	✓	✓	✓	*X*	✓	*X*	✓	*X*
XBridge® Shield RP18	✓	✓	*X*	✓	✓	✓	✓	*X*	✓	*X*	✓	*X*
Atlantis™ PREMIER BEH C18 AX	✓	✓	*X*	*X*	✓	✓	*X*	✓	✓	*X*	✓	✓

✓suitable; *X* not suitable

This work can serve as a guide for simplifying the method development—i.e. the choice of suitable column and mobile phase for particular purposes.

Experimental

Acetonitrile (Chromasolv® gradient grade, for HPLC, ≥ 99.9%), methanol (Chromasolv® gradient grade, for HPLC, ≥ 99.9%), ammonium acetate (purity ≥ 98%), ammonium formate (purity ≥ 97%), formic acid (purity ≥ 95%), acetic acid (purity ≥ 99%), and ammonium hydroxide solution (28.0–30.0% NH_3) were purchased from Sigma-Aldrich (St. Louis, USA). Sodium hydroxide solution for HPCE (0.1 N sodium hydroxide) was supplied by Agilent Technologies (Santa Clara, USA). All naphthoflavones (α-naphthoflavone, β-naphthoflavone, 3-hydroxy-α-naphthoflavone, and 3-hydroxy-β-naphthoflavone), profens (indoprofen, ibuprofen, fenoprofen, ketoprofen, carprofen) were supplied in analytical-grade purity from Sigma-Aldrich (St. Louis, USA). Dipeptides (H-Phe-Tyr-OH, H-Tyr-Phe-OH, H-Trp-Ala-OH, H-Ala-Trp-OH) were purchased from Bachem (Bubendorf, Switzerland). Cathinone derivatives (4-chloro-*N*,*N*-dimethylcathinone, 1-(4-chlorophenyl)-2-(pyrrolidin-1-yl)pentan-1-one, 4-chloro-*N*-isopropylcathinone, 4-chloro-*N*-butylcathinone, 1-(4-fluorophenyl)-2-(isopropylamino)pentan-1-one) were purchased from internet vendors. For structures of all tested compounds, see Table S1 in Supporting Material.

Instrumentation and chromatographic conditions

All chromatographic measurements were performed using the Waters Alliance system (Waters Corporation, Milford, USA) consisting of Waters 2695 Separation Module, Waters 2996 Photodiode Array Detector, autosampler 717 Plus, and Waters Alliance Series column heater. Empower software was used for system control and data acquisition. Following nine columns were tested: XSelect® HSS C18, XSelect® HSS C18 SB, XSelect® HSS PFP, XSelect® CSH™ C18, XSelect® CSH™ Phenyl-Hexyl, XSelect® CSH™ Fluoro-Phenyl, XBridge® C18, XBridge® Shield RP18, Atlantis™ PREMIER BEH C18 AX. All tested columns, particle size 5 µm, 150 × 4.6 mm, were obtained from Waters Corporation (Milford, USA).

Stock solutions of analytes were prepared by dissolving the sample in methanol at concentration 1 mg cm^{-3} (for solid samples) and 10 mm^3 cm^{-3} (for liquid samples). Dipeptides were dissolved in mixture of methanol and water (50/50 (*v*/*v*)) with addition of 10 mm^3 of sodium hydroxide because of their poor solubility in pure methanol. The first system peak was used as a dead time marker. All measurements were performed in triplicate.

For analysis of all sets of analytes, the mobile phase composed of acetonitrile and aqueous part in volume ratios 40/60 and 60/40 (*v*/*v*) was used. Some other volumetric ratios (70/30, 50/50, 30/70, and 20/80 (*v*/*v*)) were used to improve the separation in individual cases. The following aqueous parts of mobile phases were used: formic acid,

pH = 2.1, 10 mM ammonium acetate buffer, pH = 4.7, and 10 mM ammonium acetate buffer, pH = 8.0. For calculation of buffer components concentrations, and corresponding pH values, PeakMaster software was used [19]. 10 mM ammonium acetate buffer was prepared by dissolving appropriate amount of ammonium acetate in deionized water and appropriate amount of acetic acid (for reach pH = 4.7) or ammonium hydroxide (to reach pH = 8.0) was added. Aqueous solution of formic acid pH = 2.1 (365 mM) was prepared by diluting the appropriate volume of formic acid with deionized water.

Basic chromatographic conditions were set as follows: mobile phase flow rate 1 cm^3 min^{-1}, injection volume 5 mm^3, column temperature 25 °C, and sample temperature 20 °C. Detection wavelengths were 220 nm, 254 nm, and 280 nm. Marvin software (product of ChemAxon company) was used for calculation of log *D* values in corresponding pH of aqueous part of mobile phase and for calculation of pK_A values of analytes.

Supplementary Information The online version contains supplementary material available at https://doi.org/10.1007/s00706-021-02807-6.

Acknowledgements The authors gratefully acknowledge financial support from Czech Science Foundation [Project No. CSF 20-19655S]. Authors want to express their gratitude to Prof. Martin Schmid for his generous gift of cathinone derivatives and Waters Corporation for the kind gift of the columns.

References

1. Giaquinto A, Liu Z, Bach A, Kazakevich Y (2008) Anal Chem 80:6358
2. Bidlingmeyer BA, Broske AD (2004) J Chromatogr Sci 42:100
3. Cooper WT, Lin L-Y (1986) Chromatographia 21:335
4. Gritti F, McDonald T, Gilar M (2015) J Chromatogr A 1420:54
5. Taraba L, Křížek T (2017) Monatsh Chem 148:1605
6. Kadlecová Z, Kalíková K, Ansorge M, Tesařová E, Gilar M (2020) Microchem J 159:105466
7. Plachká K, Švec F, Nováková L (2018) Anal Chim Acta 1039:149
8. Zelenyánszki D, Lambert N, Gritti F, Felinger A (2019) J Chromatogr A 1603:412
9. Kozlov O, Kadlecová Z, Gilar M, Kalíková K, Gondová T, Tesařová E (2019) Sep Sci PLUS 2:81
10. BEH (Ethylene Bridged Hybrid) Technology : Waters. https://www.waters.com/waters/en_US/BEH-(Ethylene-Bridged-Hybrid)-Technology/nav.htm?cid=134618172&locale=en_US. Accessed 20 Jan 2020
11. de Villiers A, Cabooter D, Lynen F, Desmet G, Sandra P (2009) J Chromatogr A 1216:3270
12. Kiridena W, Atapattu SN, Poole CF, Koziol WW (2008) Chromatographia 68:491
13. Kadlecová Z, Kalíková K, Folprechtová D, Tesařová E, Gilar M (2020) J Chromatogr A 1625:461301
14. Walter TH, Alden BA, Field JA, Lawrence NL, Osterman DL, Patel AV, DeLoffi MA (2020) J Sep Sci 44:1005
15. Khater S, West C, Lesellier E (2013) J Chromatogr A 1319:148
16. XSelect HPLC Columns Selectivity of Basic Compounds : Waters. https://www.waters.com/waters/en_US/XSelect-HPLC-Columns-Selectivity-of-Basic-Compounds-/nav.htm?cid=10165804&alias=Alias_xselect_CHEMISTRY&locale=j. Accessed 21 Jan 2020
17. Spoof L, Neffling M-R, Meriluoto J (2009) J Chromatogr B 877:3822
18. Schmid MG, Hägele JS (2020) J Chromatogr A 1624:461256
19. Jaros M, Hruska V, Stedrý M, Zusková I, Gaš B (2004) Electrophoresis 25:3080

Publikace IV

Characterization and comparison of mixed-mode and reversed-phase columns; interaction abilities and applicability for peptide separation

Kadlecová, Z., Kozlík, P., Tesařová, E., Gilar, M., Kalíková, K.
Journal of Chromatography A, **2021**, *1648*, 462182.

Journal of Chromatography A 1648 (2021) 462182

Contents lists available at ScienceDirect

Journal of Chromatography A

journal homepage: www.elsevier.com/locate/chroma

Characterization and comparison of mixed-mode and reversed-phase columns; interaction abilities and applicability for peptide separation

Zuzana Kadlecová[a], Petr Kozlík[b], Eva Tesařová[a], Martin Gilar[c], Květa Kalíková[a,*]

[a] Department of Physical and Macromolecular Chemistry, Faculty of Science, Charles University, Hlavova 8, Prague 12843, Czech Republic
[b] Department of Analytical Chemistry, Faculty of Science, Charles University, Hlavova 8, Prague 12843, Czech Republic
[c] Waters Corporation, 34 Maple Street, Milford, MA 01757, USA

ARTICLE INFO

Article history:
Received 21 January 2021
Revised 15 April 2021
Accepted 18 April 2021
Available online 27 April 2021

Keywords:
Mixed-mode chromatography
Mixed-mode columns
Reversed-phase column
RP/anion-exchange mechanism
Peptide separation

ABSTRACT

In this work, two mixed-mode columns from a different manufacturers and one marketed as a reversed-phase column were characterized and compared in the terms of their interaction abilities, retentivity, peak symmetry, and applicability for peptide separation. All the tested columns contain octadecyl ligand and positively charged modifier, i.e. pyridyl group for the reversed-phase column XSelect CSH C18, quaternary alkylamine for mixed-mode column Atlantis PREMIER BEH C18 AX, and permanently charged moiety (details not available from the manufacturer) for mixed-mode column Luna Omega PS C18. For detailed characterization and comparison of their interaction potential, several approaches were used. First, a simple Walters test was performed to estimate hydrophobic and silanophilic interactions of the tested columns. The highest values of both parameters were observed for column Atlantis PREMIER BEH C18 AX. To investigate the effect of pH and buffer concentration on retention, mobile phases composed of acetonitrile and buffer (ammonium formate, pH 3.0; ammonium acetate pH 4.7 and pH 6.9) in various concentrations (5mM; 10mM; 15mM and 20mM) were used. The analysis of permanently charged compounds was used to describe the electrostatic interaction abilities of the stationary phases. The most significant contribution of electrostatic interactions to the retention was observed for Atlantis PREMIER BEH C18 AX column in the mobile phase with buffer of pH 3.0. A set of ten dipeptides, three pentapeptides and one octapeptide was used to investigate the effects of pH and buffer concentration on retention and peak symmetry. Each of the tested columns provides the optimal peak shape under different buffer pH and concentration. The gradient separation of the 14 tested peptides was used to verify the application potential of the tested columns for peptide separation. The best separation was achieved within 4 minutes on column Atlantis PREMIER BEH C18 AX.

1. Introduction

Mixed-mode chromatography (MMC) allows the separation of a wide range of analytes with different properties on one chromatographic column in one run [1,2]. In most traditional chromatographic systems, one major type of interaction/retention mechanism predominates, and other "secondary interactions" are usually undesirable [3]. For example, detrimental secondary interactions were observed during the development of RP stationary phases (SPs), where non-endcapped silanol groups exhibited an ion-exchange (IEX) activity, causing the peak tailing of basic analytes [4]. Although the second interaction mechanism can be observed, it is often weak and does not significantly contribute to the retention of most analytes [5]. On the other hand, MMC utilizes at least two different types of interactions between analyte and the SP simultaneously, which significantly affect the retention [6]. Compared to the conventional RP single-mode SPs, mixed-mode (MM) SPs provide alternative separation selectivity, and an improved loading capacity [7].

Several approaches for implementing MMC have been described [8–10]. Nevertheless, covalent modification of a carrier or ligand with different types of functional groups within a single SP is the current trend for preparation of MM SPs [11]. This approach guarantees a homogeneous distribution of different functional groups on the surface of the sorbent.. By combining traditional chromatographic modes, various MM columns can be prepared: RP/IEX, RP/HILIC (hydrophilic interaction liquid chromatography), HILIC/IEX and RP/HILIC/IEX [12,13].

RP/IEX LC offers the advantage for separation of charged polar compounds, over the traditional single mode RPLC [14]. Lig-

* Corresponding author.
E-mail address: kalikova@natur.cuni.cz (K. Kalíková).

https://doi.org/10.1016/j.chroma.2021.462182
0021-9673/

ands for RPLC/IEC contain hydrophobic moieties, usually alkyl chains of different lengths, e.g. octyl (C8) or octadecyl (C18), or phenyl group and ionizable functional groups, which are embedded within, bonded on the termini of the hydrophobic moieties or independently on the sorbent to provide ion-exchange interactions.

Although MMC development has been on-going for decades [4,15,16], there is only a limited number of commercially available MM columns. Due to the continuing demand for new SPs with high stability and selectivity, many scientists continue to design and develop new materials to further expand the diversity of the sorbents. Several publications on MMC are related to the synthesis of new MM SPs for a specific application [17,18]. Generally, MM SPs have been mainly used for the separation of biomolecules such as amino acids [19,20], nucleic acids [15], peptides and proteins [11,21–23], and RNA [24] derivatives. Although the MMC has been successfully used for the separation of complex mixtures of analytes, understanding of the chromatographic behaviour of commercially available MMC columns is limited [25–30].

Besides columns with the commercial designation "mixed-mode", there are also columns that are marketed as RP, but under certain conditions they may provide MM character [31,32]. This is the case of already mentioned interactions provided by dissociated free silanol groups. Another example is columns with ligand bonded on charged surface hybrid (CSH) particles. The CSH particles contain a pyridyl group as a charge modifier bonded to the surface of the particles. This low-level surface charge was designed to improve the peak shape of basic compounds in acidic low-ionic strength mobile phases (MPs) [33]. The presence of a positive charge on the SP surface is limited by pH of MP. According to the literature, pyridyl is positively charged at pH < 7 [34], but our previous work confirmed an anion-exchange (AEX) mechanism for inorganic ions at pH < 6 [35].

In this work three columns containing octadecyl ligand and positively charged modifier, i.e. pyridyl group for the column XSelect CSH C18 marketed as RP column [36], quaternary alkylamine for MM column Atlantis PREMIER BEH C18 AX [37] and positively charged moiety (details not available from the manufacturer) for MM column Luna Omega PS C18 [38,39] were characterized and compared. All the columns should provide RP/AEX retention mechanism under selected conditions. Two approaches were used for detailed characterization of the contribution of both types of interactions/mechanisms to overall retention. Simple Walters test was used to describe hydrophobic interactions (HI) and silanophilic interactions (SiOH index) of tested SPs [40]. The HI value increases with the hydrophobicity of the SP [41] and is affected by ligand chemistry, ligand bonding density, particle type, and nature of end-capping.. For conventional RP SPs, the SIOH index describes the hydrogen bonding with silanols and its value increases with the increasing number of accessible free silanol groups [31,42–44]. Since all the columns used in this work contain a positively charged modifier in addition to the C18 ligand, the SIOH index describes hydrogen bonding not only with silanols but also with other functional groups. .

To characterize (AEX) character, the chromatographic tests of permanently positively/negatively charged, zwitterionic and neutral compounds were performed [35]. The effects of buffer pH and concentration on peak symmetry were investigated. Generally, peak tailing occurs, when along with the dominant interaction mechanism, strong secondary interactions with a low density contribute to the retention. The active sites become saturated at low concentrations which leads to peak tailing [45,46]. Moreover, in MPs with a high content of aqueous part small changes in conditions can affect the concentrations of the MP solvent composition in the stationary phase. However, the electrostatic repulsion has been shown to improve peak shape [47].

The low population of ionizable groups on the surface can produce the tailing due to overloading effect (thermodynamic contribution to the tailing); in this case the peak tailing increases with the mass of injected sample [48,49]. In this work all experiments were performed with the same mass load conditions (injected volume, sample concentrations), so the trends in peaks symmetry should be unaffected by this effect.

This work aims to investigate the retention mechanism of commercially available MM columns, which combine reversed-phase and AEX modes. Obtained results were compared with "reversed-phase" CSH-based column, which provides a mixed-mode retention mechanism only in a narrow pH range. The application potential of MMC was demonstrated for peptide separation.

2. Experimental

2.1. Materials and reagents

Acetonitrile (Chromasolv® gradient grade, for HPLC, ≥ 99.9%), ammonium acetate (purity ≥ 98%), ammonium formate (purity ≥ 97%), formic acid (purity ≥ 95%), acetic acid (purity ≥ 99%), and ammonium hydroxide solution (28.0-30.0% NH_3) were purchased from Sigma-Aldrich (St. Louis, MO, USA). Sodium hydroxide solution for HPCE (0.1 N sodium hydroxide) was supplied by Agilent Technologies (Santa Clara, USA). Anthracene, benzene, caffeine, pyridine, aniline, benzoic acid, *N,N*-diethyl-*m*-toluamide, benzenesulfonic acid, toluenesulfonic acid, and trimethylphenylammonium chloride were purchased in analytical grade purity from Sigma-Aldrich (St. Louis, USA). The list of all tested dipeptides, which were supplied by Bachem (Bubendorf, Switzerland), including their pK_a values is shown in the Supporting material, Table S1. Met^5enkephalin, leucine enkephalin, leucine enkephalinamide, and angiotensin II were purchased in analytical grade purity from Sigma-Aldrich (St. Louis, MO, USA). Deionized water was purified with Rowapur and Ultrapur system from Watrex (Prague, Czech Republic).

2.2. UPLC instrumentation and columns

All chromatographic measurements were performed on the Waters Acquity UPLC H-Class system (Waters, Milford, USA). The system was equipped with a quaternary solvent manager, an autosampler, a column thermostat, and a photodiode array detector. Mass spectra of peptides were obtained from Waters Acquity UPLC H-Class system with Acquity QDa Mass Detector (Waters, Milford, USA) which is a compact single quadrupole mass detector equipped with an electrospray ionization interface. The QDa was operated in positive ion mode by applying a voltage of 0.8 kV to the ESI capillary and the cone voltage was set at 15 V. The desolvation temperature (Probe temperature) was set to 600°C. The Empower 3 software was used for system control, data acquisition, and results processing. Following columns were tested: Atlantis PREMIER BEH C18 AX (Waters, Milford, USA), Luna Omega PS C18 (Phenomenex, Torrance, USA), and XSelect CSH C18 (Waters, Milford, USA). Both Waters columns dimensions were 100 × 2.1 mm; particle size 1.7 μm; Phenomenex column dimensions were 100 × 2.1 mm; particle size 1.6 μm.

2.3. Experimental procedures

Stock solutions of all peptides were prepared by dissolving the analytes in a mixture of deionized water/acetonitrile (ACN), 50/50 (*v/v*) at concentration 0.5 mg mL^{-1} with the addition of 10 µl of 0.1M sodium hydroxide because of their poor solubility. Stock solutions of other analytes (anthracene, benzene, caffeine,

Table 1
Basic description of the columns and results of Walters test.

Column	Particle Size (μm)	Pore Size (Å)	Surface Area ($m^2 \bullet g^{-1}$)	Carbon load (%)	SIOH index	HI
Atlantis PREMIER BEH C18 AX	1.7	95	270	17	0.54	4.48
Luna Omega PS C18	1.7	100	260	11	0.49	4.06
XSelect CSH C18	1.6	130	185	15	0.51	4.08

Hydrophobicity index (HI), HI= $k_{anthracene}$ /$k_{benzene}$, MP composition: ACN/water, 65/35 (*v*/*v*); silanol index (SIOH index), SIOH index= $k_{N,N\text{-diethyl-}m\text{-toluamid}}$/$k_{anthracene}$, MP composition: 100 % ACN.

pyridine, aniline, benzoic acid, *N,N*-diethyl-*m*-toluamide, benzenesulfonic acid, toluenesulfonic acid and trimethylphenylammonium chloride) were prepared by dissolving in a mixture of deionized water/ACN, 50/50 (*v*/*v*) at concentration 1 mg mL^{-1}. The peak of injected deionized water was used as a column void time marker. Individual measurements were repeated three times and averaged. The relative standard deviations of the retention factors were lower than 1% for three consecutive injections.

In Walters test the relative retention of anthracene and benzene in ACN/water 65/35 (*v*/*v*) MP is used for description of HI, and the relative retention of anthracene and *N,N*-diethyl-*m*-toluamide in pure ACN characterize SIOH index. For the analysis of peptides MPs composed of ACN and buffer in different volumetric ratios (namely 2/98; 5/95; 10/90, 15/85 and 20/80 (*v*/*v*)) were used. Volumetric ratio ACN/buffer 30/70 (*v*/*v*) was used for the analysis of neutral and permanently charged compounds. The following buffers were used: ammonium formate, pH 3.0; ammonium acetate, pH 4.7 and ammonium acetate, pH 6.9. The effect of buffer concentration (5 to 20 mM in 5 mM steps) on retention and peak shape was studied; the correlation between buffer concentration and ionic strength can be found in Table S2 in Supporting material. Use of PeakMaster 6 software (freeware, downloadable at echmet.natur.cuni.cz) enables calculation of pH value after entering the required concentrations of all buffersćomponents into the software [50]. Ammonium formate buffer was prepared by dissolving the appropriate amount of ammonium formate in deionized water and adjusted with formic acid to reach pH 3.0. Ammonium acetate buffer was prepared by dissolving the appropriate amount of ammonium acetate in deionized water (pH 6.9) and adjusted with acetic acid to reach pH 4.7 (the added volumes of acids are summarized in Table S2 in Supporting material). Due to the chromatographic measurements in different mobile phase volumetric ratios and gradient elution, the pH of pure aqueous parts of mobile phases were measured. However, the procedure of pH description in mixed solvents can be found in literature [51]. The buffers were filtered with 0.45 μm nylon membrane filters (Whatman, GE Healthcare, Chicago, IL, USA) before use.

Flow rate was 0.4 mL min^{-1}, injection volume was 1 μL. Detection wavelengths were set at 254 nm and 280 nm, based on the UV-spectra measurements. All measurements were performed at column temperature 35°C, except for the Walters test, which was performed at column temperature 40°C. Sample temperature was 10°C for all measurements. The Marvin software (product of ChemAxon company) was used for the calculation of pK_a values and charge states of peptides.

3. Results and discussion

3.1. Walters test

The results of Walters test are summarized in Table 1. Values of both HI and SIOH index correspond to the values obtained for endcapped C18 stationary phases (HI about 4.0 and SIOH index about 0.5) [31]. The trend for SIOH index and HI is the same, that is the increase of SIOH index values correlates with the increase of HI values. Column Atlantis PREMIER BEH C18 AX exhibits the highest values of both SIOH index and HI, even though all tested columns have the same ligand (C18) and are endcapped. It correlates with the different carbon load among the tested columns (see Table 1). Interestingly, the results also show a similarity of HI and SIOH index values for MM column Luna Omega PS C18 and RP column XSelect CSH C18. Accordingly, the chromatographic behaviour of Luna Omega PS C18 and XSelect CSH C18 columns was found to be similar (see next sections).

3.2. Evaluation of electrostatic interactions

The ability of the SPs to interact by electrostatic interactions was investigated by analysis of permanently negatively charged acids (benzenesulfonic acid, pKa=-2.36; toluenesulfonic acid, pKa=-2.14), permanently positively charged trimethylphenylammonium cation, and several other ionizable compounds (benzoic acid, pKa=4.08; pyridine pKa=5.12; aniline pKa=4.64). Two neutral substances (caffeine, benzene) whose retention should not be affected by pH or buffer concentration of the MP were used for comparison of the studied SPs. All measurements were performed in MPs composed of ACN/buffer, 30/70 (*v*/*v*). The effect of buffer pH and concentration on retention was investigated as follows: three different buffers, i.e. ammonium formate, pH 3.0; ammonium acetate, pH 4.7 and 6.9, in four different concentrations, i.e. 5mM; 10mM; 15mM; 20mM, were tested. The buffers used in this work are very weak (if any) ion-pairing agents, thus the ion-pairing effect should not dominate and is not taken into account [52].

The results obtained from the analysis of caffeine and benzene confirmed that the retention and peak shape of neutral substances does not fundamentally change with the change of buffer pH and concentration (see Tables S3:A-C, S4:A-C, S5:A-C in Supporting material). The contribution of electrostatic interactions to the retention depends on the MP pH since the pH affects protonation and dissociation of both the analytes and the SP surface. The retention behaviour of positively and negatively charged compounds in various MPs (different buffer pH and buffer concentration) provides important information about the effect of electrostatic interactions on retention, and peak symmetry (see Tables S3:A-C, S4:A-C, S5:A-C in Supporting material).

Fig. 1A–C show the retention behaviour of toluenesulfonic acid on selected MM columns. Atlantis PREMIER BEH C18 AX shows higher retention of negatively charged toluenesulfonic acid compared to the other columns, most significantly in the MP with a buffer of pH 3.0. This observation confirms that there is a significant contribution of electrostatic interactions between the negatively charged analyte and positively charged SP. The same trend can be seen for benzoic acid, which is only partially negatively charged depending of buffer pH, so the increase in retention is less apparent (see Fig. S1 in Supporting material). Fig. 1A also illustrates the decrease in retention of acid with an increasing buffer concentration on column Atlantis PREMIER BEH C18 AX, due to the competition of charged analytes and buffer constituents for electrostatic interaction sites on the SP. Since charged acids are hydrophilic, their retention is lower and almost unaffected by buffer concentration on Luna Omega PS C18 and XSelect CSH C18

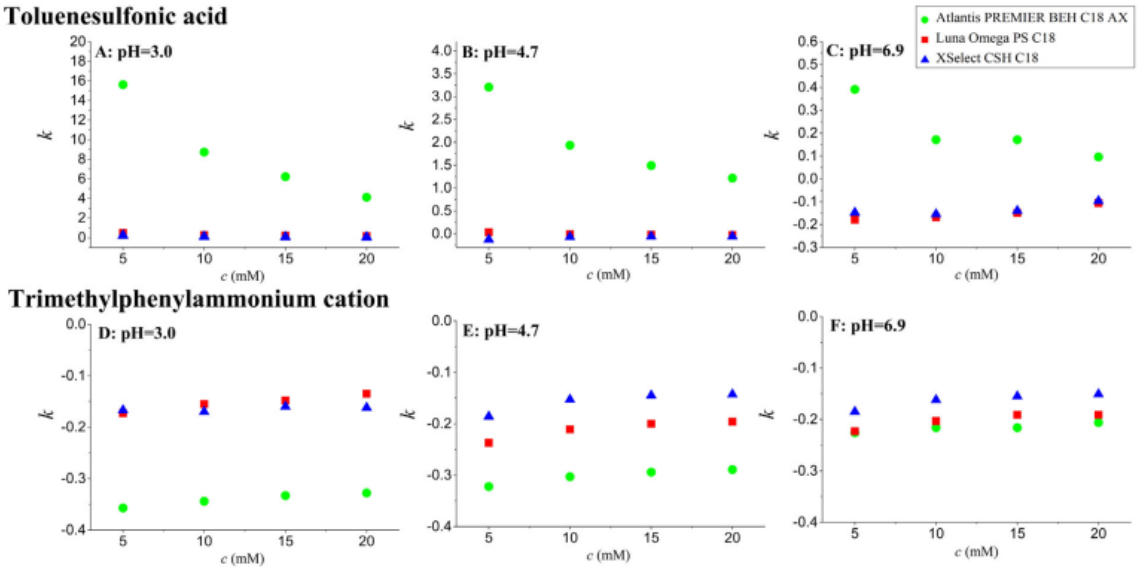

Fig. 1. The effect of buffer pH and concentration on retention of permanently charged analytes. MP composition: ACN/buffer; 30/70 (v/v). Buffers: ammonium formate, pH 3.0 (A, D); ammonium acetate pH 4.7 (B, E) and ammonium acetate pH 6.9 (C, F).

columns due to the weak contribution of electrostatic interactions (Fig. 1A–C).

Fig. 1D–F show the chromatographic behaviour of trimethylphenylammonium cation in MP with buffers of pH 3.0 – 6.9. The negative retention factors suggest an exclusion from the sorbent pores due to ionic repulsion. The reasons of exclusion effects are clearly described in Refs. [53,54]. Atlantis PREMIER BEH C18 AX column exhibits the lowest retention due to the highest electrostatic repulsion of analyte from positively charged SP. On the contrary, columns Luna Omega PS C18 and XSelect CSH C18 with lower availability of positive charge on the SP surface exhibit slightly lower repulsion of positively charged compounds compared to Atlantis PREMIER BEH C18 AX column. At higher buffer concentration the ionic repulsion is reduced (Fig. 1D–F), but due to minimal retention the observed effect is weak. Similar results were obtained for pyridine (see Fig. S1 in Supporting material).

Further inspection of Fig. 1A–C reveals, that the retention of negatively charged toluenesulfonic acid decreases with increasing pH, most apparently for Atlantis PREMIER BEH C18 AX column. Since the SP should bear positive charge in the investigated pH range, the decrease in retention may be explained by deprotonation of free silanols at higher pH, leading to partial neutralization of SP surface charge. For the same reason, the retention of positively charged analyte slightly increases at pH 4.7 and 6.9 (see Fig. 1E and F).

From the experiments discussed in Fig. 1 (and supporting Fig. S1) we conclude that Atlantis PREMIER BEH C18 AX provides stronger ionic interactions than the other two tested columns. This column contains quaternary alkylamine (pKa~10.6) as a charge modifier. Pyridyl group (pKa~5-6) present in column XSelect CSH C18 contributes less to the electrostatic interactions and Luna Omega PS C18 shows comparably low ionic contribution to retention. Although information about the charge modifier is not available for Luna Omega PS C18, we can assume that the accessibility of positive charge is similar to the XSelect CSH C18 column.

3.3. Effect of buffer pH and concentration on retention of peptides

Peptides exhibit amphoteric character; their behaviour in reversed-phase and mixed-mode (RP/AEX) chromatography depends strongly on the analyte charge, which in turn depends on the MP pH. We calculated the test peptides pI and apparent charge z according to Schimura et al. [55] for MP pHs used in this study (pH 3.0, 4.7 and 6.9; see Table 2).

Table 2
pI and charge z values of peptides at the experimental conditions.

	pI	*z* (pH 3.0)	*z* (pH 4.7)	*z* (pH 6.9)
Angiotensin II	7.00	2.70	1.21	0.10
Met^{5}enkephalin	5.60	0.80	0.07	-0.17
Leucine enkephalinamide	8.70	1.00	1.00	0.83
Leucine enkephalin	5.60	0.80	0.07	-0.17
Dipeptides	5.60	0.80	0.07	-0.17

The dipeptides, and enkephalins don't have basic or acidic amino acids in their sequence; their charge depends solely on the pKa of the carboxy and amino terminal groups. These peptides have positive charge at pH 3.0 (z = 0.80), while they are zwitterionic at pH 4.7 (z = 0.07), or carry a partial negative charge at pH 6.9 (z = -0.17). Leucine-enkephalinamide, having terminal carboxylic group amidated, and angiotensin II with two basic amino acids in the sequence (arginine and histidine) are positively charged in the entire range of experimental pH 3.0-6.9 (see Table 2).

To investigate the effect of pH and buffer concentration on peptide retention we used the same buffers as described in the previous section in following volumetric ratios ACN/buffer: 2/98; 5/95; 10/90, 15/85 and 20/80 (v/v). Fig. 2 illustrates the retention behaviour for H-Phe-Trp-OH. The cationic analyte is electrostatically repulsed from the charged surface at pH 3.0 (Fig. 2A), most notably at low buffer concentrations. Atlantis PREMIER BEH C18 AX column exhibits the lowest retention at pH 3.0 conditions, suggesting that it has the highest availability of positive charge on the SP surface (greatest ionic repulsion) from the three evaluated columns.

Fig. 2B shows the retention of H-Phe-Trp-OH at pH 4.7, where the dipeptide apparent charge is near zero (Table 2). The repulsive force is diminished, and the retention of peptide improves for Atlantis PREMIER BEH C18 AX column. Interestingly, the retention on this column is greater at low buffer concentration. This behaviour indicates that while the calculated charge is near zero

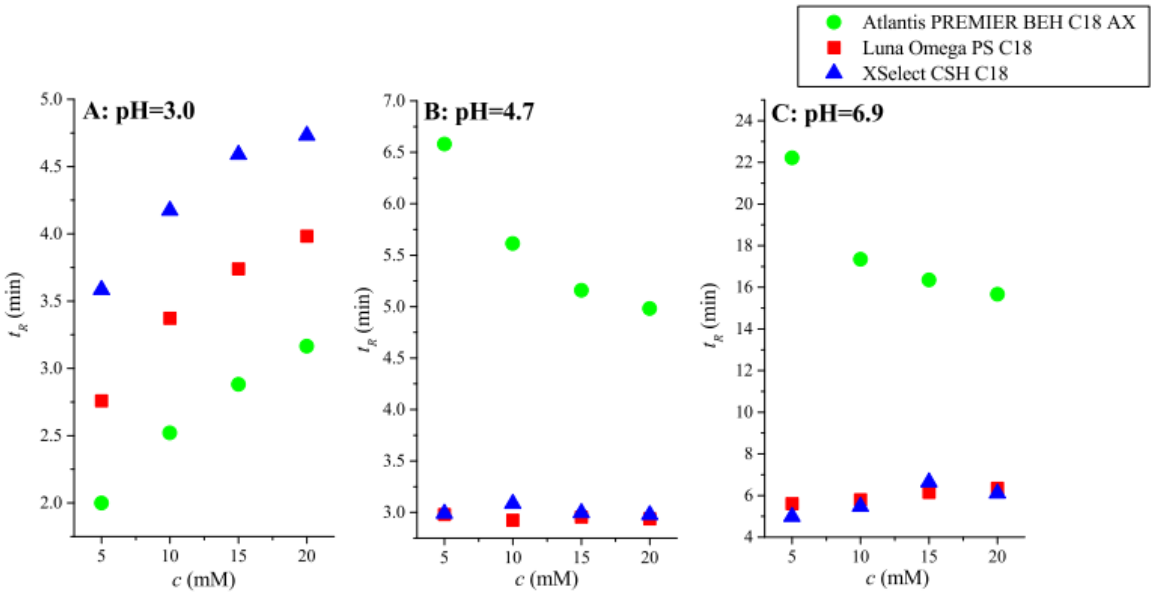

Fig. 2. The effect of buffer pH and concentration on retention of H-Phe-Trp-OH. MP composition: ACN/buffer; 15/85 (*v/v*). Buffers: ammonium formate, pH 3.0 (A); ammonium acetate pH 4.7 (B) and pH 6.9 (C).

value (Table 2) the dipeptide retention indicates that the attractive electrostatic effect of carboxy group prevails over the repulsive force of amino group at pH 4.7 (opposite trend compared to pH 3.0). The data obtained at pH 6.9 displayed in Fig. 2C show similar trends; the dipeptide retention further improves for all columns, most noticeably on Atlantis PREMIER BEH C18 AX. The electrostatic contribution to retention on XSelect CSH C18 is less apparent, presumably because the SP is mostly neutral at pH 6.9 [35]. Dipeptide retention on XSelect CSH C18 and Luna Omega PS C18 show only minor retention change with buffer concentration at pH 4.7 and 6.9 (Fig. 2B and C) suggesting that the electrostatic contribution to the peptide retention is less significant compared to Atlantis PREMIER BEH C18 AX column.

The retention data for the remaining dipeptides show similar trends to those in Fig. 2. The data are provided as Supporting material, Tables S3:A–C, S4:A–C, S5:A–C.

The peptides containing multiple charged amino acids in the sequence have more complex chromatographic behaviour; the method development is expected to be more difficult. Nevertheless, the principles of retention remain the same as for dipeptides; mixed-mode columns combine electrostatic attraction/repulsion forces and hydrophobic interactions.

The retention trends of selected peptides on the three evaluated columns are shown in Fig. 3. Retention and separation selectivity of pentapeptides and octapeptide is strongly affected by the MP composition, buffer pH and concentration (see Figs. S2 and S3 in Supporting material). At pH 6.9 the peptides charge (Table 2) and column surface charge are diminished and ion-exchange mechanism plays lesser role in the peptide retention; the retention is mostly insensitive to the MP buffer concentration (Fig. 3 C, F and I). At pH 4.7 and 3.0 the electrostatic interactions become more significant, and the MP buffer concentration effect becomes apparent. The retention of mostly positively charged leucine enkephalinamide and angiotensin II strongly decreases with decreasing buffer concentration at pH 4.7 and in particular at pH 3.0. High concentration of MP buffer can partially mitigate the retention suppression (electrostatic repulsion) and alter the retention of peptides, but the retention order remains dramatically different compared to experiment at pH 6.9. The trends in Fig. 3 validate our initial conclusions about the relative contribution of AEX retention mechanism of the three columns. The AEX strength decreases in the order: Atlantis PREMIER BEH C18 AX > Luna Omega PS C18 > XSelect CSH C18.

Additional retention data for different acetonitrile content in the MP are provided as Supporting material, Fig. S2, Tables S3, S4, and S5).

3.4. Effect of buffer pH and concentration on peak symmetry of peptides

Both the type of SP and the composition of MP significantly affect the peak symmetry of peptides. The same buffers as in previous sections were used.

Fig. 4 illustrates the trends in symmetry factor of H-Phe-Ala-OH. In MP composed of buffer of pH 3.0, H-Phe-Ala-OH is predominantly positively charged (Table 2). The strong electrostatic repulsion of analyte from charged SP surface produces enhanced peak symmetry for Atlantis PREMIER BEH C18 AX compared to other columns (Fig. 4A). The hypothesis that electrostatic repulsion is responsible for improved symmetry is supported by the observation that the peak tailing increases at higher buffer concentration when the repulsive interactions are suppressed. However the Luna Omega PS C18 shows the opposite peak symmetry trend (Fig. 4A). The reasons for this observation are unknown. No significant change in peak symmetry was observed for XSelect CSH C18 column.

In MP composed of buffer of pH 4.7 dipeptides are in zwitterionic form. Fig. 4B shows that symmetry factors are similar for Luna Omega PS C18 and XSelect CSH C18 columns; symmetry factor values are close to 1. The contribution of ionic interactions to peptide retention is minimal and a good peak symmetry was observed. However, the charge still plays a significant role on the Atlantis PREMIER BEH C18 AX column where the tailing increases at lower buffer concentrations. In MP composed of buffer of pH 6.9 dipeptides are in zwitterionic form with partial negative charge. The dipeptide peaks were severely tailing; in some cases it was impossible to reliably integrate the peaks (see

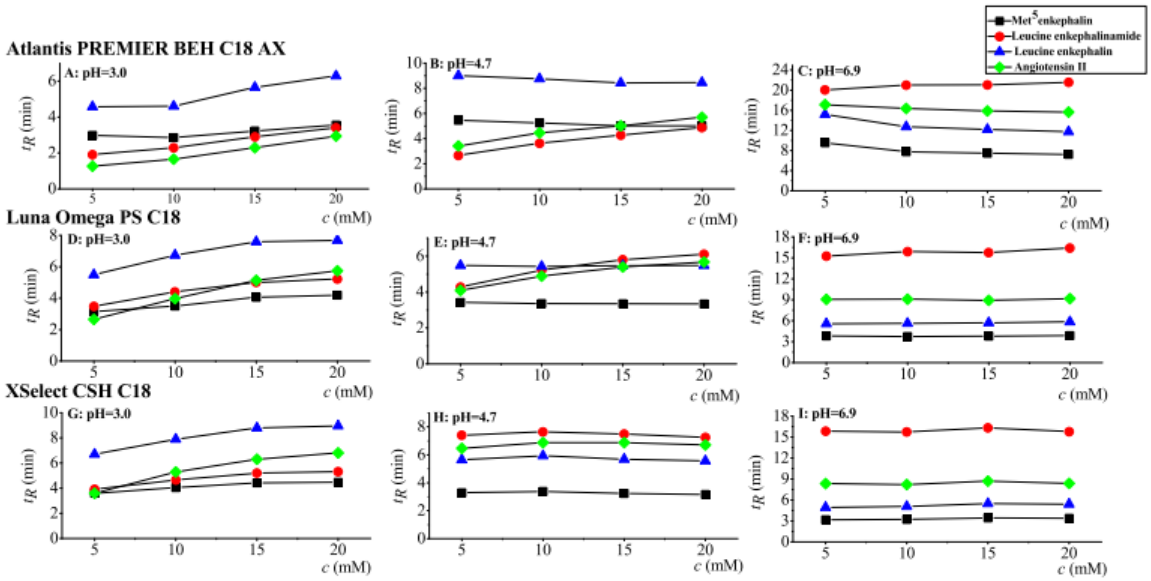

Fig. 3. The effect of buffer pH and concentration on retention of pentapeptides and octapeptide for all tested columns. MP composition: ACN/buffer; 15/85 (v/v). Buffers: ammonium formate, pH 3.0 (A,D,G); ammonium acetate pH 4.7 (B,E,H) and pH 6.9 (C,F,I). Lines are to guide the eyes only.

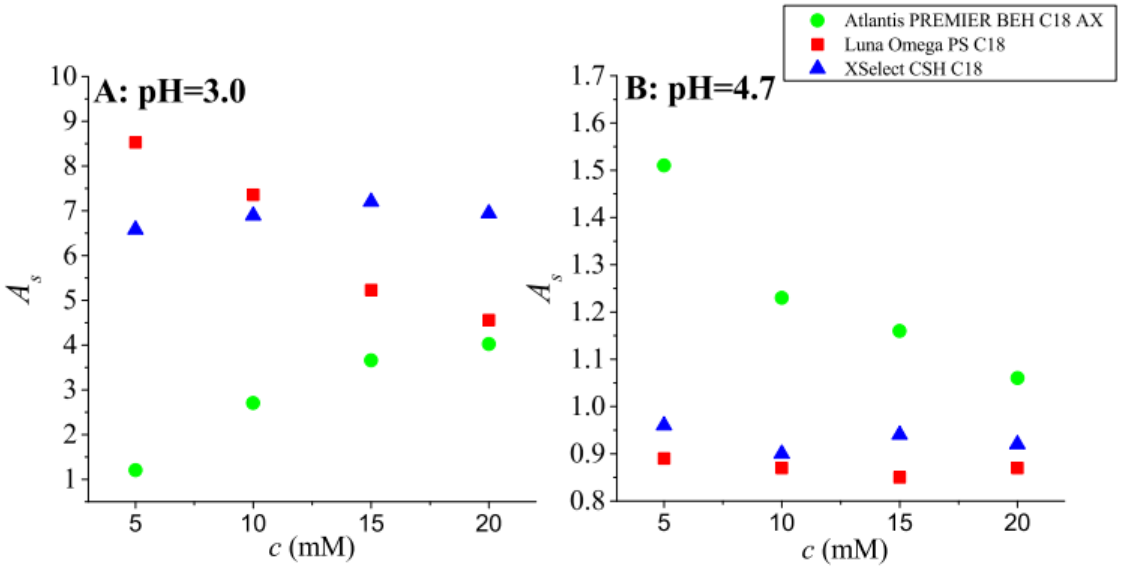

Fig. 4. The effect of buffer pH and concentration on symmetry factors of H-Phe-Ala-OH. MP composition: ACN/buffer; 2/98 (v/v). Buffers: ammonium formate, pH 3.0 (A); ammonium acetate pH 4.7 (B). Symmetry factor calculation: $A_s = w/(2 \bullet F)$, where w is peak width at 5% of peak height and F is time from width start point at 5% of peak height to peak maximum.

the symmetry factor values in Tables S5:A-C in Supporting material). Similar behaviour was observed for longer peptides, e.g. for Leucine enkephalin. On the other hand, leucine enkephalinamide with overall positive charge is observed as symmetrical peak shape under these conditions (due to electrostatic repulsion, see Fig. S4 in Supporting material). In this work we did not evaluate whether the peak tailing is driven by kinetic, thermodynamic, or combined chromatographic effects.

3.5. Peptide separation

Gradient separation of 14 peptides was performed to demonstrate the application potential of the tested columns for these compounds. Separation in MMC is strongly influenced by the charge of both the analyte and the SP, which is affected by MP pH. The contribution of electrostatic interactions to the retention is also affected by the buffer concentration. The choice of buffer concentration can attenuate or enhance electrostatic interactions. Based on the initial screening, the optimal chromatographic separation conditions for gradient elution were selected. The most effective separation of all the peptides was achieved in 5mM ammonium formate, pH 3.0. However, these conditions are not always optimal in terms of peak symmetry. Fig. 5A shows gradient separation of the set of dipeptides, pentapeptides, and octapeptide on column Atlantis PREMIER BEH C18 AX. All 14 peptides were baseline separated within 4 minutes.

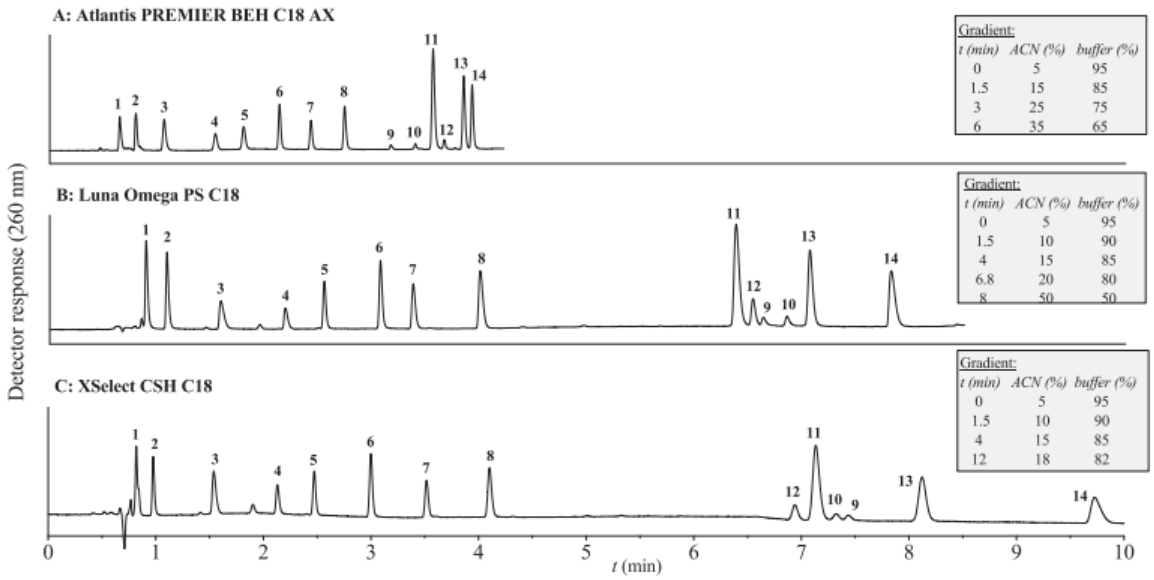

Fig. 5. Separation of set of 14 peptides, gradient elution. Buffer: 5 mM ammonium formate, pH 3.0. Analytes: 1: H-Tyr-Ala-OH; 2: H-Ala-Tyr-OH; 3: H-Phe-Ala-OH; 4: H-Ala-Phe-OH; 5: H-Trp-Ala-OH; 6: H-Ala-Trp-OH; 7: H-Phe-Tyr-OH; 8: H-Tyr-Phe-OH; 9: Angiotensin II; 10: Leucine enkephalinamide; 11: H-Phe-Trp-OH; 12: Met^{5}enkephalin; 13: H-Trp-Phe-OH; 14: Leucine enkephalin.

Due to the need for sufficient resolution of peaks 9-12, it was necessary to use a less steep gradient and thus analysis times on the other two columns are longer (Fig. 5B and C). Comparing the chromatograms at Fig. 5A–C, it is obvious that the columns provide different elution order of the peptides. The identity of all peaks was confirmed by the QDa Mass Detector. Mass spectra of all the tested peptides are shown in Fig. S5 in Supporting material.

4. Conclusion

Ultra-performance liquid chromatography with MM SPs can serve as a useful tool for the analysis and separation of various polar/charged compounds. A detailed characterization of the SPs and thus appropriate understanding of the retention/interaction mechanisms is crucial for method development. In this work, three columns containing octadecyl ligand and positively charged modifier were characterized and compared in the terms of retentivity, selectivity, and peak symmetry.

The simple Walters test was used to obtain general information about the differences in silanophilic interactions and hydrophobic interactions of the tested columns. The results show that column Atlantis PREMIER BEH C18 AX exhibits the highest values of both SIOH index and HI. The analysis of permanently charged compounds was used to evaluate the electrostatic interactions of SPs at various chromatographic conditions, such as pH and buffer concentration. The contribution of electrostatic interactions of SPs to retention was found to be most relevant at acidic conditions (pH = 3.0). The Atlantis PREMIER BEH C18 AX column shows stronger retention of negatively charged compounds in a wider pH range compared to the other two tested columns. Atlantis PREMIER BEH C18 AX also exhibited the highest contribution of electrostatic interactions to the retention of the tested analytes. MM column Luna Omega PS C18 and RP column XSelect CSH C18 showed similar retention behavior; the columns provide only modest ionic interactions. The effect of buffer pH and concentration on retention and peak symmetry of peptides confirmed the similarity of columns Luna Omega PS C18 and XSelect CSH C18. The only difference between these two columns is apparent at buffer of pH 4.7, where column Luna Omega PS C18 still exhibits significant contribution of electrostatic interactions to the retention, while column XSelect CSH C18 does not. Baseline separation of 14 peptides was achieved on all the tested columns. However, the fastest analysis within 4 minutes was obtained on column Atlantis PREMIER BEH C18 AX. These results confirm the suitability of MM columns for peptide analysis.

Declaration of Competing Interest

The authors declared no conflict of interest.

CRediT authorship contribution statement

Zuzana Kadlecová: Investigation, Methodology, Writing – original draft, Writing – review & editing. **Petr Kozlík:** Investigation, Writing – original draft, Writing – review & editing. **Eva Tesařová:** Writing – review & editing. **Martin Gilar:** Methodology, Writing – original draft, Writing – review & editing. **Květa Kalíková:** Conceptualization, Supervision, Methodology, Writing – review & editing, Funding acquisition.

Acknowledgement

The authors gratefully acknowledge the financial support of the Czech Science Foundation, Grant No. 20-19655S.

Supplementary materials

Supplementary material associated with this article can be found, in the online version, at doi:10.1016/j.chroma.2021.462182.

References

[1] M. Gilar, Y.-Q. Yu, J. Ahn, J. Fournier, J.C. Gebler, Mixed-mode chromatography for fractionation of peptides, phosphopeptides, and sialylated glycopeptides, J. Chromatogr. A 1191 (2008) 162–170, doi:10.1016/j.chroma.2008.01.061.
[2] H. Qiu, A.K. Mallik, M. Takafuji, S. Jiang, H. Ihara, New poly(ionic liquid)-grafted silica multi-mode stationary phase for anion-exchange/reversed-phase/hydrophilic interaction liquid chromatography, Analyst 137 (2012) 2553–2555, doi:10.1039/c2an35348b.

[3] K. Zhang, X. Liu, Mixed-mode chromatography in pharmaceutical and biopharmaceutical applications, J. Pharm. Biomed. Anal. 128 (2016) 73–88, doi:10.1016/j.jpba.2016.05.007.

[4] W.S. Hancock, J.T. Sparrow, Use of mixed-mode, high-performance liquid chromatography for the separation of peptide and protein mixtures, J. Chromatogr. A 206 (1981) 71–82, doi:10.1016/S0021-9673(00)82606-0.

[5] L. Zhang, Q. Dai, X. Qiao, C. Yu, X. Qin, H. Yan, Mixed-mode chromatographic stationary phases: recent advancements and its applications for high-performance liquid chromatography, TrAC Trends Anal. Chem. 82 (2016) 143–163, doi:10.1016/j.trac.2016.05.011.

[6] L.A. Kennedy, W. Kopaciewicz, F.E. Regnier, Multimodal liquid chromatography columns for the separation of proteins in either the anion-exchange or hydrophobic-interaction mode, J. Chromatogr. A 359 (1986) 73–84.

[7] Y. Yang, X. Geng, Mixed-mode chromatography and its applications to biopolymers, J. Chromatogr. A 1218 (2011) 8813–8825, doi:10.1016/j.chroma.2011.10.009.

[8] T. Marunouchi, M. Ono, T. Nakajima, Y. Ito, T. Aketo, Simultaneous determination of active ingredients in an ophthalmic solution by isocratic tandem-mode HPLC connected reverse phase column and strong cation exchange column, J. Pharm. Biomed. Anal. 40 (2006) 331–337, doi:10.1016/j.jpba.2005.08.018.

[9] J.T. Eleveld, H.A. Claessens, J.L. Ammerdorffer, A.M. van Herk, C.A. Cramers, Evaluation of mixed-mode stationary phases in liquid chromatography for the separation of charged and uncharged oligomer-like model compounds, J. Chromatogr. A 677 (1994) 211–227, doi:10.1016/0021-9673(94)80150-9.

[10] R. Nogueira, M. Lämmerhofer, W. Lindner, Alternative high-performance liquid chromatographic peptide separation and purification concept using a new mixed-mode reversed-phase/weak anion-exchange type stationary phase, J. Chromatogr. A 1089 (2005) 158–169, doi:10.1016/j.chroma.2005.06.093.

[11] G. Zhao, X.-Y. Dong, Y. Sun, Ligands for mixed-mode protein chromatography: principles, characteristics and design, J. Biotechnol. 144 (2009) 3–11, doi:10.1016/j.jbiotec.2009.04.009.

[12] L. Wang, W. Wei, Z. Xia, X. Jie, Z.Z. Xia, Recent advances in materials for stationary phases of mixed-mode high-performance liquid chromatography, TrAC Trends Anal. Chem. 80 (2016) 495–506, doi:10.1016/j.trac.2016.04.001.

[13] O. Kozlov, Z. Kadlecová, M. Gilar, T. Gondová, K. Kalíková, E. Tesařová, Systematic evaluation of selected supercritical fluid chromatography diol- and diethylamine-based columns for application in hydrophilic interaction liquid chromatography, SEPARATION SCIENCE PLUS 2 (2019) 81–88, doi:10.1002/sscp.201900023.

[14] J. Wei, Z. Guo, P. Zhang, F. Zhang, B. Yang, X. Liang, A new reversed-phase/strong anion-exchange mixed-mode stationary phase based on polar-copolymerized approach and its application in the enrichment of aristolochic acids, J. Chromatogr. A 1246 (2012) 129–136, doi:10.1016/j.chroma.2012.03.047.

[15] R. Bischoff, L.W. McLaughlin, Nucleic acid resolution by mixed-mode chromatography, J. Chromatogr. A 296 (1984) 329–337, doi:10.1016/S0021-9673(01)96427-1.

[16] R. Bischoff, L.W. McLaughlin, Chemically synthesized hydrophobic anion-exchange high-performance liquid chromatography supports used for oligonucleotide resolution by mixed mode chromatography, J. Chromatogr. A 270 (1983) 117–126, doi:10.1016/S0021-9673(01)96356-3.

[17] D. Sýkora, P. Řezanka, K. Záruba, V. Král, Recent advances in mixed-mode chromatographic stationary phases, J. Sep. Sci. 42 (2019) 89–129, doi:10.1002/jssc.201801048.

[18] H. Xian, H. Peng, X. Wang, D. Long, R. Ni, J. Chen, S. Li, Z. Zhang, J. Peng, Preparation and evaluation a mixed-mode stationary phase with imidazolium and carboxyl group for high performance liquid chromatography, Microchem. J. 150 (2019) 104131, doi:10.1016/j.microc.2019.104131.

[19] A.P. Vilches, S.H. Norström, D. Bylund, Direct analysis of free amino acids by mixed-mode chromatography with tandem mass spectrometry, J. Sep. Sci. 40 (2017) 1482–1492, doi:10.1002/jssc.201601097.

[20] M.S. Choi, S.U. Rehman, I.S. Kim, H.-J. Park, M.-Y. Song, H.H. Yoo, Development of a mixed-mode chromatography with tandem mass spectrometry method for the quantitative analysis of 23 underivatized amino acids in human serum, J. Pharm. Biomed. Anal. 145 (2017) 52–58, doi:10.1016/j.jpba.2017.06.040.

[21] G. Sun, A. Ali, Y.S. Kim, J.S. Kim, H.J. An, W.J. Cheong, An optimized mixed-mode stationary phase based on silica monolith particles for the separation of peptides and proteins in high-performance liquid chromatography, J. Sep. Sci. 42 (2019) 3621–3630, doi:10.1002/jssc.201900914.

[22] P. Yu, S. Petzoldt, M. Wilhelm, D.P. Zolg, R. Zheng, X. Sun, X. Liu, G. Schneider, A. Huhmer, B. Kuster, Trimodal mixed mode chromatography that enables efficient offline two-dimensional peptide fractionation for proteome analysis, Anal. Chem. 89 (2017) 8884–8891, doi:10.1021/acs.analchem.7b01356.

[23] P. Kozlik, J. Vaclova, K. Kalikova, Mixed-mode hydrophilic interaction/ion-exchange liquid chromatography – separation potential in peptide analysis, Microchem. J. (2021) 106158, doi:10.1016/j.microc.2021.106158.

[24] R. Bischoff, L.W. McLaughlin, Mixed-mode chromatographic matrices for the resolution of transfer ribonucleic acids, J. Chromatogr. A 317 (1984) 251–261, doi:10.1016/S0021-9673(01)91664-4.

[25] W. Yin-Mao, L. Quan-Zhou, L. Tong, G. Xin-Du, Retention model of protein for mixed-mode interaction mechanism in ion exchange and hydrophobic interaction chromatography, Chin. J. Chem. 18 (2000) 60–65, doi:10.1002/cjoc.20000180111.

[26] A. Cavazzini, N. Marchetti, R. Guzzinati, L. Pasti, A. Ciogli, F. Gasparrini, A. Laganà, Understanding mixed-mode retention mechanisms in liquid chromatography with hydrophobic stationary phases, Anal. Chem. 86 (2014) 4919–4926, doi:10.1021/ac500248b.

[27] P.G. Stevenson, J.N. Fairchild, G. Guiochon, Retention mechanism divergence of a mixed mode stationary phase for high performance liquid chromatography, J. Chromatogr. A 1218 (2011) 1822–1827, doi:10.1016/j.chroma.2011.01.078.

[28] X.-T. Peng, Z. Li, Y. Zhang, T. Liu, Q.-W. Yu, Y.-Q. Feng, Study of retention mechanism of a mixed-mode stationary phase and its application for the simultaneous determination of ten water-and fat-soluble vitamins by HPLC–UV, Chromatographia 76 (2013) 735–745.

[29] H. Hinterwirth, M. Lämmerhofer, B. Preinerstorfer, A. Gargano, R. Reischl, W. Bicker, O. Trapp, L. Brecker, W. Lindner, Selectivity issues in targeted metabolomics: Separation of phosphorylated carbohydrate isomers by mixed-mode hydrophilic interaction/weak anion exchange chromatography, J. Sep. Sci. 33 (2010) 3273–3282, doi:10.1002/jssc.201000412.

[30] M. Lämmerhofer, M. Richter, J. Wu, R. Nogueira, W. Bicker, W. Lindner, Mixed-mode ion-exchangers and their comparative chromatographic characterization in reversed-phase and hydrophilic interaction chromatography elution modes, J. Sep. Sci. 31 (2008) 2572–2588, doi:10.1002/jssc.200800178.

[31] Z. Kadlecová, K. Kalíková, M. Ansorge, M. Gilar, E. Tesařová, The effect of particle and ligand types on retention and peak shape in liquid chromatography, Microchem. J. 159 (2020) 105466, doi:10.1016/j.microc.2020.105466.

[32] L. Nováková, H. Vlčková, S. Petr, Evaluation of new mixed-mode UHPLC stationary phases and the importance of stationary phase choice when using low ionic-strength mobile phase additives, Talanta 93 (2012) 99–105, doi:10.1016/j.talanta.2012.01.054.

[33] S. Khater, C. West, E. Lesellier, Characterization of five chemistries and three particle sizes of stationary phases used in supercritical fluid chromatography, J. Chromatogr. A 1319 (2013) 148–159, doi:10.1016/j.chroma.2013.10.037.

[34] F. Gritti, G. Guiochon, Adsorption behaviors of neutral and ionizable compounds on hybrid stationary phases in the absence (BEH-C18) and the presence (CSH-C18) of immobile surface charges, J. Chromatogr. A 1282 (2013) 58–71, doi:10.1016/j.chroma.2013.01.024.

[35] Z. Kadlecová, K. Kalíková, D. Folprechtová, E. Tesařová, M. Gilar, Method for evaluation of ionic interactions in liquid chromatography, J. Chromatogr. A 1625 (2020) 461301, doi:10.1016/j.chroma.2020.461301.

[36] M.A. Lauber, S.M. Koza, S.A. McCall, B.A. Alden, P.C. Iraneta, K.J. Fountain, High-resolution peptide mapping separations with MS-friendly mobile phases and charge-surface-modified C18, Anal. Chem. 85 (2013) 6936–6944, doi:10.1021/ac401481z.

[37] T.H. Walter, B.A. Alden, J.A. Field, N.L. Lawrence, D.L. Osterman, A.V. Patel, M.A. DeLoffi, Characterization of a highly stable mixed-mode reversed-phase/weak anion-exchange stationary phase based on hybrid organic/inorganic particles, J. Sep. Sci. 44 (2021) 1005–1014, doi:10.1002/jssc.202001136.

[38] S. Chu, R.J. Letcher, A mixed-mode chromatographic separation method for the analysis of dialkyl phosphates, J. Chromatogr. A 1535 (2018) 63–71, doi:10.1016/j.chroma.2017.12.069.

[39] S.N. Atapattu, K.R.D. Johnson, C.F. Poole, System maps for the retention of neutral compounds on an electrostatic-shielded reversed-phase column, Chromatographia 82 (2019) 799–808, doi:10.1007/s10337-019-03714-z.

[40] M.J. Walters, Classification of octadecyl-bonded liquid chromatography columns, J.-Assoc. Official Anal. Chem. 70 (1987) 465–469.

[41] H.A. Claessens, M.A. van Straten, C.A. Cramers, M. Jezierska, B. Buszewski, Comparative study of test methods for reversed-phase columns for high-performance liquid chromatography, J. Chromatogr. A 826 (1998) 135–156, doi:10.1016/S0021-9673(98)00749-3.

[42] P. Kozlík, V. Šímová, K. Kalíková, Z. Bosáková, D.W. Armstrong, E. Tesařová, Effect of silica gel modification with cyclofructans on properties of hydrophilic interaction liquid chromatography stationary phases, J. Chromatogr. A 1257 (2012) 58–65, doi:10.1016/j.chroma.2012.08.004.

[43] P. Jandera, K. Novotná, M.S. Beldean-Galea, K. Jíša, Retention and selectivity tests of silica-based and metal-oxide bonded stationary phases for RP-HPLC, J. Sep. Sci. 29 (2006) 856–871, doi:10.1002/jssc.200500489.

[44] K. Vyňuchalová, P. Jandera, Selectivity tests of stationary phases for reversed-phase HPLC, Anal. Lett. 44 (2011) 1640–1662, doi:10.1080/00032719.2010.520393.

[45] A. Felinger, G. Guiochon, Validation of a chromatography data analysis software, J. Chromatogr. A 913 (2001) 221–231, doi:10.1016/S0021-9673(00)00979-1.

[46] F. Gritti, G. Guiochon, Physical origin of peak tailing on C18-bonded silica in reversed-phase liquid chromatography, J. Chromatogr. A 1028 (2004) 75–88, doi:10.1016/j.chroma.2003.11.090.

[47] M.A. Lauber, S.M. Koza, S.A. McCall, B.A. Alden, P.C. Iraneta, K.J. Fountain, High-resolution peptide mapping separations with MS-friendly mobile phases and charge-surface-modified C18, Anal. Chem. 85 (2013) 6936–6944, doi:10.1021/ac401481z.

[48] A. Felinger, Molecular dynamic theories in chromatography, J. Chromatogr. A 1184 (2008) 20–41, doi:10.1016/j.chroma.2007.12.066.

[49] F. Gritti, C. Perdu, G. Guiochon, Comparison of the performance of a few packing materials designed to minimize the thermodynamic band tailing of basic compounds in reversed-phase liquid chromatography, J. Chromatogr. A 1180 (2008) 73–89, doi:10.1016/j.chroma.2007.12.022.

[50] M. Malý, M. Dovhunová, M. Dvořák, G.S. Gerlero, P.A. Kler, V. Hruška, P. Dubský, Generalized model of the linear theory of electromigration and its application to electrokinetic chromatography: theory and software PeakMaster 6—next generation, Electrophoresis 40 (2019) 683–692, doi:10.1002/elps.201800400.

[51] S. Espinosa, E. Bosch, M. Rosés, Retention of ionizable compounds on HPLC. 5. pH scales and the retention of acids and bases with acetonitrile–water mobile phases, Anal. Chem. 72 (2000) 5193–5200. https://doi.org/10.1021/ac000591b.
[52] M. Gilar, K.J. Fountain, Y. Budman, U.D. Neue, K.R. Yardley, P.D. Rainville, R.J. Russell II, J.C. Gebler, Ion-pair reversed-phase high-performance liquid chromatography analysis of oligonucleotides:: retention prediction, J. Chromatogr. A 958 (2002) 167–182, doi:10.1016/S0021-9673(02)00306-0.
[53] I. Nischang, G. Chen, U. Tallarek, Electrohydrodynamics in hierarchically structured monolithic and particulate fixed beds, J. Chromatogr. A 1109 (2006) 32–50, doi:10.1016/j.chroma.2005.12.027.
[54] C.A. Rimmer, C.R. Simmons, J.G. Dorsey, The measurement and meaning of void volumes in reversed-phase liquid chromatography, J. Chromatogr. A 965 (2002) 219–232, doi:10.1016/S0021-9673(02)00730-6.
[55] K. Shimura, K. Kamiya, H. Matsumoto, K. Kasai, Fluorescence-labeled peptide pi markers for capillary isoelectric focusing, Anal. Chem. 74 (2002) 1046–1053, doi:10.1021/ac0108010.

Publikace V

The benefits of mixed-mode chromatography columns for separation of peptides and protein digests

Kadlecová Z., Boudová H., Kalíková K.
Monatshefte Für Chemie - Chemical Monthly, **2023,** *154*, 993-1002.

Monatshefte für Chemie - Chemical Monthly (2023) 154:993–1002
https://doi.org/10.1007/s00706-023-03088-x

ORIGINAL PAPER FOR SPECIAL ISSUE

The benefits of mixed-mode chromatography columns for separation of peptides and protein digests

Zuzana Kadlecová[1] · Hana Boudová[1] · Květa Kalíková[1]

Received: 9 March 2023 / Accepted: 26 May 2023 / Published online: 8 June 2023

Abstract

In this work, the evaluation and comparison of mixed-mode chromatography and reversed-phase chromatography for separation of peptides and protein digests have been performed. The effects of pH of aqueous part of mobile phase as well as the effects of organic modifier on retention, resolution, and peak shape were investigated on several columns including three mixed-mode columns possessing reversed-phase/anion-exchange mechanism, two reversed-phase octadecyl columns, and one column with mixed-mode reversed-phase/anion-exchange character only in defined pH range. The set of peptides varying in their polarity, length, amino acid sequence, and charge state, namely dipeptides, *N*-blocked dipeptides, and oligopeptides, was selected to describe the chromatographic behavior under different conditions properly. These measurements showed the potential of mixed-mode chromatography columns for analysis of differently charged peptides in a single run. The applicability of the tested conditions has been verified by the analysis of cytochrome C digested fragments. Two types of samples were analyzed and compared, i.e., commercial cytochrome C digested standard and cytochrome C digested via trypsin spin columns. The obtained results point to the necessity of using mass spectrometry detection because of large number of unknown peaks in cytochrome C digested standard, probably originating from chymotryptic and miscleavage activities.

Graphical abstract

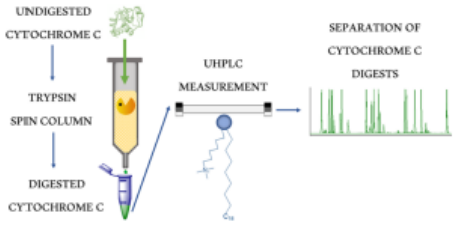

Keywords High-pressure liquid chromatography · Cytochrome C · Resolution · Mass spectrometry detection

Introduction

Mixed-mode chromatography is a promising tool for the analysis and separation of a wide range of compounds [1, 2]. The reason is utilization of at least two different types of interactions between the analyte and the stationary phase simultaneously, which can significantly affect the retention and separation [3]. Therefore, it is possible to analyze a variety of compounds differing in their physico-chemical properties (such as polarity, charge state) in a single chromatographic run [4]. This can be very advantageous for analysis of peptides/protein digests, since these analytes are usually multiply charged and differ largely in polarity [5, 6].

Mixed-mode chromatography is not an entirely new concept. For example, "hydrophobic interactions" were observed in ion-exchange chromatography and affinity chromatography, and electrostatic interactions may occur in size exclusion chromatography [7]. Before mixed-mode

✉ Květa Kalíková
kalikova@natur.cuni.cz

[1] Department of Physical and Macromolecular Chemistry, Faculty of Science, Charles University, Hlavova 8, 128 00 Prague, Czech Republic

chromatography has been reckoned as a novel individual chromatographic approach, secondary interactions (such as originating from dissociated silanols [8]) in traditional chromatography modes were often considered undesirable—they were identified as the main causes of peak tailing, and therefore there was an effort to eliminate or at least minimize them [9–11]. Mixed-mode chromatography differs from other single chromatographic modes by providing two or more significant different types of interactions, and thus all interactions contribute to the retention [3]. Generally, mixed-mode chromatography can be achieved by several approaches: (i) serial connection of two columns with different stationary phase/retention modes [12], (ii) mixing of two types of packing materials in one column [13], (iii) chemical bonding of a functional group in a ligand chain or support [14]. Covalent modification of a carrier or ligand with different types of functional groups within a single stationary phase is the dominant approach to obtain mixed-mode stationary phases nowadays.

In this work, mixed-mode stationary phases combining reversed-phase and anion-exchange retention mechanisms were used. Therefore, both "hydrophobic interaction" between the analyte and C18 ligand, and electrostatic interaction between the analyte and positively charged moiety of the stationary phase contribute to the overall retention [15]. Whether it will be electrostatic attraction or repulsion is determined mainly by the pK_a of the functional groups of the analytes and by the pH of the aqueous part of the mobile phase [16]. Hence, it is clear that mixed-mode chromatography provides an increased number of tunable mobile phase parameters, which makes the method development more flexible, but also complex [17, 18].

Specifically, three columns containing octadecyl ligand and positively charged modifier, i.e., pyridyl group for column XSelect CSH C18, quaternary alkylamine for column Atlantis PREMIER BEH C18 AX, and positively charged moiety (details not available from the manufacturer) for column Luna Omega PS C18 were used and compared in this work. Column XSelect CSH C18 is marketed as a reversed-phase column; however, the presence of pyridyl groups brings a positive charge to the stationary phase at mobile phase pH < 6 [19]. The other two mixed-mode columns should provide permanent positive charge, but our previous work reveals the similarity of the column Luna Omega PS C18 with column XSelect CSH C18 in terms of the pH range in which the electrostatic interaction with a positively charged moiety is applied [5]. The schematic structures and basic properties of stationary phases evaluated in this work are summarized in Table 1.

Mixed-mode stationary phases have been mainly used for separation of biologically active molecules, including peptides and proteins [5, 20–23]. For more complex protein molecules, digestion into smaller fragments/peptides is a necessary step preceding their analysis [1, 24]. Digestion of proteins is usually executed by trypsin, which cleaves proteins at their C-terminal arginine or lysine residues (unless proline follows) [25]. Trypsin digestion can be performed by several ways, e.g., in solution, via trypsin spin columns or on-line (immobilized trypsin reactor coupled with liquid chromatography or capillary electrophoresis systems) [26–28]. While digestion in solution requires the presence of a buffer (Tris–HCl), strict pH, and temperature control (pH = 7.8, temperature 37.0 °C) [29], and is very time consuming, digestion via spin column may be a suitable alternative, which is easy and fast [30].

As mentioned above, tested mixed-mode stationary phases combine the advantages of two separation modes (reversed phase and anion exchange) and are able to separate complex mixtures of analytes based on their polarity and charge simultaneously. For this reason, the set of various peptides differing in their properties (polarity, charge, length, amino acid sequence) was chosen for investigating the effects of chromatographic parameters on the retention, separation, and peak shape. The single mode C18 column was used for comparison. Based on the obtained results, optimal conditions for analysis of digested cytochrome C were selected.

Results and discussion

HPLC measurements

First of all, preliminary measurements of a set of 22 various peptides were performed on an HPLC system. The effects of pH of aqueous part of mobile phase on retention and resolution of individual groups of peptides (dipeptides, *N*-blocked dipeptides, and oligopeptides) were investigated on three different columns—XBridge C18 (reversed phase), XSelect CSH C18 (mixed-mode character at pH < 6), and Atlantis PREMIER BEH C18 AX (mixed mode). The goal of this study was to investigate the retention behavior of various peptides in wide pH range to describe the mixed-mode stationary phases properly and to compare mixed-mode chromatography and reversed-phase chromatography in terms of retentivity and selectivity for peptides.

Figure 1 clearly shows the importance of using gradient elution for the analysis of mixture of various peptides—while dipeptides need highly aqueous mobile phase to be retained (95 vol% of aqueous part), blocked dipeptides exhibit sufficient retention even in mobile phase composed of 60–40% by volume of acetonitrile, depending on the used column and pH of aqueous part of mobile phase. Blocked dipeptides contain benzoyl protecting group at N-terminus, and thus they are much more hydrophobic than their non-blocked counterparts. The "hydrophobic interaction"

Table 1 Schematic structures of stationary phases and their basic properties

Column name	Stationary phase structure	Interaction properties
XBridge C18 (HPLC) PREMIER BEH C18 (UHPLC)		reversed-phase column
XSelect CSH C18	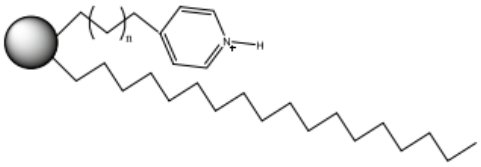	reversed-phase column with anion-exchange character at pH < 6 pK_a of pyridyl group ~ 5-6
Atlantis PREMIER BEH C18 AX	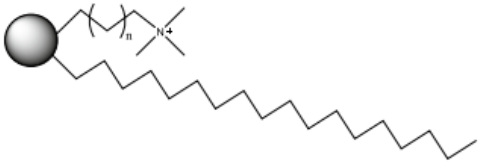	mixed-mode column (reversed-phase + anion-exchange mechanism) permanently positively charged quaternary alkylamine interactions with negatively charged dissociated silanols prevails at pH ≥ 6.8
Luna Omega PS C18		mixed-mode column (reversed-phase + anion-exchange mechanism) positively charged moiety (no details available) similar interaction behavior as column XSelect CSH C18

between the benzoyl group and C18 ligand (present in each tested stationary phase) results in higher retention in comparison with the non-blocked dipeptides.pK_a values of carboxy groups of *N*-blocked dipeptides vary within the range 3.5–3.9, i.e., as the dipeptides are more charged with increasing pH, they are becoming more polar, and thus their log *D* values decrease (Table S1 in Supporting material). This is the reason of decreasing retention of Z-Phe-Trp-OH on reversed-phase XBridge C18 column (Fig. 1A) with increasing pH (pH = 2.1 and pH = 3.0 exhibits comparable retention). For column XSelect CSH C18 (Fig. 1B), the situation is very similar, even though the stationary phase surface should be positively charged at pH < 6. In fact, pyridyl groups on CSH particles are only partially positively charged at pH = 4.7, and thus higher dipeptide polarity prevails over the electrostatic attraction (as was for peptides already shown in [5]) and the retention decreases with increasing pH.

This is not the case of mixed-mode column Atlantis PREMIER BEH C18 AX (Fig. 1C), where the highest retention was observed at mobile phase with aqueous part of pH = 4.7, where the strong electrostatic interaction between negatively charged *N*-blocked dipeptide and positively charged stationary phase surface is applied. At mobile phase with aqueous part of pH = 6.8, the electrostatic repulsion with dissociated free silanols prevails and the decrease in retention was observed. But the retention is still higher in comparison with stationary phases without positively charged moiety. The higher retention of *N*-blocked dipeptides at mobile phase with aqueous part of pH = 2.1 (where no electrostatic

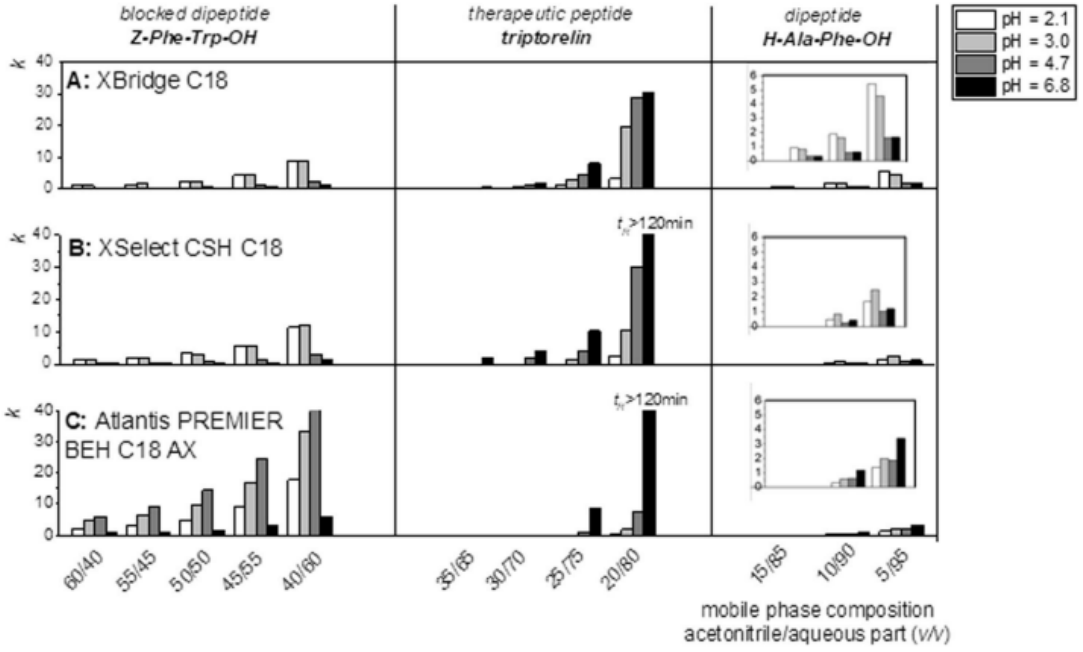

Fig. 1 Retention factors of selected representatives of peptides (Z-Phe-Trp-OH as blocked dipeptide, triptorelin as therapeutic oligopeptide, and H-Ala-Phe-OH as dipeptide) in dependence on the content of acetonitrile in mobile phase (5–60 volumetric percentages), the pH of the aqueous part of mobile phase (pH = 2.1, pH = 3.0, pH = 4.7, and pH = 6.8) and used stationary phase (**A**: XBridge C18, **B**: XSelect CSH C18, **C**: Atlantis PREMIER BEH C18 AX)

interactions take a role) on mixed-mode column in comparison with other columns can be caused by the difference in pore size (XBridge C18 pore size 130×10^{-10} m; XSelect CSH C18 pore size 130×10^{-10} m; Atlantis PREMIER BEH C18 AX pore size 95×10^{-10} m). The retention trends for other tested *N*-blocked dipeptides were the same (Fig. S1 in Supporting material).pK_a values of carboxy groups of non-blocked dipeptides vary within the range 3.5–3.8 and pK_a values of amino groups are in the range 8.0–8.5 (Table S1 in Supporting material). Log *D* values are much lower in comparison with *N*-blocked dipeptides (negative, because of missing benzoyl group) and their trend depending on pH is exactly opposite, i.e., with increasing pH, log *D* value increases and the values are almost the same for mobile phases with aqueous part of pH = 4.7 and pH = 6.8 (Table S1 in Supporting material). It may be explained by the similar charge distribution, at mobile phase with aqueous part of pH = 4.7, all amino groups are positively charged and only a part of the carboxy groups is negatively charged. Similarly, at mobile phase with aqueous part of pH = 6.8, all carboxy groups are negatively charged and only a part of the amino groups is positively charged. This is the reason why the retention of dipeptides on XBridge C18 column is not decreasing in a whole pH range, but only up to pH = 4.7 (Fig. 1A). As in the case of *N*-blocked dipeptides, retention behavior on XSelect CSH C18 column is very similar to the classical reversed-phase column (Fig. 1B). At mobile phase with aqueous part of pH = 2.1 electrostatic repulsion between positively charged pyridyl groups on the stationary phase surface and positively charged amino groups further reduces the already very low retention. No positive charge on the stationary phase surface is available above pH = 4.7, and thus only electrostatic repulsion between the negatively charged carboxy groups and negatively charged free silanols can apply. This results in very low retention in all tested pH values. Mixed-mode column Atlantis PREMIER BEH C18 AX exhibits increasing retention with increasing pH of the aqueous part of mobile phase. No retention of dipeptides was observed at mobile phase with aqueous part of pH = 2.1, because of the repulsion of positively charged amino group and positively charged stationary phase surface. With increasing pH of aqueous part of mobile phase, larger part of carboxy groups (capable of electrostatic attraction with the positively charged stationary phase surface) is dissociated and thus the retention is increasing. Moreover, free silanol groups can interact with the charged amino groups, and thereby the retention increases. The retention trends for other tested non-blocked dipeptides were similar (Fig. S2 in Supporting material).

Since oligopeptides/therapeutic peptides contain more functional groups enabling multiple charging, the description of retention behavior is more complex and differs for

individual peptides. All three tested columns exhibit no retention of oligopeptides at mobile phase with aqueous part of pH = 2.1 (the highest polarity of oligopeptides, log *D* values are summarized in Table S1 in Supporting material). Columns XBridge C18 and XSelect CSH C18 provide the same trends—the increasing retention with increasing mobile phase pH for triptorelin (Fig. 1), leuprolide, and goserelin. Individual trends in retention of other oligopeptides are shown in Fig. S3 in Supporting material. Mixed-mode column Atlantis PREMIER BEH C18 AX exhibits the same trend for all tested oligopeptides—increasing retention with increasing mobile phase pH (Fig. S3 in Supporting material).

Based on the obtained results, we can assume appropriate conditions for separation of mixture of all the tested peptides, i.e., dipeptides, blocked dipeptides, and oligopeptides. It was revealed that oligopeptides exhibit no retention at mobile phase aqueous part of pH = 2.1. In addition, pH = 2.1 shows very low selectivity for *N*-blocked dipeptides in comparison with pH = 6.8 (Fig. S4 in Supporting material). Therefore, mobile phase with aqueous part of pH = 2.1 was not used for analysis of the peptides´ mixture. For non-blocked dipeptides, it seems to be advantageous to use rather higher pH of aqueous part of mobile phase (pH = 6.8) in combination with a mixed-mode column (if pH = 2.1 was excluded). Moreover, these conditions are also suitable for analysis of blocked dipeptides.

Figure 2 shows the comparison of the best obtained results for separation of mixture of peptides. Columns XSelect CSH C18 and Atlantis PREMIER BEH C18 AX at mobile phase aqueous part of pH = 6.8 exhibited the highest selectivity and suitable resolution of most of the tested peptides in comparison with column XBridge C18 and other tested pH values of the aqueous part of the mobile phase. However, it is clearly visible that mixed-mode column Atlantis PREMIER BEH C18 AX provides higher retention times, thus inferior peak shapes (which can be obviously subjected to further optimization).

Further investigation of these two columns (XSelect CSH C18 and Atlantis PREMIER BEH C18 AX) revealed that for analysis of cytochrome C digested fragments, column Atlantis PREMIER BEH C18 AX provides better selectivity (no co-elution was observed—Fig. S5 in Supporting material).

UHPLC measurements

The obtained results from HPLC measurements revealed great potential of mixed-mode chromatography for analysis of peptides/cytochrome C digests. Therefore, we were interested in the further evaluation of two different columns marketed as mixed-mode—Luna Omega PS C18 (similar to XSelect CSH C18 column, losing positive charge at pH > 6) and Atlantis PREMIER BEH C18 AX (permanently positively charged). Just to confirm the benefits of mixed-mode

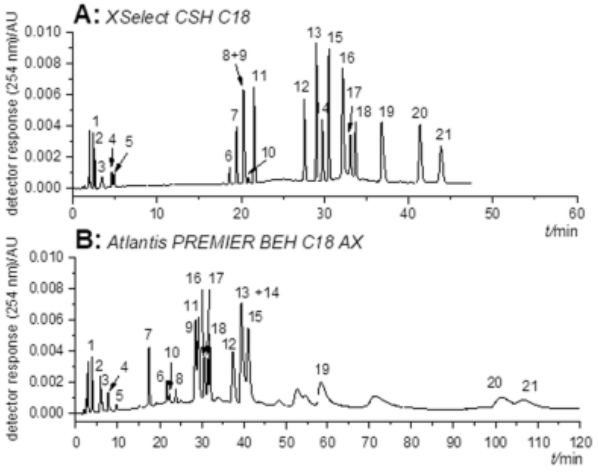

Fig. 2 Comparison of separation of mixture of peptides. **A** column XSelect CSH C18; **B** Atlantis PREMIER BEH C18 AX. Gradient elution–t_0: acetonitrile/10 mM ammonium acetate, pH = 6.8, 5/95 (*v*/*v*); t_{30min} acetonitrile/10 mM ammonium acetate, pH = 6.8, 30/70 (*v*/*v*). Detection wavelength 254 nm. Analytes: 1: H-Ala-Tyr-OH; 2: H-Tyr-Ala-OH; 3:H-Val-Tyr-OH; 4:H-Ala-Phe-OH; 5: H-Phe-Ala-OH; 6: [Met^5]-enkephalin; 7: [Lys^8]-vasopressin; 8: Z-Tyr-Ala-OH; 9: [Leu^5]-enkephalin; 10: angiotensin II; 11: Z-Ala-Tyr-OH; 12: Z-Ala-Phe-OH; 13: Z-Ala-Trp-OH; 14: Z-Phe-Ala-OH; 15: Z-Trp-Ala-OH; 16: goserelin; 17: leuprolid; 18: tritorelin; 19: Z-Phe-Leu; 20: Z-Trp-Phe-OH; 21: Z-Phe-Trp-OH

chromatography for our purpose, reversed-phase column PREMIER BEH C18 was also tested. Since UHPLC methods exhibit higher efficiency, the following experiments were carried out at UHPLC instrumentation, which additionally enables us the analysis of some other peptides, which are not UV detectable, and thus different detection, in our case mass spectrometry detection, is needed. To show the potential of mixed-mode stationary phases for separation of peptides, the effects of pH of aqueous part of mobile phase and moreover the effect of type of organic solvent (methanol vs. acetonitrile) on retention, separation, and peak shape were investigated. Two different pHs of aqueous part of mobile phase were tested: acidic pH (0.1% solution of formic acid: 26.5 mM, pH = 2.7, which is usually used for peptide analysis [31, 32]), and basic pH (26.5 mM ammonium formate, pH = 8.0, which would be appropriate for possible future on-line protein digestion by trypsin).

Figure 3 confirms the differences between mixed-mode chromatography and reversed-phase chromatography, as well as the differences between different mixed-mode columns (also previously described in [5]). For all tested peptides (the two examples are shown in Figs. 3A, B), mixed-mode columns at mobile phase aqueous part of pH = 2.7 exhibited significantly lower retention in comparison with reversed-phase column (applies for both methanol and acetonitrile). The reason is electrostatic repulsion between predominantly

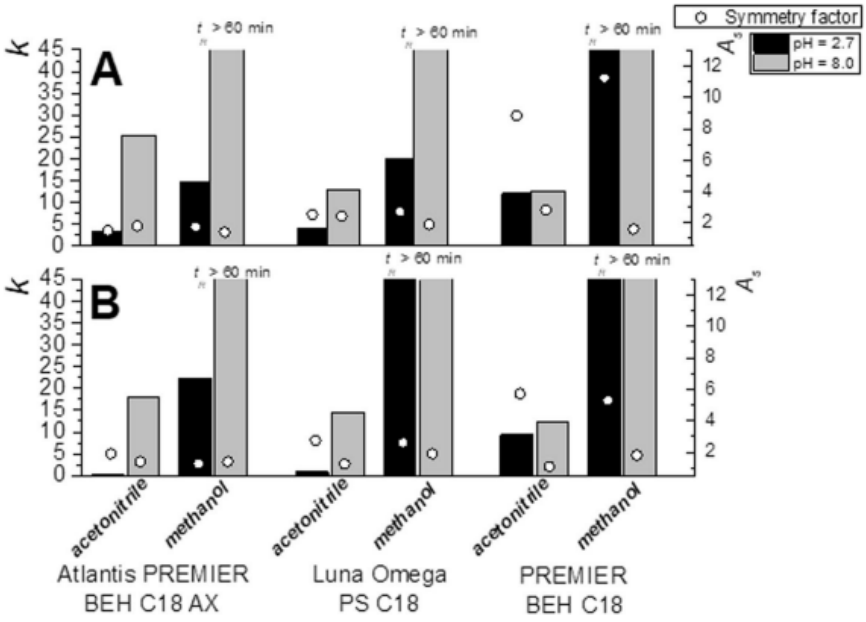

Fig. 3 The effects of pH and organic solvent on retention (k) and peak symmetry (A_s) for all tested columns. **A**: Val-Tyr-Val, mobile phase composition: organic solvent/aqueous part 5/95 (*v/v*); **B** bradykinin, mobile phase composition: organic solvent/aqueous part 15/85 (*v/v*)

positively charged peptide and mixed-mode stationary phase surface. On the other hand, at mobile phase with aqueous part of pH = 8.0, exactly opposite trend was observed, i.e., electrostatic attraction between predominantly negatively charged peptide and positively charged mixed-mode stationary phase result in higher retention on mixed-mode columns than on reversed-phase column; however, only a small difference between Luna Omega PS C18 and reversed-phase column PREMIER BEH C18 was observed (because Luna Omega loses at pH > 6 positive charge). In addition, electrostatic repulsion between the negatively charged analytes and dissociated silanol groups on the stationary phase surface also contribute to the retention. The overall retention depends on the number of free residual silanol groups, and the retention is, therefore, the result of the combination of following interaction mechanisms—"hydrophobic" interaction, electrostatic repulsion, and electrostatic attraction.

Not surprisingly, mobile phases with methanol provide significantly higher retention in comparison with acetonitrile. Comparing the symmetry factors, no meaningful differences between methanol and acetonitrile were observed (Fig. 3). Regarding the effect of mobile phase aqueous part pH on the retention and peak symmetry, it was observed that higher pH (pH = 8.0) provides higher retention in comparison with lower pH (pH = 2.7). This effect is very significant for mixed-mode columns while retention on reversed-phase column is not very affected by pH of aqueous part of mobile phase, which indicates the essential role of stationary phase charge. In addition, it was observed that higher pH mostly provides better peak shape (lower symmetry factor), which was the most significant for reversed-phase column PREMIER BEH C18 (Fig. 3).

Another goal was to find suitable conditions for separation of mixture of 12 peptides in UHPLC system. The large number of gradient types for each column in combination with each aqueous part pH and each organic modifier has been tested. Table 2 clearly shows that achieving the baseline separation of all peptides of interest was the most problematic on reversed-phase column at pH = 8.0 and on column Luna Omega PS C18. Under these conditions, it was not possible to resolve both pairs leuprolide–carbetocin and angiotensin II–leucine enkephalin—the change in gradient conditions leads to the loss of the resolution of one or the other pair. But we were able to baseline separate all the peptides on mixed-mode column Atlantis PREMIER BEH

Table 2 The success of the gradient separation of the mixture of 12 peptides and cytochrome C digests. Summary of the shortest obtained analysis times. The corresponding gradients are given in Table S2 in Supporting material

	Mixture of 12 peptides		Cytochrome c	
	pH = 2.7	pH = 8.0	pH = 2.7	pH = 8.0
Mixed-mode column Atlantis PREMIER BEH C18 AX				
Acetonitrile	✓ 7.5 min	✓ 13 min	✓ 11 min	✓ 20 min
Methanol	✓ 5.5 min	✓ 18 min	✓ 30 min	✓ 36 min
Mixed-mode column Luna Omega PS C18				
Acetonitrile	✓ 7.5 min	✗ 14 min	✓ 12 min	✓ 20 min
Methanol	✗ 10.5 min	✓ 13 min	✓ 30 min	✗ 50 min
Reversed-phase column PREMIER BEH C18				
Acetonitrile	✓ 8 min	✗ 13 min	✗ 25 min	✓ 25 min
Methanol	✓ 10.5 min	✗ 12 min	✓ 35 min	✓ 33 min

✓ baseline separated, ✗ not baseline separated

C18 AX, even within 5.5 min while using mobile phase with methanol (the fastest obtained analysis of peptide mixture is depicted in Fig. S6 in Supporting material). Generally, in mobile phases with aqueous part of pH = 8.0, very low signals from UV detection for Gly-Glu and Lys-Lys-Lys were observed (because of the significant peak deterioration); thus, usage of mass spectrometry detection is very advantageous.

Cytochrome C was selected as a model protein due to the availability of standard of its digests, which enables the comparison of digested standard and cytochrome C digested via spin columns. The list of cytochrome C digests declared in standard and corresponding *m/z* values is shown in Table S3 in Supporting material. From the HPLC measurements, it turned out that the conditions suitable for the separation of peptides may not be suitable for the separation of cytochrome C digests at the same time. Thus, analysis of cytochrome C digests (from digested standard and obtained by digestion via spin column) was performed in previously tested UHPLC conditions, i.e., three columns, acetonitrile vs. methanol, aqueous part of pH = 2.7 vs. pH = 8.0, and in large number of gradients (differing from the gradients used for analysis of 12 peptides).

Table 2 summarizes obtained results, i.e., whether it was possible to baseline separate all cytochrome C digests and the shortest analysis time. The fastest analysis of cytochrome C digested fragments was obtained using mixed-mode column Atlantis PREMIER BEH C18 AX (mobile phase with acetonitrile and aqueous part of pH = 2.7), where all 13 fragments declared in standard certificate were baseline separated within 11 min (Fig. 4A). Figure 4B shows the comparison with different mobile phase (but the same stationary phase), i.e., mobile phase with methanol in combination with aqueous part of pH = 8.0. These conditions may be very advantageous for on-line protein digestion. The comparison of Figs. 4A, B shows that in both conditions, we can achieve baseline separation of all 13 fragments, but with different elution order (different mobile phase pH).

Fragment T19C originates from chymotryptic activity (Table S3 in Supporting material, the amino acid sequence does not end with lysine or arginine), which may occur during trypsin digestion as a result of impure trypsin or trypsin autolysis [33]. This fragment was not found in the sample of cytochrome C digested via spin column, which corresponds to the statement of the manufacturer that trypsin spin columns are highly purified and immobilization prevents the trypsin autolysis [34]. Fragments T9-10, T12-13, and T13-14 are the consequence of miscleavage activity, their presence is declared in cytochrome C digested standard and they were observed also in sample digested via spin column.

The missing chymotryptic fragment is not the only difference between cytochrome C digested standard and cytochrome C digested via spin column. The comparison of analysis of these two samples (digested standard vs. digested via spin column) revealed increased number of peaks for cytochrome C digested standard, which indicates number of impurities (Fig. 5). Impurities in digested protein sample are often a consequence of chymotryptic or miscleavage activity, which is common while using in-solution digestion, especially for extended time of digestion [35]. On the other hand, lower chymotryptic and miscleavage activity can be achieved by digestion via spin columns. Obtained data point

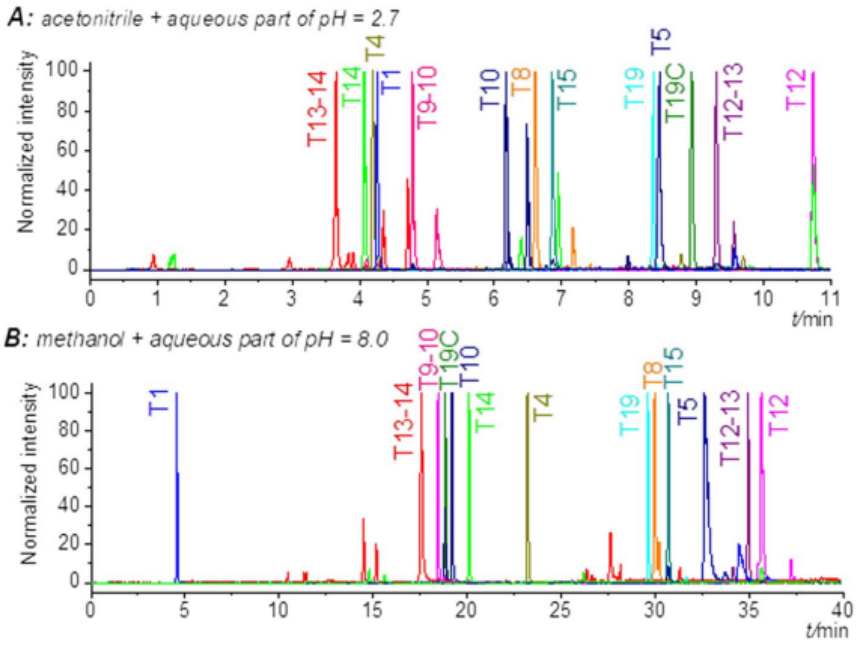

Fig. 4 Separation of 13 cytochrome C digested fragments on column Atlantis PREMIER BEH C18 AX. **A** mobile phase A—26.5 mM formic acid in acetonitrile, mobile phase B—26.5 mM formic acid in water, pH = 2.7, gradient elution: 0 min—0% A; 8 min—25% A; 10.5 min—30% A; 12 min—40% A. **B** mobile phase A—26.5 mM ammonium formate in methanol, mobile phase B—26.5 mM ammonium formate in water, pH = 8.0, gradient elution: 0 min—0% A; 40 min—75% A

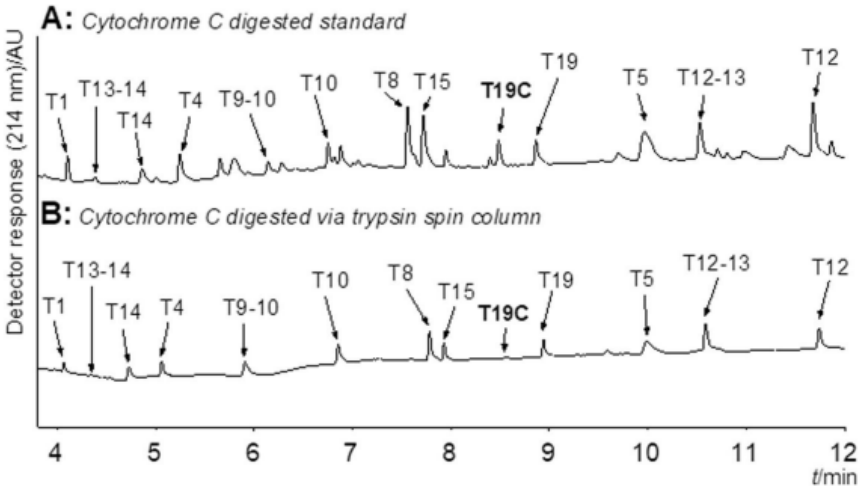

Fig. 5 Comparison of the signals from UV detection (214 nm) for **A** cytochrome C digested standard and **B** cytochrome C digested via trypsin spin column. Column: Luna Omega PS C18, mobile phase A—0.1% formic acid in acetonitrile, mobile phase B—0.1% formic acid in water, gradient elution: 0 min—0% A; 8 min—25% A; 10.5—30% A; 12 min—40% A. Table S3 in Supporting material contains information for identification of individual fragments

to the problematic nature of the analysis of protein digestion samples without mass spectrometry detection. Besides the chymotryptic peak and the number of impurities, no significant differences between the spin digestion and digested standard were observed, i.e., comparable retention of 12 fragments was achieved.

Conclusion

The goal of our study was to show the great potential of mixed-mode chromatography for analysis of peptides and protein digests. Several columns, including mixed-mode and reversed-phase columns, were used in HPLC and UHPLC systems. The effect of pH of aqueous part of mobile phase and the effect of the type of organic modifier on the retention, selectivity, resolution, and peak shape were investigated.

Analysis of dipeptides with easily defined charge state contributed to the description of mixed-mode retention behavior. It was shown that mixed-mode column Atlantis PREMIER BEH C18 AX exhibits the highest retention of negatively charged dipeptides at mobile phase aqueous part of pH = 4.7. At higher pH, the electrostatic repulsion with negatively charged residual silanols prevails. It was confirmed that column XSelect CSH C18 (marketed as reversed-phase) possesses significant mixed-mode character only in mobile phase of aqueous part of pH = 2.1 and pH = 3.0. Using HPLC, the baseline separation of various 21 peptides has been achieved on column XSelect CSH C18. In terms of the peak shape, PREMIER BEH C18 column in acidic pH (2.7) was found as the most inappropriate (symmetry factors higher than 8 for mobile phase with acetonitrile, for methanol even higher).

The analysis of cytochrome C digests on UHPLC points to the necessity of mass spectrometry detection due to the number of miscleaved/chymotryptic fragments in cytochrome C digested standard. It was shown that Atlantis PREMIER BEH C18 AX column is the most universal from the tested columns. The both acetonitrile and methanol with acidic (pH = 2.7) and basic (pH = 8.0) aqueous parts of mobile phase are suitable for baseline separation of cytochrome C digests. Mixed-mode column Luna Omega PS C18 showed comparable results except for mobile phase composed of methanol and ammonium formate buffer, pH = 8.0.

Experimental

Chemicals and materials

Acetonitrile (LC–MS grade) and methanol (LC–MS grade) were supplied by VWR International (Radnor, USA), water for LC was purchased from Honeywell (Charlotte, USA)—used for UHPLC measurements. Acetonitrile (Chromasolv® gradient grade, for HPLC, ≥ 99.9%), methanol (Chromasolv® gradient grade, for HPLC, ≥ 99.9%), ammonium acetate (purity ≥ 98%), ammonium formate (purity ≥ 97%), formic acid (purity ≥ 95%), acetic acid (purity ≥ 99%), ammonium hydroxide solution (28.0–30.0% NH_3), and trifluoroacetic acid (purity 99%) were purchased from Sigma-Aldrich (St. Louis, USA). Deionized water was purified with Rowapur and Ultrapur system from Watrex (Prague, Czech Republic). All dipeptides were purchased from Bachem (Bubendorf, Switzerland), except Z-Phe-Leu and H-Val-Tyr, which were supplied by Sigma-Aldrich (St. Louis, USA). Goserelin acetate salt, leuprolide acetate salt, bradykinin acetate salt, and carbetocin were purchased from Bachem (Bubendorf, Switzerland). Lys-Lys-Lys, Val-Tyr-Val, angiotensin I, angiotensin II, [Lys^8]-vasopressin, [Met^5]-enkephalin acetate salt hydrate, and [Leu^5]-enkephalin acetate salt hydrate were

supplied by Sigma-Aldrich (St. Louis, USA). Cytochrome C digestion standard was supplied by Waters (Milford, USA). Cytochrome C from bovine heart (purity > 95%), trypsin spin columns, and protein extraction reagent type 4 were purchased from Sigma-Aldrich (St. Louis, USA). The list of all tested analytes, their structures, log D and pK_a values is presented in Table S1 in Supporting material. Marvin software (product of ChemAxon company) was used for calculation of log D values in corresponding pH of aqueous part of mobile phase and for calculation of pK_a values of peptides.

Instrumentation and chromatographic conditions—HPLC measurements

All HPLC measurements were performed using the Waters Alliance system (Waters, Milford, USA) consisting of 2690 D Separation Module, 2487 Dual λ Absorbance Detector, 717 Plus autosampler, and Waters Alliance Series column heater. Empower 2 software was used for system control and data acquisition. Following columns were used: XSelect CSH C18, XBridge C18 and Atlantis PREMIER BEH C18 AX. All tested columns, particle size 5 µm, 150 × 4.6 mm, were obtained from Waters (Milford, USA).

Stock solutions of most of the analytes were prepared by dissolving the sample in methanol at concentration 1 mg cm^{-3}. More polar peptides (H-Val-Tyr-OH, H-Ala-Tyr-OH, H-Tyr-Ala-OH) and angiotensin II were dissolved in mixture of methanol and water (50/50 (*v*/*v*)) at concentration 1 mg cm^{-3}. Several peptides (Z-Ala-Phe-OH, Z-Ala-Tyr-OH, Z-Phe-Ala-OH, Z-Phe-Leu, and Z-Tyr-Ala-OH) needed to be dissolved at higher concentration 5 mg cm^{-3}, because of very low UV response. The first system peak was used as a dead time marker. All measurements were performed in triplicate.

Mobile phases composed of acetonitrile and aqueous part in volume ratios from 5/95 to 60/40 (*v*/*v*) with 5 volume percentage steps were used. For analysis of mixtures of peptides and cytochrome C digests, gradient elution was used. The following aqueous parts of mobile phases were used: 365 mM formic acid, pH = 2.1; 10 mM ammonium formate buffer, pH = 3.0; 10 mM ammonium acetate buffer, pH = 4.7 and pH = 6.8. For calculation of buffer components concentrations, and corresponding pH values, PeakMaster software was used [36]. Basic chromatographic conditions were set as follows: mobile phase flow rate 1 cm^3 min^{-1}, injection volume 5 mm^3, column temperature 25.0 °C, sample temperature 20.0 °C, detection wavelengths 254 nm and 280 nm. For analysis of cytochrome C digests, injection volume was 15 mm^3 and detection wavelength was 214 nm.

Instrumentation and chromatographic conditions—UHPLC measurements

Waters Acquity UPLC H-Class system (Waters, Milford, USA) was used for UHPLC measurements. The system was equipped with a quaternary solvent manager, an autosampler, a column thermostat, a photodiode array detector and a QDa mass detector. The Empower 3 software was used for system control, data acquisition, and results processing. Following columns were tested: Atlantis PREMIER BEH C18 AX; PREMIER BEH C18 (Waters, Milford, USA), both columns dimensions were 100 × 2.1 mm; particle size 1.7 µm; column Luna Omega PS C18 (Phenomenex, Torrance, USA) with dimensions 100 × 2.1 mm; particle size 1.6 µm.

Stock solutions of the peptides were prepared by dissolving the sample in deionized water at concentration 1 mg cm^{-3}. The first system peak was used as a dead time marker. All measurements were performed in triplicate.

Mobile phases were composed of acetonitrile or methanol and aqueous part in volume ratios from 0/100 to 60/40 (*v*/*v*) with 5 volume percentages steps. For analysis of mixture of peptides and cytochrome C digests, gradient elution was used. As aqueous part of mobile phase (mobile phase (B)), 0.1% formic acid, pH = 2.7 was used (corresponds to 26.5 mM solution of formic acid). Similarly, aqueous part of pH = 8.0 was prepared as 26.5 mM ammonium formate with addition of ammonium hydroxide to reach the pH = 8.0. In both cases, the same amount of formic acid/ammonium formate + ammonium hydroxide as was added to the mobile phase B was added also to the mobile phase A (to keep the ionic strength constant during the gradient). Mobile phase A contains organic solvent–pure methanol (with formic acid or ammonium formate + ammonium hydroxide), pure acetonitrile (with formic acid) or mixture acetonitrile/water, 80/20 (*v*/*v*) (ammonium formate + ammonium hydroxide), because of a low solubility of ammonium formate in pure acetonitrile. Basic chromatographic conditions were set as follows: mobile phase flow rate 0.3 cm^3 min^{-1}, injection volume 1 mm^3, column temperature 37.0 °C, sample temperature 10.0 °C, detection wavelengths 214 nm and 220 nm + QDa detection (positive mode, cone voltage 15 V, probe temperature 600 °C).

Cytochrome C trypsin digests

Two samples of cytochrome C digests were analyzed: (i) standard of digested cytochrome C, (ii) cytochrome C digested via spin column. Standard of digested cytochrome C was dissolved in 200 mm^3 of 0.055% trifluoroacetic acid. Spin digestion was performed exactly according to the manual enclosed to the trypsin spin columns (from Sigma-Aldrich). Digestion via spin column includes following steps: protein denaturation (using mixture of urea, thiourea,

and detergent protein extraction reagent type 4), spin column washing and equilibration (using 100 mM ammonium bicarbonate reaction buffer is a part of the spin column package), and digestion itself (100 µg of protein is applied, 15 min take the digestion). The products of digestion are washed from the spin column by deionized water and the sample is ready for LC analysis.

Supplementary Information The online version contains supplementary material available at https://doi.org/10.1007/s00706-023-03088-x.

Acknowledgements The authors gratefully acknowledge the financial support of the Czech Science Foundation, Grant No. 20-19655S.

Funding Open access publishing supported by the National Technical Library in Prague.

Data availability The data that support the findings of this study are available from the corresponding author, upon reasonable request.

References

1. Gilar M, Yu Y-Q, Ahn J, Fournier J, Gebler JC (2008) J Chromatogr A 1191:162
2. Cabanne C, Santarelli X (2019) Curr Protein Pept Sci 20:22
3. Kennedy LA, Kopaciewicz W, Regnier FE (1986) J Chromatogr A 359:73
4. Qiu H, Mallik AK, Takafuji M, Jiang S, Ihara H (2012) Analyst 137:2553
5. Kadlecová Z, Kozlík P, Tesařová E, Gilar M, Kalíková K (2021) J Chromatogr A 1648:462182
6. Kadlecová Z, Kalíková K (2021) Monatsh Chem 152:1081
7. McLaughlin LW (1989) Chem Rev 89:309
8. Buszewska-Forajta M, Markuszewski MJ, Kaliszan R (2018) J Chromatogr A 1559:17
9. Trammell BC, Hillmyer MA, Carr PW (2001) Anal Chem 73:3323
10. Zhu B-Y, Mant CT, Hodges RS (1992) J Chromatogr A 594:75
11. Engelhardt H, Müller H (1984) Chromatographia 19:77
12. Marunouchi T, Ono M, Nakajima T, Ito Y, Aketo T (2006) J Pharm Biomed Anal 40:331
13. Eleveld JT, Claessens HA, Ammerdorffer JL, Herk AM, Cramers CA (1994) J Chromatogr A 677:211
14. Nogueira R, Lämmerhofer M, Lindner W (2005) J Chromatogr A 1089:158
15. Yang Y, Geng X (2011) J Chromatogr A 1218:8813
16. Grybinik S, Bosakova Z (2022) Monatsh Chem 153:719
17. Zhang K, Liu X (2016) J Pharm Biomed Anal 128:73
18. Wolrab D, Frühauf P, Kolderová N, Kohout M (2021) J Chromatogr A 1635:461751
19. Kadlecová Z, Kalíková K, Folprechtová D, Tesařová E, Gilar M (2020) J Chromatogr A 1625:461301
20. Ali F, Cheong WJ, Rafique A, AlOthman ZA, Sadia M, Muhammad M (2021) J Sep Sci 44:1430
21. Liu C, Bults P, Bischoff R, Crommen J, Wang Q, Jiang Z (2019) J Chromatogr A 1603:417
22. Alharthi S, Ali A, Iqbal M, Ibrar A, Ahmad B, Nisa S, Mabood F (2022) Sci Rep 12:4061
23. Kozlik P, Vaclova J, Kalikova K (2021) Microchem J 165:106158
24. Molnarova K, Cokrtova K, Tomnikova A, Krizek T, Kozlik P (2022) Monatsh Chem 153:659
25. Olsen JV, Ong S-E, Mann M (2004) Mol Cell Proteomics 3:608
26. Nagy C, Szabo R, Gaspar A (2021) Molecules 26:5902
27. Villegas L, Pero-Gascon R, Benavente F, Barbosa J, Sanz-Nebot V (2019) Talanta 199:116
28. Yin Z, Zhao W, Tian M, Zhang Q, Guo L, Yang L (2014) Analyst 139:1973
29. Hadwan MH, Al-Obaidy SSM, Al-Kawaz HS, Almashhedy AL, Kadhum MA, Khudhair DA, Hadwan AM, Hadwan MM (2023) Monatsh Chem 154:267
30. Abe K, Shibata K, Naito T, Karayama M, Hamada E, Maekawa M, Yamada Y, Suda T, Kawakami J (2020) Anal Methods 12:54
31. Kuipers BJH, Gruppen H (2007) J Agric Food Chem 55:5445
32. Murao N, Ishigai M, Yasuno H, Shimonaka Y, Aso Y (2007) Rapid Commun Mass Spectrom 21:4033
33. Perutka Z, Šebela M (2018) Molecules 23:2637
34. Trypsin Spin Columns for proteomics Immobilized Trypsin. http://www.sigmaaldrich.com/. Accessed 1 Mar 2023
35. Hildonen S, Halvorsen TG, Reubsaet L (2014) Proteomics 14:2031
36. Malý M, Dovhunová M, Dvořák M, Gerlero GS, Kler PA, Hruška V, Dubský P (2019) Electrophoresis 40:683

Publikace VI

Mixed-mode column allows simple direct coupling with immobilized enzymatic reactor for on-line protein digestion

Vosáhlová-Kadlecová Z., Gilar M., Molnárová K., Kozlík P., Kalíková K.
Journal of Chromatography B, **2023***, 1228,* 123866.

Journal of Chromatography B 1228 (2023) 123866

Contents lists available at ScienceDirect

Journal of Chromatography B

journal homepage: www.elsevier.com/locate/jchromb

Mixed-mode column allows simple direct coupling with immobilized enzymatic reactor for on-line protein digestion

Zuzana Vosáhlová-Kadlecová [a], Martin Gilar [b], Katarína Molnárová [c], Petr Kozlík [c], Květa Kalíková [a,*]

[a] Department of Physical and Macromolecular Chemistry, Faculty of Science, Charles University, Hlavova 8, 12800 Prague, Czech Republic
[b] Waters Corporation, 34 Maple Street, Milford, MA 01757, USA
[c] Department of Analytical Chemistry, Faculty of Science, Charles University, Hlavova 8, 128 00 Prague, Czech Republic

ARTICLE INFO

Keywords:
Trypsin digestion
On-line protein digestion
Mass spectrometry
Immobilized enzymatic reactor
Mixed-mode column

ABSTRACT

Liquid chromatography coupled with mass spectrometry is widely used in the field of proteomic analysis after off-line protein digestion. On-line digestion with chromatographic column connected in a series with immobilized enzymatic reactor is not often used approach. In this work we investigated the impact of chromatographic conditions on the protein digestion efficiency. The investigation of trypsin reactor activity was performed by on-line digestion of *N*-α-benzoyl-L-arginine 4-nitroanilide hydrochloride (BAPNA), followed by separation of the digests on the mixed-mode column. Two trypsin column reactors with the different trypsin coverage on the bridged ethylene hybrid particles were evaluated.

To ensure optimal trypsin activity, the separation temperature was set at 37.0 °C and the pH of the mobile phase buffer was maintained at 8.5. The on-line digestion itself ongoing during the initial state of gradient was carried out at a low flow rate using a mobile phase that was free of organic modifiers. Proteins such as cytochrome C, enolase, and myoglobin were successfully digested on-line without prior reduction or alkylation, and the resulting peptides were separated using a mixed-mode column. Additionally, proteins that contain multiple cysteines, such as α-lactalbumin, albumin, β-lactoglobulin A, and conalbumin, were also successfully digested on-line (after reduction and alkylation). Moreover, trypsin immobilized enzymatic reactors were utilized for over 300 injections without any noticeable loss of digestion activity.

1. Introduction

Liquid chromatography (LC) coupled with mass spectrometry (MS) is the method of choice in the field of protein analysis [1]. The bottom-up approach is the most used method for protein identification in proteomics.

Protein digestion is usually performed with trypsin, a highly specific serine endoprotease, which hydrolyzes peptide bonds at the carboxyl side of arginine and lysine residues [2,3], except when the arginine and lysine is followed by proline residue. The rate of hydrolysis is slower if an acidic amino acid is located on either side of the cleavage site [4]. Trypsin digestion produces peptides with a basic residue at the carboxyl terminus, amenable for sensitive mass spectrometry analysis, and producing readily interpretable peptide mass spectra [5,6]. Before the digestion itself, protein denaturation is necessary (unfolded protein is more accessible to digestion). In case of proteins containing cysteines (formation of disulfide (S–S) bridges) the reduction and alkylation is recommended for an efficient digestion. Generally, optimal conditions for trypsin activity are temperature about 37 °C and pH around 8.0 [4]. The performance of enzymatic digestion has a fundamental influence on the success of proteomic analysis.

Besides the trypsin high activity, the specificity is also crucial. During the trypsin digestion a minor chymotrypsin or chymotrypsin-like activity can occur [7]. It leads to the nonspecific digestion of phenylalanine, tyrosine, tryptophan, or leucine residues on C-terminus [8]. This can result either from the presence of a chymotrypsin contamination

Abbreviations: ACN, acetonitrile; BAPNA, *N*-α-benzoyl-L-arginine 4-nitroanilide hydrochloride; IMER, immobilized enzymatic reactor; MeOH, methanol; MM, mixed-mode; MP, mobile phase; TIC, total ion chromatogram.

* Corresponding author at: Department of Physical and Macromolecular Chemistry, Faculty of Science, Charles University, Hlavova 8, 12800 Prague, Czech Republic.
E-mail address: kalikova@natur.cuni.cz (K. Kalíková).

https://doi.org/10.1016/j.jchromb.2023.123866
Received 4 July 2023; Received in revised form 10 August 2023; Accepted 24 August 2023
Available online 25 August 2023

(variable depending on trypsin vendor), or pseudotrypsin (ψ-trypsin), a product of trypsin autolysis, which possesses such an activity in addition to the characteristic trypsin properties [9].

Trypsin digestion can be performed in several ways. The "in-solution" procedure is predominantly used [10] with a standardized procedure described by protein digestion protocols [11]. This procedure has several drawbacks, such as long digestion time (up to 24 h), trypsin autolysis (can be reduced by addition of Ca^{2+}), need of strict temperature control and intolerance to organic solvents [12]. Some of these limitations can be overcome by enzyme immobilization on suitable support (i.e. immobilized enzymatic reactors (IMERs)) [10]. The main advantages of an IMER include the enhanced thermal, pH and autolytic stability [13]. IMERs can be prepared in various formats, e.g. membranes, capillaries, on-chip reactors, columns – spin columns or LC columns [14–16].

Immobilized enzymes can be used in either batch mode digestion or as a flow through reactors [10]. Both approaches have been investigated and several commercial products have been introduced [17]. IMERs have been shown to facilitate very fast protein digestion within minutes [18] or even seconds [17]. However, routine implementation of IMERs for protein analysis has been limited by their price, low stability, and lack of the standard digestion protocol. Another consideration is the compatibility of the LC mobile phase (MP) with the digestion buffer for the on-line digestion experiment (especially pH, presence of organic modifier, digestion buffer requirement) [19]. Therefore, the use of IMERs without direct connection to LC instrumentation (such as spin columns) or using LC trypsin columns with switching valves, fraction collectors or chromatography in 2D or 3D arrangement ("pseudo on-line") is often preferred [20–23]. Coupling the IMER online to an analytical system reduces the time needed for multi-step workflows, reduces the need for sample handling in-between steps (avoiding sample loss and contamination), and enables automation [24,25]. As this topic is of a long-term interest the progress in on-line IMER-based analytical LC platforms is thoroughly summarized in recent review [24].

In the current work, we developed a method for the direct connection of the trypsin reactor and analytical columns in series ("on-line") without need for switching valves or fraction collectors. Only one MP was used for both the protein (dissolved in the denaturant) digestion and for separation of the digests on a mixed-mode (MM) column (combining C18 ligand and positively charged quaternary alkylamine (RP/AEX retention mode) that provided superior peptide separation [26]. The effects of mobile phase composition on separation performance of peptides and cytochrome C digests using the same mixed-mode column have been investigated previously [27]. Great potential of mixed-mode column Atlantis PREMIER BEH C18 AX was shown – both acetonitrile and methanol with acidic (pH 2.7) and basic (pH 8.0) aqueous parts of mobile phase were suitable for baseline separation of cytochrome C digests. The results were compared with C18 column of the same dimensions and it was shown that higher separation performance has been achieved on mixed-mode column. C18 column provided worse separation of both set of 12 various model peptides and cytochrome C digests at both tested pHs [27]. The goal of this work was to develop simple method for on-line digestion enabling improved sample throughput and utilize a conventional unmodified LC instrumentation. An improved understanding of the digestion and separation mechanisms can improve the adoption of on-line protein digestion with the potential of speeding up the protein analysis.

2. Materials and methods

2.1. Materials and reagents

Acetonitrile (ACN, LC-MS grade) and methanol (MeOH, LC-MS grade) were supplied by VWR International (Radnor, USA). Water for LC was purchased from Honeywell (Charlotte, USA). Ammonium formate (purity > 99.995 %) and ammonium hydroxide solution (28.0–30.0 % NH_3) were purchased from Sigma-Aldrich (St. Louis, USA). Cytochrome C digestion standard was supplied by Waters (Milford, USA). *N*-α-benzoyl-L-arginine 4-nitroanilide hydrochloride (BAPNA, purity > 99 %), cytochrome C from bovine heart (purity > 95 %), bovine serum albumin (BSA, purity > 96 %), enolase from beaker's yeast, myoglobin from equine skeletal muscle (purity > 98 %), conalbumin from chicken egg white, α-lactalbumin from bovine milk, β-lactoglobulin A from bovine milk were supplied by Sigma-Aldrich (St. Louis, USA). Amino acid sequences of all tested proteins are shown in Table S1 in Supporting material. Trypsin Spin Columns, Protein Extraction Reagent Type 4 (a mixture of urea, thiourea, and C_7BzO detergent) and ProteoPrep Reduction and Alkylation Kit (tributylphosphine for reduction and iodoacetamide for alkylation) were purchased from Sigma-Aldrich (St. Louis, USA). Nylon membrane filters (0.45 μm) were supplied by Whatman (Chicago, USA).

2.2. Instrumentation and columns

Initial chromatographic measurements were performed on the Waters Acquity UPLC H-Class system (Waters, Milford, USA). The system was equipped with a quaternary solvent manager, an autosampler, a column thermostat, a photodiode array detector and a QDa mass detector. The Empower 3 software was used for system control, data acquisition, and results processing. To confirm fragment identification and to identify the unknown peaks, additional measurements using UHPLC MS/MS ToF instrumentation were performed. Agilent 1290 Infinity II LC System with a binary pump (Agilent Technologies, Inc., Waldbronn, Germany) interfaced with maXis™ Q-ToF mass spectrometer (Bruker Daltonics, Bremen, Germany) was used. Hystar 3.2 and otofControl 4.0 software were used for the information-dependent acquisition, while the LC-MS data were processed by Bruker DataAnalysis 4.4 software (Bruker Daltonics, Bremen, Germany). Two trypsin columns with dimensions 30 × 2.1 mm, and MM column Atlantis Premier BEH C18 AX (Waters, Milford, USA) with dimensions 100 × 2.1 mm; particle size 1.7 μm were used.

2.3. Experimental procedures

Stock solution of BAPNA was prepared by dissolving BAPNA in ACN/water, 25/75 (*v*/*v*) at concentration 10 mg mL^{-1} (for trypsin activity evaluation additionally: 1 mg mL^{-1}; 5 mg mL^{-1}; 15 mg mL^{-1}; 20 mg mL^{-1}). Stock solutions of proteins used for on-line digestion were prepared by dissolving in deionized water/denaturant, 50/50 (*v*/*v*) at concentration 2 mg mL^{-1}. As a denaturant, protein extraction reagent type 4 (a mixture of urea, thiourea and C_7BzO detergent) was used. Stock solutions of proteins used for digestion by trypsin spin columns or proteins required reduction and alkylation (cys–cys proteins) were prepared according to the user manual attached to the purchased equipment [28]. The first system peak was used as a column void time marker. For all measurements gradient elution was used – the gradient of MP composition as well as the gradient of flow rate (from 0.1 mL min^{-1} to 0.3 mL min^{-1}) – see the used gradients for individual proteins in Table S1 in Supporting material Part I. MP A was composed of 26.5 mM ammonium formate in ACN/water, 80/20 (*v*/*v*). As MP B 26.5 mM ammonium formate in water was used. pH of MPs was adjusted by ammonium hydroxide solution to reach ${}^{w}_{s}$pH 8.5 for MP A (${}^{w}_{s}$pH of hydro-organic MP) and pH 8.5 for MP B. For trypsin activity evaluation additional ${}^{w}_{s}$pHs/pHs were tested: pH 7.0; pH 7.5; pH 8.0; pH 9.0 (for simplicity hereafter called only as MP pH). For investigation of the effect of organic solvent on trypsin IMER activity, both ACN and MeOH based MPs were used – MP A was composed of 26.5 mM ammonium formate in organic solvent/water, 50/50 (*v*/*v*), MP B was 26.5 mM ammonium formate in water. The volume ratio 50/50 was used to be able to easily calculate organic solvent percentage in MP during initial state of digestion. All MPs were filtered before use. Injection volume was 5 μL (for trypsin activity evaluation additionally in range from 1 μL to 10 μL).

Column temperature was 37.0 °C (for trypsin activity evaluation additionally: 25.0 °C; 28.0 °C; 31.0 °C; 34.0 °C; 40.0 °C) and sample temperature was 10.0 °C for all measurements. All digestion experiments were performed in triplicate. RSD of peak intensity of individual fragments for repetitive measurements did not exceed 4 %.

QDa detector settings: mass range 50–1250 *m/z*, positive mode, cone voltage 15 V, probe temperature 600 °C. Q-ToF detector settings: mass range: 100–3500 *m/z*; fragmentation: collision-induced dissociation; spectra rate: 2 Hz, product ion spectra rate: 4–16 Hz (depending on precursor intensity), collision energy: 70 eV (50 % of the cycle time), 35 eV: (50 % of the cycle time); dry gas temperature: 350 °C; capillary voltage: 4500 V; nebulizer: 1.5 bar. Mass range for precursor selection: 300–2500 *m/z*; precursor charge between +1 and +5; precursors were selected with a 3 s cycle time and from each selected precursor 3 fragmentation spectra were acquired. Identification of peptides was performed manually based on precursor masses and characteristic fragments.

2.4. Trypsin digestion procedure

Trypsin digestion was carried out by two different ways: a) "on-line" by digestion on UHPLC trypsin columns directly connected with the analytical MM column and b) "off-line" by using commercially available trypsin spin columns (see the experimental settings in Schema S1 in Supporting material). The sequences and masses of tryptic/chymotryptic/miscleaved peptides for individual proteins were obtained from in-silico protein digests using expasy web [29].

2.4.1. Trypsin spin columns (off-line)

The whole procedure consists of several steps: protein sample denaturation, initial column preparation (washing, equilibration) and sample digestion itself. Each step was performed by centrifugation according to the attached manual, and the whole process required 1–1.5 h. For short version of trypsin spin columns usage manual see Supporting material Part I.

2.4.1.1. UHPLC columns with immobilized trypsin (on-line). Both trypsin columns were prepared using 450 Å diol sorbent, which is commonly used for size exclusion chromatography. Diol was reduced to aldehyde and trypsin was immobilized with reductive amination through the aldehyde. Two trypsin columns differing in trypsin coverage were tested and compared: IMER 1 (coverage 3.0 μmol m^{-2}) and IMER 2 (coverage 5.0 μmol m^{-2}).

3. Results and discussion

3.1. Evaluation of trypsin IMER activity

For evaluation of trypsin IMER activity *N*-α-benzoyl-L-arginine 4-nitroanilide hydrochloride (BAPNA) was used as a substrate. BAPNA is digested by trypsin into *p*-nitroaniline and benzoylarginine. Both substrate and the products of digestion are detectable with UV detection and could be used to measure the trypsin IMER activity.

In the initial experiments we used the trypsin IMER for BAPNA digestion and analysis (no separation column was used). Trypsin IMERs provided a different retentivity for BAPNA and the digestion products facilitating their slight resolution (see Fig. S1 in Supporting material).

In the subsequent experiments, BAPNA substrate was injected on IMER connected in series with MM separation column; the injected sample and the MP gradient passed through both IMER and separation column. The trypsin IMER activity was estimated from the BAPNA peak area. The calibration curve for BAPNA was constructed for nine concentration levels ranging from 1 ng to 25 μg BAPNA injections on LC column (IMER was removed from the flow path). This calibration curve is shown in Fig. S2 in Supporting material.

3.1.1. Optimization of BAPNA substrate mass for trypsin IMER activity measurement (IMER digestion capacity)

It is necessary to optimize a suitable substrate mass (and injection volume) for trypsin IMER activity measurements. We prepared five BAPNA solutions in concentrations (1 mg mL^{-1}; 5 mg mL^{-1}; 10 mg mL^{-1}; 15 mg mL^{-1}; 20 mg mL^{-1}) and injected volumes between 1 μL and 10 μL. This gave us the ability to inject 1–200 μg of substrate on trypsin IMER. Fig. 1 illustrates the relative signal of undigested BAPNA normalized to the total injected mass of BAPNA. This gave us the information about the trypsin IMER digestion capacity. When low substrate mass is injected (up to the 120 μg and 60 μg BAPNA mass for IMER 1 and IMER 2, respectively), very low BAPNA signal was detected. It indicates that within this mass range, the similar amount of BAPNA was undigested and almost no change in digestion capacity can be found. At 200 μg injected amount about 7 % and 14 % of BAPNA was undigested for IMER 1 and IMER 2, respectively (Fig. 1A and B). Based on this experiment we selected 10 mg mL^{-1} and 5 μL injection conditions for the following experiments (50 μg BAPNA mass, see the chromatogram in Fig. S3 in Supporting material). Using > 10 mg mL^{-1} concentrations of BAPNA was found to be problematic; we observed a sample precipitation in chilled autosampler.

3.1.2. Effect of mobile phase pH on trypsin IMER activity

The pH for optimal trypsin activity has been reported to be between 7 and 8 [30]. However, the optimum may be altered by the trypsin immobilization or source of enzyme. For this reason, we investigated the effect of MP pH on trypsin activity for both types of trypsin IMERs.

Fig. 2 shows that both types of immobilized trypsin reactors have better activity at pH > 7.0, with optimum near pH 8.5.

3.1.3. Effect of temperature on trypsin IMER activity

Tryptic digestions are typically performed at t = 37 °C, but other temperatures were considered. We monitored the effect of the IMER temperature on the digestion efficiency to investigate the significance of the temperature on the IMER activity. Not surprisingly, Fig. 2C and D show an increase in digestion efficiency with the temperature in a chosen temperature range. At temperatures 37.0 °C and 40.0 °C less than 0.1 % of BAPNA remained undigested on both trypsin reactors. However, from the comparison of Fig. 2A-B and Fig. 2C, D is obvious that the effect of temperature is less significant than the effect of MP pH (% of undigested BAPNA are in range up to 3 % and 22 %, respectively).

3.1.4. Effect of flow rate on trypsin IMER activity

While the temperature and pH determine the trypsin activity whether it is immobilized or not, the flow rate is relevant parameter only for column enzyme reactors. In the case of on-line digestion, it is necessary to consider the impact of MP flow rate on the substrate contact time with the immobilized enzyme.

It was observed that MP flow rate has only small influence on trypsin IMER activity (see Fig. 2E and 2F). Trypsin activity slightly decreases with increasing flow rate, but even at a highest possible flow rate (with respect to the system pressure), less than 1 % of BAPNA remains undigested. On the other hand, at flow rate 0.2 mL min^{-1}, no undigested BAPNA was observed for both trypsin columns. The results confirm that in tested flow rate range the trypsin digestion efficiency slightly depends on the time for which trypsin and substrate are in contact. Based on these results, the flow rate 0.3 mL min^{-1} in combination with the slower initial state of gradient (0.1 mL min^{-1} for first 2 min of gradient and 0.2 mL min^{-1} for third minute of the gradient, where the digestion itself takes place) was chosen for the experiments with on-line digestion of complex proteins. The rationale was to maximize the digestion efficiency while maintaining good speed and efficiency of LC analysis.

3.1.5. Effect of organic solvent on trypsin IMER activity

It is known that trypsin is sensitive to the presence of the organic modifier [31]. Therefore, we examined the effect of organic modifier

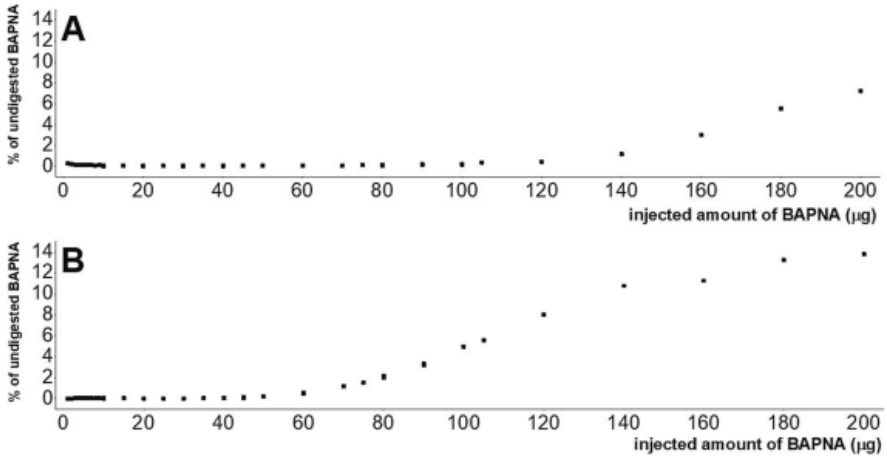

Fig. 1. Dependence of percentage of undigested BAPNA on the total amount of injected BAPNA for IMER 1 (A) and IMER 2 (B). Each point was plotted with error bars; the errors do not exceed ± 0.4 % and thus are not visible. Gradient conditions: 0–2 min constant 100 % B; 2–8 min from 100 % B to 50 % B, MP pH 8.5; column temperature: 37.0 °C; flow rate: 0.3 mL min^{-1}; detection wavelength: 280 nm.

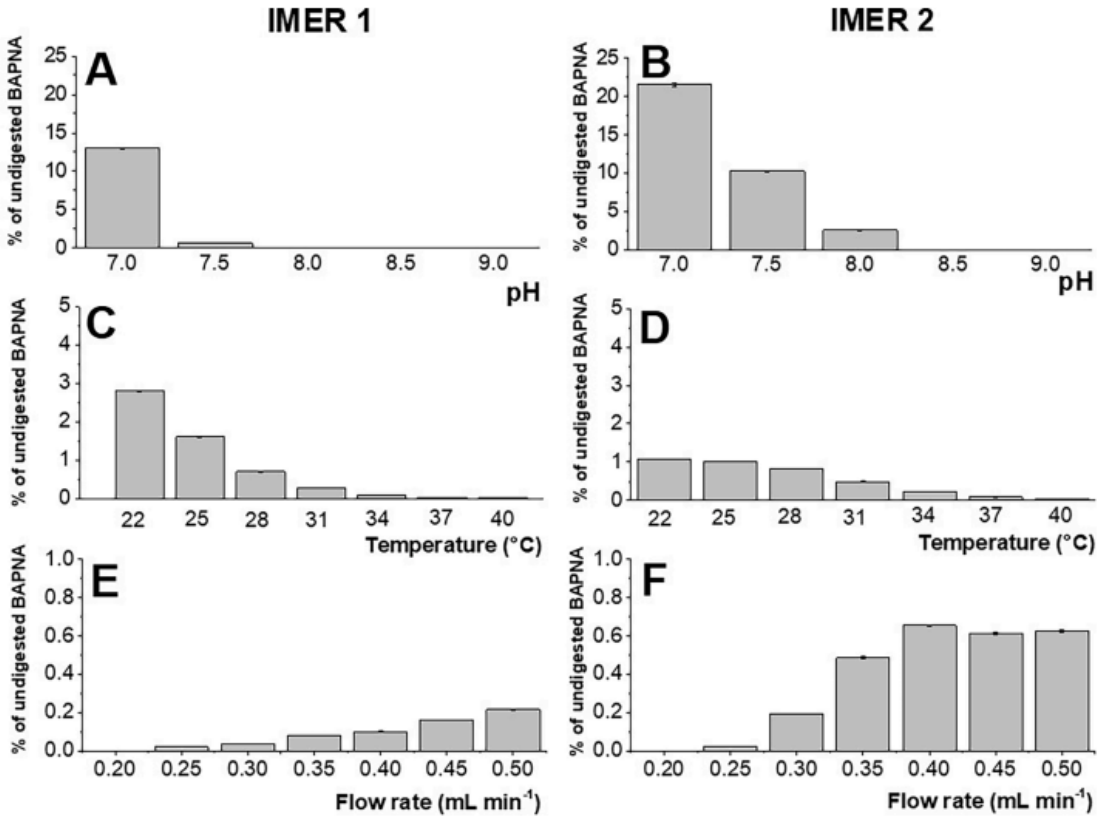

Fig. 2. Dependence of percentage of undigested BAPNA on the MP pH (A, B), column temperature (C, D) and flow rate (E, F). Each column is equipped by error bar, which does not exceed ±0.2 % for A, B; ±0.02 % for C, D and ±0.002 % for E, F. Gradient conditions: 0–2 min constant 100 % B; 2–8 min from 100 % B to 50 % B. MP pH 8.5 (except of panels A, B, - pH experiments), column temperature 37.0 °C (except of panels C, D – temperature experiments); flow rate 0.3 mL min^{-1} (except of panels E, F - flow rate experiments); detection wavelength: 280 nm; sample concentration 10 mg mL^{-1}; injection volume 5 μL.

(ACN or MeOH) percentage present in the MP during the initial/digestion state of gradient (first two minutes of gradient). The experimental results summarized in Fig. 3 reveal that higher than 5–10 % of organic solvents decrease the IMER digestion efficiency. MeOH is less detrimental to trypsin IMER activity than ACN (compare Fig. 3A/3B for IMER 1 and Fig. 3C/3D for IMER 2). Even though the MeOH reduces the digestion speed less than ACN, we preferred ACN-based MP because it maintained better peptide peak shapes in the LC analysis. Moreover, presence of ACN in MP did not visibly reduce the IMER performance over the extended time and multiple experiments (see the next section).

3.1.6. *Stability of IMER activity*

Stability of IMER was investigated over 300 injections. Even though the MP gradient passes through the IMER during each experiment with

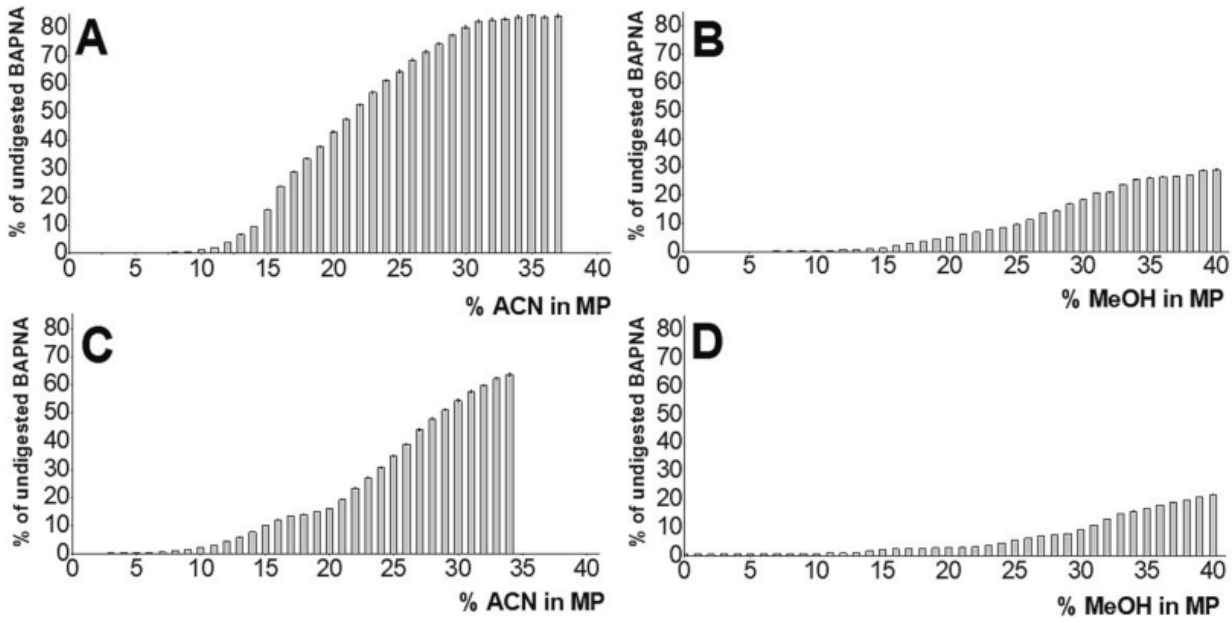

Fig. 3. Dependence of BAPNA digestion efficiency on the percentage of organic modifier (A, C: ACN; B, D: MeOH) in MP during the initial/digestion state of gradient (first two minutes) for IMER 1 (A,B) and IMER 2 (C,D). Each column is equipped by error bar, which does not exceed ±0.7 %. Gradient conditions: 0–2 min constant X% A; 2–8 min from X% A to 80 % A, where X = ⟨0; 80⟩. The percentage of organic modifier was calculated as X/2, because in MP A is 50 % of organic modifier. MP pH 8.5; sample concentration 10 mg mL^{-1}; injection volume 5 μL, for other conditions see caption to Fig. 1. Missing data at high ACN content are caused by coelution of undigested BAPNA and *p*-nitroaniline, precluding the peak quantitation.

acetonitrile content as high as 50 % (*v/v*) during the final state of gradient, no trend in decreasing the trypsin IMER digestion activity was observed (Fig. S4 in Supporting material; the percentage of undigested BAPNA remains under 0.1 % during 300 injections). We conclude that a temporary exposure of immobilized trypsin to modest percentage of organic solvent does not cause a permanent decrease of IMER activity.

3.2. On-line digestion of proteins

After the initial evaluation of trypsin IMERs with BAPNA we performed on-line digestions of selected proteins. All experiments were performed with MP containing ammonium formate, pH 8.5 (no organic solvent) in the initial phase of the gradient to maintain the optimal digestion conditions. MM column provided good retention and separation of digested peptides with 26.5 mM ammonium formate, pH 8.5 MP and ACN gradient. Peptides were identified with MS detection. Protein samples were dissolved in denaturing agent to unfold the protein and make it more amenable to digestion (see denaturing agents in experimental section).

3.2.1. Cytochrome C

Cytochrome C contains only two cysteines, hence the reduction/alkylation is not necessary for digestion. Because the digested cytochrome C standard is commercially available, we used it for comparison with different digestion methods in terms of observed peptides (tryptic *vs.* chymotryptic fragments, number of miscleavages). The amino acid sequence of cytochrome C and the expected peptides are listed in Table S1 in Supporting material Part I and Table S2 in Supporting material Part III, respectively.

The same number of tryptic fragments was observed for all three approaches, see Fig. S5-A in Supporting material Part III. Fragments T2 and T21 were not found in any sample. Neither fragment KKATNE (typical double miscleavage of terminal amino acids of Cytochrome C) was not found. For all types of the samples, we observed similar sequence coverage, 94 % (Table 1).

We further investigated the number of identified miscleaved fragments (one miscleavage was considered only) and number of chymotryptic fragments (for simplicity no miscleavage was considered). On-line digestion provided higher number of miscleaved peptides in comparison with spin digestion and digested sample (Fig. S5-B in Supporting material Part III). The number of chymotryptic fragments was comparable for all methods of digestion and standard (slightly higher number of chymotryptic fragments provided by on-line digestion – see Fig. S5-C in Supporting material Part III).

We also evaluated the relative intensity of the fragments. The ratio of

Table 1
Ratios of heights/intensities of tryptic fragment/chymotryptic fragment and tryptic fragment/miscleaved fragment for fragments declared in cytochrome C digested standard and sequence coverage for all types of samples.

	Cytochrome C digested standard	Digestion via spin column	On-line digestion IMER 1	On-line digestion IMER 2
Tryptic fragment/chymotryptic fragment				
$\frac{h_{T19}}{h_{T19C}}$	0.41	106.76	3.28	2.47
Tryptic fragment/miscleaved fragment				
$\frac{h_{T10}}{h_{T9-10}}$	1.60	1.10	1.10	1.15
$\frac{h_{T12}}{h_{T12-13}}$	0.74	0.63	0.68	0.86
$\frac{h_{T14}}{h_{T13-14}}$	3.80	20.2	1.15	1.45
Sequence coverage				
x/105 (%)	94	94	94	94

*Heights/intensities instead of areas were chosen because of problematic evaluation of MS peak area due to the necessity of smoothing. Sequence coverage: the percentage value of how many amino acids of a protein are identified/found in the digestion fragments; *x* represents the number of found amino acids in tryptic fragment sequences.

peak intensity of tryptic and chymotryptic/miscleaved version of the peptides can be used for the evaluation of the cleavage activity or fidelity. Cytochrome C digest standard has more abundant chymotryptic fragment T19C than tryptic version T19 (intensity ratio less than 1) (Table 1). On the other hand, using spin column led to significantly more tryptic than chymotryptic version of the peptide (T19C was nearly undetectable). On-line IMER experiments generated two-to-three times greater abundance of tryptic than chymotryptic fragments. The ratios of tryptic fragment/miscleaved versions of individual peptides are similar for all types of tryptic digestions. The only exception is T13-14/T14 pair, for which twenty times lower intensity of miscleaved/tryptic peptide pair was observed when using trypsin spin column.

The results suggest that miscleavage activity depends on the protein primary sequence, rather than on the trypsin digestion method. However, the chymotryptic activity is greater for in-solution digestion (the purchased digested standard was prepared in-solution) and least evident with spin column digest. We speculate that short digestion times with spin column and IMERs reduce the secondary production of chymotryptic peptides.

Similar sequence coverage was observed for all cytochrome C digests. However, Figs. S6 and S7 show that digested cytochrome C standard contains number of unidentified peaks (Fig. S7 in Supporting material). Comparison of SIR plots in Fig. S8 in Supporting material demonstrates that on-line digestion provides similar results as digestion via spin column as well as analysis of digested standard.

3.2.2. On-line digestion of proteins without disulfide bonds

To verify the activity of trypsin IMERs, two additional proteins, myoglobin and enolase, were tested. For comparison, off-line digestion with trypsin spin column was performed. Enolase contains only one cysteine, myoglobin none. Neither reduction nor alkylation was required to disrupt the disulfide bonds and achieve a complete protein digestion.

Myoglobin tryptic digestion yields 18 fully tryptic peptides (and 3 lysine short clips, see Table S3 in Supporting material Part IV). All those peptides were successfully identified in all experiments meaning 100 % sequence coverage (see Fig. S12 in Supporting material). Fig. S9 in Supporting material Part IV shows a similar number of miscleaved (Fig. S9-B) and chymotryptic peptides (Fig. S9-C) in all myoglobin digests. Selected intensity ratios for individual tryptic/miscleaved and tryptic/chymotryptic fragment pairs are summarized in Table 2. Myoglobin digestion results were similar to cytochrome C experiments; spin column digestion has significantly lower chymotryptic activity than the on-line experiments and higher relative content of tryptic peptides than miscleaved peptides (Table 2) with few exceptions. Comparison of MS TIC (total ion chromatogram) and 214 nm UV chromatograms (Figs. S10 and S11 in Supporting material Part IV) reveals that on-line digestion yields greater number of digested peptides than spin digestion. These peaks do not correspond to the expected myoglobin fragments. The most of them correspond to the miscleaved fragments (confirmed by Q-ToF measurements).

The results from both types of protein digestion revealed the number of unknown peaks occurring in all proteins with significant intensity (clearly visible on TIC plots as well as on 214 nm chromatograms). The series of the measurements has been performed and some of those peaks were the system peaks. The results showed that peaks m/z 799; m/z 400 and m/z 386 originate from the denaturing agent (present in sample of denaturant without protein, not present in sample of pure water; C_7BzO detergent has molecular weight 399.5 Da). Peaks m/z 387; **m/z 453**; **m/z 679** and m/z 327 were observed in all measurements, even without trypsin column, which excludes trypsin autolysis fragments. The bold masses represent the most intense peaks (see TIC plots in Supporting material).

Enolase is digested by trypsin into 52 fragments, from which 42 are unique fully tryptic peptides and the rest are short SK (4×), R (3×), K (2×) or L (1 ×) fragments (Table S4 in Supporting material Part V). Fig. S13-A in Supporting material Part V shows the summary of peptides found in all digestion experiments. Off-line digestion has lower number of tryptic fragments in comparison to on-line digestion; sequence coverage was 88 % and 93 %, respectively (Table 2). Spin digestion provides lower chymotryptic activity and more complete tryptic digest (lower intensity of miscleaved peptides, see Figs. S13-B and S13-C in Supporting material Part V). The only exception is ratio T4/T4-5 where opposite trend was observed. The comparison of MS TIC and UV 214 nm chromatograms (Figs. S14, S15 and S16 in Supporting material Part V) shows comparable digestion efficiency for all experiments, and presence of system peaks.

3.2.3. Proteins containing disulfide bonds (cys-cys proteins)

Proteins with multiple cysteines in the sequence can form

Table 2
Ratios of heights/intensities of tryptic fragment/chymotryptic fragment and tryptic fragment/miscleaved fragment for selected pairs of fragments; and sequence coverage for all types of samples.

MYOGLOBIN				ENOLASE			
	Digestion via spin column	On-line digestion IMER 1	On-line digestion IMER 2		Digestion via spin column	On-line digestion IMER 1	On-line digestion IMER 2
Tryptic fragment/chymotryptic fragment							
$\frac{h_{T1}}{h_{T1C}}$	18.38	9.50	12.50	$\frac{h_{T14}}{h_{T14C}}$	5.89	4.75	4.21
$\frac{h_{T17}}{h_{T17C}}$	74.40	46.41	46.42	$\frac{h_{T21}}{h_{T21C}}$	45.36	12.28	15.89
Tryptic fragment/miscleaved fragment							
$\frac{h_{T1}}{h_{T1-2}}$	1.80	0.33	0.71	$\frac{h_{T4}}{h_{T4-5}}$	3.81	5.82	7.12
$\frac{h_{T3}}{h_{T3-4}}$	1.40	0.24	0.25	$\frac{h_{T40}}{h_{T40-41}}$	32.85	1.25	1.18
$\frac{h_{T7}}{h_{T7-8}}$	1.16	1.76	2.60	$\frac{h_{T46}}{h_{T46-47}}$	2.20	1.80	1.50
Sequence coverage							
x/154 (%)	100	100	100	*x/437 (%)*	88	93	93

*Heights/intensities instead of areas were chosen because of problematic evaluation of MS peak area due to the necessity of smoothing. Sequence coverage: the percentage value of how many amino acids of a protein are identified/found in the digestion fragments; x represents the number of found amino acids in tryptic fragment sequences.

intramolecular disulfide bridges that support the protein secondary/tertiary structure. The disulfide bonds are typically reduced and alkylated prior to protein digestion. In this work four proteins, α-lactalbumin, β-lactoglobulin A, albumin, and conalbumin were reduced by tributylphosphine and alkylated with iodoacetamide prior to digestion using ProteoPrep reduction and alkylation kit according to manufacturer's manual [28].

The expected tryptic peptides are listed in Table S5 Part VI for α-lactalbumin, Table S6 in Part VII for β-lactoglobulin A, Table S7 Part VIII for albumin and Table S8 Part IX for conalbumin in Supporting material. MS SIR chromatograms of tryptic peptides for all tested proteins are shown in Supporting material (Fig. S18 in Part VI for α-lactalbumin, Fig. S20 in Part VII for β-lactoglobulin A, Fig. S22 in Part VIII for albumin and Fig. S24 in Part IX for conalbumin).

As opposed to previous digestion experiments, where the spin digestion device yielded favorable results, the on-line IMER digestions offered better sequence coverage for cys-cys proteins (Table 3). This was due to the missing peptides in off-line digestions (see Figs. S17 (Part VI), S19 (Part VII), S21 (Part VIII) and S23 (Part IX) in Supporting material) for all four proteins. Very low sequence coverage for spin digestion of α-lactalbumin was due to missing longest peptides T1, T5, T7 and T8, Fig. S17). Table 3 illustrates a significantly higher sequence coverages for IMER 2 in comparison with IMER 1. The differences were observed not only in the number of fragments found, but also in the intensity. The MS signal intensity was always higher for the IMER 2, in some cases tenfold higher.

Additional data analyses for α-lactalbumin and β-lactoglobulin A indicate lower chymotryptic activity of spin digestion (Figs. S17 (Part VI) and S19 (Part VII) in Supporting material) and lower amount of miscleaved peptides than on-line digestion (Table 3). This is consistent with previously observed results.

3.3. Evaluation of the proposed setup and comparison with other systems

One of the advantages of the proposed setup is the high-pressure, pH and temperature stability of IMERs and thus usage in UHPLC systems. It has been shown that high pressure is usually detrimental for enzyme-based flow-through systems because it may affect enzyme activity [32]. Thus, low pressure supports such as monolith or open tubular capillary are more frequently used [32]. Monolithic phases are also attractive due to the simplicity of preparation, lower flow resistance even with smaller pore sizes and can be prepared in a wide range of chemistries and morphologies compared to packed columns [33,34]. However, the high-pressure did not affect the activity of the IMERs used in this work and such stability was described previously for pepsin and trypsin IMERs [10,35]. On the other hand, compared to nano-LC systems [36,37], which are frequently used in proteomics the proposed setup is aimed for UHPLC systems and therefore higher mobile phase consumption. As UHPLC systems are known for high separation efficiency, nanoflow LC technique allows the highest level of sensitivity [38]. However, for our purpose, the sensitivity of the system was sufficient. The proposed setup is simple, suitable for any HPLC/UHPLC systems without need of any modification of common instrumentation. The mobile phase used offers a new alternative to frequently used ammonium bicarbonate or hydrogencarbonate buffers [6,39].

As the aim of the work was to show applicability of mixed-mode column for simple on-line protein digestion, other chromatographic columns/modes were not explored. Therefore, the mobile phase composition as well as gradient slope were optimized for the proposed setup. In the case of use different chromatographic modes, the separation conditions may differ. The proposed setup was evaluated using various proteins and showed very promising results and simple arrangement. The use of different chromatographic modes and more complex samples could be useful and may become a subject of the future work.

Table 3
Sequence coverages for cys-cys proteins.

	Digestion via spin column	On-line digestion IMER 1	On-line digestion IMER 2
α-Lactalbumin *x/142 (%)*	28	70	99
β-Lactoglobulin A *x/178 (%)*	42	62	75
Albumin *x/607 (%)*	72	86	90
Conalbumin *x/705 (%)*	65	85	91

*Heights/intensities instead of areas were chosen because of problematic evaluation of MS peak area due to the necessity of smoothing. Sequence coverage: the percentage value of how many amino acids of a protein are identified/found in the digestion fragments; *x* represents the number of found amino acids in tryptic fragment sequences.

4. Conclusion

In this work, rapid method for on-line trypsin digestion of proteins was developed. The simple LC setup used tryptic column reactor connected in series with mixed-mode chromatographic column without a need for switching valves. The activity and stability of two types of trypsin IMERs (IMER 1 *vs.* IMER 2) were investigated with BAPNA substrate. The effects of temperature, MP pH, flow rate and organic solvent content in the MP on the digestion efficiency were investigated. pH of the MP and the organic solvent content have the most significant effect on the immobilized trypsin activity. Based on the results, MP pH 8.5 and separation temperature 37.0 °C were chosen for the subsequent experiments with proteins. Proteins were digested using the initial aqueous gradient conditions, the fragments were trapped on mixed-mode chromatographic column and eluted with the gradient of acetonitrile.

Proteins such as cytochrome C, enolase and myoglobin were digested without sample reduction and alkylation. Spin digestion and on-line digestion provided comparable sequence coverages (>88 %). On-line digestion exhibited higher chymotryptic activity and greater amount of miscleaved peptides then spin digestion device.

The proteins containing multiple cys–cys bonds were reduced and alkylated off-line prior to tryptic digestion. In this case the off-line digestion provided significantly lower sequence coverages in comparison with on-line protein digestion.

By directly connecting the trypsin column to the MM column in a series, a higher sample throughput can be achieved compared to alternative digestion methods. This approach is uncomplicated and can be adopted in most laboratories without need for LC instrument modifications.

CRediT authorship contribution statement

Zuzana Vosáhlová-Kadlecová: Investigation, Methodology, Formal analysis, Writing – original draft, Writing – review & editing. **Martin Gilar:** Conceptualization, Methodology, Resources, Writing – review & editing. **Katarína Molnárová:** Investigation, Formal analysis, Writing – review & editing. **Petr Kozlík:** Investigation, Formal analysis, Writing – review & editing. **Květa Kalíková:** Supervision, Methodology, Conceptualization, Writing – original draft, Writing – review & editing, Funding acquisition.

Declaration of Competing Interest

The authors declare that they have no known competing financial interests or personal relationships that could have appeared to influence the work reported in this paper.

Data availability

Data will be made available on request.

Acknowledgement

The authors gratefully acknowledge the financial support of the Czech Science Foundation, Grant No. 20-19655S. The authors want to express their gratitude to Beatrice Muriithi and Oksana D. Tchoul from Waters corporation for IMERs preparation.

Appendix A. Supplementary material

Supplementary data to this article can be found online at https://doi.org/10.1016/j.jchromb.2023.123866.

References

[1] E.J. Dupree, M. Jayathirtha, H. Yorkey, M. Mihasan, B.A. Petre, C.C. Darie, A critical review of bottom-up proteomics: The good, the bad, and the future of this field, Proteomes 8 (2020) 14, https://doi.org/10.3390/proteomes8030014.
[2] J.M. Burkhart, C. Schumbrutzki, S. Wortelkamp, A. Sickmann, R.P. Zahedi, Systematic and quantitative comparison of digest efficiency and specificity reveals the impact of trypsin quality on MS-based proteomics, J. Proteomics 75 (2012) 1454–1462, https://doi.org/10.1016/j.jprot.2011.11.016.
[3] E. Vandermarliere, M. Mueller, L. Martens, Getting intimate with trypsin, the leading protease in proteomics, Mass Spectrom. Rev. 32 (2013) 453–465, https://doi.org/10.1002/mas.21376.
[4] J.V. Olsen, S.-E. Ong, M. Mann, Trypsin cleaves exclusively C-terminal to arginine and lysine residues, Mol. Cell. Proteomics 3 (2004) 608–614, https://doi.org/10.1074/mcp.T400003-MCP200.
[5] A.F.M. Altelaar, J. Munoz, A.J.R. Heck, Next-generation proteomics: towards an integrative view of proteome dynamics, Nat. Rev. Genet. 14 (2013) 35–48, https://doi.org/10.1038/nrg3356.
[6] M. Naldi, U. Černigoj, A. Štrancar, M. Bartolini, Towards automation in protein digestion: Development of a monolithic trypsin immobilized reactor for highly efficient on-line digestion and analysis, Talanta 167 (2017) 143–157, https://doi.org/10.1016/j.talanta.2017.02.016.
[7] Z. Perutka, M. Šebela, Pseudotrypsin: A little-known trypsin proteoform, Molecules 23 (2018) 2637, https://doi.org/10.3390/molecules23102637.
[8] H. Schaefer, D.C. Chamrad, K. Marcus, K.A. Reidegeld, M. Blüggel, H.E. Meyer, Tryptic transpeptidation products observed in proteome analysis by liquid chromatography-tandem mass spectrometry, Proteomics 5 (2005) 846–852, https://doi.org/10.1002/pmic.200401203.
[9] F. Dycka, V. Franc, P. Frycák, M. Raus, P. Rehulka, R. Lenobel, G. Allmaier, M. Marchetti-Deschmann, M. Sebela, Evaluation of Pseudotrypsin cleavage specificity towards proteins by MALDI-TOF mass spectrometry, Protein Pept. Lett. 22 (2015) 1123–1132.
[10] T. Šlechtová, M. Gilar, K. Kalíková, S.M. Moore, J.W. Jorgenson, E. Tesařová, Performance comparison of three trypsin columns used in liquid chromatography, J. Chromatogr. A 1490 (2017) 126–132, https://doi.org/10.1016/j.chroma.2017.02.024.
[11] L.R. Riviere, P. Tempst, Enzymatic digestion of proteins in solution, Curr. Protoc. Protein Sci. 00 (1) (1995).
[12] B. Stefansson, L. Helgadóttir, S. Olafsdottir, Á. Gudmundsdottir, J.B. Bjarnason, Characterization of cold-adapted Atlantic cod (Gadus morhua) trypsin I — Kinetic parameters, autolysis and thermal stability, Comp. Biochem. Physiol. B Biochem. Mol. Biol. 155 (2010) 186–194, https://doi.org/10.1016/j.cbpb.2009.11.004.
[13] F.E. Regnier, J. Kim, Accelerating trypsin digestion: the immobilized enzyme reactor, Bioanalysis 6 (2014) 2685–2698, https://doi.org/10.4155/bio.14.216.
[14] S.A. Currivan, W.Q. Chen, R. Wilson, E.S. Rodriguez, N. Upadhyay, D. Connolly, P. N. Nesterenko, B. Paull, Multi-lumen capillary based trypsin micro-reactor for the rapid digestion of proteins, Analyst 143 (2018) 4944–4953, https://doi.org/10.1039/C8AN01330F.
[15] S. Liu, H. Bao, L. Zhang, G. Chen, Efficient proteolysis strategies based on microchip bioreactors, J. Proteomics 82 (2013) 1–13, https://doi.org/10.1016/j.jprot.2013.02.012.
[16] K. Meller, M. Szumski, B. Buszewski, Microfluidic reactors with immobilized enzymes—Characterization, dividing, perspectives, Sens. Actuators B 244 (2017) 84–106, https://doi.org/10.1016/j.snb.2016.12.021.
[17] M. Safdar, J. Sproß, J. Jänis, Microscale immobilized enzyme reactors in proteomics: Latest developments, J. Chromatogr. A 1324 (2014) 1–10, https://doi.org/10.1016/j.chroma.2013.11.045.
[18] S. Moore, S. Hess, J. Jorgenson, Characterization of an immobilized enzyme reactor for on-line protein digestion, J. Chromatogr. A 1476 (2016) 1–8, https://doi.org/10.1016/j.chroma.2016.11.021.
[19] G. Massolini, E. Calleri, Immobilized trypsin systems coupled on-line to separation methods: Recent developments and analytical applications, J. Sep. Sci. 28 (2005) 7–21, https://doi.org/10.1002/jssc.200401941.
[20] G.W. Slysz, D.C. Schriemer, On-column digestion of proteins in aqueous-organic solvents, Rapid Commun. Mass Spectrom. 17 (2003) 1044–1050, https://doi.org/10.1002/rcm.1022.
[21] D. López-Ferrer, K. Petritis, N.M. Lourette, B. Clowers, K.K. Hixson, T. Heibeck, D. C. Prior, L. Paša-Tolić, D.G. Camp, M.E. Belov, R.D. Smith, On-line digestion system for protein characterization and proteome analysis, Anal. Chem. 80 (23) (2008) 8930–8936.
[22] A. Goyon, B. Scott, K. Kurita, C. Maschinot, K. Meyer, P. Yehl, K. Zhang, On-line sequencing of CRISPR guide RNAs and their impurities via the use of immobilized ribonuclease cartridges attached to a 2D/3D-LC–MS system, Anal. Chem. 94 (2022) 1169–1177, https://doi.org/10.1021/acs.analchem.1c04350.
[23] F. Hallez, A. Combès, C. Desoubries, A. Bossée, V. Pichon, Analysis of long-lived sulfur mustard-human hemoglobin adducts in blood samples by red blood cells lysis and on-line coupling of digestion on an immobilized-trypsin reactor with liquid chromatography-tandem mass spectrometry, J. Chromatogr. A 1665 (2022), 462830, https://doi.org/10.1016/j.chroma.2022.462830.
[24] B. Wouters, S.A. Currivan, N. Abdulhussain, T. Hankemeier, P.J. Schoenmakers, Immobilized-enzyme reactors integrated into analytical platforms: Recent advances and challenges, TrAC Trends Anal. Chem. 144 (2021), 116419, https://doi.org/10.1016/j.trac.2021.116419.
[25] C. Olsen, F.S. Skottvoll, O.K. Brandtzaeg, C. Schnaars, P. Rongved, E. Lundanes, S. R. Wilson, Investigating monoliths (vinyl azlactone-co-ethylene dimethacrylate) as a support for enzymes and drugs, for proteomics and drug-target studies, Front. Chem. 7 (2019), https://doi.org/10.3389/fchem.2019.00835.
[26] Z. Kadlecová, P. Kozlík, E. Tesařová, M. Gilar, K. Kalíková, Characterization and comparison of mixed-mode and reversed-phase columns; interaction abilities and applicability for peptide separation, J. Chromatogr. A 1648 (2021), 462182, https://doi.org/10.1016/j.chroma.2021.462182.
[27] Z. Kadlecová, H. Boudová, K. Kalíková, The benefits of mixed-mode chromatography columns for separation of peptides and protein digests, Monatsh. Chem. (2023), https://doi.org/10.1007/s00706-023-03088-x.
[28] T.P.I. Kit, ProteoPrep® Reduction and Alkylation Kit, (n.d.).
[29] PeptideMass, (n.d.). https://web.expasy.org/peptide_mass/ (accessed January 31, 2023).
[30] W. Rick, Trypsin, in: H.U. Bergmeyer (Ed.), Methods of Enzymatic Analysis, Second Ed., Academic Press, 1974, pp. 1013–1024, https://doi.org/10.1016/B978-0-12-091302-2.50099-2.
[31] L.M. Simon, M. Kotormán, G. Garab, I. Laczkó, Structure and activity of α-chymotrypsin and trypsin in aqueous organic media, Biochem. Biophys. Res. Commun. 280 (2001) 1367–1371, https://doi.org/10.1006/bbrc.2001.4282.
[32] M. Naldi, A. Tramarin, M. Bartolini, Immobilized enzyme-based analytical tools in the -omics era: Recent advances, J. Pharm. Biomed. Anal. 160 (2018) 222–237, https://doi.org/10.1016/j.jpba.2018.07.051.
[33] J. Křenková, F. Foret, Immobilized microfluidic enzymatic reactors, Electrophoresis 25 (2004) 3550–3563, https://doi.org/10.1002/elps.200406096.
[34] B. Wouters, I. Dapic, T.S.E. Valkenburg, S. Wouters, L. Niezen, S. Eeltink, G. L. Corthals, P.J. Schoenmakers, A cyclic-olefin-copolymer microfluidic immobilized-enzyme reactor for rapid digestion of proteins from dried blood spots, J. Chromatogr. A 1491 (2017) 36–42, https://doi.org/10.1016/j.chroma.2017.01.078.
[35] J. Ahn, M.C. Jung, K. Wyndham, Y.Q. Yu, J.R. Engen, Pepsin immobilized on high-strength hybrid particles for continuous flow online digestion at 10 000 psi, Anal. Chem. 84 (2012) 7256–7262, https://doi.org/10.1021/ac301749h.
[36] Z. Günyel, H. Aslan, N. Demir, C. Aydoğan, Nano-liquid chromatography with a new nano-structured monolithic nanocolumn for proteomics analysis, J. Sep. Sci. 44 (2021) 3996–4004, https://doi.org/10.1002/jssc.202100454.
[37] C. Aydoğan, B. Beltekin, S. Alharthi, C.A. Ağca, İ.Y. Erdoğan, Nano-liquid chromatography with monolithic stationary phase based on naphthyl monomer for proteomics analysis, J. Chromatogr. A 1690 (2023), 463804, https://doi.org/10.1016/j.chroma.2023.463804.
[38] C. Aydoğan, Nanoscale separations based on LC and CE for food analysis: A review, TrAC Trends Anal. Chem. 121 (2019), 115693, https://doi.org/10.1016/j.trac.2019.115693.
[39] R. Nicoli, S. Rudaz, C. Stella, J.-L. Veuthey, Trypsin immobilization on an ethylenediamine-based monolithic minidisk for rapid on-line peptide mass fingerprinting studies, J. Chromatogr. A 1216 (2009) 2695–2699, https://doi.org/10.1016/j.chroma.2008.10.046.

Publikace VII

Phosphorothioate oligonucleotides separation in ion-pairing reversed-phase liquid chromatography: Effect of ion-pairing system

Kadlecová, Z., Kalíková, K., Tesařová, E., Gilar, M.
Journal of Chromatography A, **2022**, *1676*, 463201.

Journal of Chromatography A 1676 (2022) 463201

Contents lists available at ScienceDirect

Journal of Chromatography A

journal homepage: www.elsevier.com/locate/chroma

Phosphorothioate oligonucleotides separation in ion-pairing reversed-phase liquid chromatography: Effect of ion-pairing system

Zuzana Kadlecová[a], Květa Kalíková[a,*], Eva Tesařová[a], Martin Gilar[b,*]

[a] Department of Physical and Macromolecular Chemistry, Faculty of Science, Charles University, Hlavova 8, 12800, Prague, Czech Republic
[b] Waters Corporation, 34 Maple Street, Milford, MA 01757, United States

ARTICLE INFO

Article history:
Received 19 April 2022
Revised 3 June 2022
Accepted 5 June 2022
Available online 7 June 2022

Keywords:
Phosphorothioate oligonucleotides
Ion-pairing reversed-phase chromatography
Diastereomeric separation
Ion-pairing agent
Resolution

ABSTRACT

Ion-pairing reversed-phase liquid chromatography was utilized for the analysis of native and phosphorothioate oligonucleotides of the identical sequence but different amount and position of phosphorothioate modifications. The effects of ion-pairing amines nature (alkyl chain length, hydrophobicity) and concentration on retention, *n*/*n*-1 resolution, and diastereomeric separation of phosphorothioate oligonucleotides were investigated using octadecyl column. Eight different ion-pairing agents at two concentrations (10 mM and 100 mM) buffered with acetic acid were investigated. The resolution of *n* and *n*-1 mers oligonucleotides improved with hydrophobicity and concentration of ion-pairing amines. Ion-pairing amines with moderate hydrophobicity were most successful in suppressing diastereomeric resolution. However, a partial separation of phosphorothioate oligonucleotide diastereomers was observed with all ion-pairing systems, which resulted in wider peaks compared to phosphorodiester oligonucleotides of the same sequence. This phenomenon complicates the *n* and *n*-1 mers separation of oligonucleotides with high degree of phosphorothioate modifications. Separation of oligonucleotides with different number of phosphorothioate modifications was observed, which may be useful for therapeutic oligonucleotide analysis. The aim of the work was to identify the ion-pairing systems useful for chromatographic characterization of phosphorothioate oligonucleotides.

1. Introduction

Nucleic acids with therapeutic potential and mRNA vaccines represent rapidly emerging modalities in the pharmaceutical industry [1,2]. Advances in the synthesis of chemically modified oligonucleotides (ONs) have enabled the development of novel strategies in genetic medicine [3]. Therapeutic ONs are used in antisense or gene therapy [4], *e.g.* for the treatment of Duchenne muscular dystrophy (marketed as Casimersen) [5] or for the treatment of homozygous familial hypercholesterolemia (Inclisiran) [6]. Synthetic ONs are often chemically modified to increase their *in-vivo* resistance against endo- and exo- nuclease degradation [7,8]. Moreover, suitable modification can improve cellular uptake and target binding properties.

One of the widely used modification is the phosphorothioation of internucleotide linkages. Replacement of one of the non-bridging oxygens of the phosphate group with a sulfur creates a phosphorothioate (PS) linkage [9,10]. This modification introduces a chiral center into the phosphate group leading to the formation of 2^z diastereomers, where z is the number of PS modifications [11]. Since the diastereomers have different physico-chemical properties, they can be separated on the conventional achiral stationary phases (SPs). Due to partial resolution of multiple diastereomers the chromatographic peaks of PS ONs appear wider than those of their native (phosphodiester) counterparts [12,13]. Available separation techniques do not provide sufficient separation power to resolve thousands-to-millions of diastereomers. Therefore, it is desirable to develop the separation methods capable of suppressing the separation of PS ONs diastereomers while maintaining the resolution of full-length PS oligonucleotide (*n*) from its shorter synthetic impurities (*n*-1, *n*-2..., *n*-*x*; *x* represents the number of truncated nucleotides).

Ion-pairing (IP) reversed-phase (RP) liquid chromatography (LC) methods have been applied to separation of nucleic acids, mRNA digests, plasmids [14–16], dsDNA restriction fragments [17,18] and to analysis of oligonucleotides [19–21]. The retention mechanism in IP RP LC is complex issue, which can be described by electrostatic theory. Although the electrostatic theory has not been ex-

* Corresponding authors.
E-mail addresses: kalikova@natur.cuni.cz (K. Kalíková), Martin_Gilar@waters.com (M. Gilar).

https://doi.org/10.1016/j.chroma.2022.463201
0021-9673/

Table 1
The list of all tested 21mer ONs, their sequence, number of PS linkages and number of diastereomers.

Name	Sequence	Schematic Sequence	Number of PS Linkages	Number of Diastereomers
allPO	5′-TTT TAG CAT TTT TAC GAT TTT-3′	5′——————3′	0	0
1PS3′	5′-TTT TAG CAT TTT TAC GAT TT*T-3′	5′——————*3′	1	2
1PS5′	5′-T*TT TAG CAT TTT TAC GAT TTT-3′	5′*——————3′	1	2
1PScenter	5′-TTT TAG CAT T*TT TAC GAT TTT-3′	5′——————*——————3′	1	2
2PS3′	5′-TTT TAG CAT TTT TAC GAT T*T*T-3′	5′——————**3′	2	4
2PS5′	5′-T*T*T TAG CAT TTT TAC GAT TTT-3′	5′**——————3′	2	4
2PScenter	5′-TTT TAG CAT T*T*T TAC GAT TTT-3′	5′——————**——————3′	2	4
1PS3ž′	5′-T*TT TAG CAT TTT TAC GAT TT*T-3′	5′*——————*3′	2	4
2PS3ž′	5′-T*T*T TAG CAT TTT TAC GAT T*T*T-3′	5′**——————**3′	4	16
2PScenter3ž′	5′-T*T*T TAG CAT T*T*T TAC GAT T*T*T-3′	5′**——————**——————**3′	6	64
allPS	5′-T*T*T * T*A*G * C*A*T * T*T*T * T*A*C * G*A*T * T*T*T-3′	5′**********3′	20	1,048,576

* represents PS linkage.

tended specifically to oligonucleotides yet, the retention principles of IP RP LC also apply to them [22–26]. The retention mechanism is based on interactions between positively charged IP agent (*i.e.* alkylamines) and negatively charged (thio)phosphate group of ONs [27]. Generally, both formation of neutral complex of IP agent and analytes, and the adsorption of IP agent on hydrophobic stationary phase surface leading to ion-exchange retention mechanism may explain the increasing retention of ONs with increasing hydrophobicity of IP agent (*e.g.* alkylamines) [28,29]. "Strong" IP systems such as tributylammonium acetate or triethylamine (TEA)-hexafluoroisopropanol (HFIP) systems were shown to be useful for analysis of PS ONs [20,30]. Such IP systems with strong electrostatic retention require higher amounts of organic modifier to elute ONs from RP LC columns, which reduces the hydrophobic interactions of ONs with RP stationary phase – the mechanism that is presumably responsible for diastereomeric separation [22,31].

Widely used IP systems for ONs analysis consist of TEA buffered with acetic acid or HFIP as a counter ions [32–34]. HFIP is used for LC MS applications instead of acetic or other buffering acids [35–37] because it provides useful separation with reduced amine concentration and does not suppress MS signal. However, HFIP is significantly more expensive than acetate mobile phase (MP) additive. Some other fluoroalcohols, *e.g.* trifluoroethanol, can be used as a weak acid buffering the alkylamine, however no significant changes in chromatographic behavior compared to HFIP were observed [38–40].

Chromatographic methods for ONs analysis utilize conventional RP columns, *i.e.* octyl, octadecyl (C18) and phenyl columns [41–43], although other SPs have been considered [44]. All alkyl-RP stationary phases exhibit similar retention behavior, and although phenyl columns may provide different selectivity, the retention mechanism remains the same (*i.e.* combinations of RP and electrostatic interactions) [41]. Recently, LC separation of PS ON diastereomers was investigated by several groups [14,20,41,44], however, a comprehensive study of IP agents impact of diastereomeric separation has not been published yet.

Aim of this work is to investigate the nature of IP systems and their concentration on the diastereomeric separation of PS ONs. Because the latest generation of antisense and siRNA oligonucleotides utilize selective PS modification of inter-nucleotide linkages [45], we investigated oligonucleotides with various numbers and position of PS linkages. The goal of presented study was to identify IP systems that (i) promote the separation of diastereomers to support the analysis of partially thioated ONs isomers when desired; (ii) identify IP systems that suppress the diastereomeric separation for analysis of fully thioated ONs or ONs with multiple PS linkages; and (iii) investigate the ability of selected IP systems to resolve *n* and *n*-1 species of synthetic oligonucleotides. The effect of temperature on separation of ONs diastereomers will be addressed in the subsequent report.

2. Materials and methods

2.1. Materials and reagents

Acetonitrile (ACN, Chromasolv® gradient grade, for HPLC, ≥ 99.9%), ammonium hydroxide solution (28.0–30.0% NH_3), diethylamine (DEA, purity ≥ 99.5%), triethylamine (purity ≥ 99%), diisopropylamine (DIPA, purity ≥ 99.5%), dipropylamine (DPA, purity 99%), hexylamine (HA, purity 99%), dibutylamine (DBA, purity ≥ 99.5%), octylamine (OA, purity 99%), dihexylamine (DHA, purity 97%), 1,1,1,3,3,3-hexafluoro-2-propanol (purity ≥ 99%), and acetic acid (purity ≥ 99%) were purchased from Sigma-Aldrich (St. Louis, USA). The list of 21mer ONs synthetized by Integrated DNA Technologies (Coralville, USA) with their sequences and PS linkage positions is given in Table 1. The structure of 2PScenter3ž' ON is shown in Fig. S1 in Supporting material for clarity. The shorter mers, *i.e.* 20mers, 19mer and 18mer, sequences analogous to allPS and 1PScenter ON, but truncated at 5′terminus by 1, 2, and 3 nucleobases, respectively (see the sequences in Table S1 in Supporting material), were synthesized by KRD (Prague, Czech Republic). Deionized water was purified with Rowapur and Ultrapur system from Watrex (Prague, Czech Republic).

2.2. Instrumentation and columns

All chromatographic measurements were performed on the Waters Acquity UPLC H–Class system (Waters, Milford, USA). The system was equipped with a quaternary solvent manager, an autosampler, a column thermostat, and a photodiode array detector. The Empower 3 software was used for system control, data acquisition, and results processing. Premier BEH C18 columns (Waters, Milford, USA) with dimensions 50 × 2.1 mm; particle size 1.7 μm were used. For hydrophobic alkylamines (*i.e.* DBA, HA, OA, DHA) we dedicated one column per each MP type to avoid lengthy re-equilibration of columns with different alkylamines.

2.3. Experimental procedures

Stock solutions of all tested ONs were prepared by dissolving the analytes in deionized water at concentration 50 pmol μL^{-1}. The first system peak was used as a column void time marker. Individual measurements were repeated three times. For all measurements gradient elution was used. MP B was fully aqueous, consisting of 10 or 100 mM alkylamine buffered with acetic acid to pH 8.0. Alternatively, MP B was aqueous 10 mM or 100 mM ammonium acetate (AmAc) adjusted to pH 8.0 with ammonium hydroxide solution (RP separation mode, MP does not contain alkylamine). MP A was composed of ACN/water 80/20 (*w*/*w*) with addition of the same amounts of alkylamine and acetic acid as was added to MP B to reach the same concentration. For MP composed of AmAc, ratio ACN/water 20/80 (*w*/*w*) was used because

of poor solubility of AmAc in ACN. Following IP systems were tested: diethylammonium acetate (DEAA), triethylammonium acetate (TEAA), diisopropylammonium acetate (DIPAA), dipropylammonium acetate (DPAA), dibutylammonium acetate (DBAA), hexylammonium acetate (HAA), octylammonium acetate (OAA), dihexylammonium acetate (DHAA). To prepare MP TEA-HFIP we added triethylamine (to reach 5 mM concentration) into 50 mM aqueous HFIP solution (MP B). The unadjusted pH of HFIP-based MP B was 8.5. MP A was composed of ACN/water 50/50 (*w/w*); the same amounts of TEA and HFIP were added as in MP B (5 mM and 50 mM, respectively). The gradient slope is 1% ACN per minute for all experiments regardless of IP systems used. For detailed description of MPs and gradients for all tested IP systems see Table S2 in Supporting material. All MPs were filtered with 0.45 µm nylon membrane filters (Whatman, GE Healthcare, Chicago, USA) before use. Flow rate was 0.4 mL min^{-1}, injection volume was 1 μL. Detection wavelength was set at 260 nm, based on the UV-spectra measurements. Column temperature for all experiments was 60 °C. The effect of temperature will be discussed in future work. Sample temperature was 10 °C for all measurements.

2.4. Selection of conditions

All alkylammonium acetate MPs were adjusted with acetic acid to pH 8.0. At this pH the phosphate (phosphorothioate) internucleotide linkages are negatively charged and interact with positively charged IP agents. All used alkylamines have pKa values in the range 10.5 – 11.5, thus they are fully positively charged at pH 8.0, even in the presence of organic solvent [33]. Both MPs A and B contain the same amount of IP agents ensuring that the concentration of IP agent remains constant during the gradient. Initial gradient strength was chosen so that 21mer phosphodiester ON retention is approximately 10 min with 1% ACN per minute gradient. The relative retention and diastereomeric separation of all 21mers of common sequence but different number of PS linkages was investigated with selected IP systems.

3. Results and discussion

3.1. Effects of ion-pairing systems on ONs retention

The IP additives into MP have been used to improve the retention of highly polar ionic molecules [28,46]. The retention mechanism could be explained by electrostatic theory, where hydrophobic IP agents form equilibrium between MP and SP, modify the SP surface with the charge (in case of oligonucleotides positively charged amines), which promotes the retention of ionic molecules with the opposite charge [23,47]. The type (hydrophobicity, alkyl chain length) as well as the concentration of IP amine have direct impact on the retention [24,26,31,48]. Elution of ONs in IP RP LC is realized with the gradient of organic solvent. Organic solvent reduces the population of positively charged alkylamines adsorbed on the RP SP and counter both electrostatic and hydrophobic interactions of ONs with the SP. The retention of oligonucleotides in IP RP LC primarily depends on the "hydrophobicity" of IP system, which correlates with a) the number of carbon atoms in the structure of alkylamine, and b) branching of alkyl chain in the structure of alkylamine [22,44].

Oligonucleotides are polar molecules, only few percent of ACN in the MP is required for their elution from C18 columns in the absence of IP agents or with TEAA buffers [19]. It was shown that the retention of ONs (similarly to proteins) strongly depends on the organic modifier content in the MP [49] and that ONs elute within narrow range of the organic modifier percentage [19]. This phenomenon can be utilized to compare the relative retention

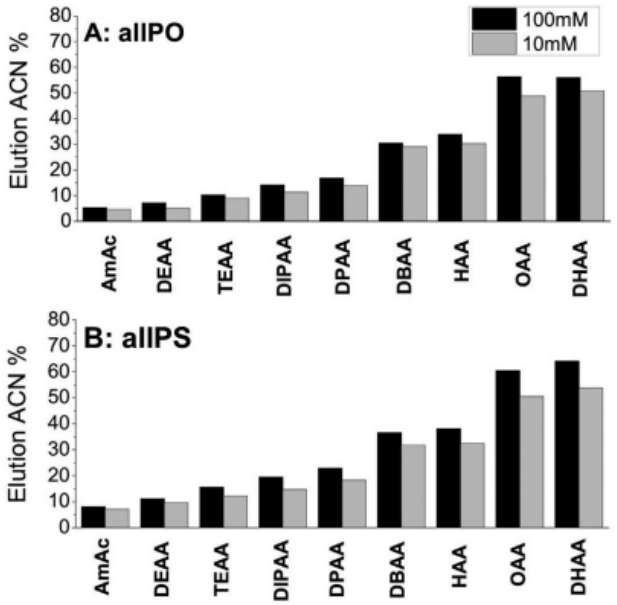

Fig. 1. ACN percentage at the time of elution of allPO (A) and allPS (B) ONs. For gradient conditions and exact values of ACN% for each system see Table S2 in Supporting material.

"strength" of the alkylamine IP systems [22]. Fig. 1 shows the percentage of ACN in MP at the time of elution for allPS and allPO analytes using 100 mM and 10 mM IP MPs. Stronger ONs retention was observed with longer (more hydrophobic) alkylamines because the IP reagents are more effectively adsorbed on the C18 SP and promote a stronger electrostatic retention (Fig. 1). AllPS exhibits somewhat higher retention compared to allPO, otherwise the ACN percentage trends are similar (see Fig. 1). This information could be used for the method development with different IP systems, *e.g.* for the choice of the acetonitrile initial percentage required to achieve a reasonable oligonucleotide elution time with the shallow gradients [19,49].

Fig. 1 can be used to rank the strength of IP system similarly to approach proposed recently [22]. Diethylamine or triethylamine could be classified as weak while the hexyl-, octyl- and dihexyl- amines as strong IP agents. The alkyl chain length is the primary factor responsible for the IP agent apparent hydrophobicity. Although TEA, DIPA, DPA and HA have 6 carbon atoms, the oligonucleotide retention increases with the IP alkyl chain lengths: TEAA < DIPAA < DPAA < HAA. The impact of alkylamine branching on oligonucleotide retention was reported previously [44]. We observed a similar behavior for OAA that afforded significantly greater retention for ONs than branched DBAA, although both IP reagents have 8 carbon atoms.

Fig. 1 shows that ON retention also depends on the buffer concentration, but the retention is dominated by the hydrophobicity of IP system.

3.2. Effects of ion-pairing systems on diastereomeric separation

The diastereomers present in phosphorothioate ONs complicate their analysis due to their partial separation in IP RP LC. This effect can be observed in Fig. 2 and in Fig. S2 in Supporting material. Fig. 2 presents the sample of five 21mer oligonucleotides of a common sequence containing none, one, two, four, or six inter-nucleotide PS modifications. The gradient was 1% ACN/min in all experiments, gradient start was adjusted to elute the oligonucleotides in a comparable elution time window using the data

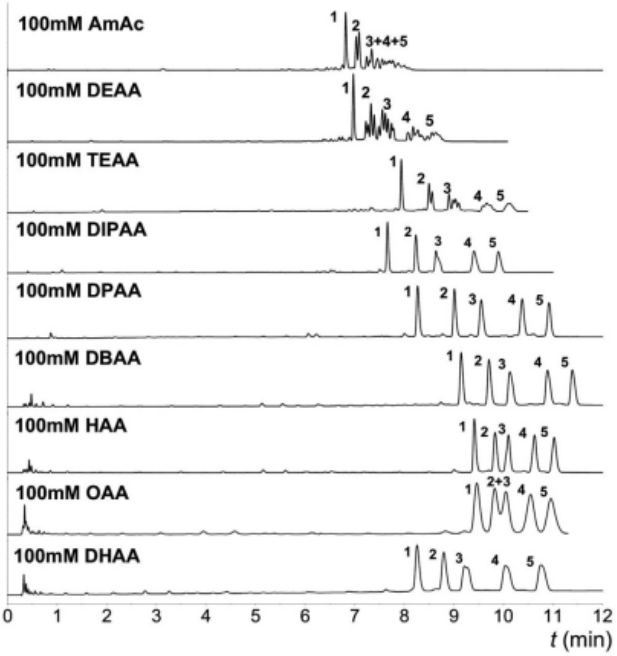

Fig. 2. Separation of 21mer oligonucleotides of the same sequence with none (allPO - 1), one (1PS5′ 2), two (2PS5′ 3), four (2PS3′5′ 4) and six (2PScenter3′5′ - 5) phosphorothioate modifications. The initial gradient strength was adjusted to achieve oligonucleotides elution in a comparable time window (retention time around 10 min). For gradient conditions see Table S2 in Supporting material.

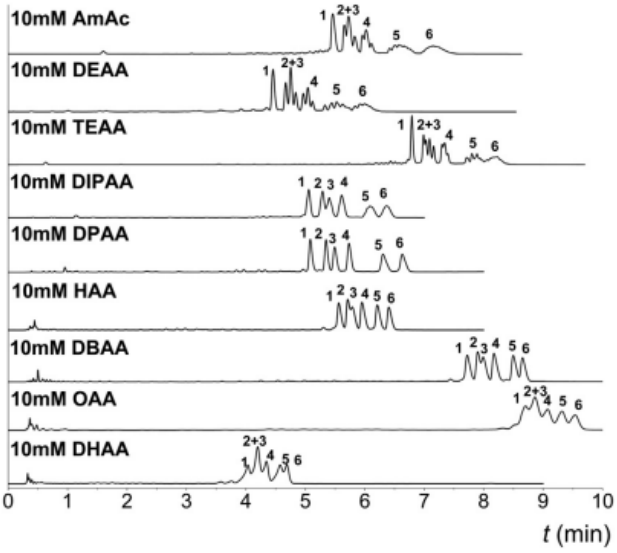

Fig. 3. Comparison of simultaneous separation of several ONs by using 10 mM IP systems. Analytes: 1: allPO; 2: 1PS3′; 3: 1PS5′; 4: 1PS3′5′; 5: 2PS3′5′; 6: 2PScenter3′5′. For gradient conditions see Table S2 in Supporting material.

obtained in Fig. 1 for allPO oligonucleotide. As noted earlier, PS oligonucleotides exhibit the effect of "peak widening" caused by the diastereomeric separation. This effect is most clearly visible in the TEAA chromatogram in Fig. 2; allPO oligonucleotide elutes first as a single peak, 1PS5' elutes second resolved into 2 isomers followed by 1PS3'5' resolved into 4 isomers. Peak 4 (2PS3'5' oligonucleotide consisting of 16 partially resolved isomers) appears as a broad peak due to partial diastereomer resolution, and the last eluting peak 5 (2PScenter3'5' oligonucleotide) is very wide due to the presence of 64 overlapping isomers (for the schematic sequences with the positions of phosphorothioation see Table 1).

Fig. 2 illustrates the mechanism of peak "broadening" reported for PS oligonucleotides [13]. The diastereomeric resolution is more pronounced for weak IP reagents, while it appears to be suppressed for stronger ion pairing systems (Fig. 2). From these results we hypothesize that the diastereomeric separation is caused by hydrophobic interactions with C18 SP that are more pronounced at low concentrations of ACN [20] used in IP RP LC with hydrophilic alkylamines (Fig. 1). Strong IP agents require high percentage of ACN to elute oligonucleotides, which leads in reduction of the diastereomeric separation. However, the diastereomeric separation suppression is incomplete. Inspection of Fig. 2 and Tables S3-S12 (Supporting material) reveals that PS oligonucleotide peaks are wider than allPO oligonucleotide for all IP systems. Apparently, electrostatic interactions also contribute to separation of diastereomers, as observed in anion-exchange (AEX) LC [50] or capillary zone electrophoresis [51]. Based on results in Fig. 2 the DPAA, DBAA and HAA IP systems are promising for separation of allPS oligonucleotides in scenarios when the suppression of isomeric separation is desired.

Fig. 3 shows separation performed in 10 mM IP buffers for another mixture of 21 mer oligonucleotides of the same sequence, but different number of PS modifications. The mixture included allPO oligonucleotide, two oligonucleotides with 1PS linkage (placed on 5′ or 3′ end), oligonucleotide with two PS linkages (5′ or 3′ end), oligonucleotide with 4PS linkages (both termini had two PS linkages), and oligonucleotide with 6PS linkages (both termini and center had two thiolations; see Table 1). The separation trends are consistent with those observed in Fig. 2; the separation of diastereomers is enhanced for hydrophilic IP reagents. The overall retention of ONs is decreased compared to 100 mM buffer experiment (Fig. 2) as expected, due to lower retention *via* IP mechanism. The retention of ONs of the same sequence increases with the number of PS linkages (both in Fig. 2 and Fig. 3). This could be explained by delocalization of negative charge that makes phosphorothioates more strongly retained in AEX and makes for stronger IP interactions with PS ON [52]. However, two oligonucleotides with single PS linkage (peaks 2 and 3 in Fig. 3) were resolved from each other in most of the IP systems in Fig. 3. Similar results were observed for additional oligonucleotides modified with 1PS and 2PS linkages placed on 3′, 5′, or in center (data are not shown in Fig. 3). Therefore, the retention of oligonucleotides does not strictly follow the degree of thiolation, it also depends on the position of PS linkage in the sequence (see Tables S3 – S12 in Supporting material). Although the separation of ONs with different amounts of PS linkages is not the primary goal of this work, it is useful for analysis of therapeutic PS oligonucleotides oxidation [13].

PS modification of ONs is known to improve oligonucleotide resistance *in-vivo* towards exo- and endo- nucleases [7]. Limited thiolation of 5′ and 3′ termini is favored over full PS oligonucleotide modification. This strategy leads to formation of limited number of diastereomers that could be resolved chromatographically. When the diastereomeric separation is desired, the results in Fig. 2 and 3 indicate that hydrophilic IP systems are recommended. However, such IP systems may be less efficient for the separation of *n* from *n-x* impurities [22]. The separation of *n* from *n-x* will be investigated in the next section.

3.3. *Effects of ion-pairing systems on resolution of* n *and* n-x *mers*

Separation of target oligonucleotides from their shorter synthetic impurities (*n-x*) or metabolites is the main goal of LC analysis [53]. Accordingly, we investigated the ability of IP systems to

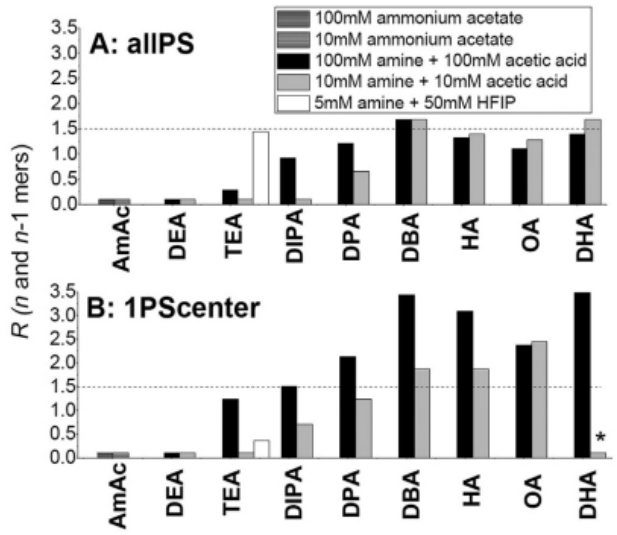

Fig. 4. Resolution of 21mer and 20mer for allPS ON (A) and 1PScenter ON (B). For gradient conditions see Table S2 in Supporting material. (*retention lost).

resolve *n* and *n*-1 (*i.e.* 21mer and 20mer) for two selected ONs, namely allPS and 1PScenter ONs (see Fig. 4). We also investigated the resolution of *n* and *n*-2 mer (21mer and 19mer), *n* and *n*-3 mer (21mer and 18mer), *n*-1 and *n*-2 (20mer and 19mer), and *n*-2 and *n*-3 (19 mer and 18mer) for allPS ON (see Table S13 in Supporting material and Fig. 5). All *n*-*x* species were prepared synthetically with the sequence truncated at 5' end by *x* number of nucleotides. Such ONs are representative of the typical impurities arising from the full-length ONs synthesis. Baseline resolution of *n* and *n*-1 mers (resolution $R > 1.5$) is desirable for oligonucleotides purity measurement and quantification.

Fig. 4 summarizes two observed trends: (i) more hydrophobic IP systems provide higher resolution of *n* and *n*-1 (21/20 mer), and (ii) 100 mM IP systems are in most cases more efficient than 10 mM IP systems for *n* and *n*-1 separation. These findings are consistent with the electrostatic hypothesis of IP separation, where higher concentration and hydrophobicity of IP agents lead to formation of greater charge density on the surface of the SP [24,26,47,48]. As discussed earlier, the suppression of diastereomeric resolution in relatively hydrophobic IP systems also improves the separation of *n* and *n*-1 oligonucleotides. The comparison of allPS ON and 1PScenter ON data (Fig. 4) shows that the *n* and *n*-1 resolution for 1PScenter ON is generally greater that for all PS ON sample. We attribute this to partial peak broadening due to multiple diastereomers present in the allPS oligonucleotides; Tables S3-S11 illustrate that allPS peak are always significantly wider than partially thioated or phosphodiester ONs of the same sequence. The only exception was observed in TEA+HFIP mobile phase (Fig. 4); the separation of ONs in TEA+HFIP IP systems will be discussed in the following section.

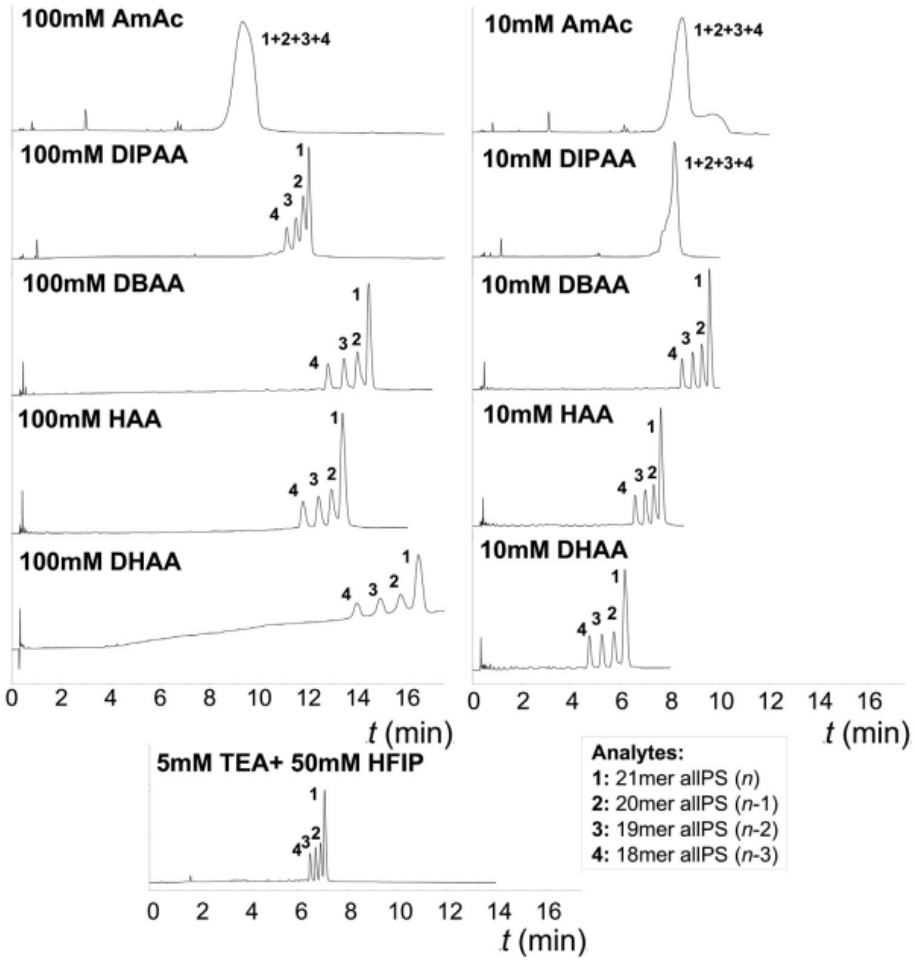

Fig. 5. Resolution of *n* and *n*-1 mer, *n*-1 and *n*-2 mer and *n*-2 and *n*-3 mer for allPS ON for selected IP systems. For gradient conditions see Table S2 in Supporting material.

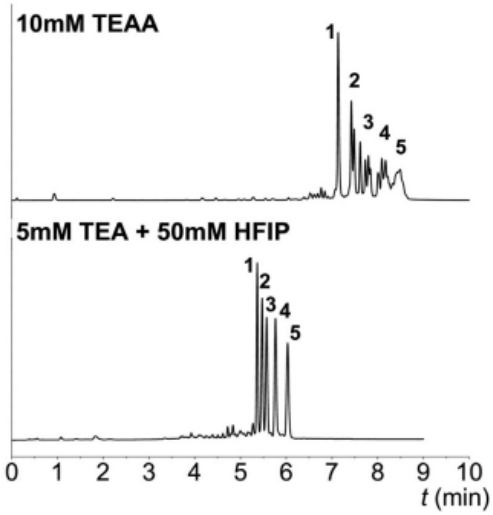

Fig. 6. Comparison of simultaneous separation of several PS ONs by using 10 mM TEAA and 5 mM TEA + 50 mM HFIP. Analytes: 1: allPO; 2: 1PS5; 3: 2PS5; 4: 2PS3; 5: 2PScenter3. For gradient conditions for each IP system see Table S2 in Supporting material.

We also analyzed the mixture of 18–21mer of allPS ON representing a full-length ON contaminated with synthetic *n-x* impurities. Fig. 5 shows that acceptable resolution of all four ONs (18–21mer) can be achieved with more hydrophobic IP systems. AmAc and DEAA do not provide resolution of 18–21mer peaks at any concentration (see Table S13 in Supporting material). TEAA, DIPAA and DPAA provide partial separation of PS ONs of different length, separation is significantly improved for 100 mM IP concentration (see example of DIPAA in Fig. 5 and data for TEAA and DPAA in Table S13 in Supporting material). Hydrophobic IP systems enable baseline resolution of all 18mer – 21mer PS ONs peaks with both 10 mM and 100 mM IP concentrations. Significantly wider peaks were observed with 100 mM concentrations, especially for 100 mM DHAA (Fig. 5).

3.4. The effect of HFIP on diastereomeric separation of PS ONs

The most common IP system used for PS ONs analysis is relatively hydrophilic TEA buffered with HFIP [19,32,54]. This seems contradictory to the results presented in the previous sections. The improved separation of ONs in TEA/HFIP systems is reportedly due to enhanced TEA adsorption on the SP due to its low solubility in HFIP solutions [22,32]. This hypothesis explains why the TEA+HFIP buffers offer significantly higher resolution of *n* and *n*-1 mer compared to 10 mM TEAA (see Fig. 4). The effect of perfluoroalcohols on the IP RP LC separation of oligonucleotides has been investigated by several groups, but it is not completely understood [19,22,33,38].

Therefore, we investigated 5 mM TEA + 50 mM HFIP IP system for separation of PS ONs. Fig. 5 shows that 5 mM TEA with 50 mM HFIP buffer system provides acceptable retention and separation of *n* and *n*-1,...*n-x* PS ONs. We also investigated the separation of 21mer ONs of the same sequence with different number of PS linkages. The comparison of 10 mM TEAA and 5 mM TEA + 50 mM HFIP buffer systems is shown in Fig. 6. The latter buffer system provides an efficient suppression of diastereomeric separation which results in narrow peaks (Fig. 6) and higher resolution then 10 mM TEAA. The suppression of diastereomeric separation is in our opinion the primary reason for the improved separation of PS ONs (see Figs. 4 and 5; Table S13) in TEA/HFIP systems. The systematic study of alkylamines other than TEA with HFIP buffer system for separation of PS ONs has not been published yet. As a next step we plan to expand this work by evaluation the effect of HFIP and other fluoroalcohols with different alkylamines as IP agents on diastereomeric separation and resolution PS ONs varying in the position and number of PS linkages.

4. Conclusion

In this study we investigated the IP systems and their effect on the separation of phosphorothioate ONs in IP RP LC. Eight IP systems at two concentrations (10 mM and 100 mM) were studied. The nature and concentration of IP systems had strong impact on retention, diastereomeric separation, resolution and resolution of PS ONs. Recommended chromatographic systems for specific applications are summarized in Table 2.

We observed strong relationship between alkylamine chain length (hydrophobicity) and IP systems ability to promote retention and separation of ONs *via* electrostatic interactions. When using more hydrophobic alkylamines a higher ACN concentration is required to elute the oligonucleotides. This results in a suppression of hydrophobic interaction of oligonucleotides with the C18 SP and corresponding suppression of diastereomeric resolution of PS ONs. While this was a general trend, a partial separation of PS ONs diastereomers was observed for very strong IP system such as OAA and DHAA. This suggests that the participation of electrostatic interactions in the separation of diastereomers cannot be completely discounted. Higher resolution of mers of different length for both tested analytes was observed for more hydrophobic IP systems, however the highest resolution was observed for DBAA.

We also observed separation of ONs of the same sequence and different degree/position of PS linkages for all investigated IP systems. This could be useful for quality control of PS ONs and resolution of their partially oxidized impurities. We briefly compared TEA/HFIP system with TEA-acetate system. TEA/HFIP MP has a

Table 2
Suitability of IP systems to individual applications.

	Suppression of Diastereomeric Separation	Resolution of *n* and *n*-1 MERS	Separation of ONs with Different Number of PS Linkages	Notes
AmAc	X	X	X	▲
DEAA	X	X	X	
TEAA	X	X	X	
DIPAA	X	X	X	•
DPAA	√	X	√	
DBAA	√	√	√	
HAA	√	√	√	
OAA	√*	√	X*	▼, ○
DHAA	√*	√	X*	▼, ○
TEA+HFIP	√	√	X	■

√ suitable; X not suitable; * broad peaks – partial diastereomeric resolution; ▲poor solubility in ACN; • higher concentration (100 mM) is significantly better; ▼ poor solubility in water, prepare buffer in ACN/water mixture; ○ lower concentration (10 mM) is significantly better; ■ limited HFIP solubility in ACN, high cost.

strong ability to suppress diastereomeric separation while concurrently provides good resolution of *n* and *n*-1 species. This work can serve as a guide for PS ONs method development, *e.g.* for selection of suitable IP system for specific oligonucleotide applications.

Declaration of Competing Interest

The authors declare that they have no known competing financial interests or personal relationships that could have appeared to influence the work reported in this paper.

CRediT authorship contribution statement

Zuzana Kadlecová: Investigation, Methodology, Writing – original draft, Writing – review & editing. **Květa Kalíková:** Supervision, Methodology, Writing – original draft, Writing – review & editing, Funding acquisition. **Eva Tesařová:** Writing – review & editing. **Martin Gilar:** Conceptualization, Methodology, Resources, Writing – original draft, Writing – review & editing.

Acknowledgement

The authors gratefully acknowledge the financial support of the Czech Science Foundation, Grant No. 20–19655S.

Supplementary materials

Supplementary material associated with this article can be found, in the online version, at doi:10.1016/j.chroma.2022.463201.

References

[1] W. Yin, M. Rogge, Targeting RNA: a transformative therapeutic strategy, Clin. Transl. Sci. 12 (2019) 98–112, doi:10.1111/cts.12624.
[2] S. Andersson, M. Antonsson, M. Elebring, R. Jansson-Löfmark, L. Weidolf, Drug metabolism and pharmacokinetic strategies for oligonucleotide- and mRNA-based drug development, Drug Discov. Today. 23 (2018) 1733–1745, doi:10.1016/j.drudis.2018.05.030.
[3] S. Benizri, A. Gissot, A. Martin, B. Vialet, M.W. Grinstaff, P. Barthélémy, Bioconjugated oligonucleotides: recent developments and therapeutic applications, Bioconjug. Chem. 30 (2019) 366, doi:10.1021/acs.bioconjchem.8b00761.
[4] E.C. Kuijper, A.J. Bergsma, W.W.M.P. Pijnappel, A. Aartsma-Rus, Opportunities and challenges for antisense oligonucleotide therapies, J. Inherit. Metab. Dis. 44 (2021) 72–87, doi:10.1002/jimd.12251.
[5] H. Wilton-Clark, T. Yokota, Casimersen for duchenne muscular dystrophy, Drugs Today Barc. Spain. 57 (2021) 707–717, doi:10.1358/dot.2021.57.12.3352740.
[6] F.J. Raal, D. Kallend, K.K. Ray, T. Turner, W. Koenig, R.S. Wright, P.L.J. Wijngaard, D. Curcio, M.J. Jaros, L.A. Leiter, J.J.P. Kastelein, Inclisiran for the Treatment of Heterozygous Familial Hypercholesterolemia, N. Engl. J. Med. 382 (2020) 1520–1530, doi:10.1056/NEJMoa1913805.
[7] B.P. Monia, J.F. Johnston, H. Sasmor, L.L. Cummins, Nuclease resistance and antisense activity of modified oligonucleotides targeted to Ha-ras, J. Biol. Chem. 271 (1996) 14533–14540, doi:10.1074/jbc.271.24.14533.
[8] A. Goyon, P. Yehl, K. Zhang, Characterization of therapeutic oligonucleotides by liquid chromatography, J. Pharm. Biomed. Anal. 182 (2020) 113105, doi:10.1016/j.jpba.2020.113105.
[9] N. Dias, C.A. Stein, Antisense oligonucleotides: basic concepts and mechanisms, Mol. Cancer Ther. 1 (2002) 347–355.
[10] E. Urban, C.R. Noe, Structural modifications of antisense oligonucleotides, Il Farm 58 (2003) 243–258, doi:10.1016/S0014-827X(03)00022-3.
[11] D. Yu, E.R. Kandimalla, A. Roskey, Q. Zhao, L. Chen, J. Chen, S. Agrawal, Stereo-enriched phosphorothioate oligodeoxynucleotides: synthesis, biophysical and biological properties, Bioorg. Med. Chem. 8 (2000) 275–284, doi:10.1016/S0968-0896(99)00275-8.
[12] W.J. Stec, G. Zon, B. Uznański, Reversed-phase high-performance liquid chromatographic separation of diastereomeric phosphorothioate analogues of oligodeoxyribonucleotides and other backbone-modified congeners of dna, J. Chromatogr. A. 326 (1985) 263–280, doi:10.1016/S0021-9673(01)87452-5.
[13] M. Gilar, K.J. Fountain, Y. Budman, J.L. Holyoke, H. Davoudi, J.C. Gebler, Characterization of therapeutic oligonucleotides using liquid chromatography with on-line mass spectrometry detection, Oligonucleotides 13 (2003) 229–243, doi:10.1089/154545703322460612.
[14] E.D. Close, A.O. Nwokeoji, D. Milton, K. Cook, D.M. Hindocha, E.C. Hook, H. Wood, M.J. Dickman, Nucleic acid separations using superficially porous silica particles, J. Chromatogr. A. 1440 (2016) 135–144, doi:10.1016/j.chroma.2016.02.057.
[15] A.O. Nwokeoji, M.E. Earll, P.M. Kilby, D.E. Portwood, M.J. Dickman, High resolution fingerprinting of single and double-stranded RNA using ion-pair reverse-phase chromatography, J. Chromatogr. B. 1104 (2019) 212–219, doi:10.1016/j.jchromb.2018.11.027.
[16] T. Jiang, N. Yu, J. Kim, J.-R. Murgo, M. Kissai, K. Ravichandran, E.J. Miracco, V. Presnyak, S. Hua, Oligonucleotide Sequence Mapping of Large Therapeutic mRNAs via Parallel Ribonuclease Digestions and LC-MS/MS, Anal. Chem. 91 (2019) 8500–8506, doi:10.1021/acs.analchem.9b01664.
[17] W. Xiao, P.J. Oefner, Denaturing high-performance liquid chromatography: a review, Hum. Mutat. 17 (2001) 439–474, doi:10.1002/humu.1130.
[18] C.G. Huber, P.J. Oefner, E. Preuss, G.K. Bonn, High-resolution liquid chromatography of DNA fragments on non-porous poly(styrene-divinylbenzene) particles, Nucleic Acids Res 21 (1993) 1061–1066.
[19] M. Gilar, K.J. Fountain, Y. Budman, U.D. Neue, K.R. Yardley, P.D. Rainville, R.J. Russell, J.C. Gebler, Ion-pair reversed-phase high-performance liquid chromatography analysis of oligonucleotides: retention prediction, J. Chromatogr. A. 958 (2002) 167–182, doi:10.1016/S0021-9673(02)00306-0.
[20] M. Enmark, M. Rova, J. Samuelsson, E. Örnskov, F. Schweikart, T. Fornstedt, Investigation of factors influencing the separation of diastereomers of phosphorothioated oligonucleotides, Anal. Bioanal. Chem. 411 (2019) 3383–3394, doi:10.1007/s00216-019-01813-2.
[21] X. Chen, Z. Liu, L. Gong, Evaluating the interplay among stationary phases/ion-pairing reagents/sequences for liquid chromatography mass spectrometry analysis of oligonucleotides, Anal. Biochem. 625 (2021) 114194, doi:10.1016/j.ab.2021.114194.
[22] M. Donegan, J.M. Nguyen, M. Gilar, Effect of ion-pairing reagent hydrophobicity on liquid chromatography and mass spectrometry analysis of oligonucleotides, J. Chromatogr. A. 1666 (2022) 462860, doi:10.1016/j.chroma.2022.462860.
[23] B.A. Bidlingmeyer, S.N. Deming, W.P. Price, B. Sachok, M. Petrusek, Retention mechamism for reversed-phase ion-pair liquid chromatography, J. Chromatogr. A. 186 (1979) 419–434, doi:10.1016/S0021-9673(00)95264-6.
[24] A. Bartha, G. Vigh, Z. Varga-Puchony, Basis of the rational selection of the hydrophobicity and concentration of the ion-pairing reagent in reversed-phase ion-pair high-performance liquid chromatography, J. Chromatogr. A. 499 (1990) 423–434, doi:10.1016/S0021-9673(00)96989-9.
[25] A. Barha, G. Vigh, J. Ståhlberg, Extension of the electrostatic retention model of reversed-phase ion-pair chromatography to include the simultaneous effect of the organic modifier and the pairing ion, J. Chromatogr. A. 506 (1990) 85–96, doi:10.1016/S0021-9673(01)91569-9.
[26] J. Ståhlberg, Á. Bartha, Extension of the electrostatic theory of reversed-phase ion-pair chromatography for high surface concentrations of the adsorbing amphiphilic ion, J. Chromatogr. A. 456 (1988) 253–265, doi:10.1016/0021-9673(86)80024-3.
[27] A. Kaczmarkiewicz, Ł. Nuckowski, S. Studzińska, B. Buszewski, Analysis of antisense oligonucleotides and their metabolites with the use of ion pair reversed-phase liquid chromatography coupled with mass spectrometry, Crit. Rev. Anal. Chem. 49 (2019) 256–270, doi:10.1080/10408347.2018.1517034.
[28] C. Horvath, W. Melander, I. Molnar, P. Molnar, Enhancement of retention by ion-pair formation in liquid chromatography with nonpolar stationary phases, Anal. Chem. 49 (1977) 2295–2305.
[29] S. Studzińska, Review on investigations of antisense oligonucleotides with the use of mass spectrometry, Talanta 176 (2018) 329–343, doi:10.1016/j.talanta.2017.08.025.
[30] S.G. Roussis, M. Pearce, C. Rentel, Small alkyl amines as ion-pair reagents for the separation of positional isomers of impurities in phosphate diester oligonucleotides, J. Chromatogr. A. 1594 (2019) 105–111, doi:10.1016/j.chroma.2019.02.026.
[31] D.S. Levin, B.T. Shepperd, C.J. Gruenloh, Combining ion pairing agents for enhanced analysis of oligonucleotide therapeutics by reversed phase-ion pairing ultra performance liquid chromatography (UPLC), J. Chromatogr. B. 879 (2011) 1587–1595, doi:10.1016/j.jchromb.2011.03.051.
[32] K.J. Fountain, M. Gilar, J.C. Gebler, Analysis of native and chemically modified oligonucleotides by tandem ion-pair reversed-phase high-performance liquid chromatography/electrospray ionization mass spectrometry, Rapid Commun. Mass Spectrom. 17 (2003) 646–653, doi:10.1002/rcm.959.
[33] N. Li, N.M. El Zahar, J.G. Saad, E.R.E. van der Hage, M.G. Bartlett, Alkylamine ion-pairing reagents and the chromatographic separation of oligonucleotides, J. Chromatogr. A. 1580 (2018) 110–119, doi:10.1016/j.chroma.2018.10.040.
[34] L. Dillen, T. Deschrijver, K. Van Mol, J.O. de Beeck, P. Jacobs, F. Cuyckens, Evaluation of micropillar array columns for chromatographic separation of phosphorothioated oligonucleotides and their diastereomers, Anal. Sci. Adv. 2 (2021) 354–363.
[35] R.S. Geary, Antisense oligonucleotide pharmacokinetics and metabolism, Expert Opin. Drug Metab. Toxicol. 5 (2009) 381–391, doi:10.1517/17425250902877680.
[36] S. Studzińska, R. Rola, B. Buszewski, The impact of ion-pairing reagents on the selectivity and sensitivity in the analysis of modified oligonucleotides in serum samples by liquid chromatography coupled with tandem mass spectrometry, J. Pharm. Biomed. Anal. 138 (2017) 146–152, doi:10.1016/j.jpba.2017.02.014.
[37] M. Huang, X. Xu, H. Qiu, N. Li, Analytical characterization of DNA and RNA oligonucleotides by hydrophilic interaction liquid chromatography-tandem mass spectrometry, J. Chromatogr. A. 1648 (2021) 462184, doi:10.1016/j.chroma.2021.462184.
[38] R. Liu, Y. Ruan, Z. Liu, L. Gong, The role of fluoroalcohols as counter anions for ion-pairing reversed-phase liquid chromatography/high-resolution

electrospray ionization mass spectrometry analysis of oligonucleotides, Rapid Commun. Mass Spectrom. 33 (2019) 697–709, doi:10.1002/rcm.8386.
[39] B. Basiri, H. van Hattum, W.D. van Dongen, M.M. Murph, M.G. Bartlett, The role of fluorinated alcohols as mobile phase modifiers for LC-MS analysis of oligonucleotides, J. Am. Soc. Mass Spectrom. 28 (2017) 190–199, doi:10.1007/s13361-016-1500-3.
[40] L. Gong, Comparing ion-pairing reagents and counter anions for ion-pair reversed-phase liquid chromatography/electrospray ionization mass spectrometry analysis of synthetic oligonucleotides, Rapid Commun. Mass Spectrom. 29 (2015) 2402–2410, doi:10.1002/rcm.7409.
[41] M. Enmark, J. Bagge, J. Samuelsson, L. Thunberg, E. Örnskov, H. Leek, F. Limé, T. Fornstedt, Analytical and preparative separation of phosphorothioated oligonucleotides: columns and ion-pair reagents, Anal. Bioanal. Chem. 412 (2020) 299–309, doi:10.1007/s00216-019-02236-9.
[42] S. Studzińska, B. Buszewski, Evaluation of ultrahigh-performance liquid chromatography columns for the analysis of unmodified and antisense oligonucleotides, Anal. Bioanal. Chem. 406 (2014) 7127–7136, doi:10.1007/s00216-014-7959-5.
[43] S. Studzińska, S. Bocian, L. Siecińska, B. Buszewski, Application of phenyl-based stationary phases for the study of retention and separation of oligonucleotides, J. Chromatogr. B. 1060 (2017) 36–43, doi:10.1016/j.jchromb.2017.05.033.
[44] S. Studzińska, F. Łobodziński, B. Buszewski, Application of hydrophilic interaction liquid chromatography coupled with mass spectrometry in the analysis of phosphorothioate oligonucleotides in serum, J. Chromatogr. B. 1040 (2017) 282–288, doi:10.1016/j.jchromb.2016.11.001.
[45] M.M.Lemaitre Meena, Stereocontrolled oligonucleotides for nucleic acid therapeutics: a perspective, Nucleic Acid Ther 31 (2021) 1–6, doi:10.1089/nat.2020.0906.
[46] J.H. Knox, J. Jurand, Separation of catecholamines and their metabolites by adsorption, ion-pair and soap chromatography, J. Chromatogr. A. 125 (1976) 89–101, doi:10.1016/S0021-9673(00)93813-5.
[47] P. Jandera, J. Churáček, B. Taraba, Comparison of retention behaviour of aromatic sulphonic acids in reversed-phase systems with mobile phases containing ion-pairing ions and in systems with solutions of inorganic salts as the mobile phases, J. Chromatogr. A. 262 (1983) 121–140, doi:10.1016/S0021-9673(01)88093-6.
[48] Á. Bartha, Gy. Vigh, H.A.H. Billiet, L. de Galan, Studies in reversed-phase ion-pair chromatography: IV. The rôle of the chain length of the pairing ion, J. Chromatogr. A. 303 (1984) 29–38, doi:10.1016/S0021-9673(01)96042-X.
[49] M. Gilar, U.D. Neue, Peak capacity in gradient reversed-phase liquid chromatography of biopolymers: theoretical and practical implications for the separation of oligonucleotides, J. Chromatogr. A. 1169 (2007) 139–150, doi:10.1016/j.chroma.2007.09.005.
[50] J.R. Thayer, Y. Wu, E. Hansen, M.D. Angelino, S. Rao, Separation of oligonucleotide phosphorothioate diastereoisomers by pellicular anion-exchange chromatography, J. Chromatogr. A. 1218 (2011) 802–808, doi:10.1016/j.chroma.2010.12.051.
[51] A. Demelenne, M.-J. Gou, G. Nys, C. Parulski, J. Crommen, A.-C. Servais, M. Fillet, Evaluation of hydrophilic interaction liquid chromatography, capillary zone electrophoresis and drift tube ion-mobility quadrupole time of flight mass spectrometry for the characterization of phosphodiester and phosphorothioate oligonucleotides, J. Chromatogr. A. 1614 (2020) 460716, doi:10.1016/j.chroma.2019.460716.
[52] P.A. Frey, R.D. Sammons, Bond order and charge localization in nucleoside phosphorothioates, Science 228 (1985) 541–545, doi:10.1126/science.2984773.
[53] B. Wei, J. Wang, L. Cadang, A. Goyon, B. Chen, F. Yang, K. Zhang, Development of an ion pairing reversed-phase liquid chromatography-mass spectrometry method for characterization of clustered regularly interspaced short palindromic repeats guide ribonucleic acid, J. Chromatogr. A. 1665 (2022) 462839, doi:10.1016/j.chroma.2022.462839.
[54] B. Koshel, R. Birdsall, W. Chen, Two-dimensional liquid chromatography coupled to mass spectrometry for impurity analysis of dye-conjugated oligonucleotides, J. Chromatogr. B. 1137 (2020) 121906, doi:10.1016/j.jchromb.2019.121906.

Publikace VIII

Impact of ion-pairing systems choice on diastereomeric selectivity of phosphorothioated oligonucleotides in reversed-phase liquid chromatography

Vosáhlová Z., Gilar M., Kalíková K.

Journal of Chromatography A, **2024,** *1730,* 465074.

Journal of Chromatography A 1730 (2024) 465074

Contents lists available at ScienceDirect

Journal of Chromatography A

journal homepage: www.elsevier.com/locate/chroma

Impact of ion-pairing systems choice on diastereomeric selectivity of phosphorothioated oligonucleotides in reversed-phase liquid chromatography

Zuzana Vosáhlová [a], Martin Gilar [b], Květa Kalíková [a,*]

[a] Department of Physical and Macromolecular Chemistry, Faculty of Science, Charles University, Hlavova 8, Prague 12800, Czech Republic
[b] Waters Corporation, 34 Maple Street, Milford, MA 01757, USA

ARTICLE INFO

Keywords:
Phosphorothioated oligonucleotides
Ion-pairing reversed-phase chromatography
Phenyl column
C18 column
Hexafluoroisopropanol

ABSTRACT

Ion-pairing reversed-phase liquid chromatography was utilized for the analysis of native and phosphorothioated oligonucleotides differing in the length (2–6mers and 21mer) and the number and position of phosphorothioate modifications. We investigated the influence of counterion (acetate vs. hexafluoroisopropanol) on the adsorption of eleven alkylamines on the stationary phases. A stronger adsorption of charged alkylamines on octadecyl- and phenyl-based stationary phases led to greater retention of oligonucleotides, and the adsorption of alkylamines was promoted with greater concentration of hexafluoroisopropanol in the mobile phase. Selected amines (triethylamine, dipropylamine, hexylamine) were used to study the resolution of *n* and *n-x* mers (main peak and its impurities shortened at 5'end), and diastereomeric separation of phosphorothioated oligonucleotides. The results confirmed a crucial role of alkylamine and counterion choice on the diastereomeric separation. The increasing hydrophobicity of alkylamine led to diminished diastereomeric selectivity which produced narrower phosphorothioated oligonucleotides peaks and led to improved *n/n-x* separation. Using hexafluoroisopropanol instead of acetate as counterion further enhances this effect (except for 100 mM concentration of hexafluoroisopropanol in combination with highly hydrophobic hexylamine). The elevated column temperature led to suppression of the diastereomeric resolution and improved resolution of *n* and *n-x* mers oligonucleotides. Baseline separation of oligonucleotides with different number of phosphorothioate linkages was achieved; this may be useful for therapeutic oligonucleotide analysis.

1. Introduction

Therapeutic oligonucleotides (ONs) are rapidly developing group of pharmaceuticals. Recent report mentioned that therapeutic ONs represent more than 4 % of the total number of new drugs approved by the U. S. Food and Drug Administration (FDA) from 2016 to 2023 [1]. ONs modification, specifically phosphorothioation, improves *in-vivo* stability, but leads to the formation of 2^z diastereomers (where *z* is the number of phosphorothioate (PS) modifications), which significantly complicates their analysis [2]. The presence of large number of diastereomers (e.g. 1,048,576 isomers of fully modified 21mer PS ON) presents a challenge for the ONs separation [3]. It has been shown that PS ONs have significantly wider peaks than unmodified (PO) ONs of the same sequence, which was attributed to the partial resolution of PS ONs diastereomers [4–7]. Due to this phenomenon, the analysis of PS ONs is more difficult. This has been also the case for siRNA drugs with smaller number of PS modifications, typically 1 or 2 PS modifications on the 3′ and 5′ ends of the ONs [8,9].

Development of nucleic acid-based therapeutics benefits from the advances of analytical methods suitable for their characterization. Capillary electrophoresis [10] and anion-exchange liquid chromatography (AEX) [11,12] exhibits very high selectivity for ONs with different length (different number of charges), but these methods are not directly compatible with mass spectrometry (MS) detection [13]. Two-dimensional (2D) chromatographic techniques can overcome this problem in case of using MS compatible mobile phase (MP) in the second dimension (e.g. AEX – RP LC combination) [14]. Nowadays, for analysis of PS ONs two approaches are mainly used: i) hydrophilic interaction liquid chromatography (HILIC), which is less prone to separation of diastereomers [15,16], however the diastereomers can be separated

* Corresponding author.
E-mail address: kveta.kalikova@natur.cuni.cz (K. Kalíková).

https://doi.org/10.1016/j.chroma.2024.465074
Received 25 March 2024; Received in revised form 28 May 2024; Accepted 10 June 2024
Available online 10 June 2024

Table 1
The list of oligonucleotides with their sequences and position of PS modification (*).

NAME	SEQUENCE
longmers	
21mer unmodified (allPO)	5'-TTT TAG CAT TTT TAC GAT TTT-3'
21mer 1PS3'	5'-TTT TAG CAT TTT TAC GAT TT*T-3'
21mer 1PS5'	5'-T*TT TAG CAT TTT TAC GAT TTT-3'
21mer 1PScenter	5'-TTT TAG CAT T*TT TAC GAT TTT-3'
21mer 2PS3'	5'-TTT TAG CAT TTT TAC GAT T*T*T-3'
21mer 2PS5'	5'-T*T*T TAG CAT TTT TAC GAT TTT-3'
21mer 2PScenter	5'-TTT TAG CAT T*T*T TAC GAT TTT-3'
21mer 1PS35'	5'-T*TT TAG CAT TTT TAC GAT TT*T-3'
21mer 2PS35'	5'-T*T*T TAG CAT TTT TAC GAT T*T*T-3'
21mer 2PScenter35'	5'-T*T*T TAG CAT T*T*T TAC GAT T*T*T-3'
21 mer fully modified (allPS)	5'-T*T*T * T*A*G * C*A*T * T*T*T * T*A*C * G*A*T * T*T*T-3'
allPS 20mer (5N-1)	5' T*T * T*A*G * C*A*T * T*T*T * T*A*C * G*A*T * T*T*T 3'
allPS 19mer (5N-2)	5' T*T*A*G * C*A*T * T*T*T * T*A*C * G*A*T * T*T*T 3'
allPS 18mer (5N-3)	5' T*A*G * C*A*T * T*T*T * T*A*C * G*A*T * T*T*T 3'
shortmers	
allPO 2mer	5' TT 3'
allPS 2mer	5' T*T 3'
allPO 3mer	5' TTT 3'
allPS 3mer	5' T*T*T 3'
allPO 4mer	5' TTTT 3'
allPS 4mer	5' T*T*T*T 3'
allPO 5mer	5' TTTTT 3'
allPS 5mer	5' T*T*T*T*T 3'
allPO 6mer	5' TTTTTT 3'
1PS 6mer	5' TTTTT*T 3'
2PS 6mer	5' TTTT*T*T 3'
3PS 6mer	5' TTT*T*T*T 3'
4PS 6mer	5' TT*T*T*T*T 3'
allPS 6mer	5' T*T*T*T*T*T 3'

allPO indicates unmodified ON, allPS indicates fully modified ON, 5N-1 indicates ON shortened about one nucleotide at 5end.

under certain conditions [17]; and ii) ion-pairing reversed-phase liquid chromatography (IP RP LC), where separation of diastereomers is suppressed by adding of ion-paring reagents into the MP [18].

The role of IP reagent in IP RP LC was investigated recently. It was shown that with increasing hydrophobicity of IP reagent the retention as well as the ability to suppress the diastereomeric separation of PS ONs is increasing. This can be explained by the fact that with increasing hydrophobicity of IP reagent increases the co-solvent fraction in the gradient, which results in the lower selectivity of diastereomers [3,6]. The comprehensive description of co-solvent gradient and ion-pairing gradient modes applied for oligonucleotides was published recently [19–21]. Notably the highly hydrophobic IP reagents (octylamine or dihexylamine) yielded broader peaks which suggests that ionic interactions also participate in diastereomeric separation [5]. IP reagents are essential for the retention of ONs [22]; however, their traces persisting in LC system can compromise the sensitivity of subsequent LC MS analyses in positive electrospray ionization (ESI) mode [23,24].

The introduction of hexafluoroisopropanol (HFIP) as an acidic modifier by Apffel et al. [25,26] was crucial for sensitive LC MS of ONs. HFIP can buffer the MP pH, but due to its high vapor pressure and volatility does not suppress the ESI of ONs, and thus provides excellent MS signal [25,27]. Moreover, it was shown that using HFIP instead of acetate as a counter ion for triethylamine (TEA) reduces PS diastereomeric selectivity [5].

Several recent studies have investigated the separation on PS ONs. The effect of IP alkylamine hydrophobicity [5–7,28] and column temperature [29,30] on diastereomeric separation and resolution of *n* and *n-x* oligonucleotides differing in the number/position of phosphorothioation was studied in detail. However, only one study investigated the HFIP based MPs [28]; thus the above-mentioned effects (the effect of temperature and HFIP concentration) were not described in details, yet. Moreover, the selectivity differences between phenyl based and C18 (alkyl) stationary phases in context of IP RP LC of oligonucleotides are not fully understood [31,32].

The aim of this work was to systematically summarize how the choice of IP alkylamine (triethylamine/dipropylamine/hexylamine), IP concentration, counterion type (acetate vs. HFIP) and its concentration influences the separation of short (2–6 mer) and longer (18–21mer) PS ONs. We investigated the differences between C18 and phenyl based stationary phases (SPs) for PS ON's separation and peak broadening due to resolution of their diastereomers. This work is an extension of recent publications that described the effects of IP reagents and temperature on analysis of various phosphorothioated ONs [5,29].

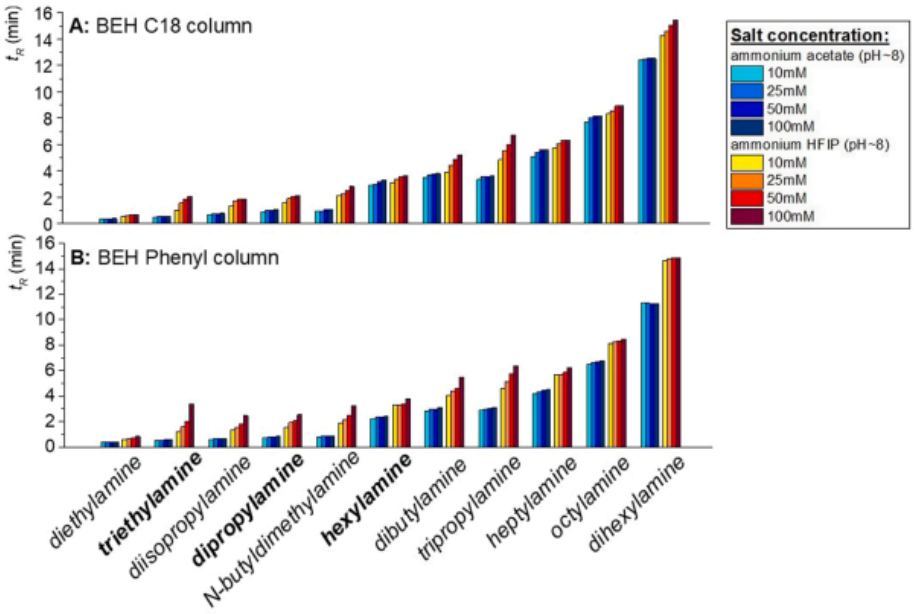

Fig. 1. Retention of alkylamines on C18 and phenyl columns using ammonium acetate or ammonium-HFIP mobile phases at various concentrations. Temperature: 60 °C. *alkylamines in bold have been selected for further studying (based on our previously published work [5]).

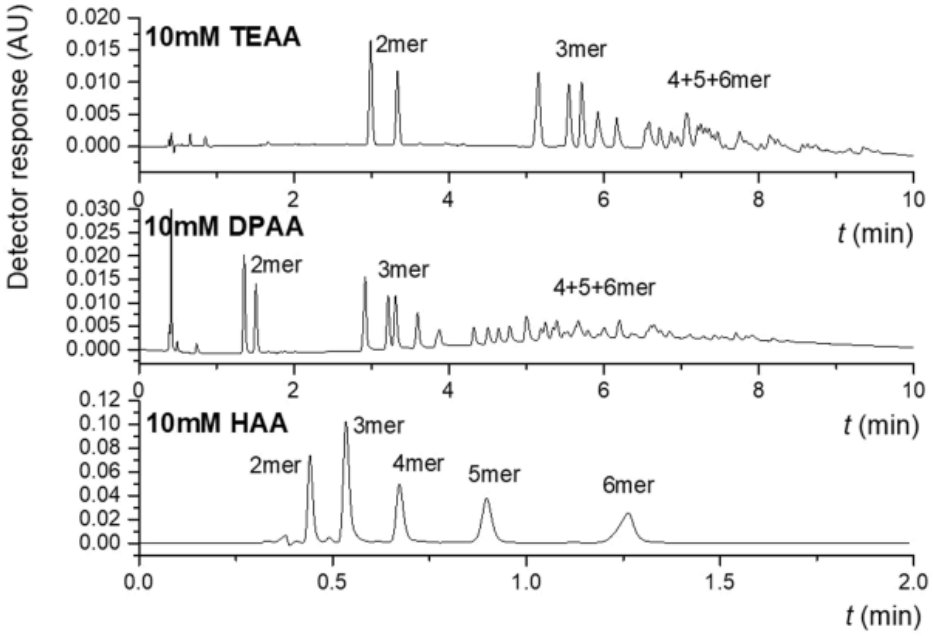

Fig. 2. Comparison of 10 mM TEAA, 10 mM DPAA and 10 mM HAA systems in terms of suppression of diastereomeric separation. Gradient conditions: TEAA: 0–20 min => 4–29 % MP A; DPAA: 0–20 min => 8–33 % MP A; HAA: 0–20 min => 25–50 % MP A. MP A contains 10 mM alkylammonium acetate in MeCN/water, 80/20 (*v/v*). MP B is fully aqueous with the same IP reagent concentration. Column: Acquity UPLC BEH Phenyl. ONs: fully modified (allPS) 2–6mers. Temperature: 60 °C.

2. Materials and methods

2.1. Materials and reagents

Acetonitrile (MeCN, Chromasolv® gradient grade, for HPLC, ≥ 99.9 %), methanol (Chromasolv® gradient grade, for HPLC, ≥ 99.9 %), ammonium hydroxide solution (28.0–30.0 % NH_3), diethylamine (purity ≥ 99.5 %), triethylamine (purity ≥ 99 %), diisopropylamine (purity ≥ 99.5 %), dipropylamine (DPA, purity 99 %), tripropylamine (purity ≥ 98 %), hexylamine (HA, purity 99 %), dibutylamine (purity ≥ 99.5 %), octylamine (purity 99 %), dihexylamine (purity 97 %), heptylamine (purity 99 %), 1,1,1,3,3,3-hexafluoro-2-propanol (purity ≥ 99 %), and acetic acid (purity ≥ 99 %) were purchased from Sigma-Aldrich (St. Louis, USA). *N*-butyldimethylamine (purity 98 %) was supplied by TCI (Tokyo, Japan). The list of tested ONs synthetized by Integrated DNA Technologies (Coralville, USA) with their sequences and PS modification positions is shown in Table 1. The 20mer, 19mer and 18mer, sequences analogous to 21mer allPS, but truncated at 5terminus by 1, 2, and 3 nucleobases, respectively (see the sequences in Table 1), were synthetized by KRD (Prague, Czech Republic). Deionized water was purified with Rowapur and Ultrapur system from Watrex (Prague, Czech Republic).

2.2. Instrumentation and columns

All chromatographic measurements were performed on the Waters Acquity UPLC H—Class system (Waters, Milford, USA). The system was equipped with a quaternary solvent manager, an autosampler, a column thermostat, photodiode array detector and QDa mass detector. The Empower 3 software was used for system control, data acquisition, and results processing. Three different columns with dimensions 50 × 2.1 mm and particle size 1.7 µm were used, namely Acquity Premier BEH C18, Acquity UPLC BEH C18 and Acquity UPLC BEH Phenyl (Waters, Milford, USA). For hydrophobic HA based MPs we dedicated one column to avoid lengthy re-equilibration of columns with less hydrophobic alkylamines.

2.3. Experimental procedures

2.3.1. Alkylamine retention

Stock solutions of alkylamines were prepared by dissolving of 10 µL of alkylamines in 1000 µL of methanol. Subsequently, 10 µL of this solution was dissolved in 1000 µL of water. MP A contained pure acetonitrile. MP B was fully aqueous, consisting of ammonium acetate (pH 8.0) or HFIP buffered with ammonia (pH 8.0), both at salt concentrations 10 mM, 25 mM, 50 mM or 100 mM. Individual measurements were repeated three times. Columns Acquity UPLC BEH C18 and Acquity UPLC BEH Phenyl were used for these experiments. For all measurements gradient elution was used as follows: 0 min = 1 % MP A; 22.5 min = 50 % MPA. Flow rate was 0.5 mL min^{-1}, injection volume was 2 µL. Column temperature for all experiments was 60 °C, sample temperature was 10 °C. MS detection using QDa detector (listed in previous subsection) in positive ESI mode was used (method parameters: cone voltage 15 V, probe temperature 600 °C, factory default setup). Individual single ion records (SIR) have been extracted using selected *m/z* (see the example in Fig. S1 in Supporting material).

2.3.2. Analysis of oligonucleotides

Stock solutions of all tested ONs were prepared by dissolving the ONs in deionized water at concentration 50 pmol μL^{-1}. Both MPs (MP A and MP B) contained 10 mM IP reagents (TEA, DPA, or HA) buffered with 10 mM acetic acid or 100 mM HFIP to reach pH 8.0 or 8.5 in aqueous part of MP, respectively. MP B was fully aqueous, MP A was composed of MeCN/water 80/20 (*w/w*) – in case of MPs with acetic acid; or MeCN/water 50/50 (*w/w*) – in case of MPs with HFIP. The change in MeCN content (from 80 % to 50 %) in MP A with HFIP is necessary due to the lower solubility of HFIP in MeCN. In addition, the change in initial gradient conditions (lowering the amount of MP A and thus additional lowering the amount of MeCN) is needed to obtain similar retention as with acetic acid.

Some other concentrations of MP constituents were also tested (5 mM and 2.5 mM for IP reagents; 50 mM, 25 mM and 10 mM for HFIP). All MPs were filtered with 0.45 µm nylon membrane filters (Whatman, GE Healthcare, Chicago, USA) before use. Individual measurements

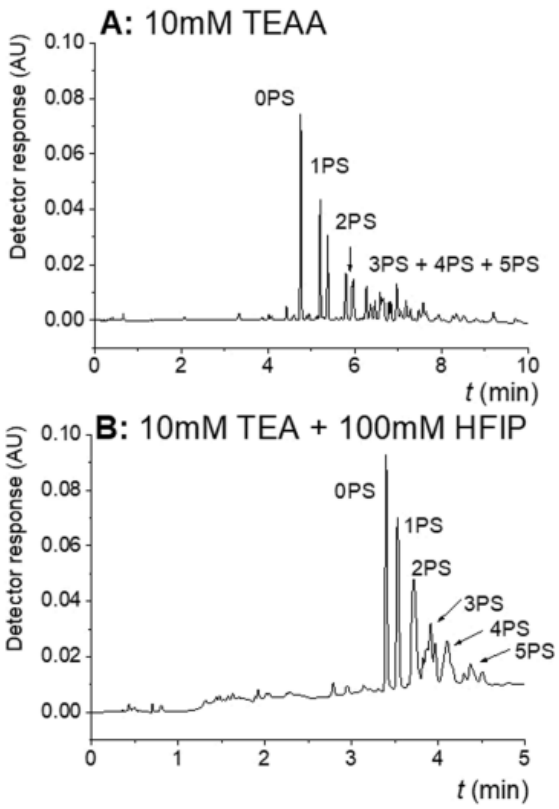

Fig. 3. Comparison of systems with acetate (A) and HFIP (B) as counterions in terms of suppression of diastereomeric separation. A: 10 mM TEAA, gradient conditions: 0–20 min => 4–29 % MP A; MP A contains 10 mM triethylammonium acetate in MeCN/water, 80/20 (*v/v*). B: 10 mM TEA + 100 mM HFIP, gradient conditions: 0–20 min => 0–40 % MP A; MP A contains 10 mM triethylamine+ 100 mM HFIP in MeCN/water, 50/50 (*v/v*). MP B is fully aqueous with the same IP reagent concentration. Column: Acquity UPLC BEH C18. ONs: 6mers with various number of PS modifications (from zero to five). Temperature: 60 °C.

were repeated three times. For all measurements gradient elution was used (see gradient description in Table S1 in Supporting material). The analyses were performed with gradients that elute 21mer allPS ON at approximately 10 min. Flow rate was 0.4 mL min^{-1}, injection volume was 2 µL. Detection wavelength was set at 260 nm, based on the UV-spectra measurements. Column temperature was set in the range 10 °C to 90 °C (with 10 °C increments), nevertheless for the most experiments the column temperature was 60 °C. The temperature was controlled by the column thermostat with active pre-heater. The mobile phase containers were kept at ambient temperature. All tested columns were packed with BEH sorbent compatible with the given temperature range. Sample temperature was 10 °C for all measurements.

3. Results and discussion

3.1. Investigation of alkylamine retention/adsorption

It has been previously reported that alkylamine retention on C18 SP correlates with their efficiency as IP reagent for separation of ON's [28]. The same report suggested that HFIP addition to mobile phase improves selected alkylamines efficiency as IP reagents, but this observation was not explored. Therefore, we investigated the impact of mobile phase buffer type (acetate vs. HFIP-based buffers) on the retention of selected IP reagents on C18 and phenyl columns. Fig. 1 confirms the published observations that the IP alkylamine hydrophobicity (retention) increases with the number of carbons in the alkylamine, but alkyl branching is also important [5–7,29]. Moreover, Fig. 1 shows that HFIP-based MPs improve retention of tested alkylamines [28] and this behaviour is HFIP concentration dependent, which implies that alkylamines are better adsorbed on SP in presence of HFIP. Similar observation was previously reported for TEA-HFIP system (enhanced resolution of ONs; higher MeCN content in MP is required for ONs elution in TEA-HFIP versus TEA-acetic acid IP systems [33–35]). In addition to these published findings we observed that tertiary alkylamines (TEA and tripropylamine) are more affected by HFIP concentration than primary amines (HA, octylamine). In contrast, alkylamine retention increases only modestly with ammonium acetate concentration in 10–100 mM buffer concentration range. Fig. 1 shows similar retention trends for both C18 and phenyl sorbents, but the alkylamine retention increase with HFIP concentration is more pronounced on the latter column. The retention data presented in Fig. 1 can be used to rank the ion-pairing MP efficiency. The ON retention and *n/n-x* resolution are expected to be greater for increasingly hydrophobic IP systems [28] and concentration of HFIP (assuming constant alkylamine concentration in the MP). However, the *n/n-x* separation is also affected by the ON sequence and presence of PS diastereomers.

3.1.1. The effect of stationary phase type on retention, resolution, and suppression of diastereomeric separation of PS ONs

Two reversed-phase SPs (C18 and phenyl-based) were selected to investigate the effect of SP chemistry on retention and resolution of PS ONs. Since ONs analysis benefits from bioinert environment, we also performed the experiments using Acquity Premier BEH C18 column. Premier columns have chemically modified metallic hardware that blocks the interactions between negatively charged analytes and metal surface [36]. Since these interactions occur more noticeably for >10 nt ONs, we did not notice significant differences between Premier and conventional C18 columns (pH of MP ~ 8) for unmodified (allPO) 2–6mer ONs. The results are shown in Fig. S2 in Supporting material for both acetic acid- and HFIP-based IP MP systems.

Recent reports demonstrated that phenyl column is less prone to the diastereomeric separation of tested PS ONs in comparison with C18 column [6,7]. This was also confirmed for HFIP MP by the data shown in Table S2 in Supporting material, where lower peak widths (indicating the suppression of diastereomeric separation) were observed for phenyl-based column in comparison with C18 column. However, based on the results summarized in Fig. 1 there is no significant difference in alkylamine adsorption on the SP surface between those columns. Table S2 also shows higher ONs retention observed for C18 column with acetate buffers, HFIP systems yielded relatively higher retention on phenyl-based column. This is illustrated in Fig. S3 in Supporting material on the separation of 6mer ONs with various number of PS modifications.

3.1.2. The effects of mobile phase composition on retention, resolution and diastereomeric separation of PS ONs

The potential of individual IP systems to resolve ONs differing in the length has been studied. Fig. S4 in Supporting material describes differences in retention of unmodified 6mer and 21mer in individual MPs (the percentage increase in retention between 6mer and 21mer). It can be clearly seen that differences in retention of 6mer (black column) and 21mer (grey column) increase with increasing hydrophobicity of IP reagent for both systems (acetate and HFIP), which indicates higher potential of hydrophobic IP systems to resolve ONs based on their length.

As has been reported previously [5–7,30], the choice of alkylamine has a significant impact on diastereomeric selectivity, which correlates with the amount of co-solvent fraction in the gradient. The reduction of diastereomeric separation with increasing alkylamine hydrophobicity is shown on the example of separation of allPS 2–6mer ON on Acquity UPLC BEH Phenyl column (Fig. 2). Similar trends were observed also for C18 columns (Fig. S5 in Supporting material).

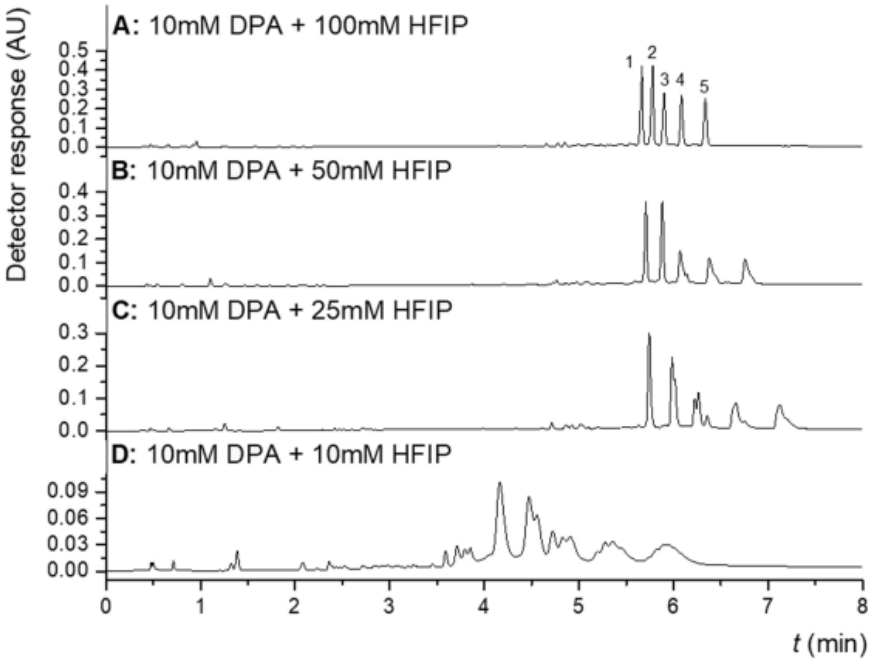

Fig. 4. The effect of HFIP concentration on suppression of diastereomeric separation. Gradient conditions: 0–20 min => 3–43 % MP A; MP A contains 10 mM dipropylamine + 10/25/50/100 mM HFIP in MeCN/water, 50/50 (*v*/*v*). MP B is fully aqueous with the same IP reagent concentration. Column: Acquity UPLC BEH C18. 21mer ONs: 1: allPO; 2: 1PS5; 3: 2PS5; 4: 2PS35; 5: 2PScenter35. Temperature: 60 °C.

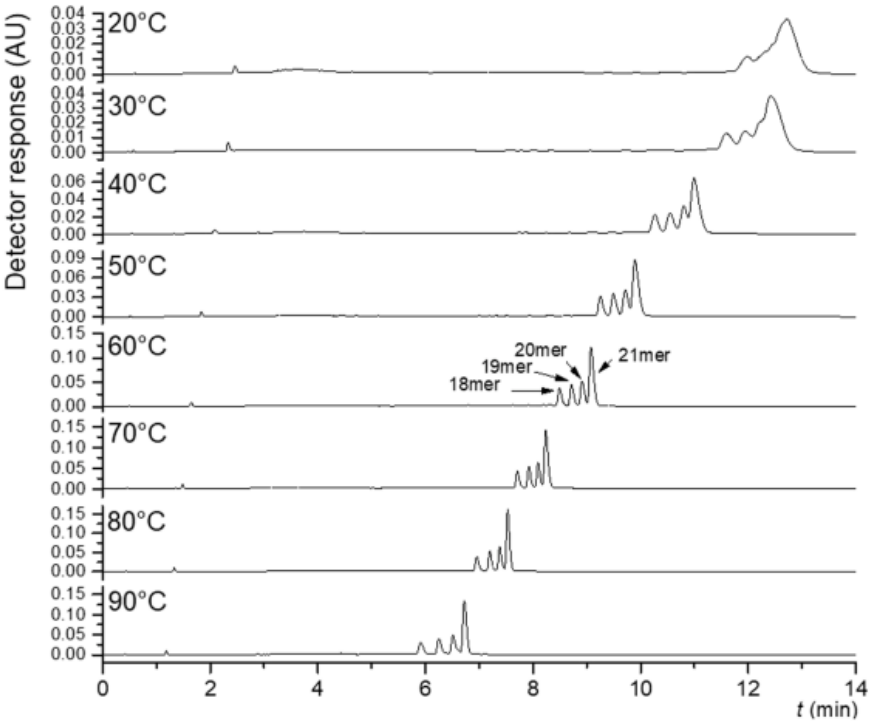

Fig. 5. Effect of temperature on resolution of *n* (fully modified allPS 21mer) and *n-x* mers (ONs shortened at 5' end about 1, 2 or 3 nucleotides, ie. *x* = *1, 2, 3*). Gradient conditions: 0–20 min => 0–40 % MP A; MP A contains 5 mM triethylamine + 50 mM HFIP in MeCN/water, 50/50 (*v*/*v*). MP B is fully aqueous with the same IP reagent concentration. Column: Acquity Premier BEH C18. Data for 60 °C have been previously published in [5].

In addition to the choice of alkylamine, the separation of diastereomers is affected also by the choice of counterion (acetate vs. HFIP). As previously reported [5,22], the HFIP-based IP MPs are more useful for suppression of diastereomeric separation of PS ONs. This is demonstrated on the example of 6mer ONs with 0–5 PS modifications in Fig. 3. Similar trends were observed for various 21mer ONs with different number and position of PS modifications (see Table S3 in Supporting material). Fig. 3 shows that the suppression of

diastereomeric separation is enhanced when using HFIP buffers compared to acetates, but it is not complete.

The choice of gradient conditions has also significant effect on diastereomeric separation of PS ONs. It is clearly visible on the example of 10 mM HAA MP in Fig. S6 in Supporting material. While in the case of a longer analysis due to the higher proportion of aqueous buffer in the MP at the beginning of the gradient, separation of diastereomers/impurities occurs, with an increase in the amount of MeCN in the MP at the start of the gradient, it is possible to achieve very fast analysis and narrow peaks.

3.1.3. The effects of buffer concentration on retention, resolution and suppression of diastereomeric separation of PS ONs

In addition to concentration of IP alkylamines in the MP, the concentration of counter ion (acetate or HFIP) can also affect the IP retention mechanism. Fig. 1 shows that the increase in HFIP concentration leads to greater adsorption of the IP reagent on RP SP, which results in higher suppression of diastereomeric separation. The effect of HFIP concentration on diastereomeric separation is illustrated in Fig. 4 for DPA-HFIP system (DPA concentration was kept constant). The same trend, i.e. increasing suppression of diastereomeric separation with increasing HFIP concentration, was reproduced also for TEA-HFIP system. For highly hydrophobic HA system we were not able to obtain the results with 100 mM HFIP concentration because of the baseline noise (Fig. S7 in Supporting material). This is probably due to a poor miscibility of HFIP MPs with high concentrations of MeCN.

3.1.4. The effects of temperature on retention, resolution and suppression of diastereomeric separation of PS ONs

A recent report investigated the effects of column temperature on diastereomers selectivity of PS ONs from both theoretical and experimental point of view [27]. In our previous work we showed that increased column temperature enhances the *n* and *n-1* resolution in IP systems containing acetic acid [29], primarily due to peak width reduction of PS ONs (suppression of diastereomeric resolution). In the present work we expanded the experiment to HFIP buffers at temperature range 10–90 °C. Fig. 5 shows the chromatographic behaviour of allPS 21mer, 20mer, 19mer and 18mer ONs test mixture in TEA-HFIP MP. The peak broadening observed at lower temperatures (20–30 °C) leading to loss of *n* and *n-x* ON resolution is presumably due to diastereomeric separation. High temperature separation conditions reduced the peak widths (diastereomeric separation) and provided an overall better resolution of 18–21mer PS ONs.

The example of separation of 21mer ONs with various number of PS modifications is shown in Fig. S8 in Supporting material. System TEA-HFIP at 90 °C lost the ability to resolve individual ONs based on number of PS modifications; this is probably related to the lower resolution power of this system [5], and low retention. Similar trends were observed for phenyl-based column (see Table S4 in Supporting material).

4. Conclusion

In this study we investigated the effect of counterion (acetate vs. HFIP) on the adsorption of selected alkylamines on the octadecyl- and phenyl-based SPs. Alkylamine ion-pairing reagent adsorption on SP (IP reagent hydrophobicity), its concentration and the counterion buffer concentration had impact on the retention and separation of PS ONs. The (undesirable) resolution of multiple PS ONs diastereomers leads to peak broadening, which lowers the achievable *n/n-x* oligonucleotide separation. The experiments with three IP alkylamines (TEA, DPA, HA) and two counterions (acetate, HFIP) illustrate that hydrophobic IP reagents and HFIP mobile phase are better suited for PS ON's analysis, if the suppression of diastereomeric separation is desired. This effect was observed for both ONs: i) 21mers, which are typical length of therapeutic ONs, and ii) shortmers, i.e. 2–6mers, which are potential metabolites of therapeutic ONs. The higher column temperature was shown to reduce the separation of diastereomers.

While the nature and concentration of alkylamine IP reagents impact on ONs separation was investigated previously, the impact of counterion on retention, diastereomer separation, and resolution of PS ONs was not systematically studied, yet. We observed that the replacement of acetate with HFIP in MP promotes the adsorption of alkylamines on the SP. HFIP-based MPs provided narrower peaks by suppressing the chromatographic resolution of PS ONs diastereomers, especially at elevated HFIP concentrations. These observations confirmed previous report that hydrophobic alkylamines (DBA, HAA) suppress the diastereomeric separation more efficiently than hydrophilic alkylamines (TEA, DPA), and the separation of PS ONs benefits from elevated temperature for both acetate and HFIP-based IP systems. The described effects for tested ONs were similar for octadecyl- and phenyl-based columns.

This research did not receive any specific grant from funding agencies in the public, commercial, or not-for profit sectors.

CRediT authorship contribution statement

Zuzana Vosáhlová: Writing – review & editing, Writing – original draft, Methodology, Investigation, Data curation, Conceptualization. **Martin Gilar:** Writing – review & editing, Writing – original draft, Methodology, Conceptualization. **Květa Kalíková:** Writing – review & editing, Writing – original draft, Visualization, Supervision, Methodology, Conceptualization.

Declaration of competing interest

The authors declare that they have no known competing financial interests or personal relationships that could have appeared to influence the work reported in this paper.

Data availability

Data will be made available on request.

Supplementary materials

Supplementary material associated with this article can be found, in the online version, at doi:10.1016/j.chroma.2024.465074.

References

[1] D. Al Shaer, O. Al Musaimi, F. Albericio, B.G. de la Torre, 2023 FDA TIDES (peptides and oligonucleotides) harvest, Pharmaceuticals 17 (2024) 243, https://doi.org/10.3390/ph17020243.
[2] F. Eckstein, Phosphorothioates, essential components of therapeutic oligonucleotides, Nucleic Acid Ther. 24 (2014) 374–387, https://doi.org/10.1089/nat.2014.0506.
[3] T. Fornstedt, M. Enmark, Separation of therapeutic oligonucleotides using ion-pair reversed-phase chromatography based on fundamental separation science, J. Chromatogr. Open 3 (2023) 100079, https://doi.org/10.1016/j.jcoa.2023.100079.
[4] W.J. Stec, G. Zon, B. Uznański, Reversed-phase high-performance liquid chromatographic separation of diastereomeric phosphorothioate analogues of oligodeoxyribonucleotides and other backbone-modified congeners of dna, J. Chromatogr. A 326 (1985) 263–280, https://doi.org/10.1016/S0021-9673(01)87452-5.
[5] Z. Kadlecová, K. Kalíková, E. Tesařová, M. Gilar, Phosphorothioate oligonucleotides separation in ion-pairing reversed-phase liquid chromatography: effect of ion-pairing system, J. Chromatogr. A 1676 (2022) 463201, https://doi.org/10.1016/j.chroma.2022.463201.
[6] M. Enmark, J. Bagge, J. Samuelsson, L. Thunberg, E. Örnskov, H. Leek, F. Limé, T. Fornstedt, Analytical and preparative separation of phosphorothioated oligonucleotides: columns and ion-pair reagents, Anal. Bioanal. Chem. 412 (2020) 299–309, https://doi.org/10.1007/s00216-019-02236-9.
[7] M. Enmark, M. Rova, J. Samuelsson, E. Örnskov, F. Schweikart, T. Fornstedt, Investigation of factors influencing the separation of diastereomers of phosphorothioated oligonucleotides, Anal. Bioanal. Chem. 411 (2019) 3383–3394, https://doi.org/10.1007/s00216-019-01813-2.

[8] B. Hu, L. Zhong, Y. Weng, L. Peng, Y. Huang, Y. Zhao, X.J. Liang, Therapeutic siRNA: state of the art, Signal Transduct. Target. Ther. 5 (2020) 1–25, https://doi.org/10.1038/s41392-020-0207-x.
[9] P. Yogendrarajah, I. Suarez Marina, W. Verluyten, E. Dejaegere, L. Napoletano, J. P. Boon, M. Hellings, M. Gilar, Analysis of siRNA with denaturing and non-denaturing ion-pair reversed-phase liquid chromatography methods, LCGC North Am. 41 (2023) 60–66.
[10] M. Gilar, A. Belenky, Y. Budman, D.L. Smisek, A.S. Cohen, Study of phosphorothioate-modified oligonucleotide resistance to 3′-exonuclease using capillary electrophoresis, J. Chromatogr. B Biomed. Sci. Appl. 714 (1998) 13–20, https://doi.org/10.1016/S0378-4347(98)00160-1.
[11] J.R. Thayer, V. Barreto, S. Rao, C. Pohl, Control of oligonucleotide retention on a pH-stabilized strong anion exchange column, Anal. Biochem. 338 (2005) 39–47, https://doi.org/10.1016/j.ab.2004.11.013.
[12] K. Kawamura, Y. Maruoka, HPLC retention behavior of oligonucleotides on an anion-exchange HPLC with a high concentration of urea, Chromatographia 87 (2024) 17–25, https://doi.org/10.1007/s10337-023-04291-y.
[13] G.S. Srivatsa, P. Klopchin, M. Batt, M. Feldman, R.H. Carlson, D.L. Cole, Selectivity of anion exchange chromatography and capillary gel electrophoresis for the analysis of phosphorothioate oligonucleotides1Presented at the Well Characterized Biotechnology Pharmaceuticals Meeting in San Francisco, 6–8 January 1997.1, J. Pharm. Biomed. Anal. 16 (1997) 619–630, https://doi.org/10.1016/S0731-7085(97)00180-5.
[14] A. Goyon, P. Yehl, K. Zhang, Characterization of therapeutic oligonucleotides by liquid chromatography, J. Pharm. Biomed. Anal. 182 (2020) 113105, https://doi.org/10.1016/j.jpba.2020.113105.
[15] Z. Vosáhlová, K. Kalíková, M. Gilar, J. Szymarek, M. Mazurkiewicz-Bełdzińska, S. Studzińska, Hydrophilic interaction liquid chromatography with mass spectrometry for the separation and identification of antisense oligonucleotides impurities and nusinersen metabolites, J. Chromatogr. A 1713 (2024) 464535, https://doi.org/10.1016/j.chroma.2023.464535.
[16] A.J. Alpert, Hydrophilic-interaction chromatography for the separation of peptides, nucleic acids and other polar compounds, J. Chromatogr. A 499 (1990) 177–196, https://doi.org/10.1016/S0021-9673(00)96972-3.
[17] A. Goyon, M.S. Blevins, J.G. Napolitano, D. Nguyen, M. Goel, B. Scott, J. Wang, S. G. Koenig, T. Chen, K. Zhang, Characterization of antisense oligonucleotide and guide ribonucleic acid diastereomers by hydrophilic interaction liquid chromatography coupled to mass spectrometry, J. Chromatogr. A 1708 (2023) 464327, https://doi.org/10.1016/j.chroma.2023.464327.
[18] M. Gilar, B.M. Koshel, R.E. Birdsall, Ion-pair reversed-phase and hydrophilic interaction chromatography methods for analysis of phosphorothioate oligonucleotides, J. Chromatogr. A 1712 (2023) 464475, https://doi.org/10.1016/j.chroma.2023.464475.
[19] M. Enmark, J. Häggström, J. Samuelsson, T. Fornstedt, Building machine-learning-based models for retention time and resolution predictions in ion pair chromatography of oligonucleotides, J. Chromatogr. A 1671 (2022) 462999, https://doi.org/10.1016/j.chroma.2022.462999.
[20] M. Enmark, J. Samuelsson, T. Fornstedt, Development of a unified gradient theory for ion-pair chromatography using oligonucleotide separations as a model case, J. Chromatogr. A 1691 (2023) 463823, https://doi.org/10.1016/j.chroma.2023.463823.
[21] M. Leśko, K. Kaczmarski, M. Jora, K. Stavenhagen, T. Leek, W. Czechtizky, T. Fornstedt, J. Samuelsson, Strategies for predictive modeling of overloaded oligonucleotide elution profiles in ion-pair chromatography, J. Chromatogr. A 1711 (2023) 464446, https://doi.org/10.1016/j.chroma.2023.464446.
[22] B. Basiri, H. van Hattum, W.D. van Dongen, M.M. Murph, M.G. Bartlett, The role of fluorinated alcohols as mobile phase modifiers for LC-MS analysis of oligonucleotides, J. Am. Soc. Mass Spectrome. 28 (2017) 190–199, https://doi.org/10.1007/s13361-016-1500-3.
[23] M. Holčapek, K. Volná, P. Jandera, L. Kolářová, K. Lemr, M. Exner, A. Církva, Effects of ion-pairing reagents on the electrospray signal suppression of sulphonated dyes and intermediates, J. Mass Spectrom. 39 (2004) 43–50, https://doi.org/10.1002/jms.551.
[24] K. Guo, J. Peng, R. Zhou, L. Li, Ion-pairing reversed-phase liquid chromatography fractionation in combination with isotope labeling reversed-phase liquid chromatography–mass spectrometry for comprehensive metabolome profiling, J. Chromatogr. A 1218 (2011) 3689–3694, https://doi.org/10.1016/j.chroma.2011.04.024.
[25] A. Apffel, J.A. Chakel, S. Fischer, K. Lichtenwalter, W.S. Hancock, Analysis of oligonucleotides by HPLC–electrospray ionization mass spectrometry, Anal. Chem. 69 (1997) 1320–1325, https://doi.org/10.1021/ac960916h.
[26] A. Apffel, J.A. Chakel, S. Fischer, K. Lichtenwalter, W.S. Hancock, New procedure for the use of high-performance liquid chromatography–electrospray ionization mass spectrometry for the analysis of nucleotides and oligonucleotides, J. Chromatogr. A 777 (1997) 3–21, https://doi.org/10.1016/S0021-9673(97)00256-2.
[27] L. Guo, A.J. Worth, C. Mesaros, N.W. Snyder, J.D. Glickson, I.A. Blair, Diisopropylethylamine/hexafluoroisopropanol-mediated ion-pairing ultra-high-performance liquid chromatography/mass spectrometry for phosphate and carboxylate metabolite analysis: utility for studying cellular metabolism, Rapid Commun. Mass Spectrom. 30 (2016) 1835–1845, https://doi.org/10.1002/rcm.7667.
[28] M. Donegan, J.M. Nguyen, M. Gilar, Effect of ion-pairing reagent hydrophobicity on liquid chromatography and mass spectrometry analysis of oligonucleotides, J. Chromatogr. A 1666 (2022) 462860, https://doi.org/10.1016/j.chroma.2022.462860.
[29] Z. Kadlecová, K. Kalíková, E. Tesařová, M. Gilar, Phosphorothioate oligonucleotides separation in ion-pairing reversed-phase liquid chromatography: effect of temperature, J. Chromatogr. A 1681 (2022) 463473, https://doi.org/10.1016/j.chroma.2022.463473.
[30] M. Enmark, S. Harun, J. Samuelsson, E. Örnskov, L. Thunberg, A. Dahlén, T. Fornstedt, Selectivity limits of and opportunities for ion pair chromatographic separation of oligonucleotides, J. Chromatogr. A 1651 (2021) 462269, https://doi.org/10.1016/j.chroma.2021.462269.
[31] M.G. Bartlett, S. Omuro, Evaluation of alkylamines and stationary phases to improve LC–MS of oligonucleotides, Biomed. Chromatogr. 35 (2021) e5045, https://doi.org/10.1002/bmc.5045.
[32] S. Studzińska, S. Bocian, L. Siecińska, B. Buszewski, Application of phenyl-based stationary phases for the study of retention and separation of oligonucleotides, J. Chromatogr. B 1060 (2017) 36–43, https://doi.org/10.1016/j.jchromb.2017.05.033.
[33] K.J. Fountain, M. Gilar, J.C. Gebler, Analysis of native and chemically modified oligonucleotides by tandem ion-pair reversed-phase high-performance liquid chromatography/electrospray ionization mass spectrometry, Rapid Communications in Mass Spectrometry 17 (2003) 646–653, https://doi.org/10.1002/rcm.959.
[34] N. Li, N.M. El Zahar, J.G. Saad, E.R.E. van der Hage, M.G. Bartlett, Alkylamine ion-pairing reagents and the chromatographic separation of oligonucleotides, J. Chromatogr. A 1580 (2018) 110–119, https://doi.org/10.1016/j.chroma.2018.10.040.
[35] M. Gilar, K.J. Fountain, Y. Budman, J.L. Holyoke, H. Davoudi, J.C. Gebler, Characterization of therapeutic oligonucleotides using liquid chromatography with on-line mass spectrometry detection, Oligonucleotides. 13 (2003) 229–243, https://doi.org/10.1089/154545703322460612.
[36] P. Bigos, MaxPeak premier solutions: improving consumer safety through innovative science, (2024) (on-line available on https://www.waters.com/webassets/cms/library/docs/720008054en.pdf).

Publikace IX

Phosphorothioate oligonucleotides separation in ion-pairing reversed-phase liquid chromatography: Effect of temperature

Kadlecová, Z., Kalíková, K., Tesařová, E., Gilar, M.
Journal of Chromatography A, **2022**, *1681*, 463473.

Journal of Chromatography A 1681 (2022) 463473

Contents lists available at ScienceDirect

Journal of Chromatography A

journal homepage: www.elsevier.com/locate/chroma

Phosphorothioate oligonucleotides separation in ion-pairing reversed-phase liquid chromatography: effect of temperature

Zuzana Kadlecová[a], Květa Kalíková[a,*], Eva Tesařová[a], Martin Gilar[b,**]

[a] Department of Physical and Macromolecular Chemistry, Faculty of Science, Charles University, Hlavova 8, 12800, Prague, Czech Republic
[b] Waters Corporation, 34 Maple Street, Milford, MA 01757, United States of America

ARTICLE INFO

Article history:
Received 21 July 2022
Revised 27 August 2022
Accepted 1 September 2022
Available online 7 September 2022

Keywords:
Phosphorothioate oligonucleotides
Ion-pairing reversed-phase chromatography
Diastereomeric separation
Temperature
Resolution

ABSTRACT

Analysis of diastereomers of phosphorothioate oligonucleotides in ion-pairing reversed-phase liquid chromatography is affected not only by the character and concentration of ion-pairing system, but also by the separation temperature. In this work, eight ion-pairing systems at two concentrations buffered with acetic acid were used with octadecyl column to investigate the effects of temperature (in the range from 20 °C to 90 °C) on retention, diastereomeric separation, resolution of mers of different length and resolution of oligonucleotides with different number of phosphorothioate linkages. It was observed that elevated temperature suppresses the diastereomeric separation and oligonucleotide peaks become narrower. This improves the resolution of *n* and *n*-1 mers at elevated temperature. Plots of ln *k* (*k* = retention factor) versus reciprocal absolute temperature show that for 100 mM ion-pairing systems the increase in temperature does not lead to simple decrease in oligonucleotides retention as generally observed in reversed-phase liquid chromatography. The aim of this work is to improve chromatographic method for analysis of phosphorothioate oligonucleotides.

1. Introduction

Phosphorothioation is one of the most common modification of oligonucleotides (ONs) utilized to minimize their *in-vivo* enzymatic degradation [1]. While the phosphorothioate (PS) modification increases *in-vivo* stability of ONs, it also makes their chromatographic analysis more challenging due to the formation of diastereomers. The presence of multiple potentially separable isomers may cause broadening of chromatographic peaks and complicate the ONs analysis. For this reason, the suppression of diastereomeric separation can be beneficial for the resolution of the target peak from the shorter ON impurities [2,3].

It has been shown that ion-pairing (IP) system nature and concentration have strong impact on ONs chromatographic analysis (see our previous work [4] and other reports [2,5–7]). The effect of IP system choice on PS ONs separation was investigated recently [8–10]. The diastereomeric separation is promoted with hydrophilic IP systems and suppressed with hydrophobic IP alkylamines [4,11]. IP mobile phases (MPs) buffered with hexafluoroisopropanol are suitable for PS ON separations and for liquid chromatography (LC) coupled with mass spectrometry (MS) applications [7,12–15]. Despite of significant number of studies, the separation temperature has been so far overlooked as a parameter for optimization of PS ONs analysis [16].

Generally, column temperature has an impact on retention, selectivity, resolution, peak shape and efficiency. Using elevated temperature in LC analysis of ONs offers several benefits, such as increased efficiency, lower backpressure, and faster analysis [17,18].

The most commonly used column temperature for the chromatographic analysis of RNA and DNA-based ONs is 60 °C [2,19,20]. Occasionally even higher temperature is required to eliminate secondary ONs structures due to formation of homoduplex loops such as hairpins or intermolecular complexes such as G-quadruplexes [21,22] which complicate chromatographic analysis. The elevated temperature minimizes the undesirable secondary structure effects on ONs retention and peak shape [23].

Although the temperature is an important parameter of the chromatographic analysis of ONs, no comprehensive study of its effects on PS ONs diastereomeric separation has been published yet. The goal of this work is to investigate the effects of separation temperature on (i) retention, (ii) diastereomeric resolution, (iii) resolution of *n* and *n-1, n-2*... short-mers, and (iv) resolu-

* Corresponding author at: Department of Physical and Macromolecular Chemistry, Faculty of Science, Charles University, Hlavova 8, 12800, Prague, Czech Republic.
** Corresponding author at: Waters Corporation, 34 Maple Street, Milford, MA 01757, USA.
E-mail addresses: kalikova@natur.cuni.cz (K. Kalíková), Martin_Gilar@waters.com (M. Gilar).

https://doi.org/10.1016/j.chroma.2022.463473
0021-9673/

Table 1
The list of all tested ONs, their sequence, number of PS linkages and number of diastereomers.

Name	Sequence	Number of PS linkages	Number of diastereomers
21mers			
allPO	5′-TTT TAG CAT TTT TAC GAT TTT-3′	0	0
1PS3′	5′-TTT TAG CAT TTT TAC GAT TT*T-3′	1	2
1PS5′	5′-T*TT TAG CAT TTT TAC GAT TTT-3′	1	2
1PScenter	5′-TTT TAG CAT T*TT TAC GAT TTT-3′	1	2
2PS3′	5′-TTT TAG CAT TTT TAC GAT T*T*T-3′	2	4
2PS5′	5′-T*T*T TAG CAT TTT TAC GAT TTT-3′	2	4
2PScenter	5′-TTT TAG CAT T*T*T TAC GAT TTT-3′	2	4
1PS3ž′	5′-T*TT TAG CAT TTT TAC GAT TT*T-3′	2	4
2PS3ž′	5′-T*T*T TAG CAT TTT TAC GAT T*T*T-3′	4	16
2PS3žčenter	5′-T*T*T TAG CAT T*T*T TAC GAT T*T*T-3′	6	64
allPS	5′-T*T*T * T*A*G * C*A*T * T*T*T * T*A*C * G*A*T * T*T*T-3′	20	1 048 576
20mers			
allPS *n*-1	5′-T*T * T*A*G * C*A*T * T*T*T * T*A*C * G*A*T * T*T*T-3′	19	524 288
1PScenter *n*-1	5′-TT TAG CAT T*TT TAC GAT TTT-3′	1	2
19mer			
allPS *n*-2	5′-T*T*A*G * C*A*T * T*T*T * T*A*C * G*A*T * T*T*T-3′	18	262 144
18mer			
allPS *n*-3	5′-T*A*G * C*A*T * T*T*T * T*A*C * G*A*T * T*T*T-3′	17	131 072

*denotes phosphorothioate linkage.

tion of ONs with various number of PS modifications. Obtained results can serve as guidelines for chromatographic method development in laboratories pursuing the analysis of therapeutic PS ONs.

2. Experimental section

2.1. Materials and reagents

Acetonitrile (ACN, Chromasolv® gradient grade, for HPLC, ≥ 99.9%), ammonium hydroxide solution (28.0–30.0% NH_3), diethylamine (purity ≥ 99.5%), triethylamine (purity ≥ 99%), diisopropylamine (purity ≥ 99.5%), dipropylamine (purity 99%), hexylamine (purity 99%), dibutylamine (purity ≥ 99.5%), octylamine (purity 99%), dihexylamine (purity 97%), and acetic acid (purity ≥ 99%) were purchased from Sigma-Aldrich (St. Louis, USA). The list of 21mer ONs synthetized by Integrated DNA Technologies (Coralville, USA) with their sequences and PS linkage positions is given in Table 1. Table 1 shows also the sequences of the shorter mers, i.e. 20mers, 19mer and 18mer, sequences analogous to allPS and 1PScenter ON, but truncated at 5′terminus by 1, 2, and 3 nucleobases, respectively, which were synthetized by KRD (Prague, Czech Republic). Rowapur and Ultrapur system from Watrex (Prague, Czech Republic) was used for water purification and deionization.

2.2. Instrumentation and columns

Waters Acquity UPLC H–Class system (Waters, Milford, USA) consisting of quaternary solvent manager, autosampler, column manager, and photodiode array detector was used for chromatographic measurements. Empower 3 software was used for system control, data acquisition, and results processing. Separation was performed with 50 × 2.1 mm; 1.7 μm Premier BEH C18 columns (Waters, Milford, USA). For hydrophobic alkylamines (i.e. dibutylamine, hexylamine, octylamine, dihexylamine) one column per each alkylamine was used to avoid lengthy re-equilibration of columns with different alkylamines. For the investigation whether the obtained temperature trends are valid also for different C18 column, the column XBridge C18 (50 × 2.1 mm; 2.5 μm; Waters, Milford, USA) was tested under one condition (100 mM triethylammonium acetate, whole temperature range) and results were compared (see Figs. S1-S3 in Supporting material).

2.3. Experimental procedures

ONs stock solutions (concentration 50 pmol μL^{-1}) were prepared by dissolving the ONs in deionized water. Gradient elution was used for all measurements. Aqueous MP B with 10 mM or 100 mM concentration of alkylamine were buffered with acetic acid to pH 8.0. Ammonium acetate (AmAc) 10 mM or 100 mM MPs B were prepared by dissolving AmAc in water and adjusted to pH 8.0 with ammonium hydroxide solution (this MP does not contain alkylamines). MP A was composed of ACN/water 80/20 (*w*/*w*) with addition of the same amount of alkylamine and acetic acid as in MP B to maintain the same buffer concentrations. MP composed of AmAc, ratio ACN/water 20/80 (*w*/*w*) was used to maintain the solubility of ammonium acetate. For experiments with various IP systems, different initial MP conditions were used, but the gradient slope was always 1% ACN per minute. Following IP systems were investigated: diethylammonium acetate (DEAA), triethylammonium acetate (TEAA), diisopropylammonium acetate (DIPAA), dipropylammonium acetate (DPAA), dibutylammonium acetate (DBAA), hexylammonium acetate (HAA), octylammonium acetate (OAA), and dihexylammonium acetate (DHAA). For the description of MPs and gradients used see Table S1, Supporting material. All MPs were filtered with 0.45 µm nylon membrane filters (Whatman, GE Healthcare, Chicago, USA) before use. Flow rate was 0.4 mL min^{-1}, injection volume was 1 μL. The first system peak was used as a column void time marker. Individual measurements were repeated three times. Based on the UV-spectra measurements, the detection wavelength was set at 260 nm. Column temperature effect on separation was investigated in range 20 °C to 90 °C with 10 °C increments. Sample temperature was 10 °C for all measurements.

2.4. Selection of conditions

All MPs were prepared with pH 8.0 to ensure that (thio)phosphate groups of ONs are negatively charged and thus available for electrostatic interaction with positively charged IP agents adsorbed on the hydrophobic surface of C18 stationary phase. MPs A and B were prepared in all cases such that the concentration of IP reagent during the gradient elution remains constant. Initial gradient ACN concentrations were chosen to ensure that the retention of ONs is approximately 10 min. 21mer PS ON (allPS), partially thioated 21 mer with PS internucleotide linkages at selected positions, and 21mer ON (denoted allPO, no PS

modification) used in the study have the same primary sequence (Table 1). This allowed us to investigate the effect of the number of PS linkages on the ONs retention and diastereomeric separation. Ammonium acetate MPs was used as reversed-phase (RP) system for comparison with IP RP LC systems. Experimental temperature range was limited by the column heater module used in this study.

3. Results and discussion

3.1. Effect of temperature on retention

IP RP LC has been described as mixed-mode chromatography where both hydrophobic and ionic interactions participate in separation [11]. The relationship between ln k and inverse temperature $1/T$ in RP LC is expected to be linear [24]. However, we observed that in IP RP LC the ln k versus $1/T$ relationship is more complex (Fig. 1) and strongly non-linear for all investigated IP systems. The retention data in Fig. 1 for 1PS3ž' oligonucleotide were successfully fitted by second-degree polynomial fit. Another observation in Fig. 1 is that ON retention (ln k) is greater for 100 mM compared to 10 mM IP system, where the contribution of IP retention mode is weaker. The retention loss at elevated temperature is more apparent for 10 mM experiments; this is evident from the steeper raise of the relationship (red line), and for weak IP systems (DEAA, TEAA);for additional data see Tables S2 – S10, Supporting material. For relatively strong IP systems (DBAA, HAA, OAA and DHAA at 100 mM concentration) we observed a retention increase with temperature at the low end of experimental temperature (20 °C); the retention maxima marked by arrow in Fig. 1 were observed close to 30 °C (see also Tables S4, S5 and S10, Supporting material). Interpretation of these observations are not straight forward. The retention in IP RP LC depends on hydrophobic retention of ONs with C18 SP, adsorption of charged IP reagents on C18 surface, that in turn provides electrostatic interactions with ONs phosphate backbone. All three "interactions" are impacted by separation temperature. While the electrostatic retention forces are enhanced at elevated temperature [25], hydrophobic adsorption strength of both ON and IP reagent on C18 surface declines with temperature, counteracting the gains in ionic retention.

Additional data for retention behavior temperature effects for two oligonucleotides are provided as Fig. S4 in Supporting material.

3.2. Effect of temperature on diastereomeric separation

Fig. 2 demonstrates a significant effect of column temperature on diastereomeric separation for 2PS3žćenter oligonucleotide analyzed with 100 mM TEAA system. The separation of diastereomers is clearly suppressed at elevated temperature, and therefore the overall peak width decreases. Additional data for all PS ONs samples and all investigated IP systems show similar trends (see Tables S3-S10 in Supporting material). As reported in our previous study [4], the separation of diastereomers is most pronounced for AmAc (non-IP MP), very weak DEAA, and weak TEAA IP systems (only TEAA system is shown in Fig. 2). Despite of this trend the separation of diastereomers can be effectively suppressed at 90 °C, at least for the 2PS3žćenter ON example (Fig. 2). The separation at more commonly used 60 °C temperature shows peak broadening due to partial separation of diastereomers. Fig. 2 illustrates a typical problem encountered in PS ONs method development. PS ONs peaks appear much wider than PO–ONs when applying similar LC conditions.

Fig. 2 illustrates that the separation of PS ONs, in case that the suppression of diastereomeric separation is needed, may benefit from a higher separation temperature. On the other hand, AmAc and DEAA systems have somewhat atypical different resolution trends compared to other IP systems (Fig. S5, Tables S2 and S3 in Supporting material).

In our previous work [4] we reported that separation of PS ONs diastereomers generally decreased with IP systems hydrophobicity (DEAA<TEA<DIPAA<DPAA<DBAA<HAA). The extremely hydrophobic (OAA<DHAA) alkylamines at 100 mM concentration showed a reversed trend; the PS ONs peaks became somewhat broader again. In the current study we aim to investigate the impact of IP systems in conjunction with separation temperature (20–90 °C). The retention data, peak widths, and resolution of diastereomers for samples

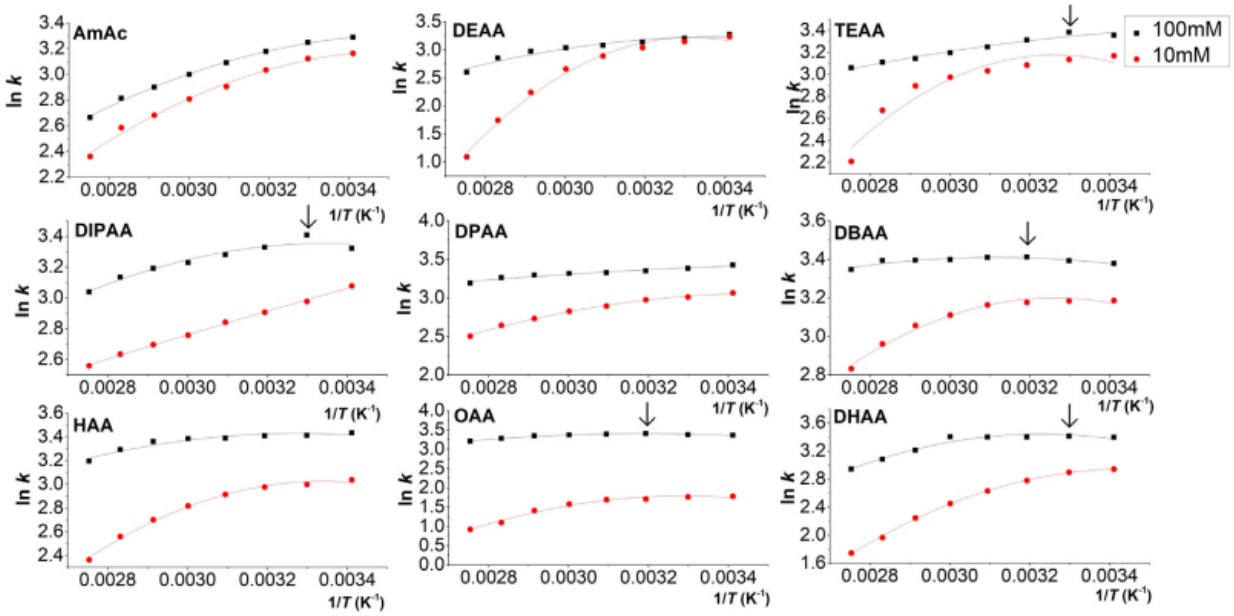

Fig. 1. Dependence of ln k on $1/T$ for all tested MPs for 1PS3žÓN. For gradient conditions for each IP system see Table S1 in Supporting material. Black squares – 100 mM buffers; red circles – 10 mM buffers.

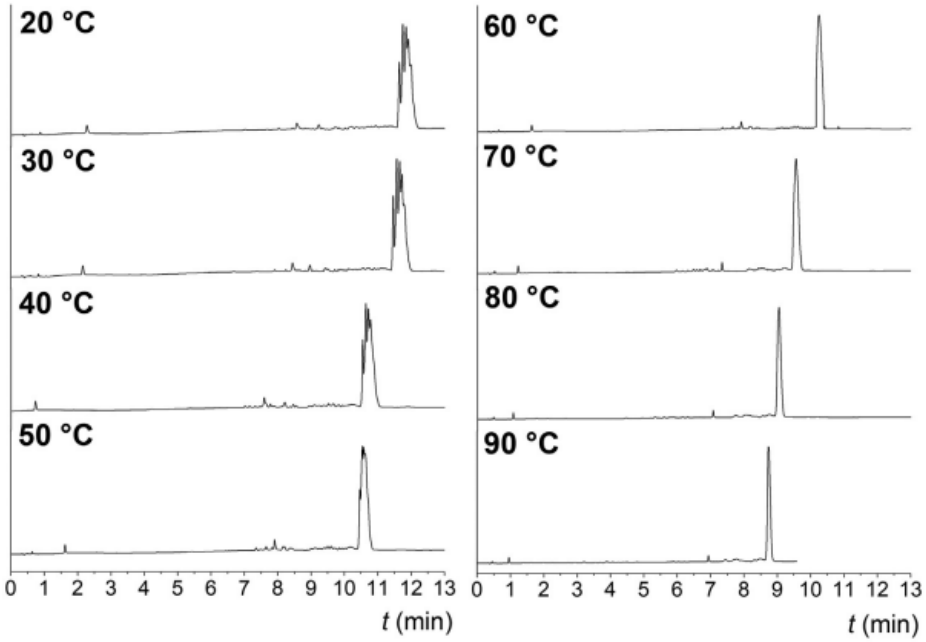

Fig. 2. Effect of temperature from 20 °C to 90 °C on diastereomeric separation of 2PS3žčenter ON. IP system: 100 mM TEAA. For gradient conditions see Table S1 in Supporting material.

specified in Table 1 are summarized in Tables S2-S10, Supporting material. In summary, moderately hydrophobic IP systems (DPAA, DBAA, HAA) and elevated temperatures (60–90 °C) are preferred choice for separation of PS ONs when the goal is to suppress the diastereomeric separation.

While the impact of temperature shown in Fig. 2 and in supplemental Tables S2-S10 is compelling, the separation goal in ONs analysis is not to reduce peak widths (which also depends on column efficiency, and gradient slope), but to resolve the full-length ON *n* from its *n-x* impurities. The impact of temperature on resolution of *n* and *n*-1 (*n-x*) for selected PS ONs will be discussed in the next section.

Additional data illustrating the effect of temperature, IP agent character and concentration on peak width for allPO and allPS oligonucleotides are shown in Fig. S6-A and S6-B in Supporting material.

3.3. Effects of temperature on resolution of n and n-x mers

Recently, we reported that resolution of *n* and *n*-1 mers improves with concentration and hydrophobicity of IP systems in the MP [4,11]. However, the effect of separation temperature was not studied. The data presented above suggest that temperature is crucial parameter for separation success of PS ONs. The peak broadening due to a resolution of diastereomers may be detrimental for separation of *n* and *n-x* species.

Fig. 3 shows the resolution of *n* and *n*-1 mers for IP systems investigated in 20 – 90 °C temperature range for allPS oligonucleotides. The resolution of *n* and *n*-1 mers increases with increasing temperature except for AmAc mobile phase and weak IP system DEAA that do not provide any resolution. The horizontal dashed line in Fig. 3 indicates a desirable value of $R \geq 1.5$ (baseline resolution). The highest resolution was obtained for DBAA in most temperature conditions. Surprisingly, moderately hydrophobic (HAA) and highly hydrophobic IP systems (OAA and DHAA) that show the highest separation performance for PO ONs [11] exhibit somewhat lower resolution between allPS and allPS *n*-1 ONs especially at low temperature (Fig. 3). This is probably due to diastereomeric resolution that leads to wider peaks and reduced resolution, in particular at low separation temperatures.

Similar trends were observed for separation of *n*/*n*-1 species of 1PScenter ON (Fig. S7); both *n* and *n*-1 samples have only two diastereomers, therefore the observed resolution is greater than for allPS species comprising of more than half million of diastereomers (Table 1).

Additional data for temperature effects on resolution of allPS 21mer, 20mer, 19mer and 18mer ONs are listed in Tables S11-S19, Supporting material. Fig. 4 shows selected chromatograms illustrating the impact of peak broadening on resolution of *n*/*n-x* species. The effect of band broadening is most significant for TEAA mobile phase at low temperature (20 °C) where no separation is achieved. High temperature (90 °C) reduced the peak widths for all IP systems and one can observe partial resolution of 18–21 mer oligonucleotides even with TEAA mobile phase. As was described earlier (also in our previous work [4]), very hydrophobic IP systems at high concentration (see 100 mM OAA in Fig. 4) promote partial diastereomeric separation. While the separation selectivity improves for HAA and OAA systems, the peak broadening reduces the resolution, most noticeably for 100 mM OAA experiment at 20 °C (Fig. 4). The peak broadening while using highly hydrophobic IP systems suggests that the participation of electrostatic interactions in the separation of diastereomers cannot be completely discounted (see our previous work [4]). The results suggest that hydrophobic IP systems offer the highest peak capacity for separation of PO ONs, but the best separation of allPS ONs is achieved with moderately hydrophobic IP agents, for example with DBAA (Fig. 3).

In the next experiment we investigated the impact of temperature on separation of 21 mer ONs of the same sequence, but with different number of PS modifications. The recent trend in design of therapeutic oligonucleotides is the minimal use of PS modifications, often just one or two PS modifications on one or both termini. The loss of PS modification due to oxidation needs to be

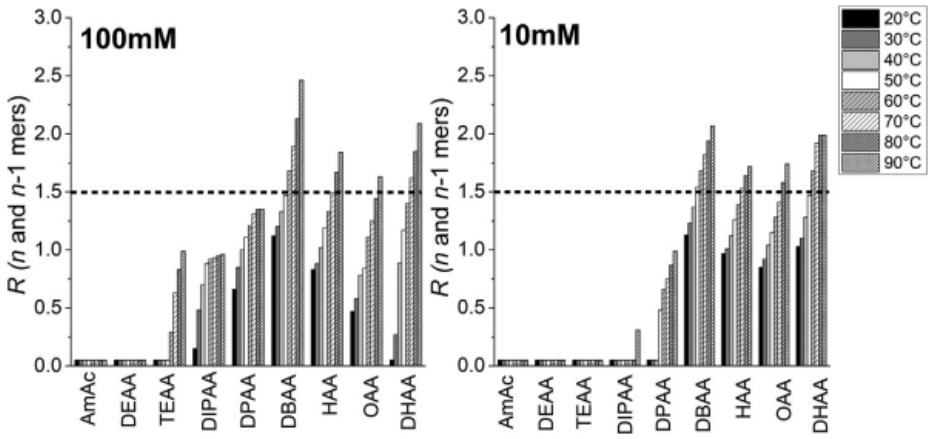

Fig. 3. Effect of temperature from 20 °C to 90 °C on resolution of allPS and allPS *n*-1. For gradient conditions for each IP system see Table S1 in Supporting material.

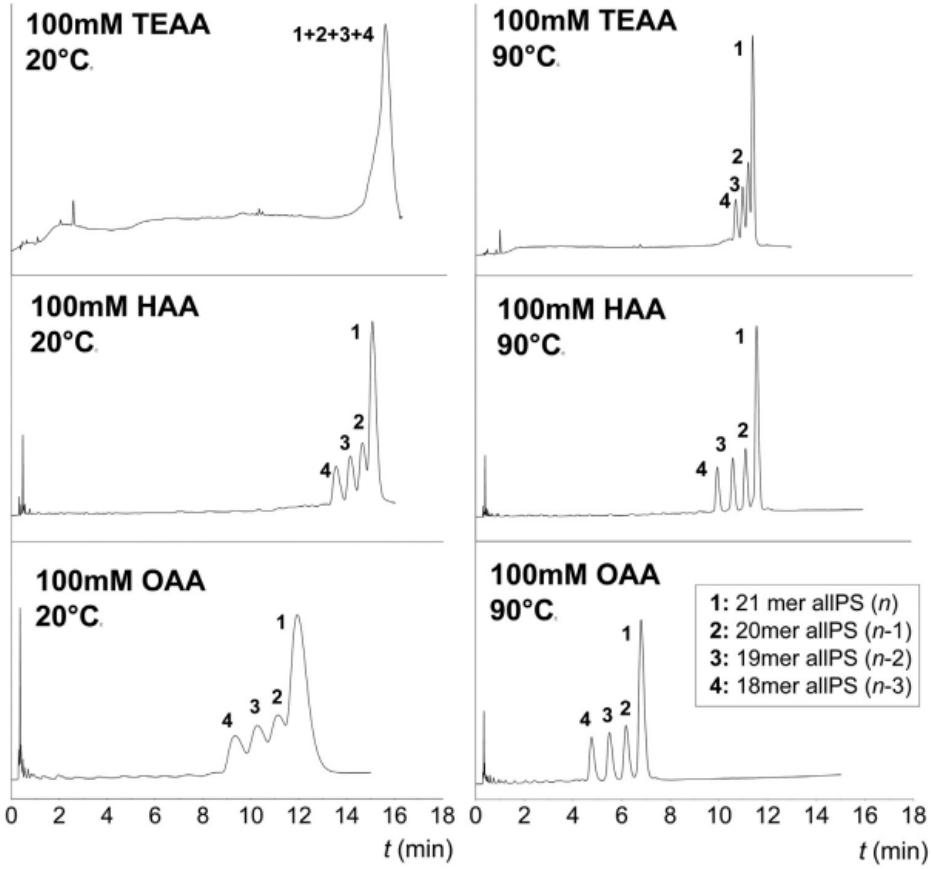

Fig. 4. Resolution of *n* and *n*-1 mer, *n*-1 and *n*-2 mer and *n*-2 and *n*-3 mer for allPS ON for selected IP systems. For gradient conditions see Table S1 in Supporting material.

tested in production quality control. Finding an IP system suitable for resolution of ONs with different number/position of PS modifications is highly desirable.

We investigated selected IP systems and temperature range for analysis of 21 mer ONs listed in Table 1. Fig. 5 shows the separation of ONs with zero (allPO), one (1PS5), two (2PS5), four (2PS3ž) and six (2PScenter3ž) phosphorothioate modifications at 20 °C and 90 °C with 100 mM mobile phases. AmAc and the weakest IP system (DEAA) enable partial diastereomeric separation at both temperatures. With multiple overlapping peaks we cannot distinguish the individual ONs. TEAA and DIPAA show partial diastereomeric separation, but the ONs are resolved into the peak groups according to number of PS modifications. All IP systems retain more strongly the oligonucleotides with greater number of PS modifications. Best resolution of the sample is achieved with DIPAA or DBAA systems at 90 °C (Fig. 5). As pointed out earlier, very hydrophobic OAA and DHAA IP systems exhibit wide peaks as the diastereomeric separation is more pronounced than with moderately hydrophobic IP systems. Table S20 in Supporting material provides detailed summary of all results.

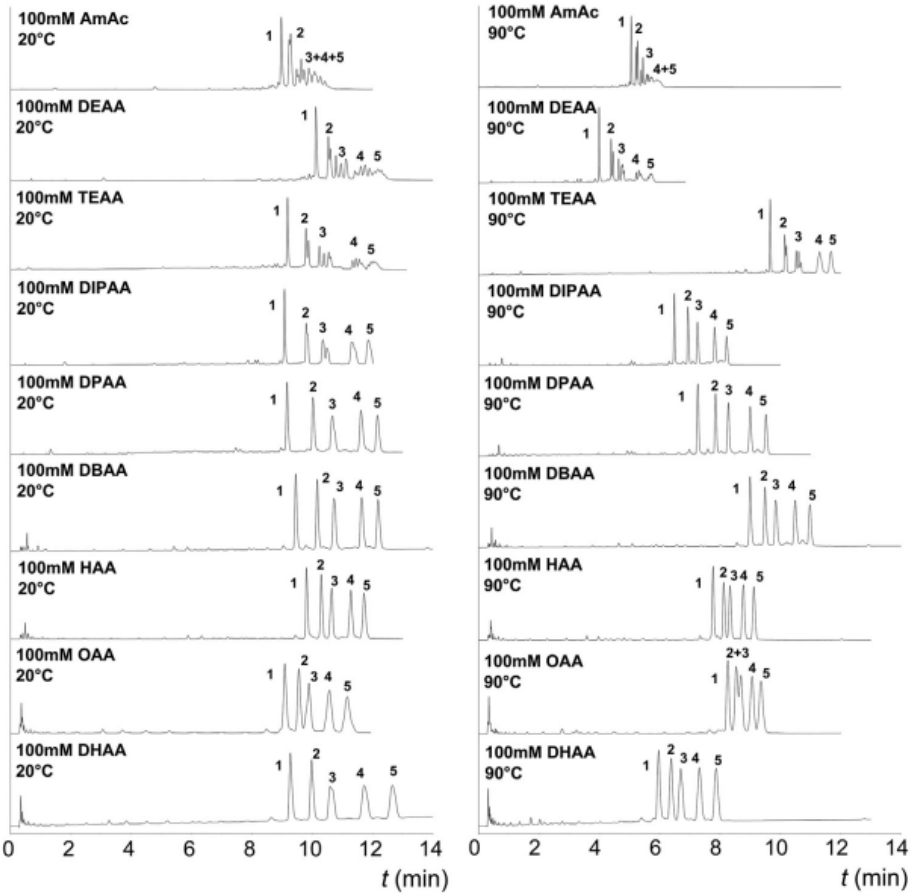

Fig. 5. Separation of 21mer ONs of the same sequence with zero (allPO - 1), one (1PS5‹ 2), two (2PS5‹ 3), four (2PS3ž‹ 4) and six (2PScenter3ž' - 5) phosphorothioate modifications. For gradient conditions see Table S1 in Supporting material.

4. Conclusion

We observed a general decrease of PS ONs peak widths with separation temperature, presumably due to reduction of hydrophobic retention component in IP RP LC. This led to suppression of diastereomeric resolution (at elevated temperature) and resulted in an improved resolution of *n* and *n-x* shorter mers. The best resolution of allPS oligonucleotides was observed with DBAA mobile phases. Highly hydrophobic IP systems (OAA, DHAA) produced relatively wide peaks for allPS ONs and other PS ONs, most noticeably at low temperatures. We speculate that the diastereomeric separation is promoted with such IP systems *via* ionic interactions, although the exact mechanism is unknown.

Separation of ONs with different number of PS modifications was achieved. The best IP systems for such application were DPAA and DBAA at elevated temperature. These moderately hydrophobic IP systems are useful for quality control of PS oligonucleotides and PS oxidation products analysis.

Overall, for the application where diastereomer separation needs to be suppressed and concurrently the resolution of *n* and *n-x* mers and resolution of ONs with various degree and position of PS modification is desired, 100 mM HAA at all temperatures seems to be the most versatile option. The suitability of individual chromatographic systems and temperatures for applications of interest are summarized in Table S20 in Supporting material.

This study provides guidelines for laboratories developing methods for analysis of PS ONs. High column temperatures in the range of 60–90 °C improve quality of PS ON's separation and are advisable despite of the expected reduction in column lifetime.

Declaration of Competing Interest

The authors declared no conflict of interest.

CRediT authorship contribution statement

Zuzana Kadlecová: Investigation, Methodology, Writing – original draft, Writing – review & editing. **Květa Kalíková:** Supervision, Methodology, Writing – original draft, Writing – review & editing, Funding acquisition. **Eva Tesařová:** Writing – review & editing. **Martin Gilar:** Conceptualization, Methodology, Resources, Writing – original draft, Writing – review & editing.

Data availability

The data are available as on-line Supporting material to the article.

Acknowledgment

The authors gratefully acknowledge the financial support of the Czech Science Foundation, grant no. 20-19655S.

Supplementary materials

Supplementary material associated with this article can be found, in the online version, at doi:10.1016/j.chroma.2022.463473.

References

[1] A. Goyon, P. Yehl, K. Zhang, Characterization of therapeutic oligonucleotides by liquid chromatography, J. Pharm. Biomed. Anal. 182 (2020) 113105, doi:10.1016/j.jpba.2020.113105.

[2] N. Li, N.M. El Zahar, J.G. Saad, E.R.E. van der Hage, M.G. Bartlett, Alkylamine ion-pairing reagents and the chromatographic separation of oligonucleotides, J. Chromatogr. A 1580 (2018) 110–119, doi:10.1016/j.chroma.2018.10.040.

[3] X. Chen, Z. Liu, L. Gong, Evaluating the interplay among stationary phases/ion-pairing reagents/sequences for liquid chromatography mass spectrometry analysis of oligonucleotides, Anal. Biochem. 625 (2021) 114194, doi:10.1016/j.ab.2021.114194.

[4] Z. Kadlecová, K. Kalíková, E. Tesařová, M. Gilar, Phosphorothioate oligonucleotides separation in ion-pairing reversed-phase liquid chromatography: effect of ion-pairing system, J. Chromatogr. A 1676 (2022) 463201, doi:10.1016/j.chroma.2022.463201.

[5] A.C. McGinnis, B. Chen, M.G. Bartlett, Chromatographic methods for the determination of therapeutic oligonucleotides, J. Chromatogr. B 883–884 (2012) 76–94, doi:10.1016/j.jchromb.2011.09.007.

[6] L. Gong, Analysis of oligonucleotides by ion-pairing hydrophilic interaction liquid chromatography/electrospray ionization mass spectrometry, Rapid Commun. Mass Spectrom. 31 (2017) 2125–2134, doi:10.1002/rcm.8004.

[7] S. Studzińska, R. Rola, B. Buszewski, The impact of ion-pairing reagents on the selectivity and sensitivity in the analysis of modified oligonucleotides in serum samples by liquid chromatography coupled with tandem mass spectrometry, J. Pharm. Biomed. Anal. 138 (2017) 146–152, doi:10.1016/j.jpba.2017.02.014.

[8] M. Enmark, J. Bagge, J. Samuelsson, L. Thunberg, E. Örnskov, H. Leek, F. Limé, T. Fornstedt, Analytical and preparative separation of phosphorothioated oligonucleotides: columns and ion-pair reagents, Analyt. Bioanalyt. Chem. 412 (2020) 299–309, doi:10.1007/s00216-019-02236-9.

[9] M. Enmark, M. Rova, J. Samuelsson, E. Örnskov, F. Schweikart, T. Fornstedt, Investigation of factors influencing the separation of diastereomers of phosphorothioated oligonucleotides, Analyt. Bioanalyt. Chem. 411 (2019) 3383–3394, doi:10.1007/s00216-019-01813-2.

[10] M. Enmark, S. Harun, J. Samuelsson, E. Örnskov, L. Thunberg, A. Dahlén, T. Fornstedt, Selectivity limits of and opportunities for ion pair chromatographic separation of oligonucleotides, J. Chromatogr. A 1651 (2021) 462269, doi:10.1016/j.chroma.2021.462269.

[11] M. Donegan, J.M. Nguyen, M. Gilar, Effect of ion-pairing reagent hydrophobicity on liquid chromatography and mass spectrometry analysis of oligonucleotides, J. Chromatogr. A 1666 (2022) 462860, doi:10.1016/j.chroma.2022.462860.

[12] K.J. Fountain, M. Gilar, J.C. Gebler, Analysis of native and chemically modified oligonucleotides by tandem ion-pair reversed-phase high-performance liquid chromatography/electrospray ionization mass spectrometry, Rapid Commun. Mass Spectrom. 17 (2003) 646–653, doi:10.1002/rcm.959.

[13] M. Gilar, K.J. Fountain, Y. Budman, J.L. Holyoke, H. Davoudi, J.C. Gebler, Characterization of therapeutic oligonucleotides using liquid chromatography with on-line mass spectrometry detection, Oligonucleotides 13 (2003) 229–243, doi:10.1089/154547033224606 12.

[14] L. Gong, Comparing ion-pairing reagents and counter anions for ion-pair reversed-phase liquid chromatography/electrospray ionization mass spectrometry analysis of synthetic oligonucleotides, Rapid Commun. Mass Spectrom. 29 (2015) 2402–2410, doi:10.1002/rcm.7409.

[15] B. Chen, M.G. Bartlett, Evaluation of mobile phase composition for enhancing sensitivity of targeted quantification of oligonucleotides using ultra-high performance liquid chromatography and mass spectrometry: application to phosphorothioate deoxyribonucleic acid, J. Chromatogr. A 1288 (2013) 73–81, doi:10.1016/j.chroma.2013.03.003.

[16] J.M. Cunliffe, D.P. Dreyer, R.N. Hayes, R.P. Clement, J.X. Shen, Using temperature to optimize resolution and reduce analysis times for bioanalytical diastereomer LC–MS/MS separations, J. Pharm. Biomed. Anal. 54 (2011) 179–185, doi:10.1016/j.jpba.2010.08.017.

[17] I. Lurie, L. Li, Use of High-Temperature Liquid Chromatography with Sub-2 µm Particle C18 Columns for the Analysis of Seized Drugs, J. Liq. Chromatogr. Relat. Technol. 32 (2009) 2615–2626, doi:10.1080/10826070903245516.

[18] S. Heinisch, J.-.L. Rocca, Sense and nonsense of high-temperature liquid chromatography, J. Chromatogr. A 1216 (2009) 642–658, doi:10.1016/j.chroma.2008.11.079.

[19] N.M. Elzahar, N. Magdy, A.M. El-Kosasy, M.G. Bartlett, Degradation product characterization of therapeutic oligonucleotides using liquid chromatography mass spectrometry, Analyt. Bioanalyt. Chem. 410 (2018) 3375–3384, doi:10.1007/s00216-018-1032-8.

[20] V.B. Ivleva, Y.-Q. Yu, M. Gilar, Ultra-performance liquid chromatography/tandem mass spectrometry (UPLC/MS/MS) and UPLC/MSE analysis of RNA oligonucleotides, Rapid Commun. Mass Spectrom. 24 (2010) 2631–2640, doi:10.1002/rcm.4683.

[21] S.M. McCarthy, M. Gilar, J. Gebler, Reversed-phase ion-pair liquid chromatography analysis and purification of small interfering RNA, Anal. Biochem. 390 (2009) 181–188, doi:10.1016/j.ab.2009.03.042.

[22] P.J. Oefner, Allelic discrimination by denaturing high-performance liquid chromatography, J. Chromatogr. B 739 (2000) 345–355, doi:10.1016/S0378-4347(99)00571-X.

[23] M. Biba, C.J. Welch, J.P. Foley, B. Mao, E. Vazquez, R.A. Arvary, Evaluation of core–shell particle columns for ion-pair reversed-phase liquid chromatography analysis of oligonucleotides, J. Pharm. Biomed. Anal. 72 (2013) 25–32, doi:10.1016/j.jpba.2012.09.007.

[24] R.J.M. Vervoort, E. Ruyter, A.J.J. Debets, H.A. Claessens, C.A. Cramers, G.J. de Jong, Characterisation of reversed-phase stationary phases for the liquid chromatographic analysis of basic pharmaceuticals by thermodynamic data, J. Chromatogr. A 964 (2002) 67–76, doi:10.1016/S0021-9673(02)00589-7.

[25] DNAPac™ PA200 Oligonucleotide HPLC Columns, (n.d.). https://www.thermofisher.com/document-connect/document-connect.html?url=https://assets.thermofisher.com/TFS-Assets%2FCMD%2Fmanuals%2FMan-065036-LC-DNAPac-PA200-RS-Columns-Man065036-EN.pdf (accessed April 19, 2022).

Publikace X

Hydrophilic interaction liquid chromatography with mass spectrometry for the separation and identification of antisense oligonucleotides impurities and nusinersen metabolites

Vosáhlová Z., Kalíková K., Gilar M., Szymarek J., Mazurkiewicz-Bełdzińska M., Studzińska S.

Journal of Chromatography A, **2024**, *1713*, 464535.

Journal of Chromatography A 1713 (2024) 464535

Contents lists available at ScienceDirect

Journal of Chromatography A

journal homepage: www.elsevier.com/locate/chroma

Hydrophilic interaction liquid chromatography with mass spectrometry for the separation and identification of antisense oligonucleotides impurities and nusinersen metabolites

Zuzana Vosáhlová [a], Květa Kalíková [a,*], Martin Gilar [b], Jakub Szymarek [c], Maria Mazurkiewicz-Bełdzińska [c], Sylwia Studzińska [a,d,e,*]

[a] Department of Physical and Macromolecular Chemistry, Faculty of Science, Charles University, Hlavova 8, 12800, Prague, Czech Republic
[b] Waters Corporation, 34 Maple Street, Milford, MA 01757, USA
[c] Department of Developmental Neurology, Medical University of Gdansk, 7 Dębinki Str., PL-80-952, Gdańsk, Poland
[d] Chair of Environmental Chemistry and Bioanalytics, Faculty of Chemistry, Nicolaus Copernicus University in Toruń, 7 Gagarin Str., PL-87-100 Toruń, Poland
[e] Centre for Modern Interdisciplinary Technologies, Nicolaus Copernicus University in Toruń, 4 Wileńska St., 87-100 Toruń, Poland

ARTICLE INFO

Keywords:
Phosphorothioate oligonucleotides
Hydrophilic interaction liquid chromatography
Impurities and metabolites
Nusinersen
Amide stationary phase

ABSTRACT

With the development of therapeutic oligonucleotides for antisense and gene therapies, the demand for analytical methods also increases. For the analysis of complex samples, for example plasma samples, where the use of mass detection is essential, hydrophilic interaction liquid chromatography is a suitable choice. The aim of the present work was to develop a method for separation and identification of the oligonucleotide impurities and metabolites by hydrophilic interaction liquid chromatography.

First of all, the effects of different chromatographic conditions (e.g. pH of the aqueous part of the mobile phase, buffer concentration, column temperature) on the retention and separation of phosphorothioate oligonucleotides standards on the amide stationary phase were investigated. A set of model oligonucleotides containing a fully modified 21mer and its typical impurities (shortmers and oligonucleotides with different number of thiophosphate modifications) was used. The results showed that the concentration of the salt in the mobile phase as well as its pH, are the most influential parameters with regard to peak shape and separation.

The knowledge gained was applied to the analysis of an unpurified 18mer oligonucleotides, analogues of the drug nusinersen used for the treatment of spinal muscular atrophy. The successful separation and identification of twenty-six and twenty-eight impurities was performed with the developed HILIC method. The method was applied to analysis of nusinersen metabolites of serum samples of patients treated with Spinraza.

1. Introduction

The importance and the use of therapeutic oligonucleotides (ONs) in gene and antisense therapy has been growing significantly in recent years [1,2]. Therapeutic ONs are used for the treatment of e.g. spinal muscular atrophy (nusinersen) [3] or cytomegalovirus infection of the retina of patients with AIDS (fomivirsen) [4]. Naturally occurring ONs are sensitive to endo- and exonuclease activities. Synthetic therapeutic ONs are chemically modified in order to increase their resistance to these enzymes, which leads to an increase in their in vivo stability and effectiveness [5,6].

One of the common modifications is phosphorothioation, where one (or more) oxygen atoms that do not participate in the phosphodiester bond are replaced by sulfur [7]. This modification leads to the formation of a chiral center on the phosphorus atom and formation of 2^n diastereomers, where n is the number of thiophosphate substitutions (PS) [8]. With a higher number of PS modifications, the number of potentially separable diastereomers increases causing the problem with analysis of PS ON synthetic impurities. Additional classes of ONs impurities are products of sugar or base residue modifications, product truncation (N-1, N-2 impurities) or incorporation of an additional nucleotide ($N + 1$ product) and other longmers [9,10]. Two trends can be currently observed in ONs analytics. The first is related to the separation of impurities formed during the synthesis of these compounds,

* Corresponding authors.
E-mail addresses: kveta.kalikova@natur.cuni.cz (K. Kalíková), kowalska@umk.pl (S. Studzińska).

https://doi.org/10.1016/j.chroma.2023.464535
Received 23 October 2023; Received in revised form 24 November 2023; Accepted 25 November 2023
Available online 26 November 2023

while the second is related to the therapeutic monitoring of antisense drugs and their metabolites. In both tasks the efficient separation of ONs is a key requirement for the separation method.

Currently, two main approaches are used for the analysis and separation of metabolites and impurities of therapeutic phosphorothioate ONs: i) ion-pair (IP) reversed-phase (RP) liquid chromatography (LC) (where the diastereomeric separation is suppressed by IP system) [11]; ii) hydrophilic interaction liquid chromatography (HILIC), which is less prone to separation of diastereomers [12]. Both approaches have their limitations—most of IP agents cause contamination of mass spectrometer (MS), while HILIC MS signal is reduced by alkali ion ON adducts (potential for impurities and metabolites signal loss) [13]. On the other hand, the main advantage of HILIC is utilization of MS compatible mobile phases, while IP RP LC provides higher MS sensitivity, better reproducibility, and many possibilities how to affects the separation of diastereomers and ONs by changing the chromatographic conditions (temperature, mobile phase composition) [14]. The resolution of modified ONs mixtures in both modes of liquid chromatography is limited due to closely related structure of target ON and its impurities or metabolites [9,10,15]. The primary drivers for application of HILIC for separation of therapeutic phosphorothioate ONs was its alternative selectivity and potential to avoid IP agents in LC MS analysis [16].

The first application of HILIC on the analysis of ONs was presented by Alpert in 1990 for the separation of oligothymidylic acids with different chain lengths (from 12 to 30) [17]. The first HILIC separation of ONs without PS modification using commercial columns, i.e., a diol-based stationary phase Luna® HILIC and a TSKgel® Amide-80 column, was reported in 2010 [18]. Separation and identification of antisense phosphorothioate ONs were first presented by Easter et al. [19], but the optimized method was able to separate only two ONs within 20 min. Next, the systematic studies of HILIC for the analysis of phosphorothioate antisense ONs and their impurities were performed [20]. The impact of stationary phase type, mobile phase (MP) salt and its concentration on the separation and determination of selected compounds by HILIC ESI MS was investigated. The comparison of IP RP LC and HILIC MS sensitivity for ONs was presented by Lobue in 2019 [21]. A few additional reports on analysis of therapeutic ONs in HILIC were presented [13,22,23]. Comprehensive study about utilization of zwitterionic stationary phases in HILIC for ONs characterization was published by Lardeux et al. [24]. Recently, HILIC was also utilized for the profiling of diastereomers of various ONs formats especially that with chemical modification at the sugar moieties [25].

The main goal of this work was to develop robust selective HILIC method suitable for the separation of impurities and metabolites of therapeutic ONs. The amide stationary phase was chosen, since the earlier studies found that it is best suited for ONs separations [18–20]. The PREMIER variant of amide column was used to minimize the ONs nonspecific adsorption to metal surfaces that can cause peak broadening (or signal loss), and poor reproducibility of chromatographic results [26,27]. Nusinersen analogues were selected for the study, due to its importance in the spinal muscular atrophy (SMA) therapy. To the best of our knowledge, such studies for nusinersen in HILIC were performed for the first time. The comprehensive retention studies were done at initial stage to identify the LC conditions suitable for analysis of phosphorothioate shortmers. The resolution of nusinersen analogues and their impurities was investigated, followed by method application to analysis of nusinersen metabolites extracted from SMA patient serum samples. The separation of ONs was crucial; HILIC with amide stationary phase permitted successful LC MS analysis of ONs.

2. Materials and methods

2.1. Materials and reagents

Acetonitrile (ACN, LC-MS grade) was supplied by VWR International (Radnor, USA). Water for LC was purchased from Honeywell (Charlotte, USA). Ammonium formate (purity >99.995 %), ammonium acetate (purity ≥99 %), ammonium hydroxide solution (28.0–30.0 % NH_3) and formic acid (purity >95 %) were purchased from Sigma-Aldrich (St. Louis, USA). Deionized water was purified with Rowapur and Ultrapur system from Watrex (Prague, Czech Republic).

21mer ONs and 2–6mer ONs were synthetized by Integrated DNA Technologies (Coralville, USA). The shortmers, i.e. 20mer, 19mer and 18mer, analogous to 21mer allPS, but truncated at 5′terminus by 1, 2, and 3 nucleobases, respectively, were synthetized by KRD (Prague, Czech Republic). Unmodified (OL1) and phosphorothioate (OL2) 18mer riboONs of similar sequence were purchased from Sigma-Aldrich (Gillingham, Dorset, UK). Both, OL1 and OL2, were desalted raw products without any purification because they were used as model compounds for the development of a method for the impurity's separation and identification. Additionally, their aqueous solutions were frozen and thawed and stored for two days at a temperature of 35 °C to increase the amount of impurities, which will be the products of the decomposition of these ONs [28]. The list of all tested ONs, their sequences and position of phosphorothioation is given in Table 1.

The following reagents were used during the serum sample preparation step: a mixture of phenol/chloroform/isoamyl alcohol (25:24:1) (VWR International, Gdańsk, Poland) and chloroform (Merck KGaA, Darmstadt, Germany).

2.2. Instrumentation and columns

Initial chromatographic experiments were performed on the Waters Acquity UPLC H-Class system (Waters, Milford, USA). The system was equipped with a quaternary solvent manager, an autosampler, a column thermostat, a photodiode array detector and a QDa mass detector. The Empower 3 software was used for system control, data acquisition, and results processing. Next, preliminarily optimized separation methods

Table 1
The list of all tested oligonucleotides, their sequences, position of phosphorothioation (marked by *) and molecular masses.

Name	Sequence	Molecular mass [Da]
MODEL OLIGONUCLEOTIDES		
allPS 21mer (DNA)	5′ T*T*T * T*A*G * C*A*T * T*T*T * T*A*C * G*A*T * T*T*T 3′	6703.4
allPS 20mer (5′N-1)	5′ T*T * T*A*G * C*A*T * T*T*T * T*A*C * G*A*T * T*T*T 3′	6383.2
allPS 19mer (5′N-2)	5′ T*T*A*G * C*A*T * T*T*T * T*A*C * G*A*T * T*T*T 3′	6062.9
allPS 18mer (5′N-3)	5′ T*A*G * C*A*T * T*T*T * T*A*C * G*A*T * T*T*T 3′	5742.7
Shortmers		
allPO 2mer	5′ TT 3′	546.4
allPS 2mer	5′ T*T 3′	562.5
allPO 3mer	5′ TTT 3′	850.6
allPS 3mer	5′ T*T*T 3′	882.7
allPO 4mer	5′ TTTT 3′	1154.8
allPS 4mer	5′ T*T*T*T 3′	1203.0
allPO 5mer	5′ TTTTT 3′	1459.0
allPS 5mer	5′ T*T*T*T*T 3′	1523.3
allPO 6mer	5′ TTTTTT 3′	1763.2
1PS 6mer	5′ TTTTT*T 3′	1779.3
2PS 6mer	5′ TTTT*T*T 3′	1795.3
3PS 6mer	5′ TTT*T*T*T 3′	1811.4
4PS 6mer	5′ TT*T*T*T*T 3′	1827.5
allPS 6mer	5′ T*T*T*T*T*T 3′	1843.5
Nusinersen analogues		
OL1 allPO 18mer (RNA)	5′ UCACUUUCAUAAUGCUGG 3′	5653.7
OL2 allPS 18mer (RNA)	5′ U*C*A*C*U*U*U*C*A*U*A*A*U*G*C*U*G*G 3′	5927.0

were transferred to liquid chromatograph coupled with Quadrupole Time-of-Flight (Q-TOF) mass spectrometer to obtain higher MS resolution and sensitivity. The 1260 Infinity Quaternary System (Agilent, Waldbronn, Germany) high-performance liquid chromatography (UHPLC) system with a binary pump, vacuum chambered microdegasser, thermostatically controlled autosampler, column compartment, and a diode-array detector (DAD) was used in the present study. The system was equipped with Agilent 6540 UHD Accurate-Mass Q-TOF mass spectrometer (Waldbronn, Germany) with electrospray ionization. The negative ion mode was applied and the full scan mass spectra were recorded within the mass range of *m/z* 500–3200. The data were collected with the use of Agilent Mass Hunter Software (version B.04.01).

Acquity Premier BEH Amide columns (Waters, Milford, USA) with particle size 1.7 μm were used, inner diameter 2.1 mm, and three different lengths (50, 100, 150 mm).

2.3. Experimental procedures

2.3.1. Sample preparation

Standards of ONs are provided in lyophilized form. Stock solutions were prepared by dissolution in deionized water at a concentration of 300 μM. These stock solutions were stored in a freezer and diluted 3 times by ACN before use (to reach the final concentration 100 μM in water:ACN; 1:2).

A pediatric patient with genetically confirmed SMA1 was enrolled at the Division of Developmental Neurology, the Medical University of Gdańsk at the University Clinical Centre. The Spinraza dosage was 5 mg in 5 ml during the lumbar puncture. The 3 ml of serum samples were taken before the administration of the first dose and after the third dose. Samples were taken by relevant guidelines of the Medical University of Gdańsk (Poland) and approved by the Independent Bioethics Committee for Scientific Research at the Medical University of Gdańsk (permission no. NKBBN/778/2022).

Serum samples were prepared by liquid-liquid extraction (LLE) with the use of a phenol/chloroform/isoamyl alcohol mixture (25:24:1 *v/v/v*). The 2 ml of serum sample was first diluted with redistilled water at a ratio of 1:3. Next, 3 ml of phenol/chloroform/isoamyl alcohol mixture and 3 ml of diluted serum were mixed and next centrifuged (RCF = 20,160 × *g* for 20 min). The supernatant was taken for an additional LLE extraction step with chloroform (at a ratio of 1:4). This step was repeated to remove residual phenol.

2.3.2. Mobile phases and analysis conditions

Generally, two types of MP composition were used (marked as MP I and MP II). Initial measurements (retention study) were performed in MP I consisting of pure acetonitrile in MP A I and aqueous part in MP B I. Several MPs B I were tested: 10 mM ammonium formate (pH 3.0, pH 4.7, pH 6.8 and pH 8.0); 10 mM ammonium acetate (pH 4.7, pH 6.8); for ammonium formate pH 8.0 concentrations from 5 mM to 25 mM (5 mM steps) were also tested. As the most optimal MP B I 25 mM ammonium formate, pH 8.0 was chosen. For analysis of impurities and metabolites MP II was used (because of need of higher MS sensitivity). MP A II was composed of 10 mM ammonium acetate in ACN/water 75/25 (*v/v*) and MP B II was 10 mM ammonium acetate, pH 6.8. For all measurements gradient elution was used. The most optimal gradient for MP I was gradient I: 0–25 (min), 97-55 (%A); for MP II gradient II: 0-1-21 (min), 100-100-50 (%A).

All MPs were filtered with 0.45 μm nylon membrane filters (Whatman, GE Healthcare, Chicago, USA) before use. The first system peak was used as a column void time marker. Flow rate was 0.4 mL min^{-1}, injection volume was 1–5 μL. Detection wavelength was set at 260 nm, based on the UV-spectra measurements. Column temperature was 40 °C, except of the testing of the effect of temperature on retention and resolution, where temperature range 10–90 °C (10 °C steps) was tested. Sample temperature was 10 °C for all measurements.

2.3.3. Mass spectrometer settings

All MS measurements were performed in negative mode. QDa detector settings: mass range 50–1250 *m/z*, cone voltage 30 V, probe temperature 600 °C. Most of Q-TOF-MS parameters were applied based on our earlier studies [29,30], consequently capillary voltage was equal to 4000 V, drying gas flow −10 L min^{-1}, shielding gas flow 10 L min^{-1}, octopole voltage 800 V, drying gas temperature 350 °C, shielding gas temperature 400 °C, and collision energy 25 eV. The nebulizer gas pressure, skimmer voltage, and fragmentor voltage were optimized during the study, as they had the greatest impact on ON signals. Finally, the selected values were as follows: 20 psi for nebulizer gas pressure, 100 V for skimmer voltage, and 200 V for fragmentor voltage.

The identification of impurities and metabolites was performed by assigning charge states of ions observed at the full scan spectra, calculation of masses, and application of deconvolution with the use of Mass Hunter Software. The sequence assignment of impurities and metabolites was done after determination of their molecular mass with the use of e.g. RoboOligo and Mongo Oligo Mass Calculator v2.06 programs [31, 32]. Both software's determine the sequence or masses of ONs provided by the MS analysis of multi-charged ions. Mongo Oligo may provide the possible CID-product ions. Furthermore, fragmentation spectra were registered and fragment ions were assigned following the scheme of McLuckey [33]. The exact process of metabolites identification was presented in detail in our previous publication [29].

3. Results and discussion

The study was divided into three parts in order to develop a suitable HILIC method for separation of ONs impurities and metabolites extracted from serum samples of patient treated by nusinersen. In the first part we were focused primarily on the retention studies of selected ONs (see selected ONs in Table 1), since this is a necessary stage in the comprehensive development of each separation method. These ONs were selected for the following reasons: 21mer and its shorter impurities as representatives of therapeutic ONs of first generation; 2–6mers with different number of PS modifications because of their similar length to metabolites of those therapeutic ONs. During the initial experiments, the effect of MP pH, salt concentration and column temperature on the retention and separation of phosphorothioated ONs varying in the length and number of PS modifications was done. The main purpose of this part of the study was to find the optimal conditions suitable for separation of ONs impurities and metabolites. The second part of our study was devoted to the optimization of MS conditions for identification of ONs. The last part was devoted to the application of the developed HILIC Q-TOF-MS method to the analysis of real samples (unpurified ONs standards, nusinersen metabolites). These studies were performed for the first time for nusinersen analogues and metabolites in HILIC.

3.1. The effects of chromatographic parameters on retention and resolution of model mixture of ONs

ON impurities and their metabolites are usually shorter sequences of the main compound. For this reason, the model sample, used during the retention studies, was a mixture of fully phosphorothioated 21mer with 5′N-1 (20mer), 5′N-2 (19mer) and 5′N-3 (18mer) ONs. The focus was to investigate the HILIC method capability to suppress diastereomer separation and concurrently to check its separation performance for the target ONs and their shorter impurities/metabolites.

The analysis of model mixture in different pH of MP showed significant differences (see Fig. 1). In MP pH 3.0 no ON was eluted within almost 60 min. This is probably caused by very strong interaction of ON with metal surface of instrumentation used. Between MPs with pH 4.7 and 8.0 only small decrease in retention with increasing pH was observed, which was in agreement with the published reports [13]. Table S1 in Supporting material summarizes obtained values of peak

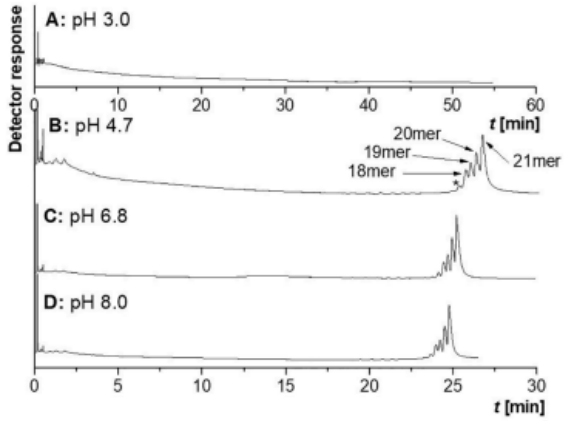

Fig. 1. The effect of MP pH on retention and resolution of model mixture (allPS 21mer - allPS 18mer). Experimental conditions: *ACQUITY* Premier BEH Amide Column (1.7 µm, 50 × 2.1 mm); MP composition MP A: ACN, MP B: 10 mM ammonium formate in water; gradient elution: 97–55 % MP A in 25 min (20 min re-equilibration); column temperature: 40 °C; autosampler temperature 10 °C; flow rate: 0.4 mL min^{-1}; injection volume 1 µL; UV detection λ = 260 nm. The scale of detector response is not the same and thus system peaks look differently. * indicates 17mer, an impurity of ONs standards.

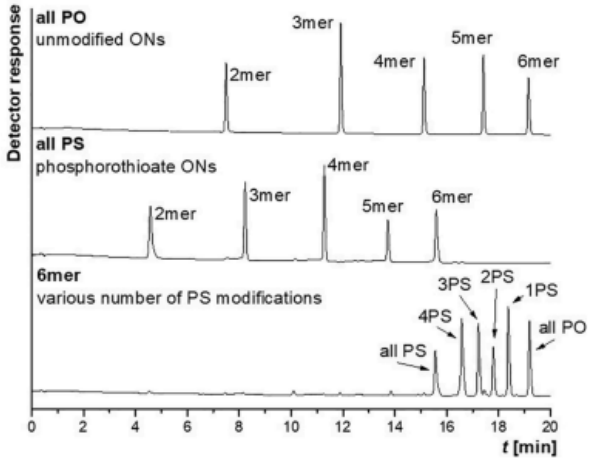

Fig. 2. Separation of ONs based on their length and the number of PS modifications. Experimental conditions: *ACQUITY* Premier BEH Amide Column (1.7 µm, 50 × 2.1 mm); MP composition MP A: ACN, MP B: 25 mM ammonium formate in water, pH 8.0; gradient elution: 97–55 % MP A in 25 min (20 min re-equilibration); column temperature: 40 °C; autosampler temperature 10 °C; flow rate: 0.4 mL min^{-1}; injection volume 1 µL; UV detection λ = 260 nm.

widths and resolutions. MP with pH 4.7 provided significantly lower resolution than pH 6.8 and 8.0. On the other hand, the highest resolution was observed for MP with pH 8.0, and the narrowest peaks provided MP with pH 6.8. Based on these results we conclude that acidic pH is not suitable for ON analysis by HILIC and amide stationary phase, while near-neutral and slightly basic pHs are. We selected pH 8.0 for the subsequent experiments, however pH 6.8 also provided sufficient peak resolution and thus it was used in another part of our study.

The effect of salt concentration on chromatographic performance is shown in Fig. S1 in Supporting material. Our results are in agreement with previously published observations [21]. An increase in concentration of ammonium formate led to the decrease in peak width, improvement in peak shape and resolution of ONs with different length. Moreover, slight increase in retention with increasing salt concentration was observed, which is usually attributed to the electrostatic repulsion between ONs and stationary phase surface. However, there should be no electrostatic interaction between neutral stationary phase and negatively charged ONs, unless there are residual silanols on the stationary phase surface [34]. Described effects were most significant in range 5–20 mM, while the results for 20 mM and 25 mM ammonium formate were very similar (Fig. S1). The highest concentration was selected for further experiments.

While the effect of column temperature has a great impact on chromatographic performance in IP RP LC, where increased temperature helps to suppress the diastereomer separation [35], in HILIC the effect of column temperature is negligible (see Fig. S2 in Supporting material). With increasing temperature only very slight increase in retention was observed, which is probably related to the size of ONs and change of their structure. Moreover, increase in retention with increasing temperature in HILIC has been previously observed [36].

Since the impurities and metabolites are shortmers, we decided to apply our optimized conditions (25 mM ammonium formate, pH 8.0, gradient elution) for the analysis of shortmers (2–6mers, different number of PS modifications). Fig. 2 shows that developed method allowed for separation of ONs based on their length (both modified and unmodified), and also based on the number of PS modifications. In addition, the retention behavior is opposite than in IP RP LC, i.e. in HILIC with increasing number of PS modifications the retention decreases. The reason is higher hydrophilicity of ONs with phosphodiester bond (PO) than phosphorothioate one (PS). Inspection of Fig. 2 reveals one additional trend—the peaks of all PS ONs are about 25 % wider than their all PO counterparts. This suggests that diastereoseparation is not completely suppressed even under HILIC conditions (similar to IP RP LC), which has been reported recently [25].

Application of amide column and HILIC makes it possible to separate ONs with different length and number of phosphorothioate modifications. Properties of stationary phase, neutral surface groups with high polarity allow successful resolution of the model ONs standards.

3.2. Application of developed HILIC method to the analysis of real samples

Two types of samples were selected to verify applicability of the method. The first type are unpurified oligonucleotides: unmodified OL1 and phosphorothioate OL2. Their analysis by HILIC with mass spectrometry will verify the applicability of this mode for the separation and identification of oligonucleotide impurities. The second type of samples are extracts from the serum of patient treated with an oligonucleotide-based drug. The purpose of the present research was only to verify if the developed HILIC method allows the separation of metabolites extracted from biological samples. Our goal, however, was not to study metabolism, as this has already been done and described extensively in earlier studies [29].

3.2.1. ONs impurities

To increase MS sensitivity while maintaining resolution and peak shape the separation conditions were slightly changed −10 mM ammonium acetate, pH 6.8 was used (Figs. S3 and S4 in Supporting material). The ammonium acetate was added into both MP A and MP B to keep the ionic strength constant. pH of 6.8 was selected to ensure easy and repeatable preparation. The same results were observed also for nusinersen analogues as shown in Fig. 3A–D, i.e. no significant difference in resolution between the two salts used in the MP and also different MP pH values (Fig. 3A,B). Lowering salt concentration caused reduction of analysis time (Fig. 3B,D). Similar effect was noticed for the change of ammonium formate to ammonium acetate (Fig. 3C,D). The sharper gradient profile (Fig. 3E) caused lowering the peaks width, due to, e.g. reduction of diastereomeric resolution. Finally, method gradient optimization significantly reduced retention time (almost twice) without loss of resolution (Figs. 3D,E and S5) in Supporting material).

The MS operating parameters were not optimized extensively, as this has already been the subject of several studies [25,26]. Nevertheless, it

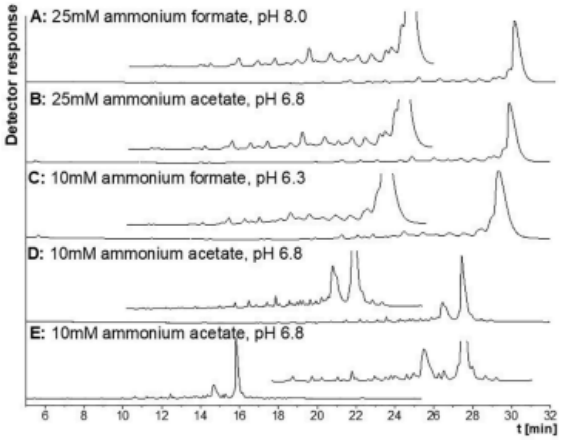

Fig. 3. The impact of salt used in the MP on the separation of OL2 impurities. Experimental conditions: *ACQUITY* Premier BEH Amide Column (1.7 µm, 50 × 2.1 mm); mobile MP: MP A: ACN, MP B: salt in water (A, B, C, D) or MP A: ACN/salt 75/25 (*v/v*), MP B: salt in water (E); gradient elution: 3–55 % MP A in 30 min (A, B, C, D) or 0–50 % MP B in 21 min (E) (20 min re-equilibration); column temperature: 40 °C; autosampler temperature 10 °C; flow rate: 0.4 mL min^{-1}; injection volume 4 µL; UV detection λ = 260 nm. Part of the chromatogram is zoomed in: 16–32 min for A,B,C,D; 8–18 min for E.

was observed that a few parameters have a particular effect on the MS response for ONs (Table S2). The peak areas increased when fragmentor voltage decreased, contrary to skimmer and nebulizer pressure. The greatest MS response for OL1, OL2, and their impurities was observed for fragmentor voltage equal to 200 V, while the skimmer equalled to 80 V and nebulizer pressure 20 psi.

The assignment of charge states of ions observed at the full scan spectra and next mass calculation, or mass deconvolution was done for the identification of impurities (Fig. 4). Next, sequence assignment was performed by impurity mass calculation with the use of the Mongo Oligo Mass Calculator v2.06 program. The masses of ONs detected in the sample were compared with the masses of impurities calculated by the software. The probable impurities were consistent with the mechanism of their formation. It is a common practice because most types of ON impurities are already well-known and described in the literature. They are formed as N-shortmers (at 5′ or 3′ end), or 3′end shortmers with additional phosphate (PO) or thiophosphate (PS) or 2′,3′-cyclic phosphate (cyc) groups [37]. Moreover, base mismatches, basic impurities (loss of adenine or guanine), or ONs with phosphate diester linkage (P═O) instead of phosphorothioate ones (P═S) may be observed [37].

Figs. 4, S7, and S8 present the exemplary full scan spectra, adducts, and deconvolution results for OL1, OL2, and some of their impurities. The accurate mass for OL1 and OL2, as well as for their impurities could be readily determined, even when additional peaks of sodium and potassium adducts were observed (Figs. 4, S7, and S8). The traces of non-volatile cations in the mobile phase [13,21] contribute to adducts present in ONs MS spectra (Figs. S7, S8 in Supporting material). Consequently, the ion current is shared over a greater number of signals, which decreases the intensity of the target ON signal and reduces the sensitivity of MS detection [13,21]. In the case of the present study, adduct peaks were of relatively low abundance (Figs. S7, S8 in Supporting material), making identification effective without significant signal intensity loss. Although metal adducts are the most frequently suggested as one of the disadvantages of HILIC application to ON analysis [13,19], our results do not entirely confirm this assertion, since the identification is possible. Nevertheless, it is likely that reduction in adducts would increase the sensitivity in HILIC. Our results are in line with previous research supporting the benefit of HILIC in the reduction (but not complete removal) the adduct formation issues [13].

The two charge states at the full scan spectra for the majority of impurities were observed (Figs. S7, S8 in Supporting material), except for one impurity for OL1 (5′N-12) and five for OL2 (3′ N-6 cyc, 3′ N-7 cyc, 3′ N-11 cyc, 3′ N-12 cyc, 3′N-12) where only one charge state was noticed. Additionally, three charge states were noticed for OL1 and OL2

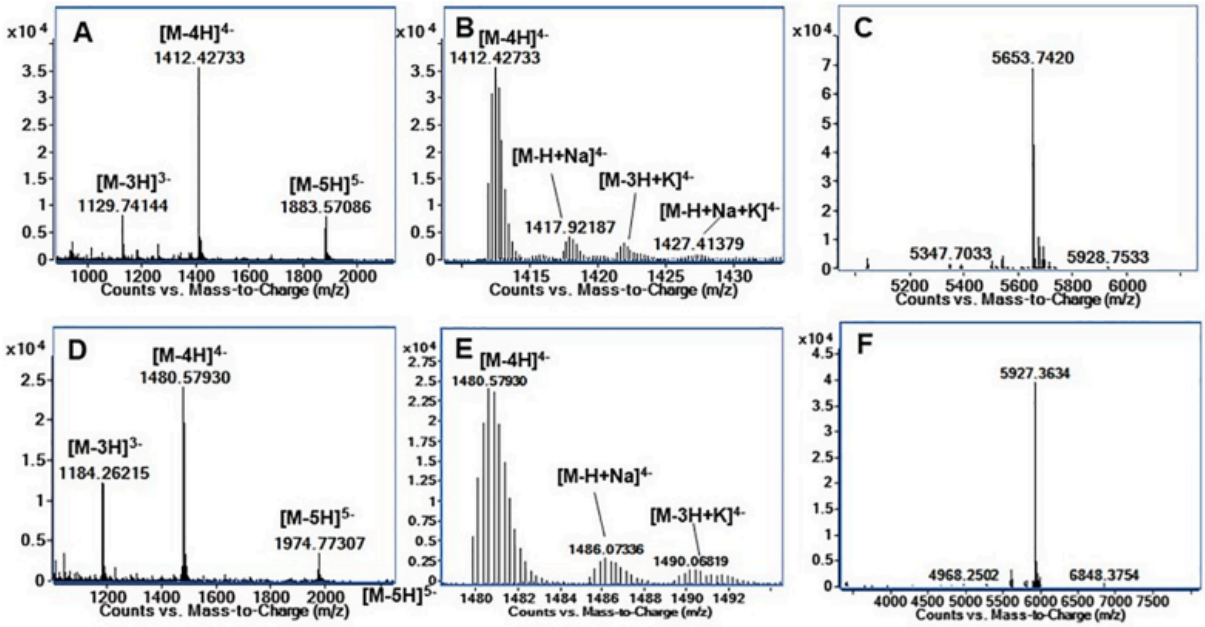

Fig. 4. The full scan spectra (A,D), adducts (B,E), and deconvoluted masses (C,F) for OL1 (A, B, C) and OL2 (D, E, F). Experimental conditions: *ACQUITY* Premier BEH Amide column (1.7 µm, 50 × 2.1 mm); MP composition MP A: ACN/10 mM ammonium acetate (pH 6.8) 75/25 (*v/v*), MP B: 10 mM ammonium acetate (pH 6.8); gradient elution program: 0–1 min. 100 % MP A, 1–21 min. 100–50 % MP A (20 min re-equilibration); column temperature: 40 °C; autosampler temperature 10 °C; flow rate: 0.4 mL min^{-1}; injection volume 5 µL; mass spectrometric conditions: nebulizer gas pressure 20 psi, skimmer voltage 80 V, capillary voltage 4000 V, fragmentor voltage 200 V; drying gas flow 10 L min^{-1}, shielding gas flow 10 L min^{-1}, octopole voltage 800 V, drying gas temperature 350 °C, and shielding gas temperature 400 °C.

(these were −3, −4, and −5 with −4 being the most abundant) (Table 2, Fig. 4). Regarding the charge state distribution at the full scan spectra of ON polyanions, it shifted to lower *m/z* values together with decreasing in the length (and simultaneously, the number of ionized phosphate groups) (Table 2, Figs. S7 and S8 in Supporting material). The charge state distribution in HILIC depends on the length of the ON, similar to the most abundant ion. These effects are not related to the modification of ONs.

Table 2 collects the most abundant ion of each impurity with its charge state, deconvoluted mass, retention time, and sequence of probable impurity based on Q-TOF-MS analysis. Twenty-six impurities were annotated for OL1, while twenty-eight for OL2. Fig. 5 presents EIC for each of identified OL1 impurities, while Fig. S9 for OL2.

In the case of OL1, mainly shortmers were identified, precisely failure sequences lacked a various number of nucleotides from both the 3′ and 5′ ends (Table 2). Characteristically, in the case of impurities resulting from the incomplete synthesis process shortmers at the 5′ end have hydroxyl groups (from 5′N-2 to 5′N-14). Shortmers formed as an ON degradation products at the 3′ end position mostly have a phosphate (PO) group (8 impurities), less often cyclic phosphate (cyc) (3 impurities) (Table 2). As for the elution order, in general, retention increases with the elongation of the ON chain, which is a result of the increasing polarity of the molecule. Moreover, 3′-shortmers always have greater retention compared to 5′ shortmers of the same number of nucleotides in the sequence, due to the presence of an additional phosphate group or a cyclic phosphate.

HILIC appeared to be efficient method for ONs impurities separation with good selectivity (lack of coelution of OL1 impurities together with the main compound) (Fig. 5). In addition, two longmers have been also identified: OL1 with an additional phosphate group (OL1 PO) and OL1 with additional guanosine (OL1 +G) (Table 2). Both impurities were completely separated from the main compound (Fig. 5).

The trends observed for OL1 are analogous to OL2 (Table 2). One impurity was also identified where the sulfur atom in one of the phosphorothioate groups was swapped for oxygen (OL2 P═O) (Table 2). It was eluted together with the main compound and its separation from OL2 was impossible under any of the conditions applied during the study (Figs. S9, S10B in Supporting material).

The application of the developed method did not provide complete separation of all identified impurities, regardless of whether the ON was modified (OL2) or not (OL1). An attempt was made to change the gradient program, however, this did not improve separation, while additionally increased the broadening of peaks. Two more amide columns with 100 mm and 150 mm lengths were also used (Figs. S10A and S11 in Supporting material). In the case of OL2, the resolution of impurities eluted before the main peak was increased when 150 mm column was applied (Fig. S10A in Supporting material), contrary to closely related impurities eluted with the main peak (Fig. S10B, C in Supporting material). Greater improvements in the resolution of impurities for longer column were observed for unmodified OL1 (Fig. S11 in Supporting material).

3.2.2. *ONs metabolites*

Generally, therapeutic ONs are metabolized/hydrolyzed in human body because of endo- and/or exonucleases present in plasma and tissues [38]. By modifying of ONs, the stability increases, but they still undergo the metabolism and can be cleaved by nucleases practically anywhere between oxygen on 3' end and phosphorous from phosphate group (cleavage of phosphodiester linkage) [39]. This results in a huge number of very short ONs as metabolites.

The simplest method of isolation of ONs from serum is phenol/chloroform LLE described in experimental section. The LLE removes proteins and lipids form the aqueous ONs sample prior to its LC MS analysis. Two plasma samples were selected for the study: sample prior to the first dose of nusinersen (control sample, no target ON was detected) and the sample after the fourth dose of the drug. The metabolites of nusinersen found in the patients plasma were short (3-,4-mers) fragments of target ON; IP RP LC does not allow their complete separation [29]. The developed HILIC method was suitable for separation and analysis of short ON metabolites.

Eleven metabolites were identified in a manner analogous to impurities, and they had also been identified previously [29]. Their probable sequence, masses, and parent ions are summarized in Table 3, while fragmentation spectra for three exemplary metabolites were presented in Fig. S12. The short sequence of metabolites made it impossible to unambiguously identify all of them with strictly defined nusinersen fragments, even with the use of fragmentation, since the masses of fragments is similar for some of the metabolites (Fig. S12). It should be noted that these ONs have two other types of modification in addition to the phosphorothioate modification (extensively tested earlier in this research): 2′-O-methoxyethyl group in ribose moieties and methylated cytosine and uridine.

For most of the detected metabolites (seven compounds), only one signal with charge state equal −2 was observed on the spectra in full scan mode (Fig. S13D in Supporting material). For the rest, there were two signals with charge −1 and −2 (Fig. S13A in Supporting material). Analogous trends were observed for impurities with short, several-nucleotide sequences (Table 2). This confirms that the shorter the ON, the lower the charge state of the main signal. However, this effect may also be related to the low number of metabolites or their poor ionization, due to the modified structure.

In the initial stage of the study, a 50 mm Amide column was used. Complete separation of the metabolites was not achieved, with the coelution of as many as four metabolites (M2-M5) in one peak and three of them (M9–M11) in the other (Fig. S14A). Decreasing the percentage of ammonium acetate at the end of the gradient increased the analysis time but did not increase the separation significantly. However, partial separation of metabolites M9, M10, M11 was achieved (Fig. S14B). In the next step, two longer columns of 100 mm and 150 mm were used. The total analysis time and metabolites retention increased, but the resolution was not higher, neither for coelution M2, M3, M4, M5 or coelution M9, M10, M11 (Fig. S15). The gradient changes for 150 mm column allow partial separation of M2 from M3, M4, M5, and increased resolution of M9, M10 and M11 (Fig. 6). At the same time, however, the analysis time is longer, and the separation is not complete anyway. The results indicate that the separation of very short, modified, and structurally similar ONs is very challenging for HILIC despite the use of UHPLC, a long column, and changes in the gradient elution program. Nevertheless, it should be emphasized that this is also difficult to achieve for IP RP HPLC [29,40], and the advantage of the developed HILIC method is the absence of ion pair reagents.

The M1 metabolite has the lowest polarity and is therefore eluted as the first one (Figs. 6, S14, S15). M3 and M5 coelute with M4, all of which are 3mers. M3 and M5 have only three phosphorothioate groups (unlike M4), but they include more polar nucleotides, no guanosine (G) (Table 3). Therefore, most likely the resultant polarity of M4, M3 and M5 is similar. Next, M2 is eluted due to increased polarity of M2 compared to the other three metabolites (additional 2′-O-methoxyethylribose) (Fig. 6B, Table 3). Somewhat surprising is the elution of M7 after M3, M4, and M5 (Figs. 6, S14, S15), since each one of them is a 3mer (Table 3). The next eluted M8, a 3mer composed of three polar mU and an additional 2′-O-methoxyethylribose (Table 3). The M9, M10 and M11 metabolites are the last to elute from the amide column (Figs. 6, S14, S15). Two of these metabolites are 4mers, and retention increases with ON length in HILIC due to greater polarity. M9, on the other hand, is a 3mer, but it has additional 2′-O-methoxyethylribose (Table 3). It is possible to partially separate these three metabolites and then M9 is eluted before M10 and M11 (Fig. 6A), which is most likely closely related to the fact that there are only three nitrogenous bases in its structure.

Table 2
Impurities identified in OL1 and OL2.

m/z values for the most abundant ion	Charge	Impurity	Impurity sequence	Deconvoluted mass [Da]	Retention time [min]
OL1					
618.5960	−2	5′ N-14	5′ CUGG 3′	1239.1923	9.57
783.59054	−2	3′ N-13 PO	5′ UCACU 3′ - PO	1569.1811	12.20
944.13064	−2	5′ N-12	5′ UGCUGG 3′	1890.2613	12.75
738.76977	−3	5′ N-11	5′ AUGCUGG 3′	2219.3111	13.39
848.45443	−3	5′ N-10	5′ AAUGCUGG 3′	2548.3655	14.01
821.75231	−3	3′ N-10 cyc	5′ UCACUUUC 3′ - cyc	2468.2581	14.31
931.77153	−3	3′ N-9 cyc	5′ UCACUUUCA 3′ - cyc	2798.3113	14.67
950.79667	−3	5′ N-9	5′ UAAUGCUGG 3′	2855.3901	14.78
827.75525	−3	3′ N-10 PO	5′ UCACUUUC 3′ - PO	2486.2677	14.98
937.77304	−3	3′ N-9 PO	5′ UCACUUUCA 3′ - PO	2816.3208	15.31
1060.48043	−3	5′ N-8	5′ AUAAUGCUGG 3′	3184.4425	15.23
1143.46167	−3	3′ N-7 cyc	5′ UCACUUUCAUA 3′ - cyc	3433.3859	15.74
1162.16075	−3	5′ N-7	5′ CAUAAUGCUGG 3′	3489.1021	15.95
1039.78193	−3	3′ N-8 PO	5′ UCACUUUCAU 3′ - PO	3122.3485	16.00
1149.46452	−3	3′ N-7 PO	5′ UCACUUUCAUA 3′ - PO	3451.3946	16.26
1264.16821	−3	5′ N-6	5′ UCAUAAUGCUGG 3′	3795.5023	16.45
1259.1498	−3	3′ N-6 PO	5′ UCACUUUCAUAA 3′ - PO	3780.4487	16.56
1024.38187	−4	5′ N-5	5′ UUCAUAAUGCUGG 3′	4101.5290	16.96
1361.1574	−3	3′ N-5 PO	5′ UCACUUUCAUAAU 3′ - PO	4086.4716	17.15
1100.88825	−4	5′ N-4	5′ UUUCAUAAUGCUGG 3′	4407.5515	17.42
1106.87875	−4	3′ N-4 PO	5′ UCACUUUCAUAAUG 3′ - PO	4431.5171	17.68
1177.14833	−4	5′ N-3	5′ CUUUCAUAAUGCUGG 3′	4713.0930	17.88
1259.66106	−4	5′ N-2	5′ ACUUUCAUAAUGCUGG 3′	5042.6456	18.01
1183.38879	−4	3′ N-3 PO	5′ UCACUUUCAUAAUGC 3′ - PO	4737.0574	18.09
1412.4273	**−4**	**OL1**	**5′ UCACUUUCAUAAUGCUGG 3′**	**5653.7093**	**18.44**
1432.41926	−4	OL1 PO	5′ UCACUUUCAUAAUGCUGG 3′ - PO	5733.6760	19.40
1482.42756	−4	OL1 + G	5′ GUCACUUUCAUAAUGCUGG 3′	5933.7076	19.85
OL2					
642.5604	−2	5′ N-14	5′ C*U*G*G 3′	1287.1203	6.64
775.56021	−2	3′ N-13	5′ U*C*A*C*U 3′	1553.1204	7.41
806.54049	−2	3′ N-13 cyc	5′ U*C*A*C*U 3′ - cyc	1615.0048	8.86
823.07247	−2	5′ N-13	5′ G*C*U*G*G 3′	1648.1473	9.37
967.54076	−2	3′ N-12 cyc	5′ U*C*A*C*U*U 3′ - cyc	1937.0815	10.25
984.07396	−2	5′ N-12	5′ U*G*C*U*G*G 3′	1970.0815	10.55
770.72496	−3	5′ N-11	5′ A*U*G*C*U*G*G 3′	2315.1760	11.29
1128.54225	−2	3′ N-11 cyc	5′ U*C*A*C*U*U*U 3′ - cyc	2259.0845	11.39
838.37969	−3	3′ N-10	5′ U*C*A*C*U*U*U*C 3′	2518.1403	11.66
886.06867	−3	5′ N-10	5′ A*A*U*G*C*U*G*G 3′	2661.2061	12.00
859.36589	−3	3′ N-10 cyc	5′ U*C*A*C*U*U*U*C 3′ - cyc	2580.5991	12.46
993.40255	−3	5′ N-9	5′ U*A*A*U*G*C*U*G*G 3′	2983.7069	12.86
1108.74565	−3	5′ N-8	5′ A*U*A*A*U*G*C*U*G*G 3′	3329.2384	13.32
1202.37925	−3	3′ N-7 PO	5′ U*C*A*C*U*U*U*C*A*U*A 3′ - PO	3609.8767	13.57
1082.04391	−3	3′ N-8 cyc	5′ U*C*A*C*U*U*U*C*A*U 3′ - cyc	3248.6324	13.63
1197.05261	−3	3′ N-7 cyc	5′ U*C*A*C*U*U*U*C*A*U*A 3′ - cyc	3594.1578	14.00
1215.75029	−3	5′ N-7	5′ C*A*U*A*A*U*G*C*U*G*G 3′	3650.2518	14.17
1312.06136	−3	3′ N-6 cyc	5′ U*C*A*C*U*U*U*C*A*U*A*A 3′ - cyc	3939.1841	14.35
1323.08361	−3	5′ N-6	5′ U*C*A*U*A*A*U*G*C*U*G*G 3′	3972.0625	14.69
1064.29721	−4	3′ N-5 cyc	5′ U*C*A*C*U*U*U*C*A*U*A*A*U 3′ - cyc	4261.1906	14.97
1072.56286	−4	5′ N-5	5′ U*U*C*A*U*A*A*U*G*C*U*G*G 3′	4294.2528	15.19

(continued on next page)

Table 2 (*continued*)

m/z values for the most abundant ion	Charge	Impurity	Impurity sequence	Deconvoluted mass [Da]	Retention time [min]
1153.31412	−4	5′ N-4	5′ U*U*U*C*A*U*A*A*U*G*C*U*G*G 3′	4616.7555	15.72
1219.56568	−4	3′ N-3	5′ U*C*A*C*U*U*U*C*A*U*A*A*U*G*C 3′	4882.2627	15.88
1299.81725	−4	3′ N-2	5′ U*C*A*C*U*U*U*C*A*U*A*A*U*G*C*U 3′	5203.2690	16.26
1233.56603	−4	5′ N-3	5′ C*U*U*U*C*A*U*A*A*U*G*C*U*G*G 3′	4938.2653	16.29
1319.57498	−4	5′ N-2	5′ A*C*U*U*U*C*A*U*A*A*U*G*C*U*G*G 3′	5283.2998	16.49
1400.32916	−4	5′ N-1	5′ C*A*C*U*U*U*C*A*U*A*A*U*G*C*U*G*G 3′	5605.3190	16.85
1480.57930	**−4**	**OL2**	**5′ U*C*A*C*U*U*U*C*A*U*A*A*U*G*C*U*G*G 3′**	**5927.0099**	**17.05**
1476.58422	−4	OL2 (P═O)	5′ U*C*A*C*U*U*U*C*A*U*A*A*U*G*C*U*G*G 3′ (P═O)	5910.8362	17.49

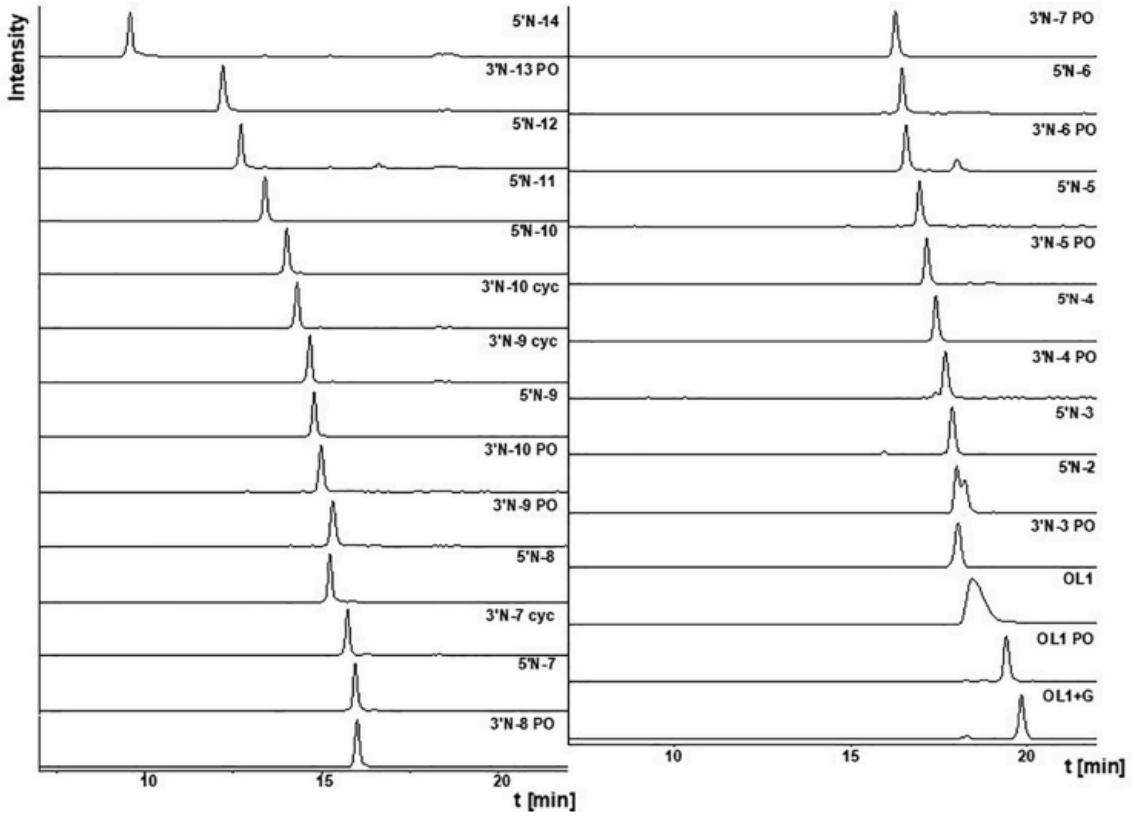

Fig. 5. Extracted ion chromatograms for impurities of OL1. Experimental conditions: *ACQUITY* Premier BEH Amide column (1.7 µm, 50 × 2.1 mm); MP composition MP A: ACN/10 mM ammonium acetate (pH 6.8) 75/25 (*v/v*), MP B: 10 mM ammonium acetate (pH 6.8); gradient elution programs: 0–1 min. 100 % MP A, 1–21 min. 100–50 % MP A (20 min re-equilibration); column temperature: 40 °C; autosampler temperature 10 °C; flow rate: 0.4 mL min^{-1}; injection volume 5 µL; mass spectrometric conditions: nebulizer gas pressure 20 psi, skimmer voltage 80 V, capillary voltage 4000 V, fragmentor voltage 200 V; drying gas flow 10 L min^{-1}, shielding gas flow 10 L min^{-1}, octopole voltage 800 V, drying gas temperature 350 °C, and shielding gas temperature 400 °C. Peak broadening of OL1 is caused by partial column overloading for the dominant oligonucleotide (OL1 concentration is 10–100 fold higher than the shorter oligonucleotide impurities detected in the sample).

4. Conclusion

The aim of this work was to develop HILIC method using amide stationary phase for analysis of phosphorothioated therapeutic ONs. We investigated the effects of several chromatographic parameters (pH of the aqueous part of the MP, buffer concentration, separation temperature) on retention and resolution of phosphorothioated ONs differing in the length and the number of PS modifications. The results showed that pH 6.8–8.0 is recommended for ONs analysis, while pH 4.7 provided broader peaks and at pH 3.0 21mer ONs were not eluted within 60 min. The separation (peak symmetry) improved with buffer concentration from 10 to 25 mM buffers. More sensitive MS detection was achieved when replacing ammonium formate with ammonium acetate. The effect of separation temperature on retention and resolution was not significant.

The impurities were identified in the sample of 18mer ONs (analogues to nusinersen). In allPO anologue 26 impurities, in allPS analogue even 28 impurities were partially separated and identified by Q-TOF. In

Table 3
The sequences of probable nusinersen metabolites, *m/z* values for observed ions, their charge states, and masses.

Abbreviation	Observed ions [*m/z*]	Charge state	Metabolite			
			Deconvoluted mass [Da]	Predicted mass [Da]	Probable sequence	Probable metabolites
M1	617.73718	−2	1237.4760	1236	A*mU*G*	5′N-11+3′N-4
	1236.47773	−1				
M2	696.77176	−2	1395.5441	1395	G*mU*mC*MoeR	5′N-15+3′N-1 or
	1394.54477	−1			mU*G*mC*MoeR	5′N-12+3′N-3
M3	601.77687	−2	1205.5537	1205	mC*A*mU*	5′N-7 + 3′N-8 or
					mU*mC*A*	3′N-15 or
					A*mC*mU*	5′N-2 + 3′N-13
M4	661.2532	−2	1324.5046	1325	*A*mU*G*	5′N-11+3′N-4
M5	595.75245	−2	1193.5049	1194	mC*mU*mU*	5′N-3 + 3′N-12 or
					mU*mU*mC*	5′N-5 + 3′N-10
M6	697.26371	−2	1396.5274	–	unidentified	–
M7	653.26689	−2	1308.5333	1308	*A*A*mU*	5′N-10+3′N-5 or
	1307.53331	−1			*mU*A*A*	5′N-9 + 3′N-6
M8	731.317095	−2	1464.6340	1464	*mU*mU*mU*MoeR	5′N-4 + 3′N-11
M9	728.76776	−2	1459.5355	1458	A*mC*mU*MoeR*	5′N-2 + 3′N-13 or
					mU*mC*A*MoeR*	5′N-6 + 3′N-9 or
					mC*A*mU*MoeR*	5′N-7 + 3′N-8
M10	771.29979	−2	1544.5995	1543	G*G*mU*mC	3′N-14
M11	806.8181	−2	1615.6362	1614	A*mU*A*A*	5′N-8 + 3′N-6

where: * – phosphorothioate group; MoeR – 2′-O-methoxyethylribose.

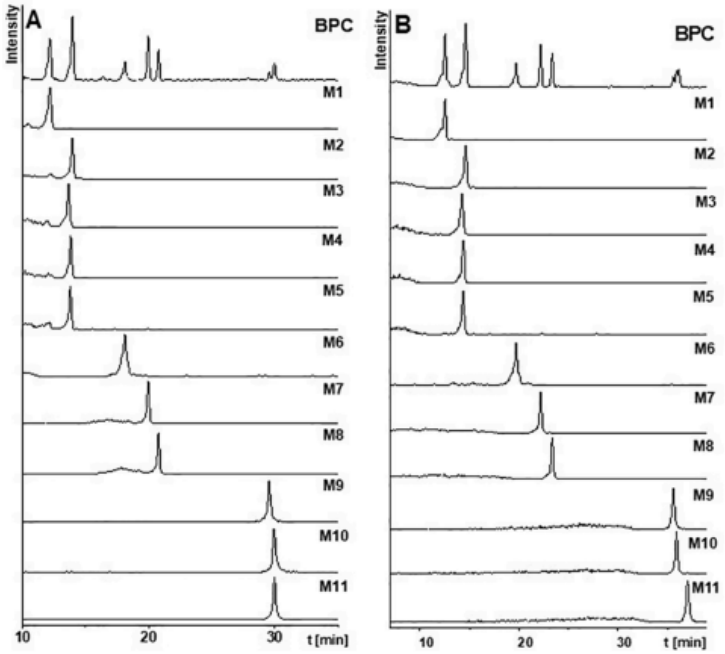

Fig. 6. Base peak chromatograms and extracted ion chromatograms for metabolites extracted from serum sample of SMA patient treated with nusinersen: (A) gradient elution program 0–1 min. 100 % MP A, 1–30 min. 100–85 % MP A (20 min re-equilibration); (B) 0–1 min. 100 % MP A, 1–60 min. 100–80 % MP A (20 min re-equilibration). Experimental conditions: *ACQUITY* Premier BEH Amide column (1.7 µm, 150 × 2.1 mm); MP composition MP A: ACN/10 mM ammonium acetate (pH 6.8) 75/25 (*v/v*), MP B: 10 mM ammonium acetate (pH 6.8); column temperature: 40 °C; autosampler temperature: 10 °C; flow rate: 0.4 mL min^{-1}; injection volume 5 µL; mass spectrometric conditions: nebulizer gas pressure 20 psi, skimmer voltage 80 V, capillary voltage 4000 V, fragmentor voltage 200 V; drying gas flow 10 L min^{-1}, shielding gas flow 10 L min^{-1}, octopole voltage 800 V, drying gas temperature 350 °C, and shielding gas temperature 400 °C.

the next step analysis of extracts from plasma samples from children treated by Spinraza has been performed. Eleven shortmer metabolites have been identified, but unfortunately it was not possible to separate all of them, even with the use of a longer column. Metabolites were very short (2–4mers), contrary to impurities. Moreover, metabolites sequences were very similar, often differing in one group. It appears that separation of this type of ONs mixtures is challenging in HILIC, contrary to resolution of dozens of impurities. Nevertheless, it should be emphasized that this is also difficult to achieve for IP RP HPLC, and the advantage of the developed HILIC method is the absence of ion pair reagents.

To conclude, MS compatible HILIC method without using of ion-pairing agents has been developed and successfully applied for the analysis of impurities in nusinersen analogues as well as for analysis of metabolites in serum samples.

CRediT authorship contribution statement

Zuzana Vosáhlová: Conceptualization, Investigation, Methodology, Writing – original draft, Writing – review & editing, Data curation.

Květa Kalíková: Conceptualization, Methodology, Resources, Supervision, Visualization, Writing – original draft, Writing – review & editing, Data curation. **Martin Gilar:** Conceptualization, Methodology, Resources, Writing – original draft, Writing – review & editing. **Jakub Szymarek:** Resources, Writing – review & editing. **Maria Mazurkiewicz-Bełdzińska:** Resources, Writing – review & editing. **Sylwia Studzińska:** Conceptualization, Data curation, Investigation, Methodology, Resources, Writing – original draft, Writing – review & editing.

Declaration of Competing Interest

The authors declare that they have no known competing financial interests or personal relationships that could have appeared to influence the work reported in this paper.

Data availability

Data will be made available on request.

Acknowledgment

This work was financially supported by Torun Center of Excellence "Towards Personalized Medicine" operating under Excellence Initiative-Research University (Sylwia Studzińska).

Supplementary materials

Supplementary material associated with this article can be found, in the online version, at doi:10.1016/j.chroma.2023.464535.

References

[1] E.C. Kuijper, A.J. Bergsma, W.W.M.P. Pijnappel, A. Aartsma-Rus, Opportunities and challenges for antisense oligonucleotide therapies, J. Inherit. Metab. Dis. 44 (2021) 72–87, https://doi.org/10.1002/jimd.12251.
[2] S. Bajan, G. Hutvagner, RNA-based therapeutics: from antisense oligonucleotides to miRNAs, Cells 9 (2020) 137, https://doi.org/10.3390/cells9010137.
[3] E.E. Neil, E.K. Bisaccia, Nusinersen: a novel antisense oligonucleotide for the treatment of spinal muscular atrophy, J. Pediatr. Pharmacol. Ther. 24 (2019) 194–203, https://doi.org/10.5863/1551-6776-24.3.194.
[4] M. Bege, A. Borbás, Rise and fall of fomivirsen, the first approved gene silencing medicine—A historical review, Acta Pharm Hung 92 (2022) 38–44, https://doi.org/10.33892/aph.2022.92.38-44.
[5] B.P. Monia, J.F. Johnston, H. Sasmor, L.L. Cummins, Nuclease resistance and antisense activity of modified oligonucleotides targeted to Ha-ras, J. Biol. Chem. 271 (1996) 14533–14540, https://doi.org/10.1074/jbc.271.24.14533.
[6] A. Goyon, P. Yehl, K. Zhang, Characterization of therapeutic oligonucleotides by liquid chromatography, J. Pharm. Biomed. Anal. 182 (2020), 113105, https://doi.org/10.1016/j.jpba.2020.113105.
[7] T.C. Roberts, R. Langer, M.J.A. Wood, Advances in oligonucleotide drug delivery, Nat. Rev. Drug Discov. 19 (2020) 673–694, https://doi.org/10.1038/s41573-020-0075-7.
[8] D. Yu, E.R. Kandimalla, A. Roskey, Q. Zhao, L. Chen, J. Chen, S. Agrawal, Stereo-enriched phosphorothioate oligodeoxynucleotides: synthesis, biophysical and biological properties, Bioorg. Med. Chem. 8 (2000) 275–284, https://doi.org/10.1016/S0968-0896(99)00275-8.
[9] D. Capaldi, A. Teasdale, S. Henry, N. Akhtar, C. den Besten, S. Gao-Sheridan, M. Kretschmer, N. Sharpe, B. Andrews, B. Burm, J. Foy, Impurities in oligonucleotide drug substances and drug products, Nucl. Acid Ther. 27 (2017) 309–322, https://doi.org/10.1089/nat.2017.0691.
[10] J. Kim, B. Basiri, C. Hassan, C. Punt, E. van der Hage, C. den Besten, M.G. Bartlett, Metabolite profiling of the antisense oligonucleotide eluforsen using liquid chromatography-mass spectrometry, Mol. Ther. - Nucl. Acids 17 (2019) 714–725, https://doi.org/10.1016/j.omtn.2019.07.006.
[11] Z. Kadlecová, K. Kalíková, E. Tesařová, M. Gilar, Phosphorothioate oligonucleotides separation in ion-pairing reversed-phase liquid chromatography: effect of ion-pairing system, J. Chromatogr. A 1676 (2022), 463201, https://doi.org/10.1016/j.chroma.2022.463201.
[12] T. Chen, S. Tang, Y. Fu, J.G. Napolitano, K. Zhang, Analytical techniques for characterizing diastereomers of phosphorothioated oligonucleotides, J. Chromatogr. A 1678 (2022), 463349, https://doi.org/10.1016/j.chroma.2022.463349.
[13] M. Huang, X. Xu, H. Qiu, N. Li, Analytical characterization of DNA and RNA oligonucleotides by hydrophilic interaction liquid chromatography-tandem mass spectrometry, J. Chromatogr. A 1648 (2021), 462184, https://doi.org/10.1016/j.chroma.2021.462184.
[14] M. Gilar, B.M. Koshel, R.E. Birdsall, Ion-pair reversed-phase and hydrophilic interaction chromatography methods for analysis of phosphorothioate oligonucleotides, J. Chromatogr. A 1712 (2023), 464475, https://doi.org/10.1016/j.chroma.2023.464475.
[15] N.M. El Zahar, N. Magdy, A.M. El-Kosasy, M.G. Bartlett, Chromatographic approaches for the characterization and quality control of therapeutic oligonucleotide impurities, Biomed. Chromatogr. 32 (2018) e4088, https://doi.org/10.1002/bmc.4088.
[16] J.M. Sutton, G.J. Guimaraes, V. Annavarapu, W.D. van Dongen, M.G. Bartlett, Current state of oligonucleotide characterization using liquid chromatography–mass spectrometry: insight into critical issues, J. Am. Soc. Mass Spectrom. 31 (2020) 1775–1782, https://doi.org/10.1021/jasms.0c00179.
[17] A.J. Alpert, Hydrophilic-interaction chromatography for the separation of peptides, nucleic acids and other polar compounds, J. Chromatogr. A 499 (1990) 177–196, https://doi.org/10.1016/S0021-9673(00)96972-3.
[18] R.N. Easter, K.K. Kröning, J.A. Caruso, P.A. Limbach, Separation and identification of oligonucleotides by hydrophilic interaction liquid chromatography (HILIC)—Inductively coupled plasma mass spectrometry (ICPMS), Analyst 135 (2010) 2560–2565, https://doi.org/10.1039/C0AN00399A.
[19] R. Easter, C. Barry, J. Caruso, P. Limbach, Separation and identification of phosphorothioate oligonucleotides by HILIC-ESIMS, Anal. Methods 5 (2013) 2657–2659. https://doi.org/10.1039/C3AY26519F.
[20] S. Studzińska, F. Łobodziński, B. Buszewski, Application of hydrophilic interaction liquid chromatography coupled with mass spectrometry in the analysis of phosphorothioate oligonucleotides in serum, J. Chromatogr. B 1040 (2017) 282–288, https://doi.org/10.1016/j.jchromb.2016.11.001.
[21] P.A. Lobue, M. Jora, B. Addepalli, P.A. Limbach, Oligonucleotide analysis by hydrophilic interaction liquid chromatography-mass spectrometry in the absence of ion-pair reagents, J. Chromatogr. A 1595 (2019) 39–48, https://doi.org/10.1016/j.chroma.2019.02.016.
[22] A. Demelenne, M.-J. Gou, G. Nys, C. Parulski, J. Crommen, A.-C. Servais, M. Fillet, Evaluation of hydrophilic interaction liquid chromatography, capillary zone electrophoresis and drift tube ion-mobility quadrupole time of flight mass spectrometry for the characterization of phosphodiester and phosphorothioate oligonucleotides, J. Chromatogr. A 1614 (2020), 460716, https://doi.org/10.1016/j.chroma.2019.460716.
[23] A. Kilanowska, B. Buszewski, S. Studzińska, Application of hydrophilic interaction liquid chromatography coupled with tandem mass spectrometry for the retention and sensitivity studies of antisense oligonucleotides, J. Chromatogr. A 1622 (2020), 461100, https://doi.org/10.1016/j.chroma.2020.461100.
[24] H. Lardeux, D. Guillarme, V. D'Atri, Comprehensive evaluation of zwitterionic hydrophilic liquid chromatography stationary phases for oligonucleotide characterization, J. Chromatogr. A 1690 (2023), 463785, https://doi.org/10.1016/j.chroma.2023.463785.
[25] A. Goyon, M.S. Blevins, J.G. Napolitano, D. Nguyen, M. Goel, B. Scott, J. Wang, S. G. Koenig, T. Chen, K. Zhang, Characterization of antisense oligonucleotide and guide ribonucleic acid diastereomers by hydrophilic interaction liquid chromatography coupled to mass spectrometry, J. Chromatogr. A 1708 (2023), 464327, https://doi.org/10.1016/j.chroma.2023.464327.
[26] G.J. Guimaraes, J.M. Sutton, M. Gilar, M. Donegan, M.G. Bartlett, Impact of nonspecific adsorption to metal surfaces in ion pair-RP LC-MS impurity analysis of oligonucleotides, J. Pharm. Biomed. Anal. 208 (2022), 114439, https://doi.org/10.1016/j.jpba.2021.114439.
[27] J.M. Nguyen, M. Gilar, B. Koshel, M. Donegan, J. MacLean, Z. Li, M.A. Lauber, Assessing the impact of nonspecific binding on oligonucleotide bioanalysis, Bioanalysis 13 (2021) 1233–1244, https://doi.org/10.4155/bio-2021-0115.
[28] D.L. Davis, E.P. O'Brie, C.M. Bentzley, Analysis of the degradation of oligonucleotide strands during the freezing/thawing processes using MALDI-MS, Anal. Chem. 72 (2000) 5092–5096, https://doi.org/10.1021/ac000225s.
[29] S. Studzińska, M. Mazurkiewicz-Bełdzińska, B. Buszewski, Development of the method for nusinersen and its metabolites identification in the serum samples of children treated with spinraza for spinal muscular atrophy, Int. J. Mol. Sci. 23 (2022) 10166, https://doi.org/10.3390/ijms231710166.
[30] A. Kilanowska, Ł. Nuckowski, S. Studzińska, Studying in vitro metabolism of the first and second generation of antisense oligonucleotides with the use of ultra-high-performance liquid chromatography coupled with quadrupole time-of-flight mass spectrometry, Anal. Bioanal. Chem. 412 (2020) 7453–7467, https://doi.org/10.1007/s00216-020-02878-0.
[31] P.J. Sample, K.W. Gaston, J.D. Alfonzo, P.A. Limbach, RoboOligo: software for mass spectrometry data to support manual and de novo sequencing of post-transcriptionally modified ribonucleic acids, Nucl. Acids Res. 43 (2015) e64, https://doi.org/10.1093/nar/gkv145.
[32] J. Rozenski, J.A. McCloskey, SOS: a simple interactive program for ab initio oligonucleotide sequencing by mass spectrometry, J. Am. Soc. Mass Spectrom. 13 (2002) 200–203, https://doi.org/10.1016/S1044-0305(01)00354-3.
[33] S.A. Mcluckey, G.J. Van Berkel, G.L. Glish, Tandem mass spectrometry of small, multiply charged oligonucleotides, J. Am. Soc. Mass Spectrom. 3 (1992) 60–70, https://doi.org/10.1016/1044-0305(92)85019-G.
[34] M. Gilar, K.D. Berthelette, T.H. Walter, Contribution of ionic interactions to stationary phase selectivity in hydrophilic interaction chromatography, J. Sep. Sci. 45 (2022) 3264–3275, https://doi.org/10.1002/jssc.202200165.
[35] Z. Kadlecová, K. Kalíková, E. Tesařová, M. Gilar, Phosphorothioate oligonucleotides separation in ion-pairing reversed-phase liquid chromatography:

effect of temperature, J. Chromatogr. A 1681 (2022), 463473, https://doi.org/10.1016/j.chroma.2022.463473.
[36] Z. Hao, B. Xiao, N. Weng, Impact of column temperature and mobile phase components on selectivity of hydrophilic interaction chromatography (HILIC), J. Sep. Sci. 31 (2008) 1449–1464, https://doi.org/10.1002/jssc.200700624.
[37] C. Rentel, H. Gaus, K. Bradley, N. Luu, K. Kolkey, B. Mai, M. Madsen, M. Pearce, B. Bock, D. Capaldi, Assay, purity, and impurity profile of phosphorothioate oligonucleotide therapeutics by ion pair–HPLC–MS, Nucl. Acid Ther. 32 (2022) 206–220, https://doi.org/10.1089/nat.2021.0056.
[38] H. Takakusa, N. Iwazaki, M. Nishikawa, T. Yoshida, S. Obika, T. Inoue, Drug metabolism and pharmacokinetics of antisense oligonucleotide therapeutics: typical profiles, evaluation approaches, and points to consider compared with small molecule drugs, Nucl. Acid Ther. 33 (2023) 83–94, https://doi.org/10.1089/nat.2022.0054.
[39] S. Andersson, M. Antonsson, M. Elebring, R. Jansson-Löfmark, L. Weidolf, Drug metabolism and pharmacokinetic strategies for oligonucleotide- and mRNA-based drug development, Drug Discov. Today 23 (2018) 1733–1745, https://doi.org/10.1016/j.drudis.2018.05.030.
[40] S. Studzińska, J. Szymarek, M. Mazurkiewicz-Bełdzińska, Improvement of serum sample preparation and chromatographic analysis of nusinersen used for the treatment of spinal muscular atrophy, Talanta 267 (2024), 125173, https://doi.org/10.1016/j.talanta.2023.125173.